Wax Ester Synthases/Acyl-CoA:Diacylglycerol Acyltransferases (WS/DGATs) from *Arabidopsis thaliana*

Dissertation

zur

Erlangung des Doktorgrades (Dr. rer. nat.)

der

Mathematisch-Naturwissenschaftlichen Fakultät

der

Rheinischen Friedrich-Wilhelms-Universität Bonn

vorgelegt von

Veronika Salewski

aus

Vechta

Bonn, 2021

Angefertigt mit Genehmigung der Mathematisch-Naturwissenschaftlichen
Fakultät der Rheinischen Friedrich-Wilhelms-Universität Bonn

1. Gutachter: Prof. Dr. Peter Dörmann
2. Gutachter: Prof. Dr. Lukas Schreiber
Tag der Promotion: 07.04.2022
Erscheinungsjahr: 2022

Abstract

Wax esters occur in the surface wax of plants and are involved amongst others in the plant's response to drought. In *Arabidopsis thaliana*, a family of 11 genes are annotated as bifunctional wax ester synthases/acyl-CoA diacylglycerol acyltransferases (WS/DGATs) and designated as *WSD1* – *WSD11*. WSD1 was previously characterized to contribute wax esters to the surface wax of stem.

In this study, the surface waxes of *Arabidopsis thaliana* stem, silique and flowers were analyzed from wild type and *wsd* insertion mutants regarding the amount and species composition of wax esters by quadrupole time-of-flight mass spectrometry. In wild type, wax ester species with 16:0 acyl moiety were most abundant in the surface waxes of stem, silique and flower. The mutant *wsd1* revealed a reduction of wax ester species with 16:0 acyl moieties in the surface waxes of stem, flower and silique. *WSD* gene expression was measured for *WSD1* – *WSD11* in root, stem, leaf, inflorescence and seed under normal growth conditions and in root and leaf after exposure to drought, salt and abscisic acid (ABA). The expression of *WSD1* was induced in leaf and the expression of *WSD6* and *WSD7* increased in both root and leaf after exposure to drought, salt and ABA. Heterologous expression of WSD1 in yeast led to the detection of an unknown lipid 1 (UL1) while wax ester synthase activity was not detected. Subcellular localization studies of WSD3, WSD4 and WSD9 indicated the three WSD proteins reside at the endoplasmic reticulum. Furthermore, the wax ester load of leaves from drought-stressed *Hordeum vulgare* was measured revealing an increased wax ester load in leaf surface wax compared to the control.

Table of Contents

Table of Figures

Table of Tables

Abbreviations

% (v/v)	Percent volume per volume (ml per 100 ml)
% (w/v)	Percent weight per volume (g per 100 ml)
ABA	Abscisic acid
CoA	Coenzyme A
DAG	diacylglycerol
ddH_2O	Double deionized water
DGAT	Diacylglycerol:acyl-CoA acyltransferase
DNA	Deoxyribonuleic acid
dNTPs	Deoxyribonuleotide triphosphates (dATP, dTTP, dGTP, dCTP)
DsRED	*Discosoma* sp. red fluorescent protein
EDTA	Ethylenediaminetetraacetic acid
ER	Endoplasmic reticulum
et al.	Latin: *et alii* and others
FAMEs	Fatty acid methyl esters
FFA	Free fatty acid
GC-FID	Gas chromatography-flame ionization detection
eGFP	Enhanced green fluorescent protein
I.S.	Internal standard
MGAT	Monoacylglycerol:acyl-CoA acyltransferase
MOPS	3-(*N*-morpholino)propanesulfonic acid
MS	Mass spectrometry
m/z	Mass-to-charge ratio
NTPs	Ribonuleotide triphosphates (ATP, UTP, GTP, CTP)
OD	Optical density
PCR	Polymerase Chain Reaction
Q-TOF MS	Quadrupole time-of-flight mass spectrometer
REB	RNA elution buffer
RNA	Ribonucleic acid
SOB	Super Optimal Broth
SPE	Solid phase extraction
SIGnAL	Salk Institute Genomic Analysis Laboratory
TAE	Tris base**,** acetic acid and EDTA
TAG	Triacylglycerol
TAIR	*The Arabidopsis Information Resource*
TIC	Total ion chromatogram
T-DNA	Transfer-DNA
TLC	Thin layer chromatography
Tris	tris(hydroxymethyl)aminomethane
UL1, UL2	Unknown lipid 1, unknown lipid 2
VLCFA	Very-long-chain fatty acid
WE	Wax ester
WS	Wax ester synthase
WSD	WS/DGAT homologs in *Arabidopsis thaliana*
WS/DGAT	Wax ester synthase/Acyl-CoA:diacylglycerol acyltransferase
WT	Wild type

Nomenclature of Wax Esters
Molecular species of WEs are described as follows W:Xol/Y:Z. W:Zol represents the fatty alcohol moiety, Y:Z represents the fatty acid moiety of the WE. The numbers of W and Y represent the number of carbon atoms, X and Z the numbers of double bonds in the respective moieties.

1 Introduction

For all living organisms, lipids play an important role by fulfilling diverse functions. Lipids are a group of diverse molecules and are defined as being soluble in nonpolar solvents. Lipids function, for example, as membrane lipids which separate cells from their environment and compartmentalize them. Lipids further serve as energy storage compounds and are involved in signaling. The main focus in the present study lies on the lipid class of wax esters.

1.1 Wax Esters (WE)

WEs are lipids which are composed of a fatty acid residue esterified to a fatty alcohol. The fatty acid and fatty alcohol moiety of wax monoesters can vary considering the degree of saturation, the moieties can be branched or straight-chained. Furthermore, not only wax monoesters are termed WEs but also more complex wax diesters and triesters (Cheng and Russell, 2004) where two or three fatty acyl residues are esterified to a diol or triol.

1.1.1 Natural Occurrence of WEs

WEs are widely distributed in eukaryotes and have also been described to occur in a few prokaryotes. In mammals, WEs are components of gland secretions of the Meibomian glands which contribute to the human eyes tear film (Nicolaides *et al.*, 1981) and of sebaceous glands which cover the body of mammals and contribute, among others, to the *vernix caseosa* of the developing fetus (Stewart *et al*., 1982). WEs are also components of secretions of preputial glands (Smith and Thiboutot, 2008; Camera *et al*., 2010) and are found in large amounts in the spermaceti organ of sperm whales (Morris (1973). In birds, the secretion of uropygial glands contains WEs and is used to preen the feathers (Biester *et al.*, 2012). Large amounts of WEs occur in diapausing deep-water copepods and, besides functioning as storage lipids, are presumed to contribute to the control of buoyancy (Lee *et al.*, 2006; Yamada *et al.*, 2016). WEs are further synthesized by insect species belonging to the family *Apoidea* and by scale insects. Honeybees and bumblebees produce wax containing WEs for their cells in which honey is stored and larvae are raised. Scale insects are covered with wax containing high amounts of WEs for their protection (Tulloch (1970)). WEs are also synthesized in algae, as for instance in *Chroomonas salina* and *Euglena gracilis* (Antia *et al.*, 1974; Teerawanichpan and Qiu, 2010).

The occurrence of WEs in prokaryotes has also been reported. For instance, WEs accumulate as intracellular inclusion bodies under growth-limiting conditions in the Gram-negative bacterium *Acinetobacter baylyi* strain ADP1 (formely *Acinetobacter calcoaceticus* strain ADP1, Vaneechoutte *et al*., 2006) and in *Mycobacterium smegmatis* mc^2155 grown under storage conditions supplemented with appropriate substrates (Kalscheuer and Steinbüchel, 2003). The pathogen

M. tuberculosis H37Rv accumulates high amounts of WEs when grown under iron-limited conditions, the function of these WEs are still unknown and may be the contribution to the cell wall under these conditions (Bacon *et al.*, 2007).
In plants, WEs are components of the cuticular waxes covering the aerial primary parts of plants. The seeds of the desert shrub *Simmondsia chinensis* (jojoba) contain of up to 60 % of WEs (of the seeds fresh weight) stored in the cotyledons of the plant embryo and used for gluconeogenesis during germination (Moreau and Huang, 1977).

1.1.2 Economic Interests in WEs

WEs are used for the generation of pharmaceutical and cosmetic products, in nutrition and as lubricants. Higher amounts of naturally occurring WEs are harvested from the seed oil of jojoba and from the epicuticular wax laying on the fronds of the carnauba palm *Copernicia prunifera*.
Due to its similarity to human sebum, the seed oil of jojoba is used in numerous cosmetic products (Alvarez and Rodríguez, 2000). WEs are also generated industrially, for instance WEs with very short alcohol moieties (methyl, ethyl) which are used as biodiesel. These WEs are synthesized by a transesterification of fatty acyl residues originating from triacylglycerols (TAGs) to methanol. The high amounts of TAGs used in biodiesel production are obtained from seed oils like rapeseed, but attempts have also been made to generate WEs for biodiesel by microorganisms (Kalscheuer *et al.*, 2006). Another field of application for WEs may be the medical treatment of obesity disease. In mouse experiments, the supplementation of WEs originating from the copepod *Calanus finmarchicus* to the diet reduced the body fat (Höper *et al.*, 2014).

1.1.3 Enzymes Involved in WE Synthesis

Few gene families are described to which enzymes involved in WE synthesis belong. For instance, mammalian wax ester synthases from mouse and human belong to the group of neutral lipid synthesizing enzymes of the monoacylglycerol acyltransferase 1 or 2 (MGAT1, MGAT2), diacylglycerol acyltransferase 1 or 2 (DGAT1, DGAT2) family (Cheng and Russell, 2004; Yen *et al*., 2005; Turkish *et al*., 2005; Yen *et al.*, 2005). The human wax ester synthase designated as multifunctional acyltransferase (MFAT) catalyzes in in vitro assays besides the synthesis of wax monoesters also the synthesis of retinyl esters and diacylglycerols (Yen *et al*., 2005). The mouse wax ester synthase catalyzes in vitro the synthesis of wax monoesters, retinyl esters and polyisoprenol esters (Cheng and Russell, 2004).
Another type of wax ester synthase was detected in the desert shrub jojoba, 12 homologous sequences of this jojoba wax ester synthase have been detected in the model plant *Arabidopsis thaliana* (Lardizabal *et al.*, 2000; Li *et al.*, 2008). Another gene family that has been found in bacteria and plants is the bifunctional wax ester synthase/ acyl-CoA:diacylglycerol

acyltransferase (WS/DGAT) family. This gene family is described below in detail. The wax ester synthases belonging to the different gene families described above use acyl-CoA and a fatty alcohol as substrates for the esterification reaction. Lipases in contrast, can generate WEs by esterifying alcohols with free fatty acids or with fatty acids hydrolyzed from triacylglycerol as well as hydrolyze WEs. These lipases are described to occur in both prokaryotes and eukaryotes (Tsujita *et al.*, 1999).

1.2 Triacylglycerols (TAGs)

TAGs are glycerolipids belonging to the neutral lipids. The TAG molecule is composed of three fatty acyl residues esterified to the three hydroxyl groups of a glycerol backbone. TAGs are synthesized by prokaryotes and eukaryotes. In prokaryotes, TAGs are synthesized under growth-limiting and stressful conditions in some bacteria like for instance in the genera *Actinomycetes*, *Mycobacterium*, *Streptomyces* and *Nocardia* (Kalscheuer and Steinbüchel, 2003; Daniel *et al.*, 2004; Olukoshi and Packter, 1994; Alvarez *et al.*, 2001). In eukaryotes, TAGs serve as energy storage lipids and as nontoxic precursor lipids for diacylglycerol (DAG) and for the phospholipid biosynthesis. Furthermore, by the incorporation into TAGs, free fatty acids (FFAs), acyl-CoAs and DAG can be efficiently removed. FFAs and acyl-CoAs are thought to be membrane-damaging (Coleman and Lee, 2004). In plants, TAGs accumulate in seeds (Zou *et al*., 1999), pollen grains (Piffanelli *et al*., 1998), and fruits like in olive or palm fruits (*Sánchez* and Harwood, 2002; Sundram *et al.*, 2003). Oilseed crops harboring high amounts of TAGs in their seeds like rapeseed are important contributors to human nutrition. In plants, TAGs can be stored in oil bodies which are cytosolic storage lipid organelles for instance in pollen and seed tissue (Napier *et al*., 1996).

1.2.1 Enzymes Involved in TAG Synthesis

TAG can be synthesized by acyl-CoA-dependent and by acyl-CoA-independent enzymes. One TAG biosynthesis pathway in which three acyl-CoA dependent enzymes are involved is the Kennedy pathway. Here the successive action of an acyl-CoA:glycerol-3-phosphate acyltransferase (GPAT; in *Arabidopsis* for instance *GPAT9*, Singer *et al*., 2016), acyl-CoA:lysophosphatidic acid acyltransferase (LPAT; in *Arabidopsis* assumed *LPAT2*, Kim *et al.*, 2005), an intervening diacylglycerol:phosphatidic acid phosphatase (PAP) (Chapman and Ohlrogge, 2012) and then acyl-CoA:diacylglycerol acyltransferase (DGAT; in *Arabidopsis DGAT1*; Hobbs *et al*., 1999; Routaboul *et al*., 1999) lead to the synthesis of TAG starting from the precursor molecule glycerol-3-phosphate. Two DGAT classes, DGAT1 and DGAT2 catalyzing the last step, the incorporation of acyl-CoA into DAG, exist. Also WS/DGAT enzymes can harbor acyl-CoA dependent DGAT activity as described above. Besides the acyl-CoA depending enzymes involved in TAG biosynthesis, also several enzymes catalyzing the last step of TAG synthesis without the need of acyl-CoA as

substrate are described: phospholipid:DAG acyltransferase (PDAT; *PDAT1* in *Arabidopsis*, Zhang *et al*., 2009); PC:DAG phosphocholine transferase (PDCT; in *Arabidopsis ROD1*) or DAG:DAG acyltransferase (Chapman and Ohlrogge, 2012).

1.3 Wax Ester Synthase/ Acyl-CoA:Diacylglycerol Acyltransferase (WS/DGAT)

The occurrence of members from the WS/DGAT family has been described so far in prokaryotes and in plants. While in prokaryotes, only species of few genera like *Acinetobacter*, *Mycobacterium* and *Streptomyces* are known to encode putative WS/DGATs (Kalscheuer and Steinbüchel, 2003), homologs of WS/DGATs are more widely distributed in plants as they have been found in many gymnosperm and angiosperm species (King *et al*., 2007; Cheng and Nikolau, 2013). In moss, only one WS/DGAT homolog has been identified so far encoded by the species *Physcomitrella patens subsp. patens* (Cheng and Nikolau, 2013). Furthermore, the genome of the flagellate *Euglena gracilis* reveals 6 putative WS/DGATs (Tomiyama *et al.*, 2017).

The eponymous activities of the WS/DGAT, the wax ester synthase (WS) activity and the acyl-CoA:diacylglycerol acyltransferase (DGAT) activity, are shown in Figure 1. The first described WS/DGAT was the *WS/DGAT* from the prokaryote *A. baylyi* strain ADP1 (formerly *A. calcoaceticus* strain ADP1, Vaneechoutte *et al*., 2006). WS/DGATs acting as both, WS and DGAT were found in *Acinetobacter baylyi* strain ADP1 and in *Arabidopsis thaliana*. Both WS/DGATs, *WS/DGAT* from *A. baylyi* ADP1 and *WSD1* from *A. thaliana*, appear to act mainly as wax ester synthase since the ratio of WS to DGAT activity was determined at approximately 10 in favor of the WS activity in enzymatic activity assays (Kalscheuer and Steinbüchel, 2003; Li *et al*., 2008). Other WS/DGATs characterized so far exhibited either only WS activity and no DGAT activity in enzymatic activity assays like *PhWS1* from *Petunia hybrida* W115 (King *et al*., 2007) or only DGAT activity like *TGS3* or *RV3087* from *Mycobacterium tuberculosis* strain H37Rv. Other WS/DGAT homologs from *M. tuberculosis* H37Rv function mainly as DGATs with minor WS activities (Daniel *et al*., 2004).

However, another species of the genus Mycobacterium, *M. smegmatis* mc^2155, contains the WS/DGAT homolog *wdh3269* which revealed higher WS than DGAT activity after heterologous expression in *Escherichia coli* and *Rhodococcus opacus* (Kalscheuer and Steinbüchel, 2003).

Besides the WS and DGAT activity, WS/DGATs can harbor further activities since for instance the WS/DGAT from *A. baylyi* ADP1 act further as acyl-CoA: monoacylglycerol acyltransferase (MGAT) and catalyzes the formation of wax diesters and monothio and dithio wax esters (Kalscheuer *et al.*, 2003; Uthoff *et al*., 2005).

Regarding wax ester synthesis, the specificity of the WS/DGAT from *A. baylyi* ADP1 was tested broadly and resulted in the finding that this WS/DGAT is highly unspecific and accepts various acyl-CoAs ranging from C_{12}-C_{20}, various chain lengths of linear alcohols ranging from C_2 toC_{30} and

aromatic alcohols (Stöveken *et al*., 2005; Kalscheuer and Steinbüchel, 2003). The specificities of other characterized WS/DGATs were tested in a lesser extent with the result that WSD1 from *A. thaliana* accepts octadecanol, tetracosanol and octacosanol for the esterification with palmitoyl-CoA and rejects short-chain alcohols like isoamyl alcohol and ethanol when expressed in yeast (Li *et al*., 2008). *Ph*WS1 from *P. hybrida* accepts these short-chain alcohols as acyl-acceptors and further prefers saturated medium chain alcohols C_8 - C_{12} and saturated very long chain acyl-CoAs though unsaturated acyl-CoAs are also accepted but with lower preference. Furthermore, PhWS1 accepts geraniol and farnesol as acyl-acceptors (King *et al*., 2007). Wdh3269 from *M. smegmatis* mc²155 accepts hexadecanol and palmitoyl-CoA, which were the only substrates tested so far for this WS/DGAT homolog (Kalscheuer and Steinbüchel, 2003).

As active-site of the WS/DGAT homologs, the highly conserved motif HH*XXX*DG has been proposed. This motif is known to be the catalytic center of nonribosomal peptide synthetases with the second histidine residue being essential for the catalyzed reaction (Stachelhaus *et al*., 1998). The active-site motif lays in the N-terminal region from different WS/DGAT homologs like the WS/DGAT from *A. baylyi* ADP1 and WSD1 as well as other homologs from *A. thaliana* and from *Mycobacterium* (Kalscheuer and Steinbüchel, 2003; Li *et al*., 2008). The HH*XXX*DG motif was demonstrated to belong to the active-site of the WS/DGAT from *A. baylyi* ADP1 with the second histidine residue being essential for the catalytic enzymatic activity (Stöveken *et al*., 2009).

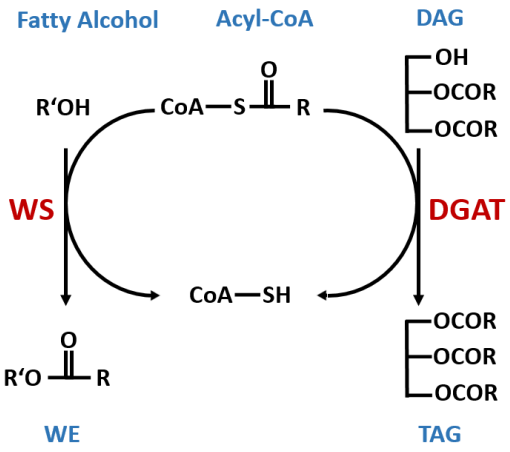

Figure 1: Reactions Catalyzed by the Bifunctional WS/DGAT.

The synthesis of a wax ester (WE) catalyzed by the wax ester synthase (WS) function of the WS/DGAT is presented on the left side, the synthesis of triacylglycerol (TAG) catalyzed by the acyl-CoA:diacylglycerol acyltransferase (DGAT) function of the WS/DGAT is presented on the right side. R' represents the fatty alcohol moiety, R represents the fatty acid moiety.

1.4 *Arabidopsis thaliana*

A. thaliana serves as model in plant biology research. The plant has many favorable properties like a short generation time of 6 weeks, a small size and is simple to grow. It belongs to the *Brassicaceae* family to which also several other agronomically important plant species like the oil

crop *Brassica napus* or different cultivated cabbage species belong. *A. thaliana* is widely distributed on earth, a variety of different ecotypes is described to occur in North America, Europe, Africa and Asia. The genome of the plant has been fully sequenced in 2000 and according to Araport 11, 27.655 protein-coding genes are encoded on five chromosomes of the plant.

1.4.1 WS/DGATs (WSDs) in *A. thaliana*

11 Genes detected in the genome of *A. thaliana* share similarity to the *WS/DGAT* from *A. baylyi* strain ADP1 and are designated as *WSD1* – *WSD11*. The *WSD* genes are distributed on chromosome 1, 2, 3 and 5 with the genes *WSD4*, *WSD5* and *WSD6* being directly neighbored on chromosome 3 and the genes *WSD10* and *WSD11* being directly neighbored on chromosome 5. Different splice variants are described for seven WSD proteins with up to four variants for WSD1 and WSD3, the residual WSD proteins WSD4, WSD5, WSD10 and WSD11 are synthesized without posttranslational modification as known so far. The sizes of the expressed WSD proteins ranges from 477 amino acids (aa) to 522 aa according to *The Arabidopsis Information Resource* (TAIR) for the largest variant each. The WSD proteins share 16-20.5 % aa sequence identity over their entire lengths (Li *et al*., 2008). As catalytic center, the WSD proteins possess the active-site motif HH*XXX*DG in the N-terminal region of the proteins, only the sequence of WSD8 reveals a replacement of the first histidine residue with asparagine, however, the second histidine residue which is assessed to be essential for the catalytic reaction is present (see Figure 2).

Figure 2: Alignment of Amino Acid Sequences from WSD Proteins Including the Putative Active Sites.

The amino acid sequences of the gene models AT5G37300.1 (WSD1), AT1G72110.1 (WSD2), AT2G38995.2 (WSD3), AT3G49190.1 (WSD4), AT3G49200.1 (WSD5), AT3G49210.1 (WSD6), AT5G12420.1 (WSD7), At5g16350.1 (WSD8), At5g22490.1 (WSD9), At5g53380.1 (WSD10), and At5g53390.1 (WSD11) found on TAIR (https://www.arabidopsis.org/) were aligned with the Clustal Omega program (Sievers *et al.*, 2011; Sievers and Higgins, 2018) on https://www.uniprot.org/help/sequence-alignments. An asterisk (*) represents a conserved residue, a colon (:) represents a conservation between residues which share strongly similar properties, a period (.) shows conservation between residues which share weakly similar properties. The putative active site, HH*XXX*DG, is depicted in a box.

1.4.2 WSD1

WSD1 was the first characterized WS/DGAT homolog from *A. thaliana*. The enzyme contributes WEs to the stem cuticle, *A. thaliana* mutants with disrupted *wsd1* gene revealed nearly complete absence of WEs in stem wax (Li *et al*., 2008). Typical stem WEs of *A. thaliana* WT are straight chain saturated wax monoesters with $C_{16:0}$ being the most abundant fatty acyl moiety esterified mainly with $C_{26:0}$, $C_{28:0}$ and $C_{30:0}$ alcohol moieties which results in WE chain lengths of C_{42}, C_{44} and C_{46} being most abundant in stem wax (Lai *et al*., 2007). WSD1 catalyzes the synthesis of these main abundant wax esters since the enzyme accepts $C_{16:0}$-CoA and diverse long-chain and very-long-chain alcohols ranging from $C_{18:0}$ to $C_{28:0}$. While the WS activity of WSD1 was demonstrated also in vivo by heterologous expression in yeast, the DGAT activity of WSD1 was only detected in vitro. In the in vitro assay, the ratio of WS to DGAT activity was determined at approximately 10 fold higher in favor of the WS activity.

As furthermore no decrease in triacylglycerol (TAG) in seeds of *wsd1* deletion mutants was measured, WSD1 is discussed to have its major role as WS and is unlikely to contribute TAG to the seed oil. WEs were measured so far only in stem wax, however, WSD1 is also expressed in leaf and flower bud tissue and the expression was not limited to epidermal cells like other genes contributing to wax synthesis (Li *et al*., 2008).

1.4.3 WSD11

wsd11 deletion mutants were described to exhibit a special flower phenotype which is characterized by folded petals. Due to the flower phenotype, *wsd11* is also designated as *fop1* (*folded petals1*). Normally, the elongation of the petals during flower development takes place smoothly through a narrow gap between sepals and anthers resulting in an unfolded petal. The folded petal phenotype of the *fop1* mutant was speculated to be caused by missing WEs acting as lubricants. This hypothesis is based further on the petals epidermal surface of *wsd11/fop1* mutants which exhibits traces of friction caused by strong pressure between elongating petal and sepal which were not present on the petal surface of the control. The analysis of WEs in floral buds of the *wsd11/fop1* mutant plant and the control resulted in no significant change, furthermore the enzymatic activity of WSD11/FOP1 was not described so far. WSD11/FOP1 is expressed only in inflorescence and flowers (Takeda *et al*., 2013).

1.4.4 WSD2 - WSD10

Regarding the other annotated WS/DGAT homologs WSD2 - WSD10, only little information derived from sequence models and electronic annotation was available over the experimental period from 2010 to 2014 of this work and need to be verified experimentally. Expression data

for several WSD proteins derived from a microarray experiment are deposited also on TAIR (see TAIR website, annotation detail for further information).

1.5 Cuticle

The outermost aerial primary tissue of a terrestrial plant is the epidermis. Hereon, the cuticle lays as thin and hydrophilic film consisting of lipid polymers and embedded (intracuticular) and overlaying (epicuticular) waxes. The cuticle constitutes thereby a border between the plant and its aerial environment. The functions of the cuticle comprise minimization of non-stomatal water loss (Vogg *et al*., 2004), the reflection of ultraviolet radiation (Holmes and Keiller, 2002), mediation of plant-pathogen interactions and being a barrier against phytophagous insects (Reina-Pinto and Yephremov, 2009). The cuticle exhibits further self-cleaning properties conferred by water repellency and prevents fusion of growing plant organs (Barthlott and Neinhuis, 1997; Sieber *et al*., 2000).

The cuticles lipid polymer cutin can be depolymerized by hydrolysis while the lipid polymer cutan is highly resistant to hydrolysis. Cutin monomers are interesterified C_{16} and C_{18} fatty acids which can be unsubstituted, ω-hydroxy or α,ω-dicarboxylic fatty acids and can have a midchain functional group like epoxy, oxo, hydroxy, vicinal diol. ω-hydroxy fatty acids are typically the most abundant cutin monomers. Furthermore, lower amounts of glycerol, fatty alcohols and phenylpropanoids are present in cutin. Cutan is thought to be structured by ether and C-C bonds (Yeats and Rose, 2013; Pollard *et al*., 2008).

The cutin polyester of the model plant *A. thaliana* is peculiar compared to other plant species since more than 50 % of the monomers are α,ω-dicarboxylic acids. The α,ω-dicarboxylic acids are derived from C_{16} and C_{18} fatty acids with $C_{18:2}$ α,ω-dicarboxylic acid being most abundant and are speculated to be directly esterified to glycerol. Besides this peculiarity, *A. thaliana* cutin contains typical ω-hydroxy and hydroxyl-epoxy fatty acid monomers derived from C_{16} and C_{18} fatty acids (Bonaventure *et al*., 2004; Pollard *et al*., 2008).

In contrast to the cuticles polymers, epicuticular and intracuticular waxes are extractable by organic solvents. The wax composition can vary between species, plant organs and developmental stages. For instance, in the model plant *A. thaliana*, alkanes are the most abundant wax components in both stem and leaf cuticle, however the molecular species vary in that the chain lengths C_{29}, C_{31} and C_{33} are dominating in leaf wax while only one chain length, C_{29}, is highly abundant in stem wax. Stem cuticular wax contains further ketones and secondary alcohols in higher amounts, these wax components occur only in trace amounts in leaf wax of *A. thaliana*. In leaf wax, primary alcohols constitute the next abundant wax component, which occur in lower amounts also in stem wax. Further wax components are WEs, aldehydes and fatty acids which occur in low amounts in stem and leaf wax (WEs only trace amounts in leaf wax) of *A. thaliana*, as

well as amyrins and other triterpenoids and minor amounts of unknown wax components (Hegebarth and Jetter, 2017; Jenks *et al*., 1995).

1.5.1 Biosynthesis of Cuticular Waxes

The abundant wax components in *A. thaliana* wax are synthesized via the alcohol-forming pathway or the alkane-forming pathway by subsequent modification of fatty acid precursors. First, C_{16} and C_{18} fatty acids are synthesized *de novo* in the plastids and exported in the cytosol. Then the fatty acids are elongated to C_{20}-C_{34} very-long-chain fatty acids (VLCFAs) at the endoplasmic reticulum (ER). The elongation is catalyzed by the multi-enzyme complex fatty acid elongase. At the ER membrane, the VLCFAs are then further modified either by the alcohol-forming pathway (also termed acyl-reduction pathway) or by the alkane-forming pathway (also termed decarbonylation pathway).

The alcohol-forming pathway leads to the synthesis of primary alcohols and WEs. The first step is the reduction of very-long-chain acyl-CoAs (VLC acyl-CoAs) to primary alcohols, fatty acyl-CoA reductase FAR3/CER4 catalyzes this reaction in *A. thaliana*. Primary alcohols are then condensed with C_{16} fatty acyl-CoAs yielding WEs by WSD1 in *A. thaliana*. The alkane-forming pathway leads to the synthesis of aldehydes, alkanes, secondary alcohols and ketones. VLC acyl-CoAs are thought to be converted by a multiprotein enzyme complex in a two-step reaction over aldehydes into alkanes, in *A. thaliana*, CER3/WAX2/YRE and CER1 are involved in these reactions, CER3/WAX2/YRE as aldehyde-generating enzyme and CER1 as aldehyde decarbonylase with CYTB5s supporting the redox reaction (Bernard *et al*., 2012). Alkanes are then further modified into secondary alcohols and ketones, in *A. thaliana* both reactions are catalyzed by the midchain alkane hydroxylase MAH1 (Lee and Suh, 2013). The other WS/DGAT homologs from *A. thaliana*, WSD2 - WSD11 might contribute also via the alcohol forming pathway to the synthesis of WEs.

1.6 Analysis of WEs

WEs can be analyzed by gas chromatography (GC) coupled with a flame ionization detector (FID). Here, intact wax ester species are separated by GC using high temperature-stable GC capillaries which are necessary due to the low volatility of wax esters. With GC-FID, different WE chain lengths can be separated and quantified, however, the species composition of WEs in one chain length cannot be identified by this method. The hydrolysis and derivatization of WEs prior to GC-FID analysis leads to the identification of the fatty acyl and fatty alcohol moieties but the information on the intact WE species is lost.

By chromatographic separation via GC or high performance liquid chromatography (HPLC) coupled with mass spectrometry (MS), WE species can be identified. First, intact WEs are

separated by their chain lengths, afterwards WEs are released into the mass spectrometer and fragmented. Diagnostic fragments are detected and thus the wax ester species identified.
Vrkoslav *et al.* (2010) and Iven *et al.* (2013) analyzed the fragmentation pattern of WEs in detail. According to them, after fragmentation of the ammonium adduct of the WE molecule, a typical diagnostic ion of a saturated WE species is the protonated fatty acid $[RCO_2H_2]^+$. With increasing degree of unsaturation in the alcohol moiety of the WE while the fatty acid moiety remains saturated, other fragments besides the most abundant protonated fatty acid fragment $[RCO_2H_2]^+$ appear: the fatty acylium ion $[RCO]^+$ and furthermore, in WE with three double bonds in the alcohol moiety, the alcohol specific fragment $[R']^+$ are here the most abundant fragments (see also Figure 3 in Iven *et al.*, 2013). For WEs with unsaturated fatty acid moieties and saturated alcohol moieties, the fatty acylium ion $[RCO]^+$ and the dehydrated acylium ion $[RCO\text{-}H_2O]^+$ appear in high intensities with the fragment $[RCO]^+$ being most abundant in WEs with three double bonds in the fatty acid moieties (Iven *et al*., 2013). Polyunsaturated WEs with two or more double bonds in the alcohol moiety and one or more double bonds in the fatty acid moiety exhibit a variety of fragments, according to Iven and coworkers the fatty acylium ion $[RCO]^+$ is the most abundant. In *A. thaliana*, only the natural occurrence of saturated WEs have been described so far and therefore, the focus in this work lays on the analysis of saturated WEs.
In this study, WEs are analyzed by MS/MS experiments using a quadrupole time-of-flight mass spectrometer (Q-TOF MS). The WEs are infused into the mass spectrometer as ammonium adducts $[M+NH_4]^+$ and then selected WEs are fragmented. The typical product ion of a saturated WE, the protonated fatty acid $[RCO_2H_2]^+$ served as diagnostic ion for the qualitative and quantitative analysis of the molecular WE species. In Figure 22, the fragmentation pattern of the saturated WE standard 18:0ol/17:0 used in this study is depicted.

1.7 Water Stress

Drought and salt stress are major abiotic stresses to which plants are exposed. Plants respond to the stress exposure by versatile adaptation mechanisms, general adaptive responses to water stress are ion and osmotic homeostasis, stress damage control and growth control (Zhu, 2003; Xiong *et al.*, 2002). After reception of the stress signal, intracellular signaling cascades are started by the cytosolic increase in Ca^{2+} ions and by other signaling molecules like the phytohormone abscisic acid (ABA) whose synthesis is also upregulated as a response to water stress. Protein phosphorylation cascades are started and regulation of gene expression in response to the exposed stress is induced by the activation of transcription factors. One transcription factor activated by ABA is MYB96 which induces the expression of numerous genes involved in cuticular wax biosynthesis, among those also the expression of the wax ester synthase WSD1 is induced (Seo *et al*., 2009; Seo *et al*., 2011). As described above, the cuticle with its embedded and

overlaying epicuticular waxes plays an important role as barrier against water loss in nonstomatal tissue. In response to water stress, the cuticular wax load increases and minimizes further water loss (Gonzáles and Ayerbe, 2010; Sheperd and Wynne Griffiths, 2006; Wang *et al*., 2012). One of the increasing cuticular wax components synthesized as a response to water stress are WEs (Larsson and Svenningsson, 1986; Wang *et al*., 2012).

1.8 *Hordeum vulgare* – Cuticular Wax Composition and Changes in Response to Drought

Barley (*Hordeum vulgare*) belongs to the family of Poaceae and is an important crop plant cultivated in temperate regions all over the world. The crop is used for instance for brewery and serves as nutrition for humans and as animal food. Barley is diploid in contrast to other members of the Poaceae family like the polyploid rye and wheat and therefore well suited for genetic analysis. The barley genome comprises approx. 5.3 Gbps distributed on 7 chromosomes on which 39.809 coding genes are encoded (according to http://plants.ensembl.org/Hordeum_vulgare/Info/Annotation/).

The cuticular wax on the primary leaf of barley is mainly composed of primary alcohols (around 80 % of the total leaf cuticular wax), residual wax components are constituted mainly by WEs (4.2 – 9.3 % depending on the cultivar), aldehydes and free fatty acids. Alkanes are rare in leaf wax (around 1 %) (Larsson and Svenningsson, 1986) which is in contrast to *A. thaliana* where alkanes constitute the major wax component as described above. WE species in barley range from C_{38} – C_{52} chain lengths with C_{42}, C_{44}, C_{46} and C_{48} being the major WE chain lengths. Exposure to water deficit causes a strong increase in WEs in the cuticular leaf wax (from 4.2 – 9.3 % in the unstressed cultivars to 6.3 – 17.2 % in the stressed cultivars) while the amount of primary alcohols or aldehydes remained unaffected or even decreased upon the stress exposure (Larsson and Svenningsson, 1986). For genetic studies related wax biosynthesis, many mutants exhibiting little or no wax on single plant organs or the entire plant have been generated in different plant species. Wax-deficient mutants from *Arabidopsis* and barley are termed *eceriferum* (*cer*) mutants (from Latin: cera = wax, ferre = bear), 85 *cer* loci have been identified so far in barley (Lundqvist and Wettstein, 1962; Kunst and Samuels, 2003).

1.9 Objectives

Wax esters (WEs) are widely distributed in nature and occur among others in mammals, birds, insects, prokaryotes and plants. In plants, WEs are mainly found in the cuticle which covers the aerial surface of the primary plant tissues. The cuticle functions as a barrier of the plant against its environment and is thereby involved in responses of the plant to environmental conditions like drought. The increase in WEs in the cuticle has been described to be involved in the response to

drought stress (Larsson and Svenningsson, 1986; Patwari *et al*., 2019). Besides the jojoba wax ester synthase type, another type of wax ester synthase has been detected in plants which is the WS/DGAT type. WS/DGAT was named after the wax ester synthase (WS) and acyl-CoA:diacylglycerol acyltransferase (DGAT) activity detected for the first described WS/DGAT from *Acinetobacter baylyi* ADP1 (formerly *A. calcoaceticus* ADP1, Vaneechoutte *et al*., 2006) (Kalscheuer and Steinbüchel, 2003). In *Arabidopsis thaliana*, 11 WS/DGAT homologs are known and designated WSD1 - WSD11. WSD1 contributes WEs to the surface wax of stem (Li *et al*., 2008) and *wsd11* mutants show a folded petal phenotype (Takeda *et al*., 2013). However, little was known about the functions of WSD11 and the other WSD proteins.

The aim of this work is to characterize the WS/DGAT homologs WSD1 - WSD11 from *A. thaliana* with the focus on WSD2 – WSD11, since WSD1 was extensively described by Li *et al.*, 2008. To this end, numerous *Arabidopsis wsd* mutant lines will be genotyped and homozygous *wsd* mutants will be investigated regarding the composition and amount of WEs on the surface wax of stem, flower and siliques and compared to the respective WT ecotypes. Furthermore, *WSD* gene expression analysis will be performed for the plant organs stem, leaf, root, inflorescence and silique derived from plants grown under optimal growth conditions and for leaf and root derived from plants exposed to drought, abscisic acid (ABA) and salt treatment. Heterologous expression studies in *Saccharomyces cerevisiae* will be performed for WSD1 and expression constructs of the other *WSD* genes except *WSD3* and *WSD10* will be cloned. The cloning of the constructs will include the generation of cDNA of *WSD3* and *WSD10* from inflorescence and root tissue. Furthermore, subcellular localization will be investigated for WSD3, WSD4 and WSD9 by expressing fusion constructs with eGFP in *Nicotiana benthamiana* leaves. In addition to *A. thaliana*, the crop *Hordeum vulgare* will be analyzed regarding WE amount and composition in leaf surface wax of plants exposed to optimal growth conditions and to drought stress.

2 Materials and Methods

2.1 Equipment

6530 Accurate Mass Quadrupole Time-of-Flight (Q-TOF) Liquid Chromatography/Mass Spectrometry	Agilent, Böblingen, Germany
Araponics for hydroponic cultivation	Araponics SA, Liège, Belgium
7890 Gas Chromatograph with Flame Ionization Detector (GC-FID)	Agilent, Böblingen, Germany
Heating block	Bioer, Hangzhou, China
Incubation Shaker Multitron 28570	INFORS HT, Einsbach, Germany
Laser Scanning Microscope LSM 780	Zeiss, Jena, Germany Device of Prof. Dr. Andreas Meyer, INRES institute, University Bonn, Germany
Light microscope BH2	Olympus, Hamburg, Germany
Microcentrifuge 5417R	Eppendorf, Hamburg, Germany
MicroPulser™ electroporator	Biorad Laboratories GmbH, München, Germany
Phytochamber SIMATIC OP17	York International, York, USA
Precellys® 24 homogenizer	PeQlab, Erlangen, Germany
Spectrophotometer Nanodrop 1000	PeQlab, Erlangen, Germany
Sterile bench model 1.8	Holten LaminAir, Allerød, Danmark
Table top centrifuge 5810R	Eppendorf, Hamburg, Germany
Thermocycler TPersonal	Biometra, Göttingen, Germany
Ultracentrifuge	Beckman Coulter, Krefeld, Germany
Vortex Certomat® MV	Braun, Melsungen, Germany
Water bath	Köttermann, Uetze, Germany

2.2 Materials

2.2.1 Consumables

Glass tubes threaded, 8 ml	VWR, Darmstadt, Germany
Pasteur pipettes (glass)	Brand, Wertheim, Germany
Pots and trays for plant cultivation	Pöppelmann, Lohne, Germany
PTFE Screw caps for 8 ml glass tubes	Schott, Mainz, Germany
Soil Einheitserde Classic VE type “Topf”	Rolfs, Siegburg, Germany
SPE columns Strata Si-1 silica, 55 µm, 70 Å (500 mg/6 ml and 100 mg/1 ml)	Macherey and Nagel, Düren, Germany

Teflon septa for screw caps	Schmidlin, Neuheim, Switzerland
TLC plates Silica 60 Durasil	Macherey and Nagel, Düren, Germany
Vermiculite	Rolfs, Siegburg, Germany

2.2.2 Chemicals

Abscisic acid (ABA), Product 51010	Precision Biochemicals, Canada (obtained from Prof. Dr. Dorothea Bartels, IMBIO, University Bonn, Germany)
Acetosyringone	Sigma-Aldrich, Taufkirchen, Germany
Adenine	Merck, Darmstadt, Germany
Agarose	PeQlab, Erlangen, Germany
Ammonium acetate	Sigma-Aldrich, Taufkirchen, Germany
Ammonium nitrate	AppliChem, Darmstadt, Germany
Bacto™ Agar	Becton Dickinson GmbH, Heidelberg, Germany
Bacto™ Peptone	Becton Dickinson GmbH, Heidelberg, Germany
Bicinchoninic acid solution (BCA)	Sigma-Aldrich, Taufkirchen, Germany
Boric acid	Thermo Fisher Scientific, Karlsruhe, Germany
Calcium nitrate	Sigma-Aldrich, Taufkirchen, Germany
Cetyl trimethylammonium bromide (CTAB)	AppliChem, Darmstadt, Germany
Chloroform	Merck, Darmstadt, Germany
Citric acid	Sigma-Aldrich, Taufkirchen, Germany
Cobalt(II) chloride	Merck, Darmstadt, Germany
Copper(II) sulfate	Merck, Darmstadt, Germany
Diethyl ether	AppliChem, Darmstadt, Germany
Difco Yeast Nitrogen Base w/o Amino Acids	Becton Dickinson GmbH, Heidelberg, Germany
Ethanol 99% denatured, technical grade	AppliChem, Darmstadt, Germany
Ethidium bromide	Roth, Karlsruhe, Germany
Ethylenediaminetetraacetate (EDTA)	Roth, Karlsruhe, Germany
Fe-EDTA	Sigma-Aldrich, Taufkirchen, Germany
Formaldehyde	AppliChem, Darmstadt, Germany
Formic Acid	Sigma-Aldrich, Taufkirchen, Germany
D-(+)Galactose	Sigma-Aldrich, Taufkirchen, Germany

α-D(+)Glucose	Sigma-Aldrich, Taufkirchen, Germany
Glycerol	AppliChem, Darmstadt, Germany
Heptadecanoic acid (17:0)	Sigma-Aldrich, Taufkirchen, Germany
Heptacosanoic acid (27:0)	Sigma-Aldrich, Taufkirchen, Germany
n-Hexane	Merck, Darmstadt, Germany
Isoamyl alcohol	Sigma-Aldrich, Taufkirchen, Germany
Lauroylsarcosine-sodium-salt	Sigma-Aldrich, Darmstadt, Germany
Lithium chloride	AppliChem, Darmstadt, Germany
Magnesium chloride	AppliChem, Darmstadt, Germany
Magnesium sulfate	AppliChem, Darmstadt, Germany
Manganese(II) chloride	AppliChem, Darmstadt, Germany
Methanol	VWR, Darmstadt, Germany
2-Mercaptoethanol	AppliChem, Darmstadt, Germany
3-(*N*-morpholino)propanesulfonic acid (MOPS)	AppliChem, Darmstadt, Germany
Murashige & Skoog Medium, including Vitamins	Duchefa Biochemie, Haarlem, the Netherlands
1-Octadecanol (18:0ol)	Sigma-Aldrich, Taufkirchen, Germany
Oxalyl chloride	Sigma-Aldrich, Taufkirchen, Germany
Peptone	ForMedium, Norfolk, United Kingdom
Phyto agar	Duchefa Biochemie, Haarlem, the Netherlands
Pyridine dried	AppliChem, Darmstadt, Germany
Potassium chloride	Merck, Darmstadt, Germany
Potassium nitrate	Grüssing, Filsum, Germany
Potassium hydrogen phosphate	Roth, Karlsruhe, Germany
D(+)-Raffinose	AppliChem, Darmstadt, Germany
Roti®-Phenol	Roth, Karlsruhe, Germany
Sodium acetate, anhydrous	Sigma-Aldrich, Taufkirchen, Germany
Sodium chloride	Duchefa Biochemie, Haarlem, the Netherlands
Sodium dodecyl sulfate (SDS)	AppliChem, Darmstadt, Germany
Sodium molybdate	Merck, Darmstadt, Germany
D(-)-Sorbitol pure (Ph. Eur., NF)	AppliChem, Darmstadt, Germany
Sucrose	Duchefa Biochemie, Haarlem, the Netherlands

Toluene	VWR, Darmstadt, Germany
Tris-(hydroxymethyl)-aminomethane	Duchefa Biochemie, Haarlem, the Netherlands
Triton® X 100	Roth, Karlsruhe, Germany
Tryptone	AppliChem, Darmstadt, Germany
Yeast extract	DuChefa Biochemie, Haarlem, the Netherlands
Zinc sulfate	Merck, Darmstadt, Germany

Amino Acids

L-Arginine, L-lysine, L-methionine, L-phenylalanine, L-tyrosine and L-valine were purchased from DuChefa Biochemie, Haarlem, the Netherlands. L-Aspartic acid, L-glutamic acid, L-histidine and L-leucine were purchased from Sigma-Aldrich, Taufkirchen, Germany. L-Threonine was bought from Carl Roth, Karlsruhe, Germany. L-Tryptophan was purchased from AppliChem, Darmstadt, Germany.

2.2.3 Antibiotics

All antibiotics used in this study were purchased from Duchefa Biochemie, Haarlem, the Netherlands.

2.2.4 Kits and Enzymes

Ambion TURBO DNA-*free*™ kit	Thermo Fisher Scientific, Karlsruhe, Germany
CloneJET PCR Cloning Kit	Thermo Fisher Scientific, Karlsruhe, Germany
DCSPol DNA Polymerase	DNA Cloning Service, Hamburg, Germany
First Strand cDNA Synthesis Kit	Fermentas, St. Leon-Rot, Germany
High Speed Plasmid Mini Kit	DNA Cloning Service, Hamburg, Germany
MinElute Gel Extraction Kit	Qiagen, Hilden, Germany
Pfu DNA Polymerase	Thermo Fisher Scientific, Karlsruhe, Germany
T_4 DNA Ligase	Fermentas, St. Leon-Rot, Germany
Zymoprep Yeast Plasmid Miniprep™ I	Zymo Research Products, Freiburg, Germany

All restriction endonucleases used in this study were purchased from Thermo Scientific or New England Biolabs.

2.2.5 Internal Standard for Lipid Quantification

Mixture of 18:0ol/17:0 (1 nmol/50 µl) and 18:0ol/27:0 (3 nmol/50 µl) wax esters dissolved in chloroform. As explained in 3.8.3, only the 18:0ol/17:0 wax ester was used for quantification.

2.2.6 Plants

Arabidopsis thaliana Columbia 0 (Col-0)

Arabidopsis thaliana Landsberg erecta (Ler)

Arabidopsis thaliana Nossen (No-0)

Hordeum vulgare cv. Barke

Nicotiana benthamiana

Table 1: *Arabidopsis* Mutant Lines Used in this Study.

Genotype	Ecotype	Gene	Stock Center Code	Origin	Seed Stock (Acyltransferase box number/ label on the cap)
wsd1(Li *et al.*, 2008)	Col-0	At5g37300	SALK_067714 (AR), N567714	NASC	VII / 1
wsd2-1	Col-0	At1g72110	GK-761F11, N473031	NASC	VII / 6
wsd2-2	Ler	At1g72110	GT_5_77861, N162325	NASC	VII / 11
wsd3-1	Col-0	At2g38995	SALK_069403C, N657666	NASC	VII / 16
wsd3-2	Col-0	At2g38995	SALK_084218 (BA), N584218	NASC	VII / 21
wsd4-1	Col-0	At3g49190	SALK_006729C, N665183	NASC	VII / 35
wsd4-2	Col-0	At3g49190	SALK_080002, N580002	NASC	VII / 26
wsd5	Col-0	At3g49200	SAIL_607_H05, N826007	NASC	VII / 36
wsd6-1	Col-0	At3g49210	SAIL_1257_G12, N846506	NASC	VII / 41
wsd6-2	Col-0	At3g49210	SALK_130459, N630459	NASC	VII / 46
wsd7-1	Col-0	At5g12420	SALK_062207 N562207	NASC	VII / 56
wsd7-2	Col-0	At5g12420	SALK_028121, N528121	NASC	VII / 51
wsd8-1	Col-3	At5g16350	SAIL_213_D06, N809938	NASC	VII / 70
wsd8-2	Col-0	At5g16350	SALK_011026, N511026	NASC	VII / 61
wsd9-1	Col-0	At5g22490	SM_3_34439, N121150	NASC	VII / 76
wsd9-2	Col-0	At5g22490	SM_3.34454, N121165	NASC	VII / 71
wsd10-1	No-0	At5g53380	RATM15-3267-1_H (pst18787)	Riken	VII / 81

wsd10-2	No-0	At5g53380	RATM53-3039-1_H (pst00785)	Riken	VIII / 5
wsd11 (Takeda *et al*., 2013)	Col-0	At5g53390	SALK_137481C, N660206	NASC	VIII / 10
wsd1 x wsd4 (double homozygous)[a]	Col-0		SALK_080002 x SALK_067714		VIII / 15

Homozygous seeds were identified in the progeny of the original mutant line ordered from the stock center and were bulked by harvesting seeds of a single plant. The seeds are stored in glass vials. *Arabidopsis thaliana* ecotypes Landsberg (Ler), Nossen (No-0) and Columbia (Col-0) were used as controls.
NASC, Nottingham Arabidopsis Stock Centre (http://arabidopsis.info/)
Riken, Riken BRC Experimental Plant Division (http://epd.brc.riken.jp/en/seed)
[a] Seeds harvested from crossed parent plants were obtained from Dr. Felix Lippold, University of Bonn, now: Aevotis GmbH, Potsdam, Germany.

2.2.7 Bacteria and Fungi

Table 2: Microorganisms Used in this Study.

Organisms	Strain	Specification	Reference
E. coli	ElectroSHOX	Electrocompetent cells	Bioline
E. coli	*XL10-Gold® ultracompetent cells*	Electrocompetent cells	Agilent Technologies
A. tumefaciens	GV3101-pMP90	Electrocompetent cells	DNA cloning service, Hamburg
S. cerevisiae	H1246 (glycerol stocks bn31 and bn508)	Electrocompetent cells	Dr. Sten Stymne, Department of Plant Breeding and Biotechnology, Alnarp, Sweden Sandager *et al.* (2002)

2.2.8 Vectors and Recombinant Plasmids

Table 3: Cloning Vectors.

Vector	Selection Marker	Reference
pJET1.2/blunt	Amp^R	Thermo Fisher Scientific
pGEM-T	Amp^R	Promega
pLGCSATRNAi (modified pLH9000)	Sm/Sp^R (bacteria), Kan^R (plants)	Dr. Georg Hölzl, IMBIO, University of Bonn, Germany
pDR196	Amp^R (bacteria), URA3 (yeast)	Rentsch *et al*., 1995
pYES2	Amp^R (bacteria), URA3 (yeast)	Thermo Fisher Scientific
pESC-URA[a]	Amp^R (bacteria), URA3 (yeast)	Agilent Genomics

[a] the vector was kindly provided by Prof. Dr. Ljerka Kunst, University of British Columbia, Vancouver, British Columbia, Canada.

Table 4: Recombinant Plasmids.

Construct (Stock Number)	Specification	Recipient Species
pL-35S-*WSD3-eGFP*	Expression in *N. benthamiana*	*A. tumefaciens* GV3101-pMP90
pL-35S-*eGFP-WSD4* (bn616)	Expression in *N. benthamiana*	*A. tumefaciens* GV3101-pMP90
pL-35S-*eGFP-WSD9*	Expression in *N. benthamiana*	*A. tumefaciens* GV3101-pMP90
pCB-*DsRed*-ER (HDEL)[a] (bn545)	Expression in *N. benthamiana*	*A. tumefaciens* GV3101
pDR196-*WSD1* (bn459)	Expression in yeast	*S. cerevisiae* H1246
pYES2-*WSD1* [b] (PD812)	Expression in yeast	*S. cerevisiae* H1246
pESC-URA-*WSD1*[c] (bn556)	Expression in yeast	*S. cerevisiae* H1246
pESC-URA-*MaFAR* (bn557)	Expression in yeast	*S. cerevisiae* H1246
pESC-URA-*MaFAR-WSD1*	Expression in yeast	*S. cerevisiae* H1246

[a] A clone was kindly given by Dr. Boris Voigt, University of Bonn, Germany and employed as ER marker for subcellular localization studies of the *WSD* genes.
[b] The construct was cloned by Dr. Antje Lohmann, MPI Golm, now: Merck KGaA, Darmstadt, Germany.
[c] WSD1 cDNA was kindly given by Prof. Dr. Ljerka Kunst, University of British Columbia, Vancouver, British Columbia, Canada.
Further cloned constructs are listed in Table 11 in the Appendix.

2.3 Methods

2.3.1 Molecular Cloning Techniques

2.3.1.1 Polymerase Chain Reaction (PCR)

PCR was performed with *Pfu* DNA polymerase if high accuracy was necessary, e. g., for cloning. Due to its 5' → 3' exonuclease proofreading activity, the *Pfu* DNA polymerase exhibits a low error rate and therefore amplifies highly accurate products from DNA templates. A typical PCR reaction contained 1 x concentrated *Pfu* buffer with $MgSO_4$, 0.2 mM of dNTP mix, 1 µl of 10 µM forward primer, 1 µl of 10 µM reverse primer, 1 ng – 1 µg of template DNA, and 1.25 u of *Pfu* DNA Polymerase (2.5 U/1 µl), ddH_2O was added to a final volume of 50 µl.

Cycle step	Temperature, °C	Time	Number of cycles
1) Initial denaturation	95	2 min	1
2) Denaturation	95	30 s	
3) Annealing	Tm-5	30 s	30-40 (cycle step 2 to 4)
4) Extension	72	2 min / kb	
5) Final extension	72	10 min	1
6) Hold	4	∞	1

Tm-5 means melting temperature (Tm) of the primers minus 5 °C.

2.3.1.2 Agarose Gel Electrophoresis

Prior to the ligation, DNA fragments were separated from interfering salts and DNA fragments of other sizes to improve the ligation efficiency and to control the size of the expected DNA molecule. To this end, agarose gel electrophoresis was applied. DNA samples were mixed with 6 x loading dye to reach a 1 x dye concentration. The agarose gel consisted of 1 % agarose boiled in 1 x TAE buffer. Prior to pouring the agarose into the gel carrier, 5 µg/ml ethidium bromide (stock solution: 1 mg/ml in ddH_2O) was added to the agarose gel. After the agarose gel became solid, it was placed into the gel chamber and submerged in 1 x TAE buffer. To determine the DNA fragment sizes, 0.5-1 µl of GeneRuler™ 1 kb DNA ladder was pipetted into another gel slot. To separate the DNA fragments, a voltage of 120 V was applied to the gel for 20 minutes. The separated DNA fragments were visualized by UV light λ= 302 nm.

For the purification of DNA molecules, a gel slice containing the desired DNA fragment was cut from the gel. The elution of the DNA out of the gel was performed with the MinElute Gel Extraction Kit, according to the manufacturer's protocol. The last step of the protocol was modified by using 30 µl ddH_2O to elute the DNA from the columns.

6 x loading dye	50 x TAE Buffer
10 mM Tris, pH 7.6 adjusted with HCl	2 M Tris base
0.03 % (w/v) bromophenol blue	2 M glacial acetic acid
0.03 % (w/v) xylene cyanol FF	50 mM EDTA pH 8.0 adjusted with HCl
60 % (v/v) glycerol	

2.3.1.3 Ligation

Gel-purified DNA fragments and linearized vectors with compatible ends were ligated by applying a vector:insert ratio of 1:3 to 1:5. Blunt-end inserts as products of *Pfu* DNA Polymerase PCRs were ligated with blunt-end pJET1.2/blunt vectors. The inserts of the plasmids were sequenced on one strand and employed for preparative digestion. Sticky-end inserts as products of digestion by different restriction endonucleases were ligated with the target vectors using compatible sticky ends. The desired 1:3 to 1:5 ratio was applied after evaluation of the DNA concentration on a gel by comparing fluorescence intensities or by measuring the DNA concentration in a photometer.
A typical ligation reaction contained the following components: DNA insert and DNA vector (up to 100 ng) in a molar ratio of 3:1 to 5:1, 1 x T4 DNA ligase buffer and 0.5 U of T4 DNA ligase. The ligation mixture was normally filled up with ddH_2O to a final volume of 10 µl. The ligation reaction was carefully mixed and then incubated either at room temperature for 30 min or overnight at 4 °C.

2.3.1.4 Desalting of the Ligated DNA Prior to Transformation

Prior to transformation by an electric shock, the ligation reaction was desalted. This was achieved by pipetting the DNA sample onto a filter membrane laying on the surface of H_2O. After 30 min to 2 h of dialysis, the DNA was desalted and was ready for transformation. Alternatively, DNA was precipitated with sodium acetate and ethanol. In this method, 1 volume of DNA sample was mixed with 2.5 volumes of absolute ethanol and 1/10 volumes of 3 M sodium acetate. The mixture was then cooled at -20 °C for half an hour. Afterwards, the sample was centrifuged at 18000 x g at 4°C for 20 min. The supernatant was removed and the DNA pellet was washed once with ice-cold 75 % ethanol (in ddH_2O). After another centrifugation step and removal of the supernatant, the DNA was dried and dissolved in ddH_2O.

2.3.1.5 Restriction of DNA by Endonucleases

The DNA was digested prior to ligation or for the verification of the identity of DNA constructs. A standard digestion contained 1 x concentrated buffer, 0.01 – 1 µg DNA, 0.1 to 0.5 U enzyme and was filled up with ddH_2O to the appropriate volume. The digestion was performed at 37 °C for

30 – 120 min. The manufacturers of the enzymes and buffers were Thermo Scientific or New England Biolabs.

2.3.1.6 Cloning of DNA constructs

Constructs for Subcellular Localization of WSD Proteins

The *WSD* cDNAs (except for *WSD1* and *WSD11* since for both proteins the subcellular localizations were published by Li *et al*., 2008 and Takeda *et al*., 2013) and *eGFP* were amplified with primers listed in the Appendix in Table 10. For *WSD3*, the cDNA of splice variant 1 (Figure 16) was amplified. The amplified DNA was subcloned into pJET1.2/blunt, sequenced on one strand, digested with the respective restriction enzymes (Appendix Table 10). For the pL-35S-*eGFP*-*WSD4* construct, the digested and purified *WSD4* and *eGFP* DNAs were ligated in one ligation reaction with a modified pLH9000 vector designated as pLHGCSATRNAi (Dr. Georg Hölzl, IMBIO, University Bonn, Germany; vector map see Figure 46 in the Appendix). The fused cDNA was driven by a 35S promoter and terminated by an OCS terminator. For the pL-35S-*eGFP*-*WSD9* construct, the pL-35S-*eGFP*-*WSD4* construct was digested with *Bam*HI and *Sal*I to remove *WSD4* and afterwards ligated with *WSD9*. Same was done with the construct pL-35S-*WSD3*-*eGFP* by using the restriction sites from *Spe*I and *Bam*HI for *WSD3*, *Bam*HI and *Sal*I for *eGFP* and *Spe*I and *Sal*I for the modified pLH9000.

Constructs for Heterologous Expression of WSD Genes in Yeast

The *WSD* (except *WSD3* and *WSD10*) and *MaFAR* DNAs were amplified with primers (Appendix Table 11), subcloned in pJET1.2/blunt, sequenced on one strand and then digested with respective restriction enzymes (Appendix Table 11). The *WSD* DNAs were then ligated with pDR196 digested with the appropriate restriction enzymes (Appendix in Table 11). *WSD1* (the construct pESC-TRP-*WSD1* was obtained from Prof Dr. Ljerka Kunst, University of British Columbia, Vancouver, British Columbia, Canada) was further ligated into pESC-URA, both digested with *Bam*HI and *Xho*I. *MaFAR* was either inserted in pESC-URA alone or into pESC-URA-*WSD1* by using the restriction sites of *Spe*I and *Pac*I (Appendix Table 11).

2.3.2 Extraction of Genomic DNA from Plant Tissue

For the analysis of plant genotypes, genomic DNA was isolated as template for PCRs. For this purpose, 2 ml reaction tubes were filled to one tenth of the volume with ceramic beads. One leaf per plant was cut and placed into the reaction tube, the lid and the plant were labeled in the same manner. The samples were flash frozen in liquid nitrogen and the leaf was homogenized at 6000 rpm for 30 s using the Precellys homogenizer. Afterwards the samples were flash frozen again before 500 µl of CTAB buffer was added to each sample. An incubation time at 65 °C for 10 min followed. The samples were cooled down to room temperature. 0.2 ml of chloroform was

added to each sample, then the samples were vortexed and centrifuged for 2 min at 18000 x g at room temperature. The upper phases were transferred into fresh tubes each containing 0.35 ml of isopropanol. After vortexing, the samples were incubated on ice for 2 min. The DNA was precipitated by centrifugation at 18000 x g for 3 min. The supernatants were discarded and the DNA pellets were washed with 500 µl of 75 % (v/v) ethanol. After another centrifugation step, the supernatants were carefully removed with a pipette leaving behind the loose DNA precipitates. The DNA pellets were dried at room temperature until no droplets were visible and then dissolved in 60 µl of ddH_2O containing 0.5 µl of RNase A (10 µg/ml). The DNA extracts were stored at – 20 °C until used.

CTAB buffer
140 mM sorbitol
220 mM Tris-HCl, pH 8
22 mM EDTA
800 mM NaCl
1 % (w/v) *N*-Lauroylsarcosine sodium salt
0.8 % CTAB

2.3.3 Genotyping of Plants by PCR

A. thaliana T-DNA and transposon insertion lines whose genotypes were not known were analyzed by PCR. Several seeds of each mutant line were sown on soil, the seedlings singularized and a few weeks later, DNA of the leaves from each labeled plantlet was extracted (see 2.3.2). These DNA samples were used as templates for PCRs which should reveal the genotype of the respective plant. In a first step, PCRs with a three primer system (two primers annealing to wild type sequences around the insertion site, one primer annealing to the border of the inserted T-DNA / transposon DNA) were performed with all isolated DNA templates of the mutants and with wild type DNA template as control. Those mutants appearing homozygous for the mutation were again checked, this time by PCRs using two primers annealing only to wild type sequences. Again control PCRs with wild type DNA were also performed. The analyzed mutant lines are listed in Table 1 and the appropriate primers used for the PCRs are listed in Appendix Table 6. For the PCRs, DCSPol DNA polymerase (a modified DNA polymerase from *Thermus aquaticus*) was employed using a protocol as described below.

PCR reaction mix

39 µl ddH_2O

4 µl 10 x Buffer B

3 µl 25 mM $MgCl_2$

0.5 µl 2 mM dNTP mix

1 µl 10 µM forward primer

1 µl 10 µM reverse primer

1 µl 10 µM border primer

1 µl genomic plant DNA (5 – 1000 ng)

0.5 µl DCSPol DNA Polymerase (5 U/µl)

PCR program

Cycle step	Temperature, °C	Time	Number of cycles
1) Initial denaturation	95	3 min	1
2) Denaturation	95	30 sec	
3) Annealing	Tm-5	30 sec	30-40 (cycle step 2 to 4)
4) Extension	72	1 min / kb	
5) Final extension	72	10 min	1
6) Hold	4	∞	1

Tm-5 means melting temperature (Tm) of the primers minus 5 °C.

2.3.4 cDNA Synthesis and Semi-Quantitative Reverse Transcription PCR

2.3.4.1 Extraction of RNA from Plant Tissue

For gene expression studies, RNA was extracted from diverse plant tissues including roots, stems, leaves, inflorescences and siliques of *A. thaliana* Col-0 wild type grown under normal conditions or exposed to drought or drought stress mimicking conditions (see 2.3.8.2).

For the RNA extraction procedure, only clean sterile tips and reaction tubes were used. To inactivate RNases, ddH_2O was mixed with 0.1 % (v/v) DEPC for 10 min by shaking and then incubated at 37 °C overnight. Afterwards it was autoclaved twice.

2 ml reaction tubes were filled to one tenth with ceramic beads. The plant tissue was cut and placed into the reaction tube, then the sample was immediately flash frozen in liquid nitrogen. Roots were taken from plants growing in hydroponic cultures (see 2.3.8.2). The root samples were shortly dried after cutting by placing the tissue on a paper towel. All other tissues were taken from plants growing on soil. Inflorescences included floral buds and opened flowers, but no siliques in early stages of development. Siliques were harvested when they had reached mature size (about 1 cm) but were still green. Stem segments were cut from the lower one third of the stem. The

tissue samples were homogenized at 6500 rpm for 30 sec using the Precellys homogenizer. For firm tissue like stem or silique tissue, the homogenization step was repeated several times with intermediate flash freezing in liquid nitrogen. 0.5 ml of REB buffer and 0.5 ml of phenol:chloroform:isoamyl alcohol 25:24:1 (v/v/v) were added into the reaction tubes. The samples were vortexed and incubated at room temperature for 5 min. A phase separation was achieved by a centrifugation at 18000 x g for 5 min at 4 °C. The upper aqueous phases were transferred into fresh tubes and re-extracted with 0.4 ml of phenol:chloroform:isoamyl alcohol 25:24:1 (v/v/v) each. Phase separations were achieved by another centrifugation step. The upper phases were again transferred into fresh tubes and re-extracted with 0.4 ml of chloroform each. After another centrifugation step and another transfer of the aqueous phases into fresh tubes, the samples were mixed with 8 M LiCl (DEPC treated) to final concentrations of 2 M LiCl. The samples were incubated overnight at – 20 °C. The next day, the samples were centrifuged at 18000 x g and 4 °C for 15 min. The supernatants were discarded and the RNA pellets were rinsed with 500 µl of precooled 2 M LiCl (DEPC treated) each. After another centrifugation step and removal of the supernatants, the RNA pellets were washed with 70 % (v/v) ethanol in DEPC treated ddH_2O. The samples were incubated at – 20 °C for 10 min. Afterwards they were centrifuged at 18000 x g and 4 °C for 10 min. The supernatants were discarded and the residual droplets were carefully removed by pipetting. The RNA pellets were then dissolved in 50 µl of ddH_2O (DEPC treated).

<u>REB buffer</u>
25 mM Tris-HCl, pH 8.0
25 mM EDTA
75 mM NaCl
1 % (w/v) SDS
1mM 2-Mercaptoethanol (freshly added)

2.3.4.2 RNA Gel Electrophoresis

Before the extracted RNA was utilized for cDNA synthesis, its quantity and quality was analyzed by RNA gel electrophoresis. For this purpose, the RNA concentration was first measured with the Nanodrop photometer. For the RNA gel, the agarose was boiled with ddH_20 and MOPS buffer in the microwave. The dissolved agarose was cooled down for 5 min and the formaldehyde solution was added and mixed by swaying carefully. The melted agarose gel was then immediately poured into the gel carrier. For sample preparation, 50 ng of RNA in 10 µl of ddH_2O (DEPC treated) was mixed with 10 µl of RNA sample loading buffer. The mixture was incubated at 65 °C for 10 min and was then loaded into the slots of the gel. The gel electrophoresis was carried out for 30 – 60 min at 90 V. The RNA bands (with ethidium bromide) were visible under UV light (λ = 302 nm).

Only RNA samples with distinct separated ribosomal RNA bands were used for cDNA synthesis. RNA samples were stored at – 80 °C until used.

RNA gel	Gel buffer
1.5 % (w/v) agarose	1 x MOPS buffer pH 7
1 x MOPS buffer pH 8	10 % (v/v) formaldehyde
6 % (v/v) formaldehyde	

RNA sample loading buffer	10 x MOPS buffer
65 % (v/v) formamide	0.2 M MOPS
8 % (v/v) formaldehyde	50 mM sodium acetate
1 x MOPS pH 8	10 mM EDTA adjusted to pH 7 or pH 8 with NaOH
54 µg/ml ethidium bromide	

2.3.4.3 Removal of Genomic DNA

The extracted RNA could contain genomic DNA in low concentrations. After controlling the RNA quality by a RNA gel and prior to cDNA synthesis, the genomic DNA was digested. This was performed by using a "Turbo DNA-free kit" (Ambion) according to manufacturer's instructions. Afterwards, the RNA concentration and quality were analyzed again by measuring the absorption with the Nanodrop photometer and by electrophoresis in a second RNA gel. RNA samples with distinct bands were used for cDNA synthesis or stored at – 80 °C.

2.3.4.4 First Strand cDNA Synthesis

Due to the susceptibility of RNA to degradation, the RNA was transcribed into the complementary cDNA strand. 1.2 µg of RNA was employed for cDNA synthesis which was performed by using a "First Strand cDNA Synthesis Kit" (Fermentas) according to manufacturer's instructions. Oligo(dT) primers hybridizing to the poly(A) tail of mRNAs were applied for cDNA synthesis. cDNA samples were diluted with ddH_2O by 1:10 and stored at – 80 °C until used.

2.3.4.5 Semi-Quantitative Reverse Transcription PCR and Gradient PCR

For expression studies of the *WSD* genes in different plant organs and under drought stress and drought mimicking conditions, a semi-quantitative reverse transcription PCR (sqRT-PCR) was performed.

Prior to sqRT-PCR, a gradient PCR was performed for all genes involved to analyze the optimal annealing temperature. The optimal annealing temperature is important to assure high gene specificity of the primers. The gradient PCR components and program were used as described in

2.3.3, the annealing temperature was modified by using a temperature gradient from 55 °C to 68 °C. The highest annealing temperatures that still resulted in a PCR product were employed for sqRT-PCR. Optimal annealing temperatures for primers of *ACT2*, *rd29A* and *WSD* genes are listed in the Appendix Table 7.

ACT2 was chosen as the housekeeping gene. Therefore, PCRs for all tissue samples were first performed for *ACT2*, with different cDNA template volumes to obtain similar intensities for the gene for all samples that should be compared. Additionally, 27 to 30 PCR cycles were performed to ensure the linear increase in DNA products after each additional PCR cycle.

After these preliminary experiments, *ACT2* was amplified for all tissue samples in 29 cycles and volumes of 0.8 to 2.5 µl of cDNA tissue samples were employed. Residual differences in fluorescence intensities of *ACT2* bands on the gel were adjusted by pipetting different volumes of the PCR product on the gel. For example, the *WSD* gene expression study performed for different plant organs of *A. thaliana* wild type revealed slight differences of the fluorescence intensity on the gel of *ACT2* amplified from the silique cDNA compared with the fluorescence intensities of the other samples. To remove this difference, the following volumes of the PCR products for *ACT2* were pipetted onto the gel: root 7 µl, stem 7 µl, leaf 7 µl, inflorescence 7 µl and silique 9 µl. By pipetting these volumes, the *ACT2* bands fluoresced with same intensities on the gel. The pipetted volumes of the analyzed genes were proportionally related to the volumes used for *ACT2*, following volumes of PCR products were pipetted for all analyzed *WSD* genes onto the gel: root 15 µl, stem 15 µl, leaf 15 µl, inflorescence 15 µl and silique 19.2 µl (15 multiplied by 9/7).

The respective cDNA volume of a tissue sample used for *ACT2* was used for all analyzed genes. As a positive control for drought stress, a PCR for *rd29A* (a drought stress marker gene, see Yamaguchi-Shinozaki and Shinozaki, 1994) was performed. Additionally to the cDNA templates, genomic wild type DNA of *A. thaliana* was amplified to demonstrate the absence of genomic DNA in the cDNA samples (different sizes for most analyzed genes on the gel compared to amplified fragments obtained from cDNA templates). ddH_2O as template was used to confirm the absence of other templates than the cDNA template in the PCR reaction mix.

The sqRT-PCR was performed by pipetting 1 x concentrated buffer B, 1.9 mM $MgCl_2$, 0.1 mM dNTP mix, 1 µl of 10 µM forward primer, 1 µl of 10 µM reverse primer, 1 – 2.5 µl of template (cDNA, genomic DNA or ddH_2O), 2 U of DCSPol DNA Polymerase per sample and by adding ddH_2O to a total volume of 25 µl. Primers applied for sqRT-PCRs as well as the employed annealing temperatures are listed in the Appendix Table 7. The PCR program was used as described in 2.3.3, the number of cycles from denaturation to extension varied between 29 cycles for *ACT2*, 35 cycles for *rd29A* and 38 cycles for the *WSD* genes. sqRT-PCR products were mixed with 1x concentrated loading dye and separated by gel electrophoresis (see 2.3.1.2). The gene expression level in the different tissues revealed by the fluorescence intensity of the amplified DNA fragments on the gel was recorded.

2.3.5 Working with *Escherichia coli*

2.3.5.1 Cultivation of *E. coli*

Generally, *E. coli* cultures grew at 37 °C in liquid cultures under permanent shaking or on plates. Cultures were grown in LB medium. For selection, antibiotics in the following final concentrations were added to the medium: ampicillin 100 µg/ml, carbenicillin 100 µg/ml, kanamycin 25 µg/ml, spectinomycin and streptomycin 25 µg/ml each, tetracycline 10 µg/ml. All antibiotics except tetracycline were dissolved in ddH_2O in 1000 x concentrated stocks prior to use, sterilized by filtration and stored at – 20 °C. Tetracycline was dissolved in ethanol.

LB medium
0.5 % (w/v) NaCl
1 % (w/v) tryptone
0.5 % (w/v) yeast extract

2.3.5.2 Generation of Electro-Competent *E. coli* Cells

E. coli cells were handled under sterile conditions and were cooled on ice at 4°C, from the time of harvesting on. 20 ml of SOB medium with appropriate antibiotics was inoculated with *E. coli* under sterile conditions and cultivated under shaking overnight at 37°C. On the next day, 400 ml of SOB medium was inoculated with the whole preculture and cultivated until an OD_{600} = 0.5 was achieved. The culture was transferred into a sterile centrifuge tube and incubated on ice for 30 min. The cells were then harvested by centrifugation at 4.000 x g and 4°C for 15 min. The supernatant was discarded and the cell pellet was resuspended in 400 ml of ice-cold 1 mM HEPES pH7. After a centrifugation step, the cell pellet was resuspended in 200 ml, then 100 ml, then 50 ml of ice-cold H_2O, with centrifugation and removal of the supernatants in between. The cell pellet was then resuspended in 20 ml of ice-cold 20 % (v/v) glycerol, again centrifuged and finally resuspended in 2 ml of ice-cold 10 % (v/v) glycerol. Aliquots with 60 µl of cell suspension were flash frozen in liquid nitrogen and stored at - 80°C until use.

SOB medium
2 % (w/v) bacto-peptone
0.5 % (w/v) yeast extract
0.06 % (w/v) NaCl
0.018 % (w/v) KCl
The following sterile solutions were added after autoclaving
2 mM $MgSO_4$
2 mM $MgCl_2$

2.3.5.3 Generation of Chemically Competent *E. coli* cells

The first steps were performed as described in Generation of Electro-Competent *E. coli* Cells (see 2.3.5.2).

After the centrifugation step to remove the SOB medium from the cell pellet, the cells were resuspended in 100 ml of ice-cold TB buffer. The suspension was incubated on ice for 10 min and then centrifuged at 4000 x g and 4°C for 15 min. After removal of the supernatant, the cells were resuspended in 5 ml of ice-cold TB buffer with 7 % DMSO. Aliquots with 200 µl of cell suspension were flash frozen in liquid nitrogen and stored at - 80°C until used.

TB buffer

10 mM PIPES pH 6.7 with KOH

55 mM $MnCl_2$

15 mM $CaCl_2$

250 mM KCl

2.3.5.4 Transformation of *E. coli* by Electroporation

An aliquot of electro-competent *E. coli* cells was thawed on ice. Up to 5 µl of the desalted DNA was pipetted into the cell suspension and the sample was swirled gently. After an incubation on ice for 2-5 min, the suspension was filled rapidly into the ice-cold electroporation cuvette. A pulse of 1800 V was applied. Immediately after the pulse, 500 µl of ice-cold LB medium was added to the suspension. The cells were incubated at 37° for 40 min and then sedimented by centrifugation for 1 min at 4000 x g. The supernatant was discarded, the cell pellet resuspended in the residual LB medium and the cells plated on selective medium containing appropriate antibiotics.

2.3.5.5 Transformation of *E. coli* by Heat Shock

An aliquot of chemically competent cells was thawed on ice. The cell suspension was incubated with up to 5 µl of DNA for 20 min on ice. The heat shock was applied for 90 s at 42°C, the suspension was incubated afterwards for 1 min on ice. The cells were incubated at 37°C for 40 min and then harvested by centrifugation for 1 min at 4000 x g. The supernatant was removed, the cells resuspended in the residual LB medium and plated on medium containing appropriate antibiotics.

2.3.5.6 Colony PCR

A colony PCR was performed as fast check for positive clones containing the desired DNA construct. Therefore, small colonies visible on the day after transformation and growing on selective LB were picked as templates. Colony and PCR sample were labeled in the same manner.

The template DNA was added to the PCR reaction (components see 2.3.3) by dipping with a sterile pipette tip first into the colony and afterwards into the PCR reaction. Primers were chosen to hybridize with the flanking vector DNA and with the insert DNA to confirm successful ligation. The PCR program was used as described in 2.3.3. The PCR products were analyzed by gel electrophoresis. Colonies which were checked to contain the desired DNA construct were grown in overnight cultures and the plasmids prepared (see 2.3.5.7).

2.3.5.7 Preparation of Plasmid DNA from *E. coli*

A 2 ml overnight culture was harvested by centrifugation at 16.000 x g. The supernatant was discarded and the cell pellet was resuspended in 200 µl of BF buffer and 10 µl of 20 mg/ml lysozyme. The suspension was incubated for 1 min at 95°C, after 20 s incubation the lid was opened shortly to release pressure. The suspension was then cooled down on ice for 1 min. After a centrifugation step of 20 min at 16.000 x g, the supernatant was transferred into a fresh tube containing 400 µl of isopropanol and 80 µl of 5 M ammonium acetate. The sample was gently mixed by inverting several times, followed by centrifugation for 12 min at 16.000 x g. The supernatant was discarded and the DNA precipitate was washed with 500 µl of 75 % ethanol and again centrifuged for 6 min at 16.000 x g. The supernatant was discarded. The DNA precipitate was completely dried before adding 80 µl of ddH_20 and 1 µl of 10 mg/ml RNase A. The plasmid preparation was stored at – 20 °C until used.

BF buffer
8 % (w/v) sucrose
0.5 % (v/v) Triton X-100
50 mM EDTA pH 8
10 mM Tris-HCl pH 8

2.3.6 Working with *Agrobacterium tumefaciens*

2.3.6.1 Cultivation of *A. tumefaciens*

A. tumefaciens grew at 28 °C in YEP medium either under shaking in liquid medium at 180 – 200 rpm or on solidified medium in a Petri dish. For selection of desired DNA constructs, the medium was supplemented with appropriate antibiotics. The utilized antibiotics were stored as sterile filtered 250 x (rifampicin dissolved in DMSO) to 1000 x (the other antibiotics dissolved in ddH_2O) concentrated stock solutions at -20 °C until use. Final concentrations applied in the medium were rifampicin 60 µg/ml, streptomycin 300 µg/ml, spectinomycin 100 µg/ml and kanamycin 50 µg/ml.

YEP medium

1 % (w/v) Bacto™ Peptone

1 % (w/v) yeast extract

0.5 % (w/v) NaCl

For solid medium 1.5 % (w/v) Bacto™ Agar was added.

2.3.6.2 Generation of Electro-Competent *A. tumefaciens* Cells

5 ml of an overnight culture of the *A. tumefaciens* strain GV3101 pMP90 were used for the inoculation of 400 ml of YEP medium containing 60 µg/ml rifampicin. The cultures grew under shaking at 28 °C. When the culture reached an OD_{600} = 0.7, it was transferred into sterile centrifugation tubes and placed on ice for 30 min. All subsequent steps were carried out under sterile conditions at 4 °C. The cells were harvested by centrifugation at 4000 x g for 20 min in a precooled centrifuge, the supernatant was discarded and the cell pellet was resuspended in 400 ml of H_20. The suspension was incubated for 15 min on ice and then the centrifugation step was repeated. The cell pellet was washed another three times and then resuspended in 1 ml of 10 % (v/v) glycerol. Aliquots of 40 µl were flash frozen in liquid nitrogen and stored at – 80 °C until used.

2.3.6.3 Transformation of *A. tumefaciens*

An aliquot of electro-competent *A. tumefaciens* cells was thawed on ice. The cell suspension was mixed with 2-4 µl of plasmid DNA and then incubated on ice for 30 min. The suspension was transferred into a precooled electroporation cuvette and the electric pulse of 1250 V was applied. The cells were immediately mixed with 1 ml of ice-cold YEP medium without antibiotics. After an incubation at 28 °C for at least 2 h, the cells were plated on YEP medium containing appropriate antibiotics and cultivated for at least 2 days at 28 °C. The culture conditions for floral dipping can be found at 2.3.8.3.

2.3.7 Working with *Saccharomyces cerevisiae*

2.3.7.1 Cultivation of *S. cerevisiae*

The *S. cerevisiae* strain H1246 lacks steryl esters and triacylglycerols due to the disruption of the four genes *ARE1*, *ARE2*, *DGA1* and *LRO1* (Sandager *et al.*, 2002). Therefore the strain is well suited for the expression of genes that are related to triacylglycerol, steryl ester and also wax ester biosynthesis.

S. cerevisiae H1246 was cultivated at 30°C, either in liquid medium under shaking at 180 – 200 rpm or on solid medium. The medium used for cultivation was either YPD medium (see 2.3.7.2) or CMdum medium which was employed for the yeast expression experiments.

CMdum

0.116 % (w/v) dropout powder

2 % (w/v) galactose, 2 % (w/v) raffinose or 2 % (w/v) glucose

0.67 % (w/v) Yeast Nitrogen Base w/o Amino Acids (YNB)

0.002 % (w/v) L-histidine

0.006 % (w/v) L-leucine

0.004 % (w/v) L-tryptophan

For solid medium 2 % (w/v) of Bacto-Agar was added.

YNB, galactose, raffinose and glucose were prepared separately as 10 x concentrated sterile stock solutions and were added to the autoclaved medium prior to use. For L-histidine, L-leucine and L-tryptophan, also higher concentrated stock solutions were prepared. Sterilization of the solutions were performed by filtration (galactose and raffinose) or by autoclaving (glucose, YNB, L-histidine, L-leucine and L-tryptophan). Dropout powder was prepared by mixing and pestling the components (below) to a fine powder in a mortar.

Dropout powder

2.5 g adenine, hemisulfate

1.2 g L-arginine

6.0 g L-aspartic acid

6.0 g L-glutamic acid, sodium salt

1.8 g L-lysine, hydrochloride

1.2 g L-methionine

3.0 g L-phenylalanine

22.5 g L-serine

12.0 g L-threonine

1.8 g L-tyrosine

9.0 g L-valine

2.3.7.2 Generation of Electro-Competent *S. cerevisiae* Cells

For the generation of electro-competent yeast cells which were used for the transformation of DNA constructs, the *S. cerevisiae* strain H1246 was used. A culture containing 5 ml of sterile YPD medium was inoculated with the yeast cells and grown overnight. The next morning, 400 ml of YPD medium was inoculated with the overnight culture and grown to an OD_{600} =1.3 - 1.5. The cell suspension was then transferred into a sterile centrifugation tube. All following steps were carried out at 4°C. The cells were harvested by centrifugation (4000 rpm for 10 min) and the supernatant was discarded. The cell pellet was resuspended in 400 ml of ice cold ddH_20 and the cells separated

from the supernatant by another centrifugation step. The washing step was repeated once. Afterwards, the cell pellet was resuspended in 20 ml of ice cold 1 M sorbitol. After another centrifugation step and removal of the supernatant, the cell pellet was resuspended in ice cold 0.5 – 1 ml of 1 M sorbitol in 10 % glycerol (v/v). Aliquots of 60 µl were either directly employed for transformation, or frozen first for 10 min at -20 °C, then stored at -80 °C.

YPD
1 % (w/v) yeast extract
2 % (w/v) peptone
2 % (w/v) glucose (from 10x concentrated sterile stock solution, added to the autoclaved medium prior to use)
For solid medium 2 % (w/v) of Bacto-Agar was added.

2.3.7.3 Transformation of *S. cerevisiae*

An aliquot of competent cells stored at -80 °C was thawed on ice and used for transformation. In some experiments, freshly prepared electro-competent yeast cells were prepared because they showed a higher transformation efficiency.
The cell suspension was placed on ice and mixed with 5 µl of desalted plasmid DNA and incubated for 5 min. The mixture was then transferred into an ice cold electroporation cuvette. The transformation was performed by applying an electric pulse of 750 V to the yeast cells. Afterwards the suspension was mixed immediately with 500 µl of ice cold 1 M sorbitol and then incubated on ice for 2 min. After a centrifugation step (3000 x g, 1 – 2 min), the supernatant was removed and the cell pellet was resuspended in the residual liquid. The cell suspension was then plated on selective CMdum medium lacking uracil. After an incubation time of 2 – 3 days at 30 °C, transformed clones became visible.

2.3.7.4 Plasmid Preparation of *S. cerevisiae*

A transformed yeast clone growing on selective medium was further analyzed concerning the DNA construct. The transformed plasmid DNA was prepared according to Zymoprep Yeast Plasmid Miniprep™ I. To confirm the identity of the isolated plasmid DNA, a PCR was performed.

2.3.7.5 Heterologous Expression of *WSD1* in *S. cerevisiae*

One approach to study enzymatic activity of WSD1 in yeast was the expression of the cDNA inserted in yeast expression vectors (pESC-URA-*WSD1*, pDR196-*WSD1*, pYES2-*WSD1*). These DNA constructs as well as an empty vector control (pDR196) were freshly transformed in the yeast strain *S. cerevisiae* H1246. Positive clones were selected and then grown overnight in precultures

containing 5 ml of CMdum medium (see 2.3.7.1) lacking uracil. Those clones carrying a pYES2 or pESC-URA plasmid were grown with raffinose instead of glucose. The expression of *WSD1* was started when the culture reached an OD_{600} of 0.02 in a total volume of 50 ml. For the induction of the *WSD1* expression, the clones carrying a pYES2 or pESC-URA construct were grown with galactose instead of glucose by transferring the cells into a new medium with galactose. At the same time when protein expression was started, each expression culture was grown with and without (=control) the addition of 0.1 % (w/v) 1-octadecanol (18:0ol) and 0.1 % (w/v) palmitic acid (16:0), both added from 100 x concentrated stock solutions dissolved in ethanol. To enable the pipetting of the fatty acid and fatty alcohol substrates, the stock solutions were thawed by immersing the vials in warm water. After induction of protein expression and addition of the alcohol and fatty acid, the yeast cultures were grown for 48 h, then the OD_{600} was measured. The volumes used for the OD_{600} measurement were first centrifuged to separate the medium from the cell pellet. Then, the supernatant was carefully removed and the cell pellet was resuspended in ddH_2O and afterwards used for OD_{600} measurements. The removal of the yeast medium and resuspension of the cell pellet in ddH_2O prior to OD_{600} measurements was performed due to the fatty acid and fatty alcohol supplements being in the medium. Thereby, a more precise OD_{600} measurement was achieved.

The expression cultures were harvested by centrifugation (4000 x g for 15 min), the cell pellets were washed by resuspension in ddH_2O and again centrifuged. This washing step was performed twice. Lipids were extracted by adding chloroform:methanol:formic acid 1:1:0.1 (v/v/v) to the cell pellet. By centrifugation, two phases were separated from each other and the lower phase which contained the extracted lipids dissolved in chloroform was transferred into a fresh glass vial. The cell pellet was reextracted twice and the chloroform phases containing the extracted lipids were combined. 50 µl of wax ester standard containing 1 nmol of 18:0ol/17:0 and 3 nmol of 18:0ol/27:0 was added. The supernatant was then mixed with a small volume of 0.9 % (w/v) KCl in ddH_2O, again centrifuged and the chloroform phase was transferred into a fresh vial. The chloroform was evaporated under a stream of air until the extracted lipids were completely dried. The dried lipids were then dissolved in 10 ml of freshly prepared hexane:diethyl ether 99:1 (v/v). Then a solid phase extraction was performed. To this end, a 500 mg silica column was equilibrated five times with 6 ml (= 30 ml in total) of freshly prepared hexane:diethyl ether 99:1 (v/v). After the equilibration, 4 ml of the dissolved lipid extract was applied to the column. The flow through containing the wax ester fraction was collected and residual wax esters were eluted with another addition of 9 ml of hexane:diethyl ether 99:1 (v/v) and again collected. The wax ester containing fractions were combined. The solvent was evaporated by a stream of air and the dried lipid extract was dissolved in 1 ml of chloroform. Therefrom, 100 µl were transferred into a new tube, the solvent was evaporated under a stream of air and then dissolved in Q-TOF running buffer prior to Q-TOF MS/MS analysis. The Q-TOF MS/MS analysis was performed as described in 2.3.11.7. The

residual 900 µl of the sample were used for TLC. The volume that was pipetted onto the TLC plate was calculated in consideration of the measured OD_{600} of the yeast culture to achieve a loading on the TLC plate that represents similar amounts of cells. The TLC was developed and stained as described in 2.3.11.2.

2.3.7.6 Coexpression of *MaFAR* and *WSD1* in *S. cerevisiae*

Another approach to study enzymatic activity of WSD1 in yeast was the coexpression of a fatty acyl-coenzyme A reductase from *Marinobacter aquaeolei* VT8 (*MaFAR*) together with *WSD1*. The idea of this strategy was that yeast clones expressing *MaFAR* are able to synthesize long chain fatty alcohols like 1-octadecanol (18:0ol) and thus, both substrates needed for WSD1 activity are synthesized by the yeast itself. By the coexpression of *MaFAR* and *WSD1*, the synthesis of wax esters in yeast would be independent from the uptake of nonpolar substrates (fatty alcohol, fatty acid) being added into the aqueous CMdum medium, therefore the addition of fatty acids and fatty alcohols into the medium was not necessary.

The following DNA constructs were transformed freshly in *S. cerevisiae* H1246: pESC-URA-*WSD1*, pESC-URA-*MaFAR*, pESC-URA-*WSD1-MaFAR* and pESC-URA empty vector. Positive clones were grown overnight in precultures containing 5 ml of CMdum medium lacking uracil with raffinose instead of glucose (see 2.3.7.1).

The expression of *WSD1* was started with an OD_{600} of 0.02 in a total volume of 30 ml. To induce the gene expression, the culture medium was CMdum containing galactose instead of glucose. The expression cultures were grown for 48 h, then the OD_{600} was measured. The yeast cultures were harvested and the lipids extracted as described in 2.3.7.5. The lipid extracts were separated by solid-phase extraction and the solvent evaporated. The dried wax ester fraction was dissolved in Q-TOF running buffer and then analyzed by Q-TOF MS/MS.

2.3.8 Working with *Arabidopsis thaliana*

2.3.8.1 Cultivation of *A. thaliana*

Seeds of *A. thaliana* wild type and mutant lines were sown onto the surface of pots filled with a soil/vermiculite mixture (3:1). The seeds were sprayed with water and a transparent hood covered the pots during germination. *A. thaliana* plants were grown in growth chambers wherein the plants were exposed to 16 h light per day, a photon flux of 160 µmol m^{-2} s^{-1}, 22 °C and an air humidity of 65 %. Five seedlings per pot with 10 cm diameter were arranged in equidistance. If necessary, herbivorous insects or mites were controlled by spraying the plants with Calypso insecticide.

2.3.8.2 Hydroponic Cultures

A. thaliana was grown in hydroponic cultures to enable the harvest of soil-free roots prior to RNA extraction and to enable the easy application of different stresses like drought stress, salt stress and hormonal stress. The *araponics* container and the seed-holders were first thoroughly cleaned with water and dishwashing detergent "Priva Spülmittel Konzentrat Zitrone", the dishwashing detergent was then thoroughly washed away. Later, the container was wiped clean with ethanol, to avoid a contamination with algae and fungi, also a tray and transparent hood were cleaned thoroughly. The seed-holders were filled with autoclaved 0.7 % (w/v) Phyto agar. After solidifying, up to 2 seeds were placed onto the agar. Surface sterilization of the seeds was not necessary. The container was filled with sterile *Arabidopsis* nutrient medium (2 strength) (Estelle and Somerville, 1987), until the agar of the seed-holders was in contact with the medium. The container was placed in the middle of the cleaned tray, the surface of the tray's base was covered with water and the transparent hood was set onto the tray.

Arabidopsis nutrient medium (2 strength)

2.5 mM KNO_3

1 mM $MgSO_4$

1 mM $Ca(NO_3)_2$

1 mM KH_2PO_4

1 mM NH_4NO_3

25 µM Fe-EDTA (Ethylenediaminetetraacetic acid iron(III) sodium salt)

35 µM H_3BO_4

7.0 µM $MnCl_2$

0.25 µM $CuSO_4$

0.50 µM $ZnSO_4$

0.10 µM Na_2MoO_4

5.0 µM NaCl

5.0 nM $CoCl_2$

The medium was autoclaved after preparation.

For drought stress experiments, *A. thaliana* wild type plants were grown in hydroponic culture until the age of 4 weeks. Then, the *Arabidopsis* nutrient (2 strength) was replaced by *Arabidopsis* nutrient (2 strength) containing either 150 mM NaCl or 100 µM abscisic acid (ABA). While the medium containing 150 mM NaCl was autoclaved, the medium intended for ABA stress was autoclaved without ABA. ABA, dissolved in ethanol in a concentration of 0.025 mg/µl, was added at the starting point of stress treatment into the fresh medium. A third container was emptied to expose the plants to drought. A fourth container was filled with new original *Arabidopsis* nutrient

(2 strength) solution and served as control. Roots and leaves were harvested after 12 h and 24 h of stress and flash frozen in liquid nitrogen.

2.3.9 Working with *Nicotiana benthamiana*

2.3.9.1 Cultivation of *N. benthamiana*

Seeds of *N. benthamiana* wild type were sown onto the surface of pots of a soil/vermiculite mixture (3:1). The seeds were sprayed with water and a transparent hood covered the pots while the seeds germinated. The cultivation of *N. benthamiana* was done in growth chambers where the plants were exposed to 12 h light per day, a photon flux of 160 µmol m^{-2} s^{-1}, 22 °C and air humidity of 60 %. The seedlings were separated by growing one plant per pot with 10 cm in diameter.

2.3.9.2 Transient Transformation of *N. benthamiana*

Transient transformation was performed to localize gene products subcellularly. The presumption was that WSD2 to WSD10 localize at the ER, like WSD1 (Li *et al.*, 2008). Three cultures were grown for the transformation: *A. tumefaciens* carrying a *WSD* cDNA fused either N- or C-terminally with *eGPF* (details of the constructs see 2.3.1.6), *A. tumefaciens* carrying the ER-marker HDEL fused C-terminally with *DsRed* and *A. tumefaciens* carrying *p19* from the tomato bushy stunt virus (TBSV). P19 is known to improve the level of protein expression by suppressing post-transcriptional gene silencing (Voinnet *et al*., 2000). The cultures were grown each in 20 ml of YEP medium supplemented with appropriate antibiotics for 24 h. On the day of transformation, *N. benthamiana* plants were watered in the morning to achieve an opening of the stomata. The *A. tumefaciens* cultures were harvested by centrifugation for 10 min at 3500 x g at room temperature. The supernatant was properly discarded and the cell pellet was resuspended in 1 ml of infiltration medium. The OD_{600} was determined by measuring 1:50 dilutions of the suspensions. A mixture of 6 ml of the three suspensions in infiltration medium was prepared: 3 ml of *p19* with OD_{600} =0.5 and 1.5 ml of *WSD* gene as well as 1.5 ml of HDEL, both with OD_{600} =0.5. The mixture incubated under shaking at 28 °C in the dark for 2 – 3 h. Afterwards, *N. benthamiana* leaves were infiltrated on the lower side using a syringe. The infiltrated leaves were labeled. The plants grew for 2 to 4 days in the growth chamber until fluorescence was visible under a fluorescence microscope. For the determination of the subcellular localization, a laser scanning microscope LSM 780 was used.

Infiltration medium

20 mM citric acid

2 % (w/v) sucrose

pH adjusted to 5.2 with NaOH

100 mM acetosyringone (freshly added)

2.3.10 Working with *Hordeum vulgare*

2.3.10.1 Cultivation of *H. vulgare*

Cultivation of *H. vulgare* differed from cultivation of *A. thaliana* by growing one plant per pot. The pots had diameters of 15 cm each and were filled with soil type "Topf"/vermiculite 2:1 (v/v) before one barley seed per pot was sown. The plants grew in growth chambers with the following conditions: 16 h light per day, a photon flux of 160 µmol m^{-2} s^{-1}, 22 °C and an air humidity of 65 %. After 6 weeks, the plants were not watered anymore and exposed to drought for 2 weeks, while control plants were watered normally. After 2 weeks of drought stress, limp leaves of the stressed plants and firm leaves of the control plants were harvested to measure wax esters.

2.3.11 Methods in Biochemistry

2.3.11.1 Synthesis of WEs

WEs were synthesized to utilize them as standards. The synthesis was performed according to a modified protocol of Gellerman *et al.*, 1975. Due to volatile toxic by-products, the whole procedure was conducted under the hood.

0.2 mmol of fatty acid, 1 ml of toluene and 0.28 mmol of oxalyl chloride were filled into a screw cap glass tube. The tube was firmly closed and the mixture incubated for 2 h at 65 °C in a water bath. Afterwards the sample was dried by a stream of air. 1 ml of dry diethyl ether, 0.2 mmol of primary fatty alcohol and 0.25 ml of dry pyridine were added to the sample. The tube was firmly closed and the reaction incubated at 80 °C for 3 h. After the reaction cooled down to room temperature, the wax esters were extracted twice with hexane. The hexane phases were combined and then washed with ddH_2O to remove polar compounds. After a centrifugation step, the upper hexane phase was transferred into a fresh tube.

Prior to quantification of the synthesized wax esters by GC-FID, the wax ester extract was purified to remove free fatty alcohols and free fatty acids. This was performed either by TLC or SPE.

2.3.11.2 Thin Layer Chromatography (TLC)

TLC was performed to purify lipid extracts from other unwanted compounds, e. g., synthesized wax esters from free fatty acids and free fatty alcohols, and in general, to separate lipid classes according to their polarity.

The lipid samples were applied to the TLC plate in a small volume of chloroform, each sample as a small spot on a horizontal line (drawn with pencil) at the base of the TLC plate. 30 - 50 µg of wax esters was applied as standard. After the chloroform was evaporated, the plate was placed into the separation chamber that was filled with 101 ml of the developing solvent, hexane:diethyl ether:acetic acid 85:15:1 (v/v/v). The TLC plate was developed until the mobile phase reached as far as 0.5 cm distant from the plate's end. Then the plate was dried for 30 min prior to visualizing the lipids. For preparative TLC, the plate's site of the standard was carefully broken and by this separated from the other lipid samples. The plate's part of the standard was then exposed to iodine vapor. The lipid spots were identified by co-migration with the standard. Silica material containing the lipid spots was scraped from the TLC plate. The lipids were extracted from the silica material with 4 ml of chloroform thrice. The extracted lipids were combined and stored at – 20 °C until further analysis.

The separation of yeast lipid extracts was conducted by TLC in the same way as described above. After the developed plate was dried, the whole plate was exposed to iodine vapor to visualize all lipid spots. To increase the visibility of lipids that were saturated and highly unpolar (like wax esters), a charring was performed. To this end, the TLC plate exposed to iodine vapor was only used after the iodine spots had disappeared. Then the TLC plate was first sprayed with α-naphthol-sulphuric acid reagent (8 g of α-naphthol in methanol/ddH_2O/concentrated H_2SO_4, 250/20/30 (v/v/v)) and afterwards heated up at 150 °C until the lipid spots became visible.

2.3.11.3 Solid Phase Extraction (SPE)

In addition to TLC, solid phase extraction (SPE) can be used to fractionate a lipid extract into its lipid classes. The method was applied to isolate wax esters from other lipid classes (according to cyberlipid.org).

For this procedure, silica columns (100 mg or 500 mg) were equilibrated with hexane prior to sample application. The sample solvent was evaporated by a stream of air and the dry lipid extract was dissolved in n-hexane and applied to the equilibrated column. After the lipid extract was absorbed into the silica material, 1 ml (for 100 mg columns) or 6 ml (for 500 mg columns) of n-hexane was applied to the column. By the application of n-hexane, alkanes which are highly abundant in cuticular waxes, were eluted from the silica material. The next step was the elution of wax esters from the silica material. The column was placed into a fresh glass vial and hexane:diethyl ether 99:1 (v/v) which was freshly prepared was applied to the silica material. The eluted wax ester fraction was dried under a stream of air and solved in Q-TOF running buffer. By this way, the wax ester sample was prepared for MS/MS analysis and either measured immediately via Q-TOF (see 2.3.11.7) or stored at – 20 °C.

2.3.11.4 Synthesis of Fatty Acid Methyl Esters

The synthesized wax ester standards were analyzed by gas chromatography using a flame ionization detector (FID). To this end, the wax ester lipids had to be converted into fatty acid methyl esters (FAMEs). FAMEs were synthesized using a protocol according to Browse *et al*., 1986. The lipids were filled into a fresh glass tube and the solvent was evaporated. 1 ml of 1 N HCl in methanol was added to the lipid sample. 5 µg of pentadecanoic acid was used as internal standard. The samples were incubated at 80 °C for up to 60 min and then cooled down to room temperature. 1 ml of 0.9 % (w/v) NaCl and 1 ml of n-hexane was added to the sample. The sample was vortexed and a centrifugation step, 1000 x g for 3 min, followed. The upper phase containing the FAMEs was transferred into a fresh glass vial with a Pasteur pipette. The solvent was concentrated by a stream of air and transferred into the glass inlay of a GC vial. The sample was either analyzed directly by GC-FID or stored at – 20 °C until analyzed.

2.3.11.5 Gas Chromatography

The temperature gradient for FAMEs applied to the GC column (HP-5MS, 30 m, Agilent) started with 100 °C, increasing to 160 °C by 25 °C/min. The temperature was then increased to 220 °C by 10 °C/min and afterwards decreased to 100 °C by 25 °C/min. The FAMEs were detected by a flame ionization detector. For the identification of the FAMEs, the GC device was calibrated with a FAME rapeseed standard mixture (Supelco) and the retention times of the FAMEs in the sample were compared to those of the standard mixture.

2.3.11.6 Extraction and Preparation of Wax Esters from Plant Tissue for Q-TOF MS/MS Analysis

For the analysis of *Arabidopsis* T-DNA and transposon insertion mutant lines, total wax was extracted from the respective plant tissue and then purified by SPE. For all samples, lipid extraction was performed in glass vials first rinsed with chloroform:methanol 2:1 (v/v) that were closed by caps with Teflon septa. Pipetting of organic solvents was conducted with Pasteur pipettes. Working with plastic was avoided. All samples were stored at – 20 °C.

Stem wax was extracted by using inflorescence stems and cutting a piece of 2-3 cm in the lower part of the stem (below the middle of the stem). The piece of stem was laid on millimeter paper and a photograph was taken. Later, the projected cross section area of the stem was determined by the software cellSens (Olympus), converted in cm^2 by the help of the underlying millimeter paper and multiplied by π to calculate the surface area. Directly after taking the photograph, the piece of stem was dipped for 30 s in a glass vial filled with about 1.5 ml of chloroform (volume of one Pasteur pipette). While the 30 s went by, the sample was vortexed several times. The chloroform was transferred into a fresh glass vial and another same volume of chloroform was added to the stem. The stem wax was again extracted for 30 s supported by vortexing. Then the

lipid extracts were combined. 50 µl of the standard mixture 18:0/17:0 and 18:0/27:0 (50 µl represents 1 nmol and 3 nmol of the respective wax ester species) was added to the sample. The sample was vortexed and then completely dried under a stream of air. The wax was then dissolved in hexane. A 100 mg silica column was equilibrated with 1 ml of hexane and the sample was applied to the column. After the sample had sunk in the silica material, another 1 ml of hexane was added to elute hydrocarbons from the silica material (according to cyberlipid.org). When all solvent had passed the column, the column was placed into a new glass vial and was filled by and by with 2 ml of freshly prepared hexane:diethyl ether 99:1 (v/v). By this, the WEs were eluted from the column. The WE eluate was completely dried under a stream of air and the WEs were solved in Q-TOF running buffer and stored at – 20 °C until analyzed.

WEs from other plant tissues were isolated as follows:

5 siliques of mature sizes being still greenish were harvested by cutting at the border between peduncle and silique. The fresh weight was determined for the usage as reference value. Then the siliques were extracted two times (for 30 s each) with chloroform. The WEs were purified by SPE as described above.

10 flowers were harvested directly after opening of the buds and they represented all together one sample. WEs were extracted two times (for 30 s each) in chloroform followed by SPE purification. After the Q-TOF MS/MS analysis, the wax esters were referred to one flower as reference value.

Leaves were harvested from barley and were used to extract the lipids by dipping two times into chloroform and SPE purification as described above. After the extraction procedure the extracted leaves were placed in a glass petri dish filled with tap water. The leaves were unfolded. Beneath the glass disc millimeter paper was laid. The unfolded leaves were photographed. Surface areas were determined by multiplying the calculated leaf areas by two (upper and lower side of the leaf).

2.3.11.7 Q-TOF MS/MS Analysis of WEs

For the analysis of WEs, the 6530 Accurate-Mass Quadrupole Time-of-Flight (TOF) LC/MS mass spectrometer (Agilent) was employed. The lipid sample dissolved in Q-TOF running buffer (chloroform:methanol:300 mM ammonium acetate 300:665:35 (v/v/v)) was directly infused via Chip Cube technology. 5 µl of the sample was injected into the source of the mass spectrometer with a flow rate of 1 µl/min. WEs were analyzed in the positive mode, ammonium adducts of intact wax esters $[M+NH_4]^+$ were selected in the first mass analyzer (targeted lists in Appendix Table 13 – Table 15) and then fragmented by collision with nitrogen gas. The collision energy was set to 15 V, the fragmentor voltage to 200 V. The protonated fatty acid ion $[FA+H]^+$ was used as product ion for quantification. WEs were quantified by relating the respective product ion to the product ion of the internal standard. Although the added internal standard contained 1 nmol of 18:0ol/17:0 and 3 nmol of 18:0ol/27:0 WEs, only the product ion of the 18:0ol/17:0 standard was

used for quantification. Explanations are found in the results, see 3.8.3. The targeted lists applied for plant tissue and for lipid extracts of yeast can be found in the Appendix Tables 13, 14 and 15. Since Lai *et al*., 2007; Li *et al*., 2008, and others described only saturated WE species were detected in *Arabidopsis* wax, only saturated WE species were measured in *Arabidopsis* wax and no isotopic correction was performed. For all analyzed wax ester species, the product ion $[FA+H]^+$ was used for quantification relative to the product ion $[C_{17}H_{34}O_2H]^+$ of the internal standard 18:0ol/17:0.
The obtained data were interpreted by Agilent Mass Hunter Qualitative Analysis Software (Version B.02.00). The exact molecular masses listed in the targeted list were calculated by the Agilent Mass Hunter Calculator. Calculation of absolute amounts was done with Microsoft Excel. The detected signal intensities of the product ions $[FA+H]^+$ of all measured WEs were extracted by the Agilent Mass Hunter Qualitative Analysis Software (Version B.02.00) and saved as a csv file for each analyzed sample. Five signal intensity values of the product ion of the respective WE were used for the quantification for each analyzed WE species per sample. These signal intensity values were averaged and divided by the average of the five signal intensity values of the standard product ion $[C_{17}H_{34}O_2H]^+$. This was done with Microsoft Excel. The averaged signal intensity value of the standard product ion represented 1 nmol. By this, the amount of the measured WE was calculated in nmol. To relate the calculated nmol amounts of the WE species to mg fresh weight, to the surface area, to 10 flowers or to OD_{600}, the nmol amount was divided by the respective reference figure (for example: nmol wax ester species / mg fresh weight). To calculate µg amounts of the measured WEs, the nmol amount was multiplied by the molar mass of the respective WE species and divided by 1000.

3 Results

3.1 Genotyping of T-DNA/ Transposon Insertion Lines

For genotyping, all *wsd* mutant lines and the respective wild type ecotypes were grown on soil, genomic DNA was isolated from leaf tissue and PCRs were performed (see 2.3.3). The determination of the mutant line's genotype comprised at least three PCRs per mutant:

Two PCRs were performed with a three primer system, either with wild type DNA (control) or with mutant DNA as template. The three primers included one T-DNA/transposon border insertion primer and two primers hybridizing to the flanking wild type sequence.

A third PCR was performed with two primers hybridizing only on flanking wild type sequences using mutant DNA as template as control.

Primers recommended on the site of Salk Institute Genomic Analysis Laboratory (SIGnAL) were used and are enlisted in Table 6 in the Appendix. The expected sizes of the PCR products indicating the wild type alleles and the insertions were specified on the site of SIGnAL when recommended primers were used. Here, the sizes of the PCR products were given approximated as the size of the sequence between the actual insertion site and the flanking sequence was specified inaccurately as 0 – 300 bps.

Thus, the size of the expected PCR product defined by the border primer and the wild type primer comprised a sequence of the inserted DNA plus an approximated sequence size of 0 – 300 bps plus the genomic sequence (see also http://signal.salk.edu/tdnaprimers.2.html).

The expected sizes of the PCR products indicating the mutations for the *wsd* mutants below are therefore described as inaccurate "approximate values" originating from the SIGnAL site. The PCR products indicating the wild type alleles were specified with accurate values. For determination of the exact site of the insertion, flanking DNA of homozygous *wsd* mutants were amplified with the respective T-DNA/transposon insertion primer and WT primers and forwarded for sequencing. In Figure 3 to Figure 13, schemes of the *WSD* genes with respective insertion sites and primer hybridizing sites are depicted. Furthermore, agarose gels displaying the PCR results of the homozygous mutants as well as the primer combinations used for the PCRs are presented.

From homozygous mutant lines, seeds were collected and stored at 4°C (see Table 1 for the labeling of the seed storage vials).

Regarding *WSD1*, one mutant line was isolated that was homozygous for the disruption of the gene. The PCR of the mutant line ***wsd1*** resulted in a PCR product with a size being consistent with 532 - 832 bps (inaccurate values from SIGnAL as described above) (Figure 3B b). This PCR product indicates the mutation. A PCR product of this size was absent from the wild type control. The PCR of the wild type control resulted in a PCR product with a size of 1115 bps (Figure 3B a). This size was expected for the wild type allele and was present only in the control PCR with WT DNA. The

T-DNA is inserted with its left border at +733 bps downstream from the translation start site in the second exon of the gene as determined by sequencing.

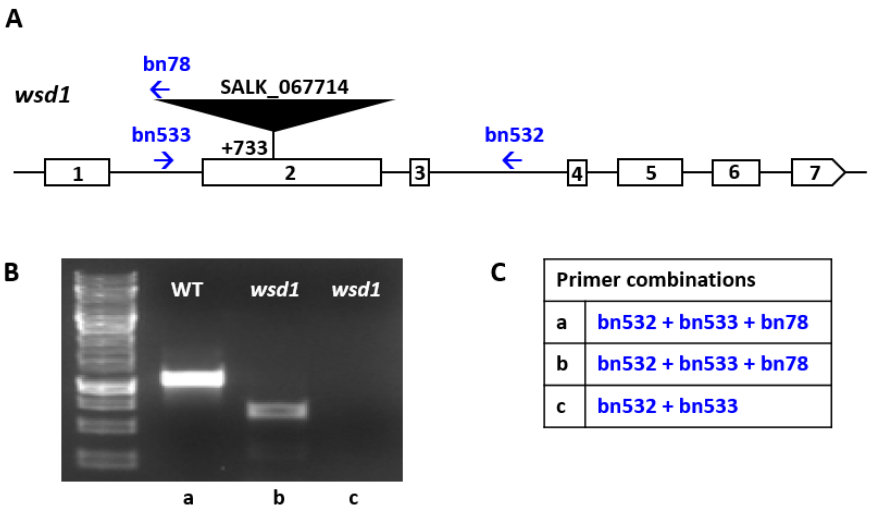

Figure 3: T-DNA Insertion Mutant Line *wsd1* of *A. thaliana*.

A scheme of the gene *WSD1* is depicted including the site of the T-DNA insertion in the second exon of the gene, primer hybridizing sites and the accurate insertion site at + 733 bps downstream from the translation start site (**A**). (**B**) PCR was done with genomic DNA from WT (control) and homozygous *wsd1* mutants. (**C**) The primer combinations included (a) three primers including the T-DNA insertion primer (with WT DNA), (b) three primers including the T-DNA insertion primer (with *wsd1* mutant DNA) or (c) two primers hybridizing only at wild type sites of the gene (*wsd1* mutant DNA).

Regarding *WSD2*, two homozygous mutant lines were isolated. The PCR of the mutant line ***wsd2-1*** resulted in a PCR product with a size being consistent with 580 - 880 bps (SIGnAL) (Figure 4B b). This PCR product indicates the mutation. A PCR product of this size was absent from the wild type control. The PCR product of the wild type control showed a size of 1250 bps (Figure 4B a). This size was expected for the wild type allele and was present only in the WT control PCR. The T-DNA is inserted with its left border at -112 bps upstream of the translation start site in the region of the promoter as determined by sequencing.

The PCR product of the mutant line ***wsd2-2*** had a size being consistent with 460 - 760 bps (SIGnAL) (Figure 4B e). This PCR product indicates the mutation, therefore, from the wild type control, a PCR product of this size was absent. The PCR product of the wild type control showed a size of 1097 bps (Figure 4B d). This size was expected for the wild type allele and was present only in the control PCR. The transposon is inserted with its left border at +1478 bps downstream from the translation start site in the fifth exon of the gene as determined by sequencing.

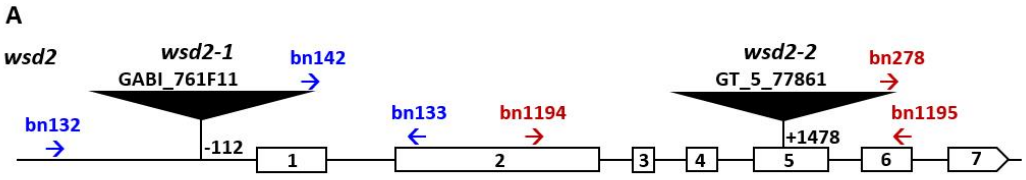

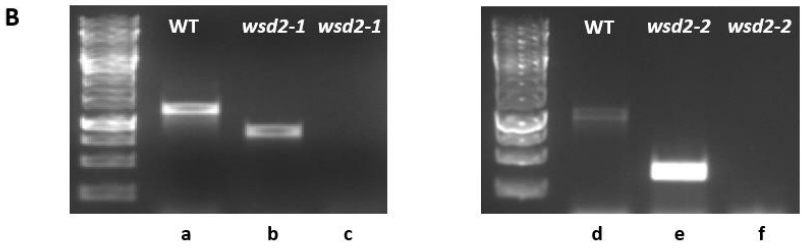

C

Primer combinations	
a	bn132 + bn142 + bn133
b	bn132 + bn142 + bn133
c	bn132 + bn133

Primer combinations	
d	bn1194 + bn278 + bn1195
e	bn1194 + bn278 + bn1195
f	bn1194 + bn1195

Figure 4: T-DNA Insertion Mutant Line *wsd2-1* and Transposon Mutant Line *wsd2-2* of *A. thaliana*.

A scheme of the gene *WSD2* is depicted including the sites of the T-DNA insertion in the region of the promoter and of the transposon insertion in fifth exon of the gene, primer hybridizing sites and the exact insertion site at -122 bps upstream of and +1478 bps downstream from the translation start site (**A**). (**B**) PCR was done with genomic DNA from WT (control) and homozygous *wsd2-1* or *wsd2-2* mutants. (**C**) The primer combinations included (a, d) three primers including the T-DNA insertion primer (PCR with WT DNA), (b, e) three primers including the T-DNA insertion primer (PCR with mutant DNA) or (c, f) two primers hybridizing only at wild type sites of the gene (PCR with mutant DNA).

Regarding *WSD3*, two homozygous mutant lines were isolated. The size of the PCR product of the mutant line ***wsd3-1*** is consistent with 474 - 774 bps (SIGnAL) (Figure 5B b) and indicates the mutation. A PCR product of this size was absent from the wild type control. The size of PCR product of the wild type control was 988 bps (Figure 5B a). This size was expected for the wild type allele and was present only in the WT control PCR. The T-DNA is localized in the second exon of the gene according to SIGnAL, the exact position of the insertion is not known as the PCR product was not sequenced.

The PCR product of the mutant line ***wsd3-2*** had a size which is consistent with 515 - 815 bps (SIGnAL) (Figure 5B e). This PCR product indicates the mutation. A PCR product of this size was absent from the wild type control. The PCR product of the wild type control had a size of 1063 bps (Figure 5B d). This size was expected for the wild type allele and was present only in the WT control PCR. The T-DNA is localized in the third intron of the gene according to SIGnAL, the exact position of the insertion is not known as the PCR product was not sequenced.

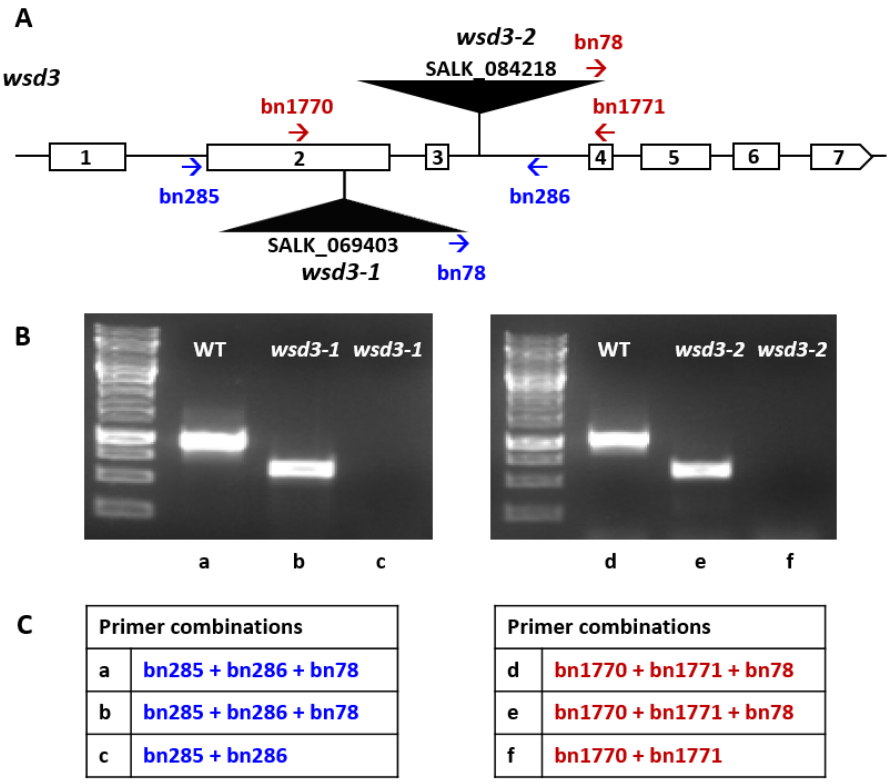

C

Primer combinations	
a	bn285 + bn286 + bn78
b	bn285 + bn286 + bn78
c	bn285 + bn286

Primer combinations	
d	bn1770 + bn1771 + bn78
e	bn1770 + bn1771 + bn78
f	bn1770 + bn1771

Figure 5: T-DNA Insertion Mutant Lines *wsd3-1* and *wsd3-2* of *A. thaliana*.

A scheme of the gene *WSD3* is depicted including the sites of the T-DNA insertions in the second exon and in the third intron of the gene and primer hybridizing sites (**A**). (**B**) PCR was done with genomic DNA from WT (control) and homozygous mutants. (**C**) The primer combinations included (a, d) three primers including the T-DNA insertion primer (PCR with WT DNA), (b, e) three primers including the T-DNA insertion primer (PCR with mutant DNA) or (c, f) two primers hybridizing only at wild type sites of the gene (PCR with mutant DNA).

Regarding *WSD4*, two homozygous mutant lines were isolated. The PCR product of the mutant line ***wsd4-1*** had a size which is consistent with 474 - 774 bps (SIGnAL) (Figure 6B b). This PCR product indicates the mutation. A PCR product of this size was absent from the wild type control. The PCR of the wild type control resulted in a PCR product with a size of 1119 bps (Figure 6B a). This size was expected for and was present only in the wild type allele. The T-DNA is inserted with its left border at +1190 bps downstream from the translation start site in the third intron of the gene as determined by sequencing.

The mutant line ***wsd4-2*** showed a PCR product which is consistent with 468 - 768 bps (SIGnAL) (Figure 6B e). This PCR product indicates the mutation, therefore, a PCR product of this size was absent from the wild type control. The PCR of the wild type control resulted in a PCR product of 1027 bps (Figure 6B d). This size was expected for the wild type allele and was present only in the WT control PCR. The T-DNA is localized in the sixth intron of the gene according to SIGnAL, the exact position of the insertion is not known as the PCR product was not sequenced.

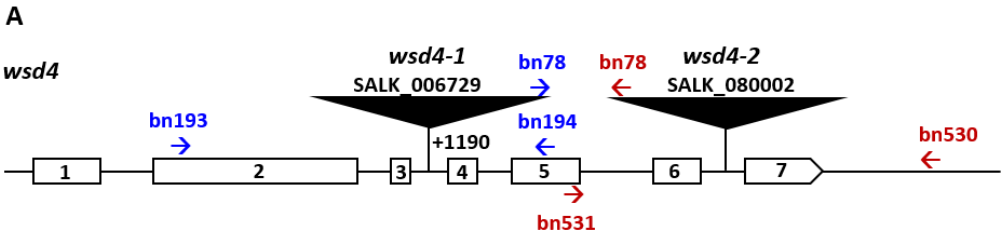

C

Primer combinations	
a	bn194 + bn193 + bn78
b	bn194 + bn193 + bn78
c	bn194 + bn193

Primer combinations	
d	bn530 + bn531 + bn78
e	bn530 + bn531 + bn78
f	bn530 + bn531

Figure 6: T-DNA Insertion Mutant Lines *wsd4-1* and *wsd4-2* of *A. thaliana*.

A scheme of the gene *WSD4* is depicted including the sites of the T-DNA insertions in the third intron and in the sixth intron of the gene, primer hybridizing sites and the exact insertion site at +1190 bps downstream from the translation start site for the T-DNA of *wsd4-1* (**A**). (**B**) PCR was done with genomic DNA from WT (control) and homozygous mutants. (**C**) The primer combinations included (a, d) three primers including the T-DNA insertion primer (PCR with WT DNA), (b, e) three primers including the T-DNA insertion primer (PCR with mutant DNA) or (c, f) two primers hybridizing only at wild type sites of the gene (PCR with mutant DNA).

Regarding *WSD5*, one homozygous mutant line was isolated. PCR products were only obtained if two primers instead of three primer were used.

The PCR product of the mutant line ***wsd5*** obtained by the use of the primers bn1795 and bn1474 showed a size which is consistent with 1250 - 1450 bps (Figure 7B b). This PCR product indicates the mutation. A PCR product of this size was absent from the wild type control. The PCR of the wild type control obtained by the use of the primers bn1795 and bn1796 showed a size of 1598 bps (Figure 7B a). This size was expected for the wild type allele and was present only in the WT control PCR. The T-DNA is localized in the second exon of the gene according to SIGnAL, the exact position of the insertion is not known as the PCR product was not sequenced.

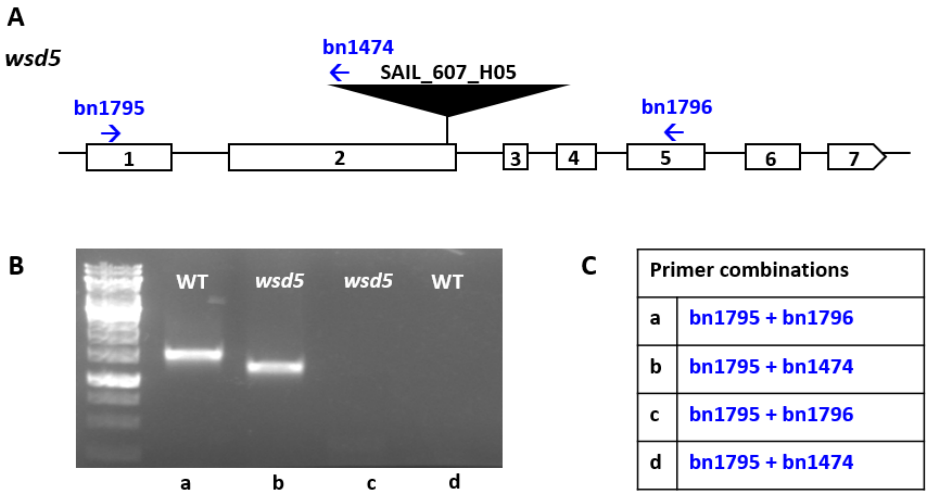

Figure 7: T-DNA Insertion Mutant Line *wsd5* of *A. thaliana*.

A scheme of the gene *WSD5* is depicted including the site of the T-DNA insertion in the second exon of the gene and primer hybridizing sites (**A**). (**B**) PCR was done with genomic DNA from WT (control) and homozygous mutants. (**C**) The primer combinations included (a) two primers hybridizing only at wild type sites of the gene (PCR with WT DNA), (b) one primer to flanking genomic DNA and one T-DNA insertion primer (PCR with mutant DNA), (c) two primers hybridizing only at wild type sites of the gene (PCR with mutant DNA), (d) one primer to flanking genomic DNA and one T-DNA insertion primer (PCR with WT DNA).

Regarding *WSD6*, two homozygous mutant lines were isolated. The PCR product of the mutant line ***wsd6-1*** had a size which is consistent with 525 - 825 bps (SIGnAL) (Figure 8B b). This PCR product indicates the mutation. A PCR product of this size was absent from the wild type control. The PCR product of the wild type control resulted had a size of 1169 bps (Figure 8B a). This size was expected for the wild type allele and was present only in the WT control PCR. The T-DNA is inserted with its left border at +907 bps downstream from the translation start site in the first intron of the gene as determined by sequencing.

The PCR product of the mutant line ***wsd6-2*** had a size which is consistent with 554 - 854 bps (SIGnAL) (Figure 8B e). This PCR product indicates the mutation. A PCR product of this size was absent from the wild type control. The PCR product of the wild type control had a size of 1132 bps (Figure 8B d). This size was expected for the wild type allele and was present only in the WT control PCR. The T-DNA is inserted with its left border at +1275 bps downstream from the translation start site in the second exon of the gene as determined by sequencing.

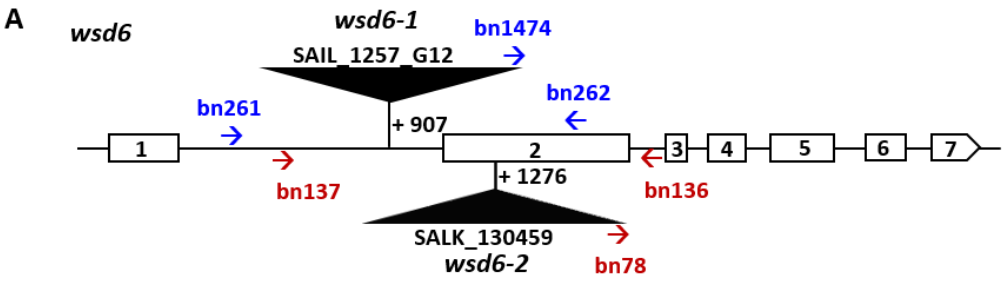

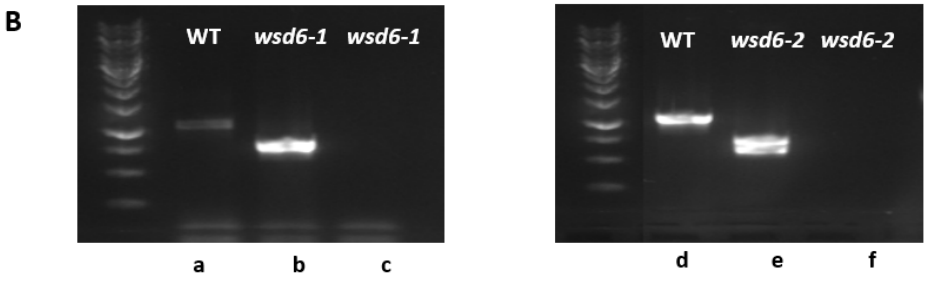

C

Primer combinations	
a	bn261 + bn262 + bn1474
b	bn261 + bn262 + bn1474
c	bn261 + bn262

Primer combinations	
d	bn136 + bn137 + bn78
e	bn136 + bn137 + bn78
f	bn136 + bn137

Figure 8: T-DNA Insertion Mutant Lines *wsd6-1* and *wsd6-2* of *A. thaliana*.

A scheme of the gene *WSD6* is depicted including the sites of the T-DNA insertions in the first intron and in the second exon of the gene, primer hybridizing sites and the exact insertion sites at +907 bps and +1276 bps downstream from the translation start (**A**). (**B**) PCR was done with genomic DNA from WT (control) and homozygous mutants. (**C**) The primer combinations included (a, d) three primers including the T-DNA insertion primer (PCR with WT DNA), (b, e) three primers including the T-DNA insertion primer (PCR with mutant DNA) or (c, f) two primers hybridizing only at wild type sites of the gene (PCR with mutant DNA).

Regarding *WSD7*, two homozygous mutant lines were isolated. The PCR product of the mutant line ***wsd7-1*** had a size which is consistent with 531 - 831 bps (SIGnAL) (Figure 9B b). This PCR product indicates the mutation. A second PCR product was detected in the homozygous mutant line when the three primer system was used (Figure 9B b). The size of this second PCR product was in agreement with 1073 bps indicating the wild type allele. This PCR product was absent if only two primers annealing to the wild type sequences of the gene were used with mutant DNA, therefore the mutant line was assumed to be homozygous.

The PCR product of the wild type control had a size in agreement with 1073 bps indicating the wild type allele (Figure 9B a). The T-DNA is inserted with its left border at +167 bps downstream from the translation start site in the first exon of the gene as determined by sequencing.

The PCR product of the mutant line ***wsd7-2*** had a size which is consistent with 592 - 892 bps (SIGnAL) (Figure 9B e). A PCR product of this size was absent from the wild type control. The PCR product of the wild type control had a size of 1235 bps (Figure 9B d). This size was expected for the wild type allele and was present only in the WT control PCR. The T-DNA is localized in the

second exon of the gene according to SIGnAL, the exact position of the insertion is not known as the PCR product was not sequenced.

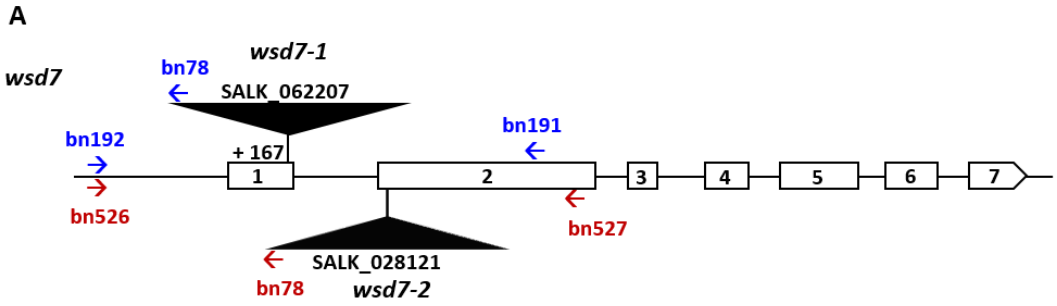

C

Primer combinations	
a	bn192 + bn193 + bn78
b	bn192 + bn193 + bn78
c	bn192 + bn193

Primer combinations	
d	bn526 + bn527 + bn78
e	bn526 + bn527 + bn78
f	bn526 + bn527

Figure 9: T-DNA Insertion Mutant Lines *wsd7-1* and *wsd7-2* of *A. thaliana*.

A scheme of the gene *WSD7* is depicted including the sites of the T-DNA insertions in the first exon and in the second exon of the gene, primer hybridizing sites and the exact insertion site at +167 bps downstream from the translation start site for the T-DNA of *wsd7-1* (**A**). (**B**) PCR was done with genomic DNA from WT (control) and homozygous mutants. (**C**) The primer combinations included (a, d) three primers including the T-DNA insertion primer (PCR with WT DNA), (b, e) three primers including the T-DNA insertion primer (PCR with mutant DNA) or (c, f) two primers hybridizing only at wild type sites of the gene (PCR with mutant DNA).

Regarding *WSD8*, two homozygous mutant lines were isolated. The PCR product of the mutant line ***wsd8-1*** had a size which is consistent with 650 - 850 bps (SIGnAL) (Figure 10B b). This PCR product indicates the mutation. A PCR product of this size was absent from the wild type control. The PCR product of the wild type control had a size of 1686 bps (Figure 10B a). This size was expected for the wild type allele and was present only in the WT control PCR. The T-DNA is inserted with its left border at +442 bps downstream from the translation start site in the first intron of the gene as determined by sequencing.

The PCR product of the mutant line ***wsd8-2*** had a size which is consistent with 503 - 803 bps (SIGnAL) (Figure 10B e). This PCR product indicates the mutation. A PCR product of this size was absent from the wild type control. The PCR product of the wild type control had a size of 1045 bps (Figure 10B d). This size was expected for the wild type allele and was present only in the WT

control PCR. The T-DNA is inserted with its left border at +1819 bps downstream from the translation start site in the fifth intron of the gene as determined by sequencing.

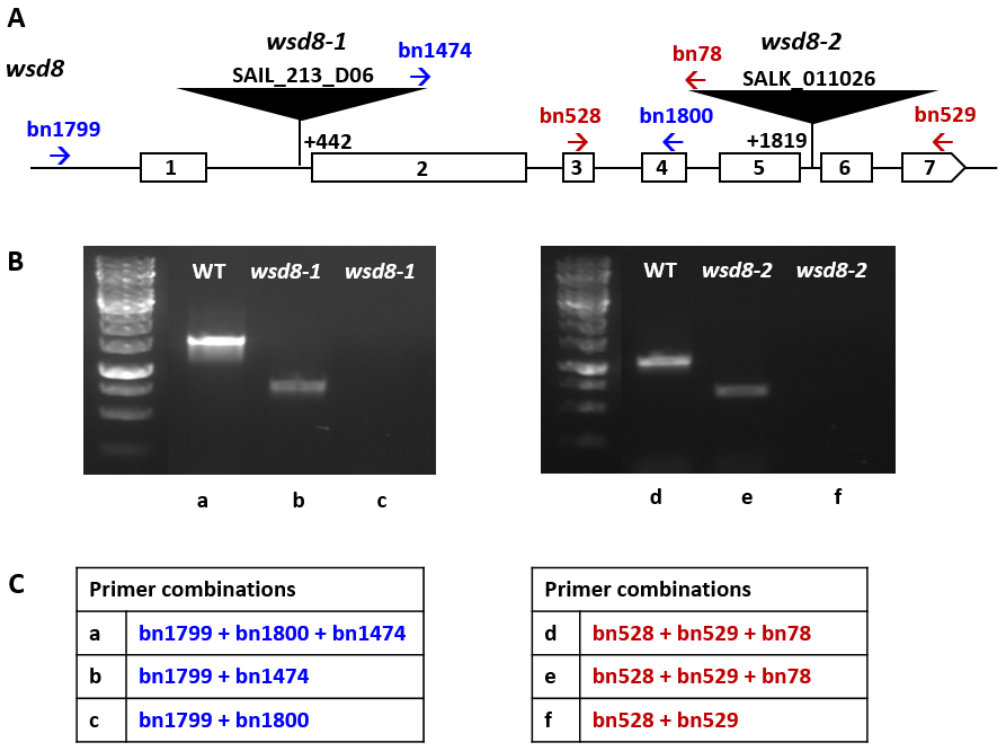

C

Primer combinations	
a	bn1799 + bn1800 + bn1474
b	bn1799 + bn1474
c	bn1799 + bn1800

Primer combinations	
d	bn528 + bn529 + bn78
e	bn528 + bn529 + bn78
f	bn528 + bn529

Figure 10: T-DNA Insertion Mutant Lines *wsd8-1* and *wsd8-2* of *A. thaliana*.

A scheme of the gene *WSD8* is depicted including the sites of the T-DNA insertions in the first intron and in the fifth intron of the gene, primer hybridizing sites and the exact insertion sites at +442 bps and +1819 bps downstream from the translation start site (**A**). (**B**) PCR was done with genomic DNA from WT (control) and homozygous mutants. (**C**) The primer combinations included (a, d) three primers including the T-DNA insertion primer (PCR with WT DNA), (b) two primers including the T-DNA insertion primer (PCR with mutant DNA), (e) three primers including the T-DNA insertion primer (PCR with mutant DNA) or (c, f) two primers hybridizing only at wild type sites of the gene (PCR mutant DNA).

Regarding *WSD9*, two homozygous mutant lines were isolated. The PCR products of the mutant line ***wsd9-1*** and the mutant line ***wsd9-2***, had sizes which are consistent with 522 - 822 bps (SIGnAL) (Figure 11B b, e). This PCR product indicates the mutation. A PCR product of this size was absent from the two wild type controls. The PCR products of the wild type controls had sizes of 1098 bps (Figure 11B a, d). This size was expected for the wild type allele and was present only in the WT control PCRs.

For *wsd9-1*, the T-DNA is localized in the fourth exon of the gene according to SIGnAL, the exact position of the insertion is not known as the PCR product was not sequenced. For *wsd9-2*, the T-DNA is inserted with its left border at +1194 bps downstream from the translation start site in the fourth exon of the gene as determined by sequencing. Because of the proximity of the two insertions, and the fact that they are derived from the same mutant population, it is possible that the two lines are not independent but originate from the same insertion event.

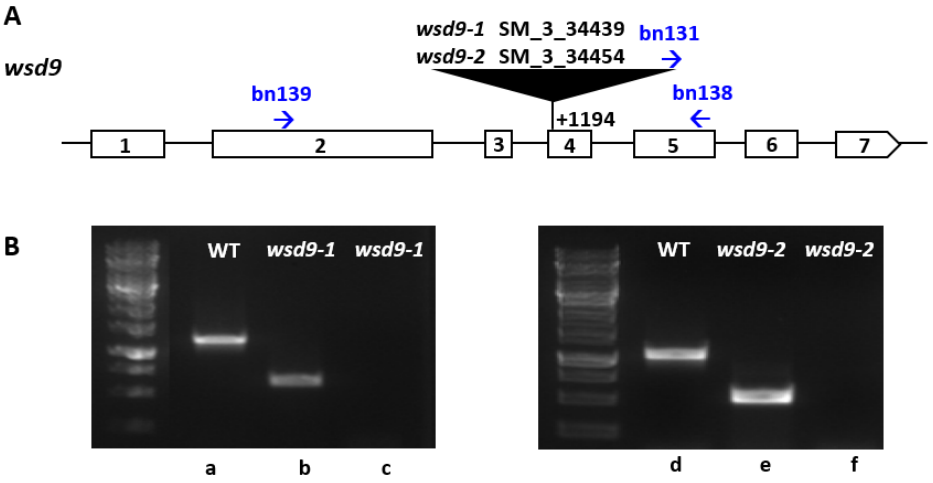

C

Primer combinations	
a, d	bn138 + bn139 + bn131
b, e	bn138 + bn139 + bn131
c, f	bn138 + bn139

Figure 11: T-DNA Insertion Mutant Lines *wsd9-1* and *wsd9-2* of *A. thaliana*.

A scheme of the gene *WSD9* is depicted including the sites of the T-DNA insertions in the fourth exon of the gene, primer hybridizing sites and the accurate exact insertion sites at +1194 bps downstream from the translation start site for the T-DNA of *wsd9-2* (**A**). (**B**) PCR was done with genomic DNA from WT (control) and homozygous mutants. (**C**) The primer combinations included (a, d) three primers including the T-DNA insertion primer (PCR with WT DNA), (b, e) three primers including the T-DNA insertion primer (PCR with mutant DNA) or (c, f) two primers hybridizing only at wild type sites of the gene (PCR with mutant DNA).

Regarding *WSD10*, two homozygous mutant lines were isolated. The PCR product of the mutant line ***wsd10-1*** had a size which is consistent with 500 - 700 bps (SIGnAL) (Figure 12B b). This PCR product indicates the mutation. A PCR product of this size was absent from the wild type control. The PCR product of the wild type control had a size of 1039 bps (Figure 12B a). This size was expected for the wild type allele and was present only in the WT control PCR. The transposon is localized in the second exon of the gene according to SIGnAL, the exact position of the insertion is not known as the PCR product was not sequenced. The PCR product of the mutant line ***wsd10-2*** had a size which is consistent with 600 - 800 bps (SIGnAL) (Figure 12B e). A PCR product of this size was absent from the wild type control. The PCR product of the wild type control had a size of 1162 bps (Figure 12B d). This size was expected for the wild type allele and was present only in the WT control PCR. The transposon is inserted with its left border at +1577 bps downstream from the translation start site in the sixth exon of the gene as determined by sequencing.

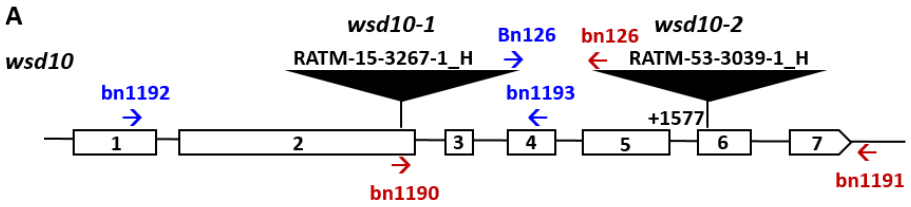

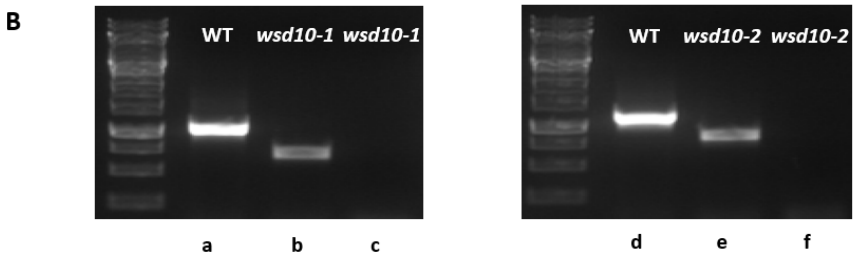

C

Primer combinations	
a	bn1192 + bn1193 + bn126
b	bn1192 + bn1193 + bn126
c	bn1192 + bn1193

Primer combinations	
d	bn1190 + bn1191 + bn126
e	bn1190 + bn1191 + bn126
f	bn1190 + bn1191

Figure 12: Transposon Mutant Lines *wsd10-1* and *wsd10-2* of *A. thaliana*.

A scheme of the gene *WSD10* is depicted including the sites of the transposon insertions in the second exon and in the sixth exon of the gene, primer hybridizing sites and the exact insertion sites at +1577 bps downstream from the translation start site for the transposon of *wsd10-2* (**A**). (**B**) PCR was done with genomic DNA from WT (control) and homozygous mutants. (**C**) The primer combinations included (a, d) three primers including the transposon insertion primer (PCR with WT DNA), (b, e) three primers including the transposon insertion primer (PCR with mutant DNA) or (c, f) two primers hybridizing only at wild type sites of the gene (PCR with mutant DNA).

For the gene *WSD11*, one homozygous mutant line was isolated. The PCR product of the mutant line ***wsd11*** had a size which is consistent with 500 - 700 bps (SIGnAL) (Figure 13B b). A PCR product of this size was absent from the wild type control. The PCR product of the wild type control had a size of 1128 bps (Figure 13B a). This size was expected for the wild type allele and was present only in the WT control PCR. The T-DNA is inserted with its left border at +1231 bps downstream from the translation start site in the third exon of the gene as determined by sequencing.

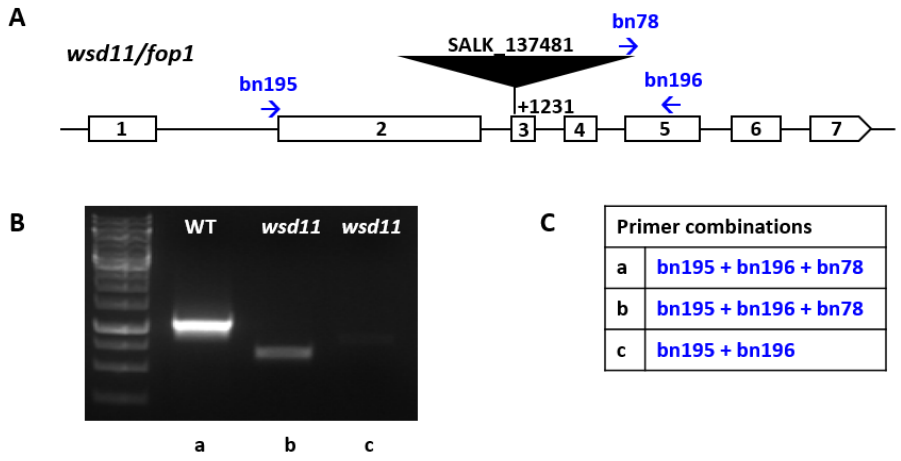

Figure 13: T-DNA Insertion Mutant Line *wsd11* of *A. thaliana*.

A scheme of the gene *WSD11* is depicted including the site of the T-DNA insertion in the third exon of the gene, primer hybridizing sites and the accurate insertion site at + 1231 bps downstream from the translation start site (**A**). (**B**) PCR was done with genomic DNA from WT (control) and homozygous mutants. (**C**) The primer combinations included (a) three primers including the T-DNA insertion primer (PCR with WT DNA), (b) three primers including the T-DNA insertion primer (PCR with mutant DNA) or (c) two primers hybridizing only at wild type sites of the gene (PCR with mutant DNA).

3.2 Expression Analysis of *WSD* Genes in Different Plant Tissues

For the analysis of the expression of the *WSD* genes in *A. thaliana* Col-0, RNA was extracted from different plant organs, including siliques, inflorescences, leaves, stems and roots. While the RNA of siliques, inflorescences, leaves and stems were extracted from plants grown on soil, the root tissue originated from plants grown in hydroponic cultures (see 2.3.8.2). After RNA extraction, residual genomic DNA was removed from the samples with DNAse and cDNA was synthesized by reverse transcription. The concentrations of the cDNA samples were adjusted such that they gave rise to bands with similar intensity upon RT-PCR with the control gene ACT1, and a semiquantitative RT-PCR was performed for all WSD genes. Two control PCRs were performed, one using genomic wild type DNA and one using ddH_2O as template.

The results of the RT-PCRs are depicted in Figure 14. While the expression of several *WSD* genes is limited to one or two plant tissues, mostly inflorescences and siliques, other *WSD* genes are expressed in all analyzed tissues.

WSD1 as well as *WSD2* and *WSD3* are expressed in inflorescence and silique tissue. *WSD4* is expressed in roots and also in inflorescences and slightly in siliques. *WSD5* is slightly expressed in inflorescences and siliques. *WSD6* and *WSD7* are expressed with similar levels in all tested plant organs: in roots, stems, leaves, inflorescences and siliques. *WSD8* is slightly expressed in stems and inflorescences and with a higher expression level in siliques. *WSD9* is expressed in stems and siliques. *WSD10* is only expressed in root tissue and *WSD11* is expressed in inflorescences.

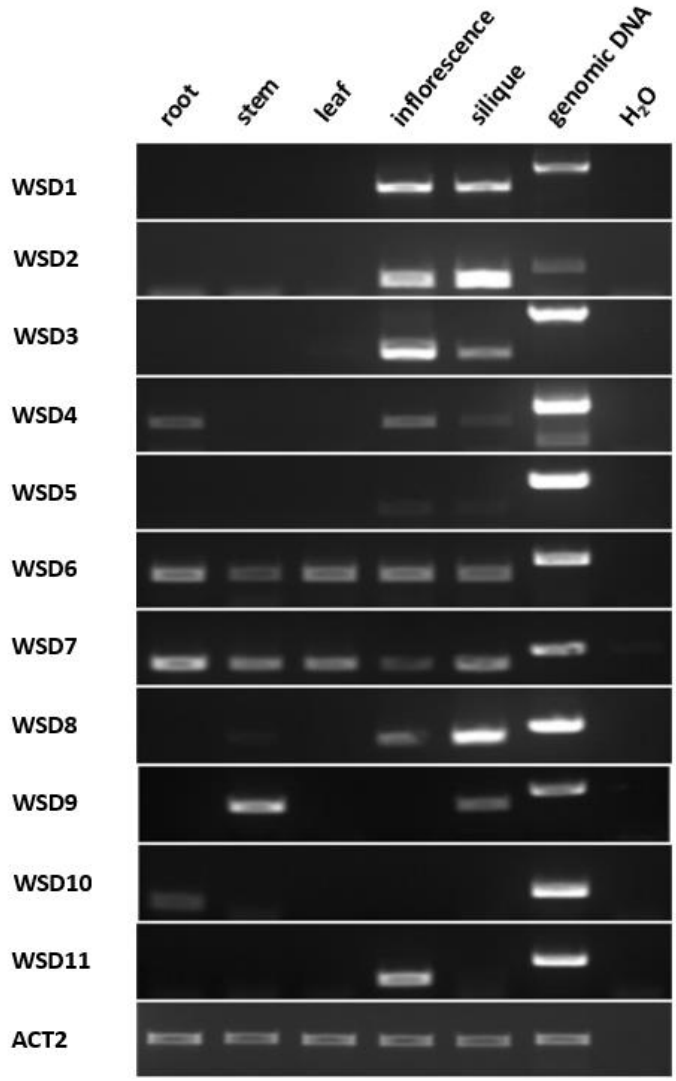

Figure 14: Expression of *WSD* Genes in Different Plant Organs.

Arabidopsis thaliana wild type was grown in hydroponic cultures (for harvesting roots) or on soil (for all other tissues). Tissues were harvested and used for RNA extraction at inflorescence stage (siliques were harvested when they were still green). *ACT2* was employed as housekeeping gene. Genomic DNA was used for a control PCR to show differences in PCR product sizes. Semiquantitative RT-PCR was performed, the PCR products separated by agarose gel electrophoresis and visualized by UV light after ethidium bromide staining.

3.3 Expression of *WSD* Genes in Leaves and Roots after Exposure to Stress

WSD1 is known to contribute to the wax ester synthesis of the waxy stem cuticle (Li *et al*., 2008). Furthermore, the cuticle is known to have important functions in response to different environmental stresses (Wang *et al*., 2011; Riederer and Schreiber, 2001). Therefore, it is likely that expression of *WSD* genes is induced after exposure to different environmental stresses. The gene expression levels of the *WSD* genes were analyzed by semiquantitative RT-PCR.

Arabidopsis thaliana wild type Col-0 plants were grown in hydroponic cultures and the roots were exposed to three different stress conditions: drought stress by removing the *Arabidopsis* nutrient (2 strength) medium, osmotic stress by exposure of the roots to 150 mM NaCl or a hormonal stress

by adding 100 µM abscisic acid into the medium. Another hydroponic culture was not exposed to stress and used as control (= 0 h of exposure to stress). After 12 and 24 h of stress exposure, root and leaf tissues were harvested and the RNA extracted. cDNA was synthesized and semiquantitative RT-PCR was performed for all *WSD* genes. The expression of *RD29A* was recorded as control, because it is known that rd29A transcription is upregulated during drought stress (Yamaguchi-Shinozaki and Shinozaki, 1994).

As depicted in Figure 15, *RD29A* was expressed in all stressed leaf and root tissues while it was not expressed in the control (0 h of stress application). The expression of *WSD1* was induced in leaf tissue (Figure 15 A) after exposure to all stresses, ABA, NaCl and drought: However WSD1 was not expressed in the unstressed control (= 0 h). In root tissue, *WSD1* was not expressed at all, neither in the stressed tissues, nor in the unstressed control. *WSD2* and *WSD3* were not expressed in leaf or root tissue regardless of stress exposure. *WSD4* was not expressed under any tested conditions in leaf tissue, but was expressed in root tissue (Figure 15 B) in the unstressed control as well as in all stressed tissues. The expression of *WSD4* in roots was always higher in those tissues which were exposed for 12 h to one stress condition than in those tissues which were exposed for 24h to the same stress condition. While the expression of *WSD4* appeared to be lower after exposure to ABA or drought compared to the expression of the gene in the unstressed plant root, the expression of *WSD4* was higher after 12 h of exposure to salt stress compared with the unstressed plant root. *WSD5* was not expressed in the unstressed plant root and leaf, but after 12h of exposure to ABA a very weak expression product was visible in the stressed leaf sample (Figure 15 A). Furthermore, after 24 h of exposure to drought stress, *WSD5* expression was clearly induced in leaves and also in roots. In roots, *WSD5* expression was induced upon exposure to salt stress with similar expression levels after 12 h and 24 h of stress. ABA treatment resulted in no detectable expression of *WSD5* in roots. While the expression of *WSD6* was low in the unstressed leaf and root controls, the expression level increased strongly upon exposure to ABA, salt and drought stress in leaf and root tissue. Similarly, *WSD7* which was expressed in the unstressed leaf and root controls, was slightly higher expressed in leaves after exposure to all stress conditions and in roots after exposure to ABA and drought. Exposure to NaCl did not change the expression level of *WSD7* in roots compared to the unstressed control. In leaves, *WSD8* was expressed with similar low levels in the unstressed control and under all applied stress conditions. Only after 24 h of exposure to drought stress, expression of *WSD8* was not detectable anymore (Figure 15 A). *WSD8* was not expressed in roots neither with nor without stress application (Figure 15 B). *WSD9* was not expressed at all in leaves and very weakly expressed in roots after 12 h of exposure to 150 mM NaCl stress. *WSD10* was not expressed in leaf tissue and the expression was also not induced after exposure to stress. In roots, by far the highest expression level of *WSD10* was detectable in the unstressed control plant (Figure 15 B). The exposure to ABA resulted in the complete loss of the gene expression of *WSD10* in roots. The exposure to salt resulted in a decrease

in the expression level after 12 h compared to the control (0 h) and a further decrease in the gene expression level after 24 h. The exposure to drought resulted in a similar decrease in gene expression level after 12 h and 24 h compared to the control for *WSD10*. *WSD11* was not expressed in any leaf or root sample, independent if the plants were stressed or not.

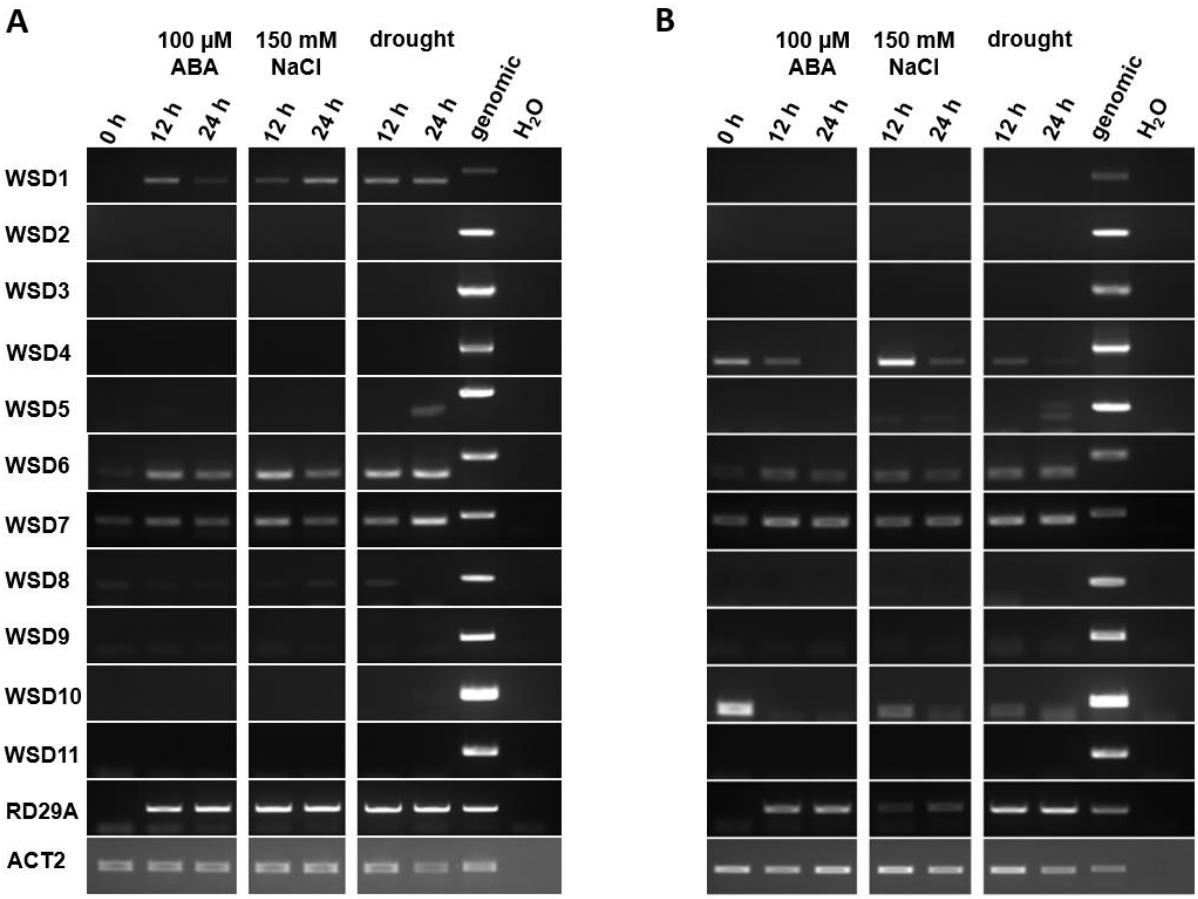

Figure 15: Expression of WSD Genes under Exposure to Different Stresses.

Arabidopsis thaliana wild type plants were grown in hydroponic cultures for 3 weeks. Then the plants were exposed for 12 or 24 hours to ABA, NaCl or drought and after that, leaf and root tissues were harvested for RNA extraction. 0 h represents plants which were not stressed (controls). RD29A was employed as control for drought stress. ACT2 was used as housekeeping gene. A PCR with H_2O as template was done to demonstrate absence of contaminating templates. Genomic DNA was used to show the differences in size between genomic PCR product and RT-PCR products. Semiquantitative PCR was performed for leaf tissue (**A**) and root tissue (**B**), the PCR products separated by agarose gel electrophoresis and visualized by UV light after ethidium bromide staining.

3.4 *WSD3* and *WSD10* cDNA Sequences

As no complete cDNAs of *WSD3* and *WSD10* were available in the stock centers, the sequences were amplified by RT-PCR using cDNA generated from inflorescences (*WSD3*) or roots (*WSD10*). The PCR was performed with the *Pfu* DNA polymerase and oligonucleotides as listed in Table 8 in the Appendix. Two PCR products were obtained for *WSD3* and one PCR product for *WSD10*. All PCR products were cloned into the pJET1.2/blunt vector and subjected to sequencing on one strand. Oligonucleotides used for sequencing are listed in Table 9 in the Appendix. Furthermore,

the full-length cDNA sequences, aligned to the genomic sequences found at TAIR are shown in the appendix (see Figures 44 and 45).

Sequencing of the two RT-PCR products for *WSD3* showed that the pre-mRNA of this gene is spliced into two splice variants: the larger splice variant 1 (Figure 16 A) has the size of 1464 bps encoding a protein of 487 amino acids (aa), the smaller splice variant 2 features only 891 bps encoding a protein of 296 aa. Compared to the different sequences found at TAIR, the large splice variant 1 is composed of all seven annotated exons, while for splice variant 2 the second exon is completely absent explaining the shorter size. Additionally, the first base triplet of the annotated exon 4 was absent in both splice variants. These three bases were spliced out and therefore represent the endmost base triplet of the third intron. Although the annotated intron-exon border was shifted for the third intron/fourth exon, the third intron ends with the codons A and G according to the GT-AG-rule which implies that many introns start with GT and end with AG.

The sequenced *WSD10* RT-PCR product is also different from the annotated sequences found at TAIR. While the *WSD10* sequence obtained from root tissue has a size of 1434 bps encoding a

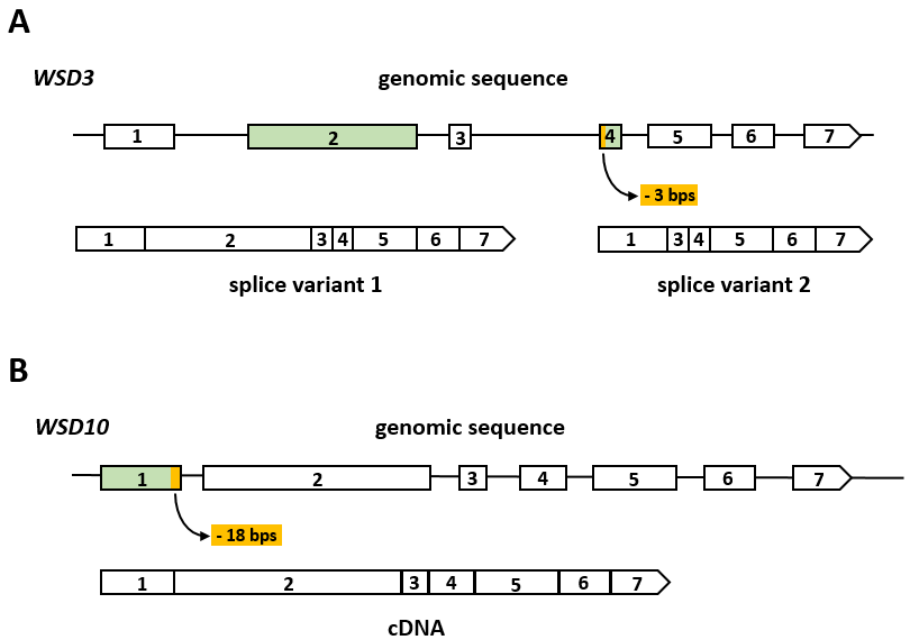

Figure 16: cDNAs of *WSD3* and *WSD10* - Splice Variants and Differences from Gene Annotations at TAIR.

RNA was isolated from different plant organs of *Arabidopsis thaliana* Col-0 wild type and cDNA was synthesized. Semiquantitative RT-PCR was performed for all 11 *WSD* genes indicating that *WSD3* is expressed in inflorescence and *WSD10* in root tissue. The cDNAs of both genes were amplified with *Pfu* DNA Polymerase resulting in two RT-PCR products for *WSD3* and one for *WSD10*. The RT-PCR products were subcloned and sequenced and compared to the annotated coding sequences found at *The Arabidopsis Information Resource* (TAIR). For *WSD3*, both sequenced RT-PCR products lack three base pairs, TAG, annotated to be the first triplet of the fourth exon (**A**). While splice variant 1 of *WSD3* is composed of all seven exons, the second and largest exon is completely missing in splice variant 2. Regarding *WSD10*, the sequenced cDNA lacks the last 18 bps of the annotated exon 1 (**B**).

477 aa protein, the sequence annotated at TAIR is 18 bps larger (Figure 16 B). This is due to the first annotated exon in which the endmost 18 bps are present in the TAIR sequence while they are removed in the sequenced RT-PCR product from roots, where these 18 bps are part of the first intron. Similar to *WSD3*, despite the shifting of the intron-exon border, the first intron of *WSD10* (according to the sequenced RT-PCR product) starts with GT following the GT-AG rule.

3.5 Subcellular Localization of WSD Proteins

While WSD1 was characterized to reside at the ER membrane (Li *et al*., 2008) and WSD11 was found to be localized in the plasma membrane (Takeda *et al*., 2013), the subcellular localization of the other WSD proteins were not known during the experimental part of this work. Therefore, it was aimed at cloning DNA constructs for subcellular localization studies of the WSD proteins except for WSD1 and WSD11. The aim was to introduce the *WSD* cDNAs together with *eGFP* fused either with its 5' or with its 3' end to the *WSD* cDNAs into the modified pLH9000 vector designated as pLHGCSATRNAi (Dr. Georg Hölzl, IMBIO, University Bonn, Germany; vector map see Figure 46 in the Appendix) thereby yielding the constructs pL-35S-*eGFP*-*WSD* or pL-35S-*WSD*-*eGFP*. For subcellular localization studies, *N. benthamiana* leaves were infiltrated with *A. tumefaciens* cultures carrying the pL-35S-*eGFP*-*WSD* or pL-35S-*WSD*-*eGFP* constructs. Furthermore the leaves were co-infiltrated with cultures carrying the pCB-*DsRed*-ER containing the HDEL retention signal and with cultures carrying the *p19* construct supporting the efficient expression of the cDNAs.
In Figure 17, the results of the subcellular localization studies obtained so far are depicted for WSD3 (splice variant 1 was used for cloning, see Figure 16), WSD4 and WSD9. At the end of this work, the cloning of the residual *WSD* cDNAs was at the point of moving the sequenced cDNAs from pJET1.2/blunt into the pLHGCSATRNAi vector. While WSD3 is fused with its C-terminus to eGFP, WSD4 and WSD9 are fused N-terminally to eGFP. The merged pictures of the green fluorescing WSD3-eGFP and eGFP-WSD4 and eGFP-WSD9 proteins with the coexpressed red fluorescing (DsRED) ER marker resulted in an overlay of green and red fluorescing structures. These results suggest that the three WSD proteins, WSD3, WSD4 and WSD9, localize at the ER.

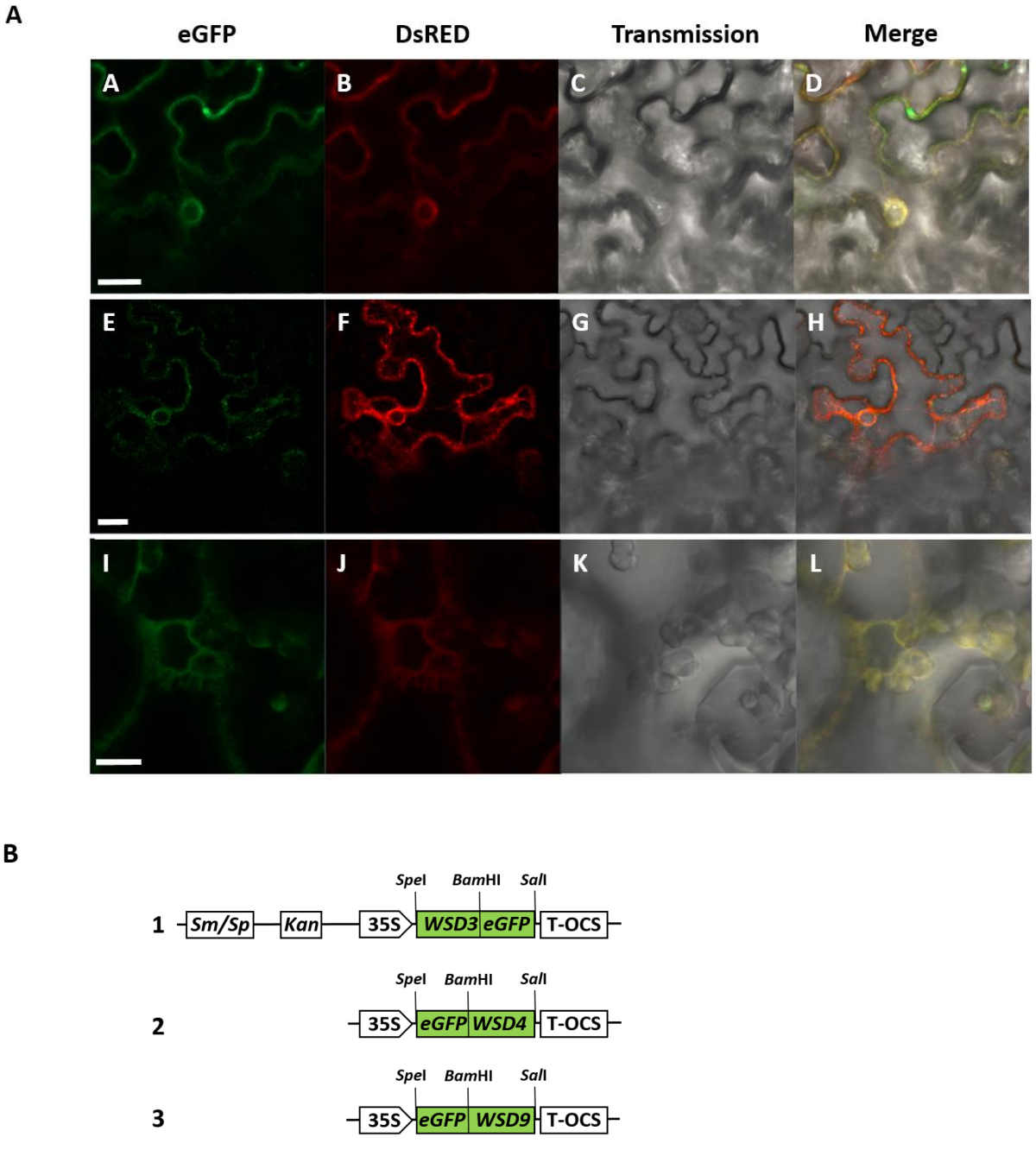

Figure 17: Subcellular Localization of WSD3, WSD4 and WSD9.

WSD cDNAs fused N-terminally or C-terminally to *eGFP* were co-expressed with the ER-marker HDEL-DsRED in *N. benthamiana* leaf epidermal cells. Three days after leaf infiltration, green and red fluorescences were measured by confocal fluorescence microscopy. Merged photos of green and red fluorescing leaf cells suggest that WSD3, WSD4 and WSD9 localize at the ER. The individual photos show the eGFP signal of WSD3 (A), WSD4 (E) and WSD9 (I), the DsRED signal of the ER-Marker (B, F, J), the bright field (C, G, K) and the merged picture (D, H, L). Size bars = 20 µm (A, E), size bar = 10 µm (I) (**A**). In (**B**) information about the fusion constructs are given (1, 2, 3: detail from pLGCSATRNAi).

3.6 Heterologous Expression of WSD1 in *Saccharomyces cerevisiae*

As it was published in Li *et al.*, 2008, expression of WSD1 in the yeast mutant *S. cerevisiae* H1246 (Sandager *et al*., 2002) supplemented with palmitic acid and primary fatty alcohols should lead to wax ester synthase activity. *S. cerevisiae* H1246 lacks the genes of four acyltransferases involved in triacylglycerol and steryl ester synthesis and therefore represents an optimal host for the expression of the putative bifunctional *WSD* cDNAs from *Arabidopsis*.

As it was described by Li *et al.*, 2008, *WSD1* was introduced into the vector pESC-URA which was then transferred into the yeast mutant *S. cerevisiae* H1246. Positive transformed clones were cultivated in minimal dropout medium lacking uracil for selection and glucose to ensure repression of the GAL promoter of pESC-URA. Expression of *WSD1* was induced with galactose. Palmitic acid (16:0) and a long chain fatty alcohol, either octadecanol (18:0ol), tetracosanol (24:0ol) or octacosanol (28:0ol), were added. Li *et al*., 2008, detected wax esters in *WSD1* expressing cultures after separating the respective lipid extracts on a TLC plate. Li and coworkers further confirmed the identity of the synthesized wax ester species 18:0ol/16:0, 24:0ol/16:0 and 28:0ol/16:0 by isolating the wax esters from a TLC plate and analyzing them by GC-MS.

In the present work, *WSD1* and the other *WSD* cDNAs (except *WSD3* and *WSD10*) were cloned into pDR196, a yeast expression vector with a constitutive PMA promoter. Therefore, the induction of gene expression was not necessary. Besides pDR196-*WSD1*, another two constructs, pESC-URA-*WSD1* and pYES2-*WSD1*, were employed for the heterologous expression of WSD1 in *S. cerevisiae* H1246. While pYES2-*WSD1* (glycerol stock number PD812) was previously generated by Dr. Antje Lohmann (MPI Golm, now: Merck KGaA, Darmstadt, Germany), pESC-URA-*WSD1* was generated by moving *WSD1* from pESC-TRP into an empty pESC-URA vector (both, the pESC-TRP-*WSD1* and pESC-URA, were obtained from Prof. Dr. Ljerka Kunst, University of British Columbia, Vancouver, British Columbia, Canada). For the later construct, both, the *WSD1* cDNA and the pESC-URA vector were the same as used in the publication of Li *et al.*, 2008, and the cloning of the *WSD1* cDNA was performed with same restriction sites (*Xho*I, *Bam*HI).

The heterologous expression of WSD1 was performed as described in Li *et al*., 2008 using *S. cerevisiae* H1246 as host. While WSD1 expression in the pESC-URA and pYES2 constructs was induced by galactose, expression of WSD1 in pDR196 was constitutive. Octadecanol (18:0ol) and palmitic acid (16:0) were added into the culture medium. After harvesting the cells, the lipids were extracted and purified by SPE. The wax ester fraction was then analyzed by TLC (Figure 18) and after preparative TLC by Q-TOF MS/MS (Figure 20). Detailed information on the analysis of WEs by Q-TOF MS/MS is given below in 3.8.

As shown in Figure 18, no WEs were detectable for any of the WSD1 constructs on the TLC plate, neither after exposure to iodine vapor, nor after charring of the plate. The 20:0ol/15:0 WE used as standard was hardly detectable after exposure to iodine vapor which is due to the lack of C=C double bonds (Fuchs *et al*., 2011). However, since unsaturated fatty acids like palmitoleic acid

(16:1) and oleic acid (18:1) are abundant in yeast, WE species with a higher degree of unsaturation which might have been synthesized by WSD1 should be detectable by iodine staining.

Interestingly, an unknown lipid ("unknown lipid 1" = UL1) spot became visible below the wax ester band on the TLC plate (Figure 18) and was only present in those samples in which WSD1 has been expressed.

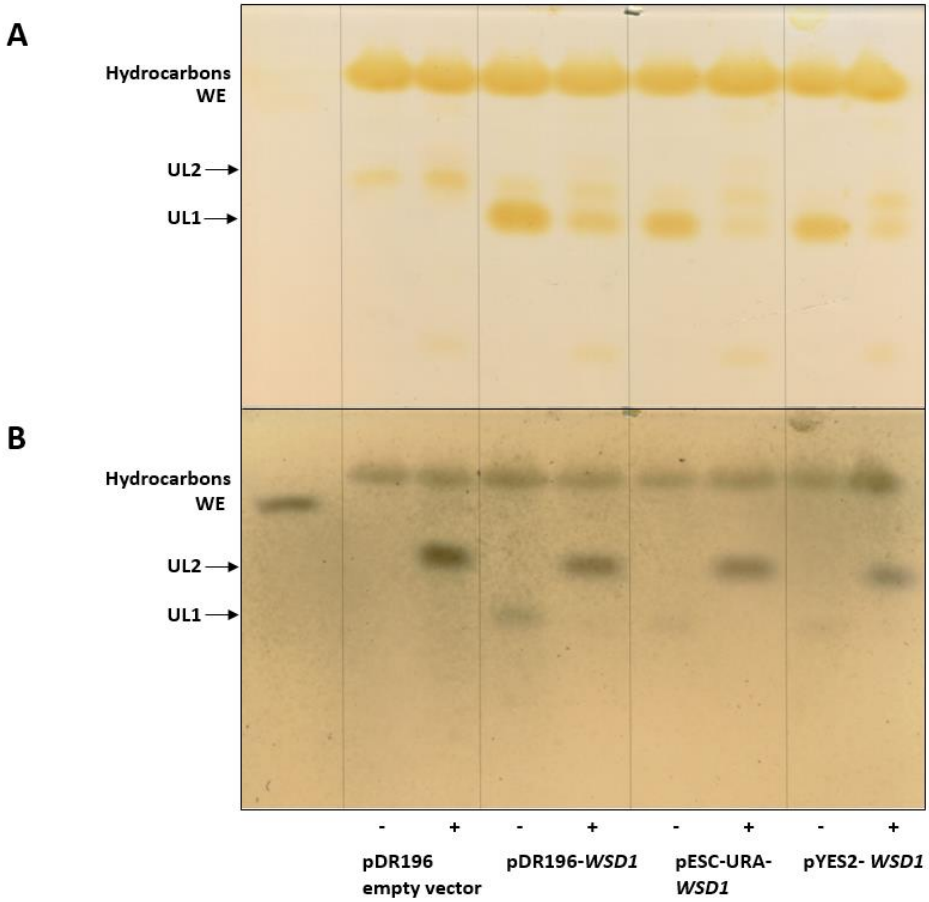

Figure 18: TLC Plate of Yeast Lipids Representing Different WSD1 Expressing Cultures.

Yeast cultures, *S. cerevisiae* H1246, were grown with or without 18:0ol fatty alcohol and 16:0 fatty acid. Yeast cultures were harvested and the lipids extracted and further purified by solid phase extraction. These wax ester fractions were separated by TLC, afterwards the separated lipids were first visualized by staining with iodine (**A**), later the same plate was incubated with α-naphthol and charred (**B**). 50 µg of 20:0ol/15:0 wax ester (WE) was used as reference. While no wax esters were detected, unknown lipids 1 and 2 (=UL1, UL2) were found either only in cultures expressing WSD1 (UL1) or in samples of cultures supplemented with palmitic acid and octadecanol (UL2). +, cells grown in the presence of 18:0ol and 16:0; -, cells grown without 18:0ol and 16:0.

This unknown lipid is clearly absent in the control (pDR196 empty vector). The unknown lipid spots appeared more intense after exposure to iodine vapor compared to the intensity of the spots after charring. Furthermore, a higher amount of the unknown lipid appeared to be synthesized in those expression cultures that were not supplemented with octadecanol and palmitic acid. This

was visible by larger and more intense spots compared to the cultures which were supplemented with octadecanol and palmitic acid. Besides the unknown lipid spots found only in the lanes of the WSD1 expression samples, a further unknown lipid ("unknown lipid 2" = UL2) was detected on the TLC plate in the lanes of those cultures that were supplemented with octadecanol and palmitic acid (Figure 18 B). Thus, UL2 occurred not only in the WSD1 expression samples but in the control sample as well. While UL1 spots were much more intense after incubation of the TLC plate in iodine vapor, UL2 spots were much better visible after the lipids were charred. Since UL2 occurred also in the lane of the empty vector control, the synthesis of this lipid was independent of WSD1. Therefore, the identity of UL2 was not examined further.

A preparative TLC was performed to separate the unknown lipid UL1 from all other lipids present in the wax ester fraction. UL1 spots of the pDR196-*WSD1* construct were scraped out from the plate. Furthermore, the comigrating areas of the pDR196 empty vector control containing no visible lipid spots were scraped out. The lipids were extracted and dissolved in Q-TOF running buffer and analyzed by direct infusion Q-TOF MS (Figure 19A). Later, the solvent was evaporated and the sample was dissolved in tetrahydrofuran/methanol (2:1 (v/v)) for direct infusion Q-TOF MS/MS analysis in which molecules with m/z of 300 - 1000 were selected and fragmented.

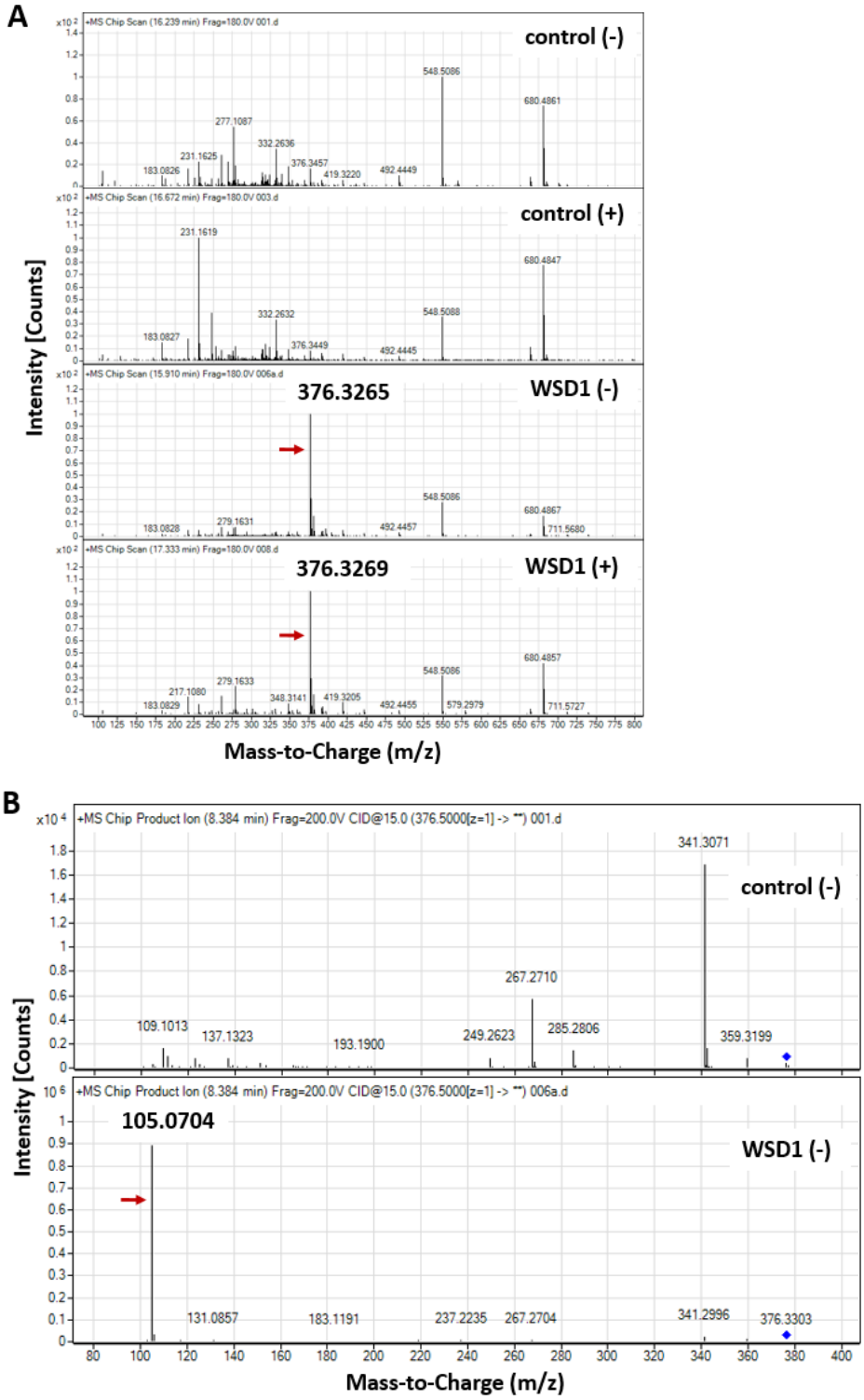

Figure 19: Q-TOF MS and MS/MS Analysis of the Unknown Lipid 1 (UL1) Synthesized in WSD1 Expressing Yeast Cultures.

S. cerevisiae H1246 cells expressing WSD1 inserted in pDR196 or harboring the empty vector as control were grown with 18:0ol alcohol and 16:0 fatty acid (+) or without these supplements (-). Lipids were extracted and purified by SPE to isolate wax esters, the purified wax ester fraction contained also UL1. A portion of the purified wax ester fraction was analyzed by TLC (see Figure 18), another portion by Q-TOF MS/MS (see Figure 20). A third portion of the total wax extract was separated by TLC and the unknown lipid UL1 migrating a little slower than wax esters was isolated from the plate. The UL1 samples were analyzed by Q-TOF MS without fragmentation (total ion chromatograms, **A**) and MS/MS (fragmentation of m/z around 376.5, **B**).

As visible in Figure 19 A, the total ion chromatogram of the WSD1 expressing samples has relatively high amounts of an ion with m/z of 376.3265. Looking at the total ion chromatogram (TIC) of the control, a peak at m/z of 376.3449 or 376.3457 is present, but in clearly lower abundance. The accuracy of the MS experiments shown in Figure 19A is about m/z of 0.001 as most of the background signals are different by m/z of 0.001 or less. However, the signals of the WSD1 sample (376.3265) and of the controls (376.3449 or 376.3457) differ by m/z of 0.02, indicating that the molecular ions are distinct. Also the fragmentation of ions with m/z around 376.5 reveals a very different pattern comparing WSD1 and the control sample (Figure 19 B). Therefore, the ions occurring after fragmentation in the MS/MS spectra of the WSD1 expressing samples and of the control samples do not originate from the same parental ion. Therefore, the ion with m/z of 376.3265 can represent the unknown lipid UL1 found in WSD1 expressing samples which is absent in the control samples (see Figure 18A).
The fragmentation of the parental ion with m/z of 376.3265 found in the WSD1 expressing sample revealed as main fragment an ion with m/z of 105.0704 (Figure 19 B).
Besides the highly abundant ion with m/z of 376.3265, also parental ions with other m/z ratios with a fragmentation pattern containing the fragment ion with m/z of 105.07 occur in the TIC of the WSD1 expressing sample. Additional parental ions that after fragmentation give rise to a fragment ion with m/z of 105.07 and that only occur in the TIC of WSD1 have m/z of around 277, 294, 308, 310, 326, 350, 359, 362, 376, 392, 404 or are larger (between 1000 and 1058). In addition, parental ions with m/z of 322 and 326 with a distinct peak of m/z of 105.07 occur in both, the control and WSD1 expressing samples, and therefore are unspecific.

The third part of the SPE purified wax ester extract was used for Q-TOF MS/MS analysis (Figure 20). Wax esters, both 18:0ol/16:0 and 18:0ol/18:0, were detected in samples of those cultures which were supplemented with octadecanol and palmitic acid. The synthesis of wax esters occurred independently of WSD1 expression, in fact, the highest amount for the two molecular wax ester species was synthesized in the control yeast cells harboring an empty pDR196 vector.

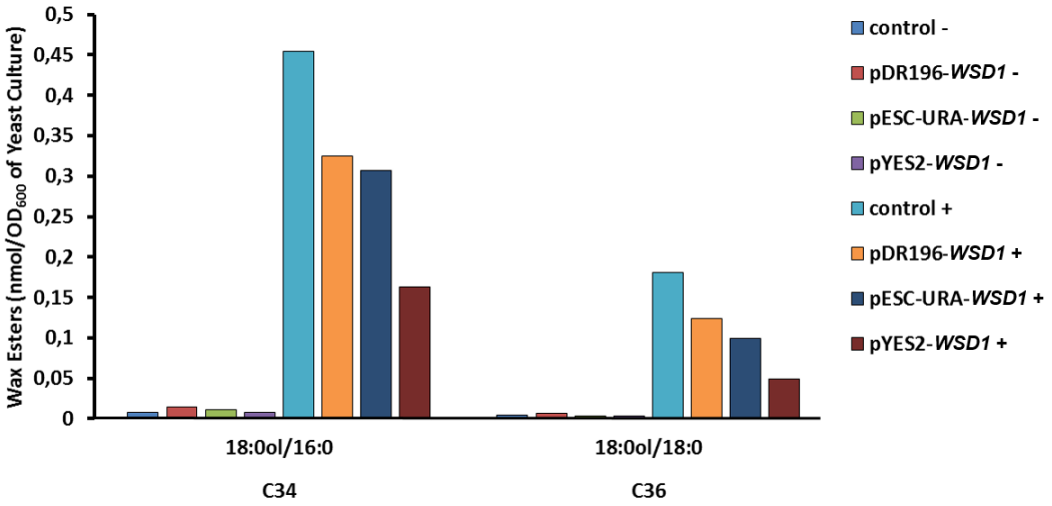

Figure 20: Wax Ester Species Synthesized in Yeast Cultures Grown with 16:0 Fatty Acid and 18:0ol Fatty Alcohol.

Yeast cultures were grown with 16:0 fatty acid and 18:0ol fatty alcohol (+) or without these substrates (-). The lipids were extracted and purified by solid phase extraction. The wax ester fraction was analyzed by Q-TOF MS/MS. Data represent one measurement of one sample.

3.7 Coexpression of *Ma*FAR and WSD1 in *Saccharomyces cerevisiae*

Another approach to demonstrate wax ester synthase activity of WSD1 after heterologous expression in yeast was the coexpression of the *WSD1* cDNA with the fatty acyl-coenzyme A reductase from *Marinobacter aquaeolei* VT8 (*MaFAR*) (Hofvander *et al*., 2011). *Ma*FAR is known to reduce various fatty acyl-CoA substrates to the respective fatty alcohols, including 16:0-CoA, 18:0-CoA, 18:1-CoA (Hofvander *et al*., 2011). These acyl-CoA species together with 16:1-CoA are abundant in yeast (Kalscheuer *et al*., 2004; Suutari *et al*., 1990). Additionally, 18:0ol alcohol was shown to be a substrate of WSD1 (Li *et al*., 2008).

Thus, coexpression of *Ma*FAR with WSD1 should lead to the synthesis of fatty alcohols like octadecanol in yeast and thereby provide WSD1 with endogenous substrates, the fatty alcohol and fatty acyl-CoA. Thus, it should be excluded that the lack of enzymatic activity found in WSD1 expressing yeast was caused by a lack of uptake of supplemented fatty alcohol substrate from the medium.

In preparation of the coexpression experiment, *WSD1* or *MaFAR* were inserted into the pESC-URA vector (which harbors two expression cassettes), either alone or together. The four constructs, pESC-URA-*WSD1*, pESC-URA-*MaFAR*, pESC-URA-*WSD1-MaFAR* and empty pESC-URA vector were transferred into *S. cerevisiae* H1246 and clones growing on selective medium were employed for the expression study. The clones were cultivated without supplementation of fatty alcohol and fatty acid substrates. After extracting the lipids of the cultures, a wax ester fraction was isolated by SPE. The dried wax ester fraction was dissolved in Q-TOF running buffer and the samples were analyzed by Q-TOF MS/MS. Wax ester amounts of saturated and unsaturated molecular species were calculated relative to the internal standard of 1 nmol of 18:0ol/17:0.

As depicted in Figure 21, wax esters were synthesized especially in the cultures expressing *Ma*FAR alone or, coexpressing WSD1 and *Ma*FAR. Wax ester levels differing slightly from the control were also found in samples expressing WSD1 alone.

The most abundant wax esters produced contained only saturated alcohols and fatty acids. However, also wax esters harboring a double bond in the alcohol or fatty acid moiety occurred in lesser amounts. The highest amounts of wax esters were measured in those cultures expressing *Ma*FAR alone: Therefore, wax ester synthesis in *S. cerevisiae* H1246 was independent from WSD1.

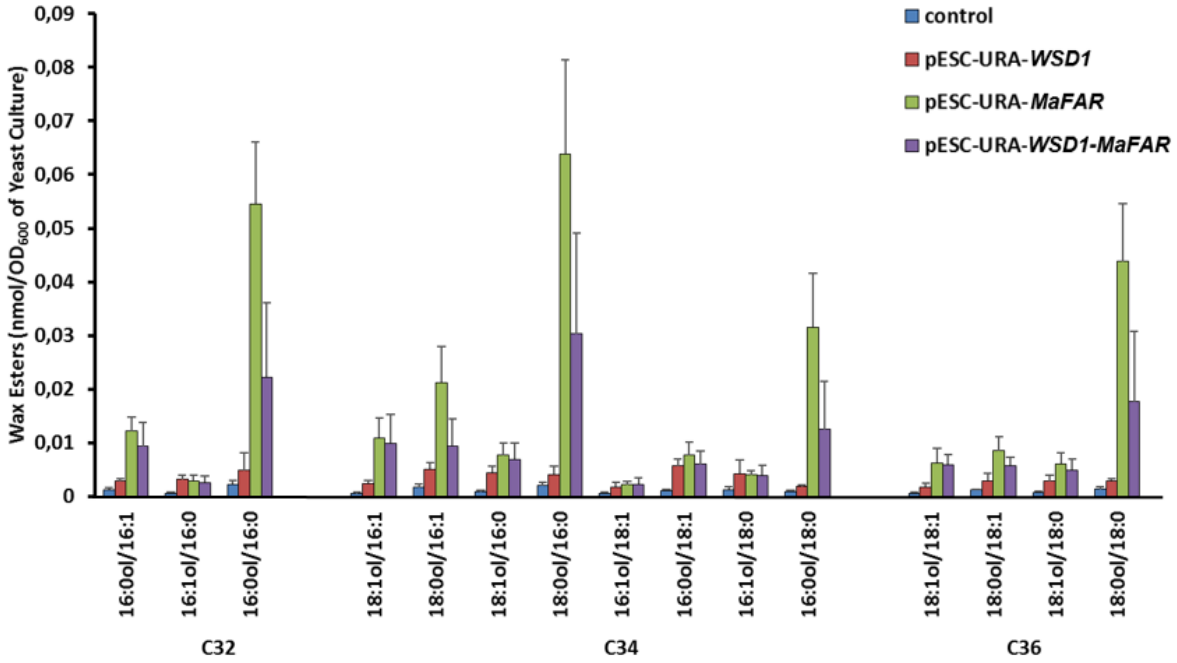

Figure 21: Heterologous Coexpression of WSD1 and *Ma*FAR in Yeast.

Cultures of *S. cerevisiae* H1246 expressing either WSD1, *Ma*FAR or WSD1 and *Ma*FAR as well as cultures harboring the empty vector control, pESC-URA, were harvested and the lipids extracted. The wax ester fractions were isolated by solid phase extraction and quantified by Q-TOF MS/MS analysis. Data represent mean and standard deviations of 3 measurements.

3.8 Analysis of Wax Esters by Q-TOF MS/MS

3.8.1 Sample Preparation prior to MS/MS Analysis

For the measurement of WEs, the 6530 Accurate-Mass Quadrupole Time-of-Flight (TOF) LC/MS mass spectrometer (Agilent) was used. The WEs were selected by their m/z ratios as ammonium adducts (see Tables 13 -14 in the Appendix), fragmented in the collision cell and the protonated fatty acids which were accompanied with the neutral loss of the alcohol and NH_3 were identified. The typical fragmentation pattern of a saturated wax ester is demonstrated in Figure 22. Here, the 18:0ol/17:0 WE species which was used as internal standard for the WE measurements in plants and yeast was fragmented. Figure 22 A displays the high abundance of the protonated heptadecanoic acid fragment $[C_{17}H_{34}O_2+H]^+$ with a calculated m/z of 271.2632. This product ion

was used for the quantification of the WE species. Figure 22 B presents the site of fragmentation of the WE 18:0ol/17:0 by a dashed line. It also shows that the precursor molecule is positively charged by forming an ammonium adduct $[C_{35}H_{70}O_2+NH_4]^+$.

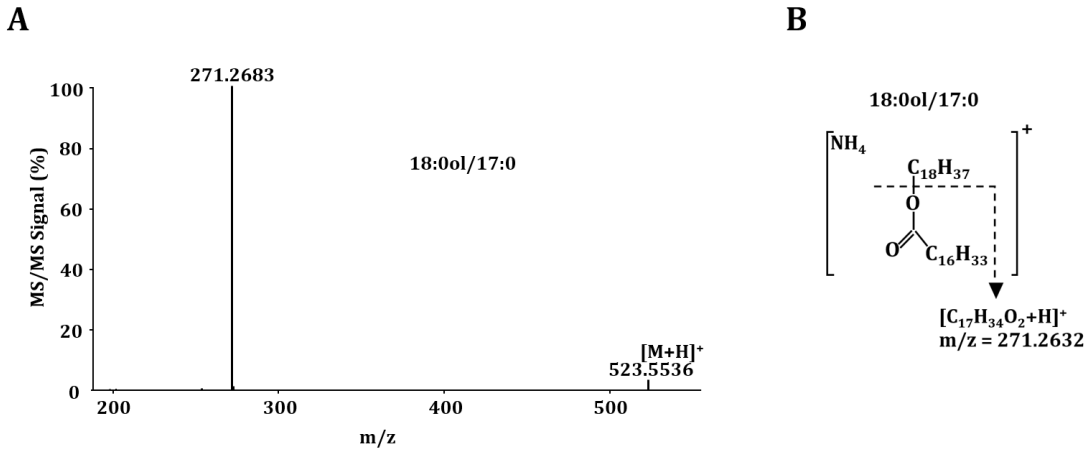

Figure 22: Typical Fragmentation Pattern of a Saturated Wax Ester Species.

The fragmented wax ester species 18:0ol/17:0 displayed a high MS/MS signal of a fragment with m/z of 271.2683 (**A**). This product ion is the protonated heptadecanoic acid which is in later studies used for the quantification of WEs. (**B**) displays the fragmentation site of 18:0ol/17:0 by a dashed line. Furthermore, it shows that the WE molecule forms an ammonium adduct prior to fragmentation which is positively charged.

Prior to MS/MS analysis, the extracted wax esters were purified to avoid false positive signals by contaminants and a suppression of ionization of the wax esters by other highly abundant lipids in the samples. Purification of wax esters was also applied by Iven *et al*., 2013; Fitzgerald and Murphy, 2007; Vrkoslav *et al*., 2010 to separate WEs from other lipids (except from steryl esters) by preparative TLC prior to analysis. In these publications, no preferential loss of any wax esters during purification was mentioned (Iven *et al*., 2013; Fitzgerald and Murphy, 2007; Vrkoslav *et al*., 2010). In this work, wax esters from *A. thaliana* leaf and flower wax which was either purified or not purified were measured by MS/MS analysis without purification and after purification. The unpurified samples contained the wax from 10 flowers per sample which was extracted for 30 s with chloroform. The wax extract was collected, the plant tissue was reextraced with fresh chloroform, and then both extracts were combined as described in 2.3.11.6. Leaf wax esters were extracted from three rosette leaves in the same way and the surface area of the leaves were determined as described in 2.3.11.6.

The purification of leaf and flower wax was performed at a later date with wax originating from another sets of plants. The plants grew under the same conditions like the plants from which the wax esters were measured without purification. Again, wax from 10 flowers per sample and this time, from 20 rosette leaves was extracted. The purification of the flower wax extract was done by SPE, the leaf wax extract was portioned and one portion was purified by SPE and another portion was purified by TLC as described in 2.3.11.2 and 2.3.11.3. The results obtained from the

MS/MS analysis for the purified and unpurified samples are presented in one single diagram for leaf wax esters and one single diagram for flower wax esters. This was done to ease the comparison of purified with unpurified samples though they originate from plants grown at different dates (Figure 23 and Figure 24). In both diagrams, high amounts of ions with m/z's resembling m/z's of wax esters are present in the unpurified leaf and flower samples (Figure 23 and Figure 24, "chloroform"). In leaf wax, ions with m/z resembling the m/z of the 20:0ol/20:0 wax ester are most abundant followed by lower amounts of ions with m/z's resembling m/z's of 16:0ol/24:0 and 20:0ol/22:0 (Figure 23 "chloroform"). In flower wax, ions with m/z's resembling m/z's of three C_{48} wax ester species 34:0ol/14:0, 32:0ol/16:0 and 30:0ol/18:0 are most prominent, additionally ions with m/z resembling the m/z of the 20:0ol/20:0 wax ester which are also found in the unpurified leaf wax are measured in flower wax (Figure 24 "chloroform"). However, in leaf and flower wax which was purified prior to MS/MS analysis, these highly abundant ions with m/z's resembling the above mentioned wax ester species are hardly present (Figure 23 and Figure 24, "SPE" and "TLC"). Therefore, it is likely that these ions represent disturbing contaminations which are removed by purification of wax esters. Furthermore, purification by SPE and TLC resulted in similar amounts of the analyzed WE species thereby

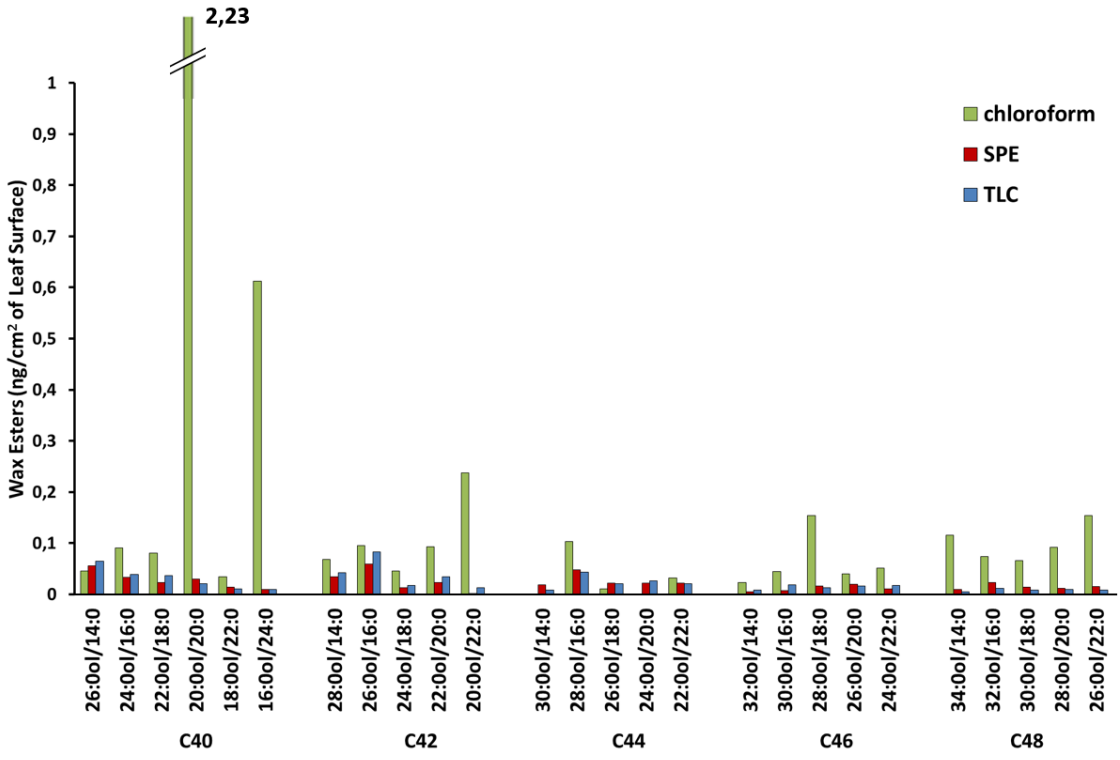

Figure 23: Leaf Wax Esters – Analysis of Unpurified and Purified Wax Extracts.

Leaf wax from *A. thaliana* wild type was extracted by chloroform and an internal standard (18:0ol/17:0) was added. The solvent was evaporated and the wax extract used directly for Q-TOF MS/MS analysis ("chloroform"). Separately, leaf wax extract was further purified by TLC (hexane/diethyl ether/acetic acid 85:15:1 (v/v/v)) ("TLC") or by SPE (hexane/diethyl ether 99:1 (v/v))("SPE"). WEs from purified samples originated from another set of plants grown at a later date under the same conditions than WEs from unpurified samples. Data are derived from one measurement.

indicating that both purification methods are likewise suitable for the purification of WEs. Jenks *et al.*, 1995, analyzed leaf wax components by first isolating the wax esters from other wax components by TLC and then measuring them by GC-FID. By this method, they found a total wax ester amount of 2 ng/cm² for *Arabidopsis thaliana* ecotypes Ler and WS. This total amount of WEs of 2 ng/cm² lays between the total amounts of unpurified and purified samples measured in this study. Jenks and coworkers did not mention the high amount of the single wax ester species 20:0ol/20:0. Regarding flower WEs, Bernard and Joubès, 2013 published the occurrence of WEs with chain lengths from C_{38} to C_{46} in *Arabidopsis* flower wax, while the occurrence of WEs with the chain length of C_{48} was not mentioned. This supports the assumption that the measured ions with m/z's resembling m/z's of WEs with C_{48} chain lengths in the unpurified flower wax samples represent contaminants.

Therefore, since the purification of wax esters is established (Iven *et al.*, 2013; Fitzgerald and Murphy, 2007; Vrkoslav *et al.*, 2010) and since the assumed contaminants are virtually absent in purified flower and leaf wax samples, all wax extracts from all *Arabidopsis* organs were purified by SPE as described in 2.3.11.6 prior to Q-TOF MS/MS analysis.

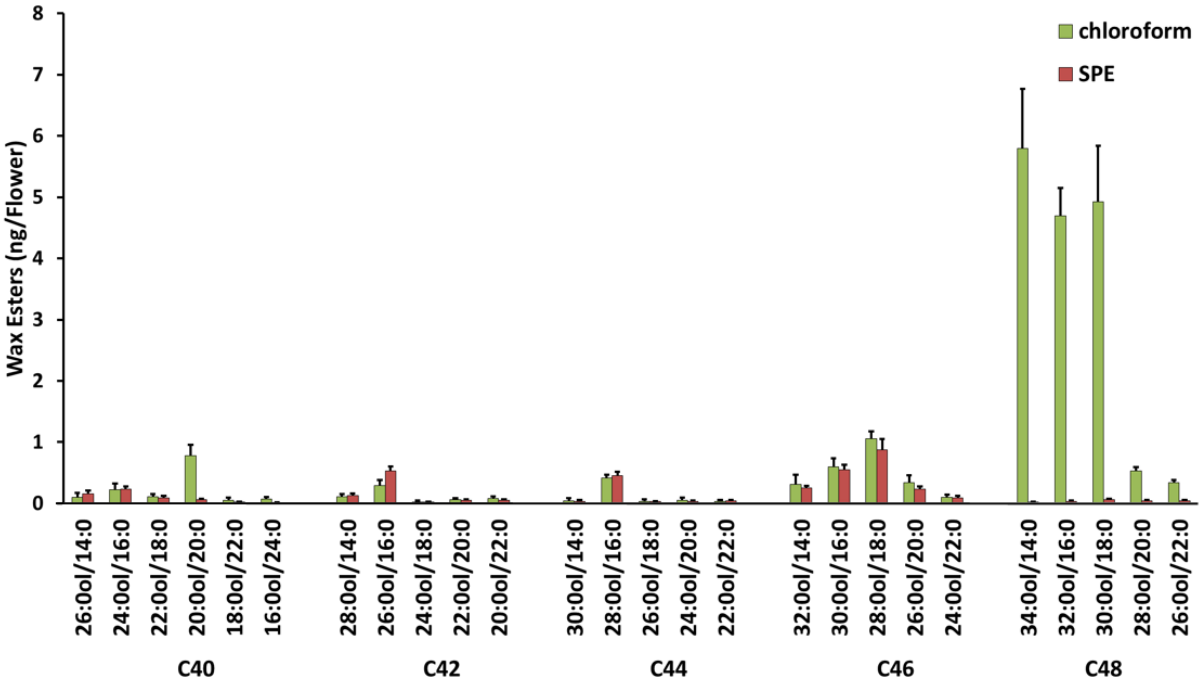

Figure 24: Flower Wax Esters – Analysis of Purified and Unpurified Wax Extracts.

Total cuticular wax of 10 flowers per sample from *A. thaliana* wild type was extracted with chloroform. The wax extract was either dissolved directly in Q-TOF running buffer and analyzed by Q-TOF MS/MS, or purified by SPE (hexane/diethyl ether 99:1 (v/v)) and then analyzed by Q-TOF MS/MS. WEs from purified samples originated from another set of plants grown at a later date under the same conditions than WEs from unpurified samples. Data represent mean and standard deviation of 5 measurements.

3.8.2 Isobaric Species of WEs

In principle, it is possible that the WE fraction contains steryl esters as contaminants although the wax extract was purified by SPE. Steryl esters accumulate in intracellular oil bodies (together with triacylglycerol), and therefore should not be extracted by isolating surface waxes. However, since also the cut edges of the analyzed plant organs were immersed in the solvent, little amounts of steryl esters might have been extracted.

Despite the purification of wax extracts by TLC or SPE, it is not possible to separate wax esters from steryl esters which co-migrate with wax esters on the TLC plate (Iven *et al*., 2013) and which are eluted in the same fraction as wax esters by hexane / diethyl ether 99/1 (v/v) from the silica column. Some steryl ester species harbor very similar m/z's of parental ions and of product ions compared to those of some wax ester species (Iven *et al.*, 2013). These isobaric species occurring in *A. thaliana* like sitosterol esters and cholesterol esters (Wewer *et al*., 2011; Iven *et al*., 2013) could lead to false positive signals and therefore, the measurement of those wax ester species was not considered. Wax ester species which are isobaric with steryl ester species, as well as their respective m/z of parental ions and of product ions are listed in Table 12 in the Appendix.

3.8.3 Wax Ester Standard and Carry-Over Effects

18:0ol/17:0 and 18:0ol/27:0 wax esters were chemically synthesized as standards for Q-TOF MS/MS analysis. The two wax ester species were quantified by GC-FID of the fatty acid methyl esters using 15:0 as internal standard after acidic methanolysis. After quantification, a standard mix containing 1 nmol of 18:0ol/17:0 and 3 nmol of 18:0ol/27:0 wax esters in 50 µl of chloroform was prepared.

The 18:0ol/27:0 wax ester turned out to be not useful as the signal intensity was very low. This was due to the low intensity of the product ion, $[C_{27}H_{54}O_2H]^+$ detected by the Q-TOF MS/MS compared to the product ion $[C_{17}H_{34}O_2H]^+$ of the 18:0ol/17:0 WE.

The second problem was the finding that the detection of the 18:0ol/27:0 wax ester was delayed in many runs compared to the 18:0ol/17:0 wax ester and the other wax esters. Apparently, the 18:0ol/27:0 wax ester was bound in the injection loop or ion source and only later desorbed.

Therefore, only the 18:0ol/17:0 wax ester was used as internal standard for data evaluation. The measurement of one wax ester sample was alternated with at least three other lipid samples to avoid occurrence of contaminants in the wax ester signals due to carry-over effects.

3.9 Wax Esters from Stem Surface Wax of the *wsd* Mutant Lines

For the qualitative and quantitative analysis of stem wax esters, homozygous *wsd* mutant lines and the corresponding wild type ecotypes as controls were used. Stem wax was extracted from inflorescence stems and the wax esters were then separated from other wax compounds by SPE

(see 2.3.11.3). The solvent of the purified wax ester fraction was evaporated and the dried lipids were dissolved in Q-TOF running buffer and analyzed by Q-TOF MS/MS (see 2.3.11.7). For quantification, 1 nmol of the standard 18:0ol/17:0 wax ester was used.
The stem wax esters of all homozygous mutant lines were measured. Here, most WE species searched for showed very low intensities (<100 counts per scan) for their respective product ions. Furthermore, the peaks of the product ions were often not higher than background peaks which hindered the clear identification of the wax ester species. Therefore, only few wax ester species could be clearly identified in stem wax. These WE species are 22:0ol/16:0, 24:0ol/16:0, 26:0ol/16:0 and 28:0ol/16:0. The other WE species displayed in the diagrams of stem wax esters showed very low intensities with peaks as low as background peaks which hinders their clear identification. Nevertheless, differences of these WE species between mutants and WT are mentioned in the results. Significant differences between mutant lines and the WT control were indicated only for the clearly identified WE species.

Below only the results showing differences between the WT and the mutant line(s) are depicted. When two mutant lines of one gene were analyzed, the results were only presented below when the differences between WT and mutant lines were present in both mutant lines.
All other results are found in the Appendix (see Figures 48 to 56). As depicted in Figure 25, wax ester chain lengths of C_{42}, C_{40}, C_{44} and C_{38} are most prominent in stems of Col-0 WT with amounts of approx. 0.023 µg/cm^2 for C_{40} and C_{42} chain lengths. Other less abundant wax ester chain lengths are C_{46}, C_{48}, C_{50}, C_{52} and C_{54}. As shown in Figure 26, the most abundant wax ester species measured in stems of Col-0 WT contain a 16:0 fatty acid moiety. The by far most abundant wax ester species occuring in wild type stems are 26:0ol/16:0, 24:0ol/16:0, 28:0ol/16:0, with amounts of approx. 0.017 µg/cm^2, 0.012 µg/cm^2 and 0.009 µg/cm^2 respectively.

As published by Li *et al*., 2008, WSD1 contributes to the wax ester synthesis in stem cuticles. The wax ester analysis of the *wsd1* mutant line confirms this result (Figure 26). The amounts of the most abundant wax ester species found in the wild type control (those with 16:0 acyl moiety: 26:0ol/16:0, 24:0ol/16:0, 28:0ol/16:0) are strongly reduced in the *wsd1* mutant line. Also other less abundant wax ester species, like 24:0ol/14:0, 26:0ol/14:0, 22:0ol/16:0 and 26:0ol/18:0 have reduced amounts in the mutant line. However, other wax ester species, like 20:0ol/20:0, 14:0ol/24:0, 20:0ol/22:0 and 30:0ol/18:0, have slightly increased amounts in the mutant line compared to the control.

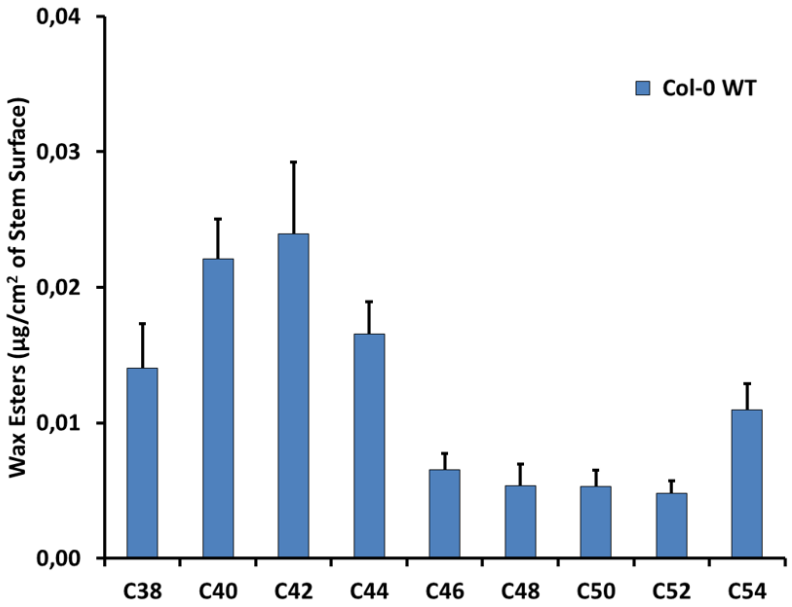

Figure 25: Stem Wax Esters from *A. thaliana* WT Col-0.

Wax from inflorescence stems was extracted with chloroform. The wax extract was fractionated by SPE (hexane/diethyl ether 99/1 (v/v)) and the wax ester fraction analyzed by Q-TOF MS/MS. The wax ester species with the same total chain length (alcohol + fatty acid) were summed up for each replicate. Five replicates were averaged and a standard deviation was calculated.

Another mutant line which showed an altered wax ester amount in stem compared to the wild type control is *wsd5* (Figure 27). Here, the mutant reveals a significant reduction in the wax ester species 24:0ol/16:0 compared to the wild type control.

The mutant lines *wsd7-1* and *wsd7-2* showed an altered wax ester amount in stem compared to the wild type control (Figure 28). Here, the wax ester species 24:0ol/16:0 and 28:0ol/16:0 revealed reduced amounts in both mutant lines, while the wax ester species 26:0ol/16:0 was only reduced to a significant extent in *wsd7-1*. The amounts of other wax ester species remained unaffected from the reduction.

Also the mutant line *wsd11* revealed a wax ester phenotype similar to *wsd5*, *wsd7-1* and *wsd7-2* (Figure 29): the amounts of the wax ester species with 16:0 acyl moiety showed reduced amounts in the stem wax. The amounts of other wax ester species like 20:0ol/20:0, 20:0ol/22:0, 30:0ol/16:0, 26:0ol/20:0 and 30:0ol/18:0 increase slightly compared to the wild type control.

The homozygous double mutant line *wsd1* x *wsd4-2* showed a very similar reduction of the same WE species compared to the WT control like the mutant *wsd1* (Figure 26). Therefore, the results are presented in the Appendix (Figure 57).

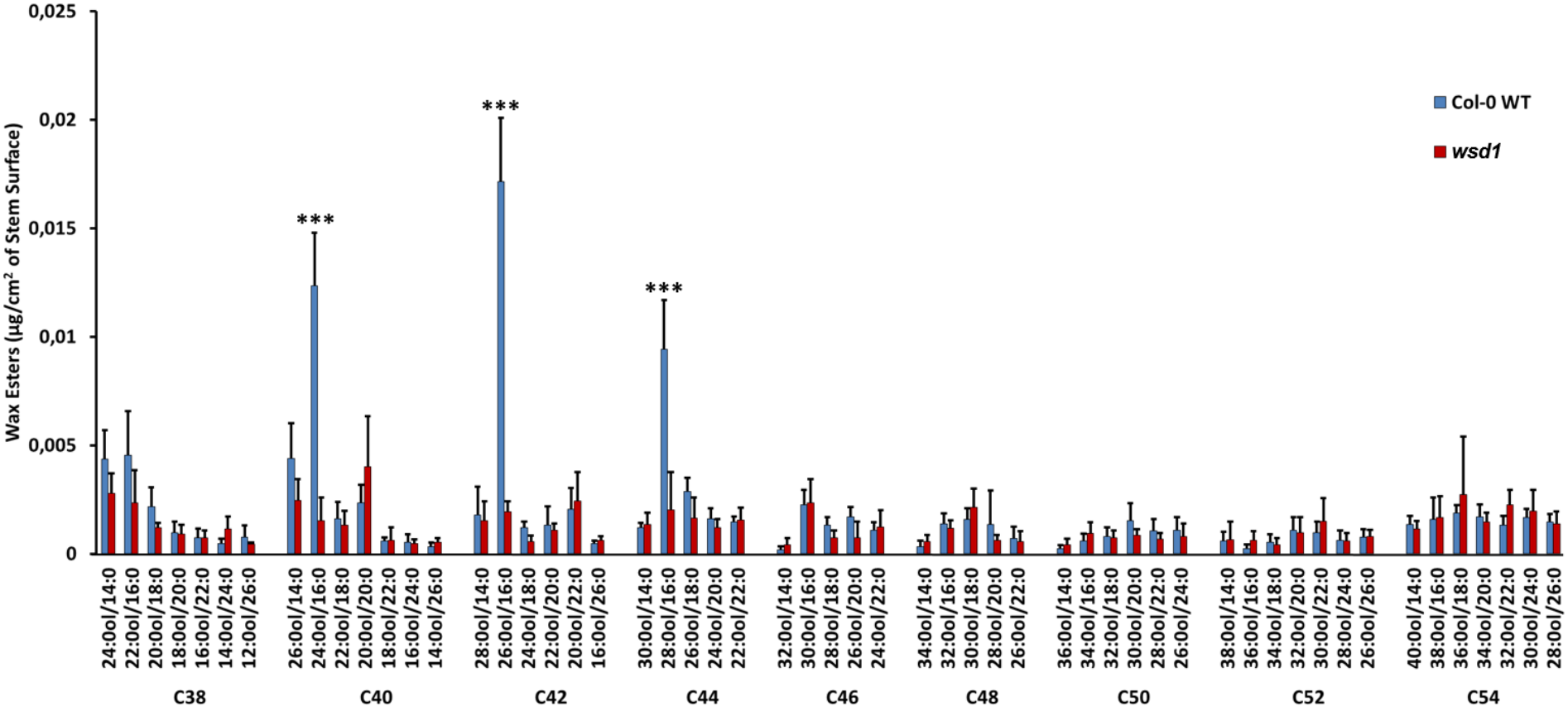

Figure 26: Stem Wax Esters from *A. thaliana* WT and Mutant Line *wsd1*.

Wax from inflorescence stems was extracted by chloroform. The wax extract was fractionated by SPE (hexane/diethyl ether 99/1 (v/v)) and the wax ester fraction analyzed by Q-TOF MS/MS. Data represent mean and standard deviation of 5 measurements. Asterisks indicate values that differ significantly from the wild type control (Student's *t* test, Welch correction, $P<0.01$ (***)).

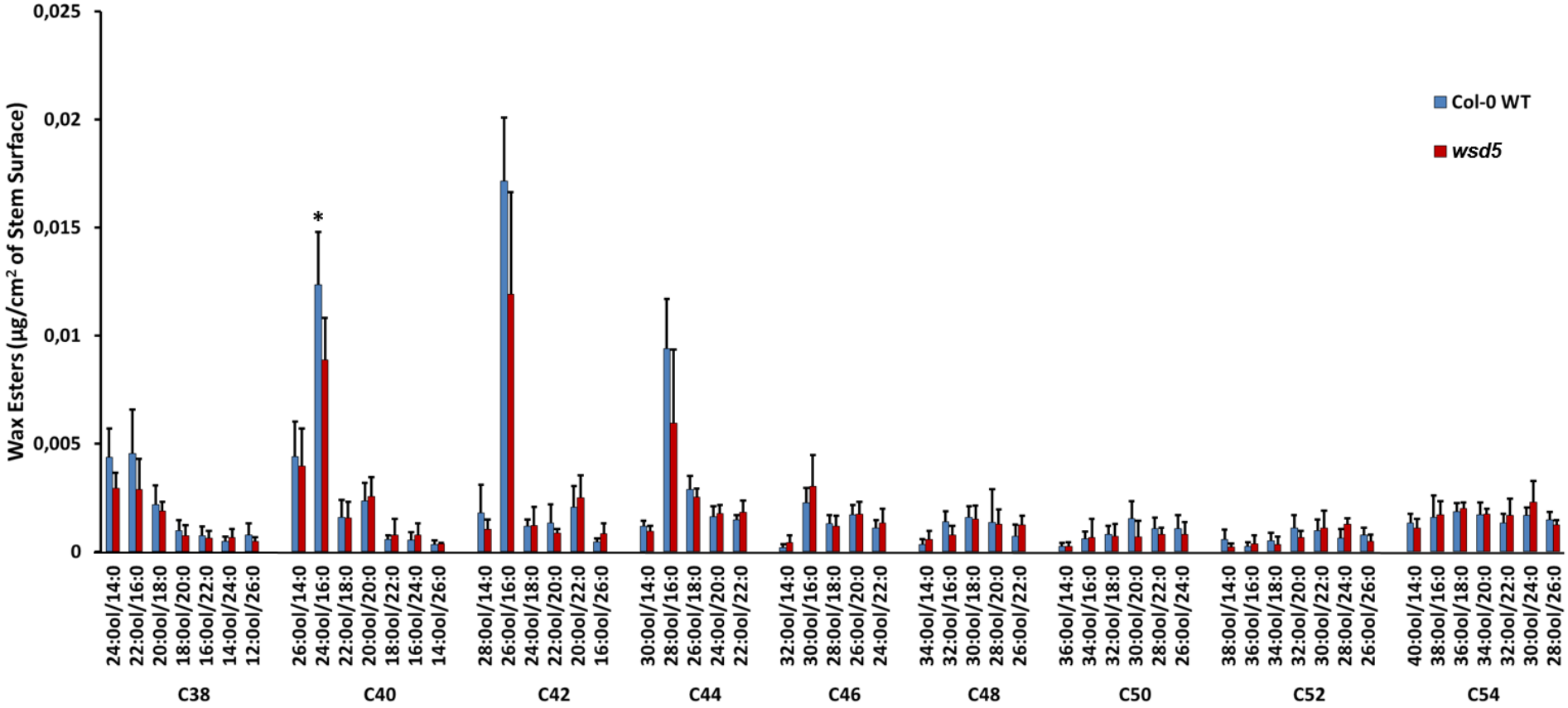

Figure 27: Stem Wax Esters from *A. thaliana* WT and Mutant Line *wsd5*.

Wax from inflorescence stems was extracted by chloroform. The wax extract was fractionated by SPE (hexane/diethyl ether 99/1 (v/v)) and the wax ester fraction analyzed by Q-TOF MS/MS. Data represent mean and standard deviation of 5 measurements. Asterisks indicate values that differ significantly from the wild type control (Student's *t* test, Welch correction, $P<0.05$ (*)).

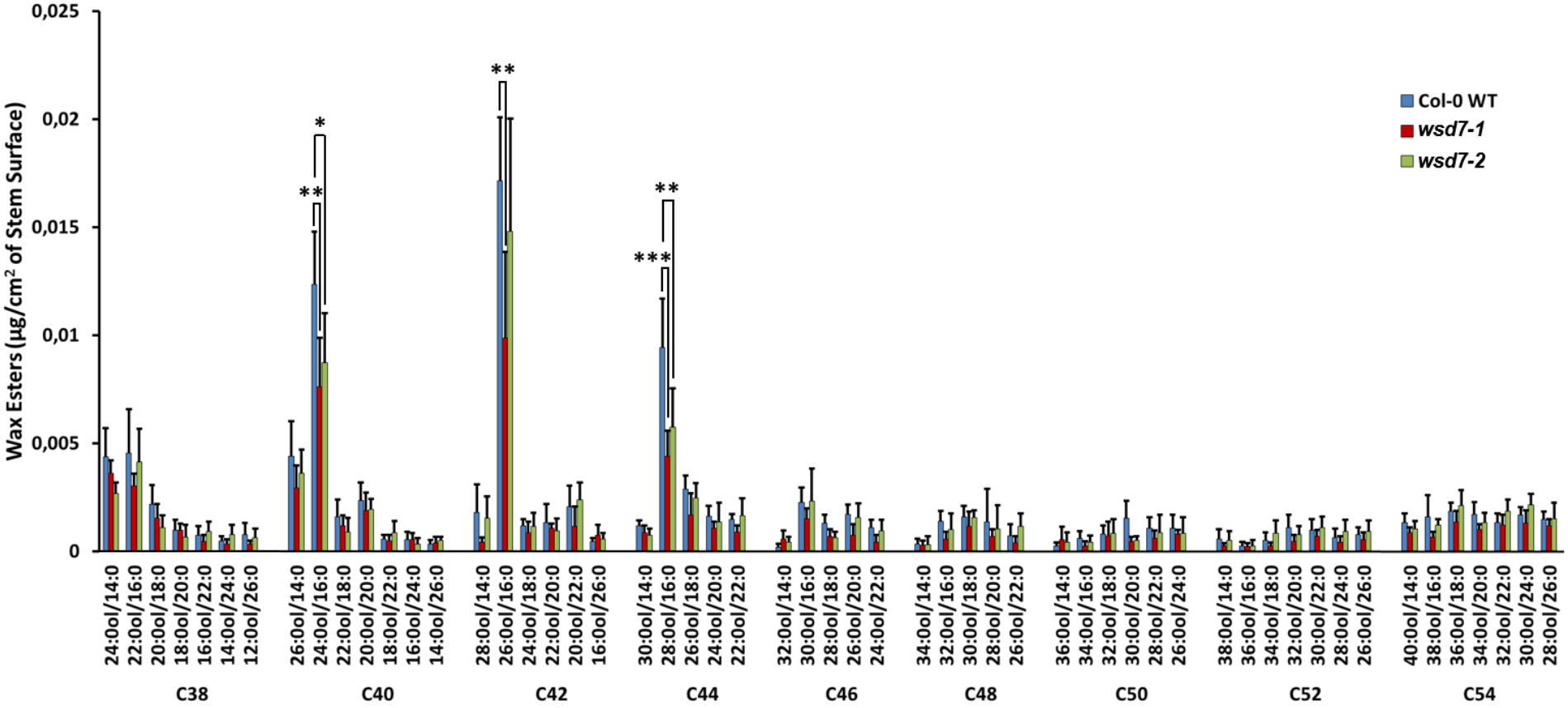

Figure 28: Stem Wax Esters from *A. thaliana* WT and Mutant Lines *wsd7-1* and *wsd7-2*.

Wax from inflorescence stems was extracted by chloroform. The wax extract was fractionated by SPE (hexane/diethyl ether 99/1 (v/v)) and the wax ester fraction analyzed by Q-TOF MS/MS. Data represent mean and standard deviation of 5 measurements. Asterisks indicate values that differ significantly from the wild type control (Student's *t* test, Welch correction, $P<0.05$ (*), $P<0.02$ (**) and $P<0.01$ (***)).

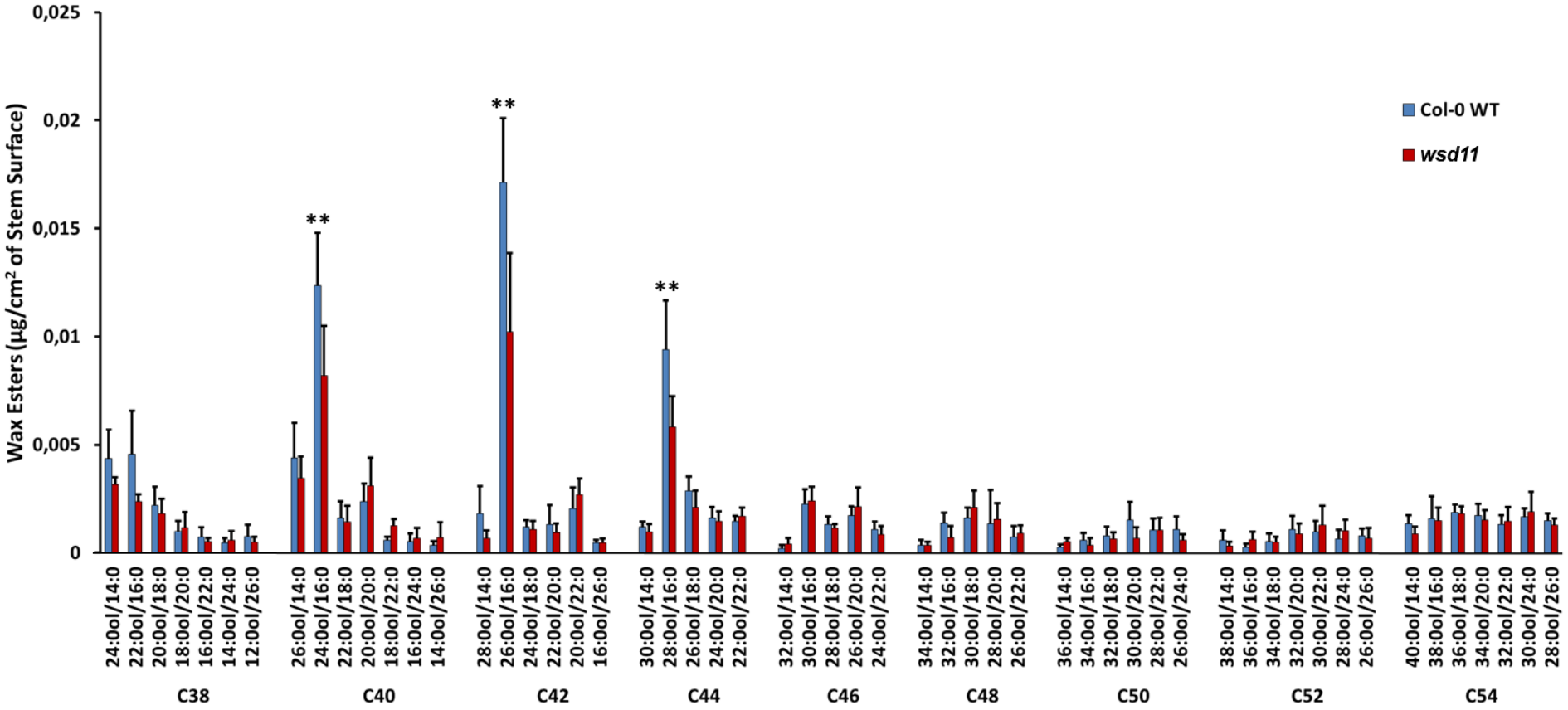

Figure 29: Stem Wax Esters from *A. thaliana* WT and Mutant Line *wsd11*.

Wax from inflorescence stems was extracted by chloroform. The wax extract was fractionated by SPE (hexane/diethyl ether 99/1 (v/v)) and the wax ester fraction analyzed by Q-TOF MS/MS. Data represent mean and standard deviation of 5 measurements. Asterisks indicate values that differ significantly from the wild type control (Student's *t* test, Welch correction, $P<0.02$ (**)).

3.10 Wax Esters from Flower Surface Wax of the *wsd* Mutant Lines

For the qualitative and quantitative analysis of flower wax esters, homozygous mutants and corresponding wild type ecotypes were used. Flower wax was extracted from freshly opened flowers, using 10 flowers per replicate, and the wax esters were separated from other wax compounds by SPE (see 2.3.11.3). The solvent of the purified wax ester fraction was evaporated and the dried lipids were dissolved in Q-TOF running buffer and analyzed by Q-TOF MS/MS (see 2.3.11.7). For quantification, 1 nmol of the standard 18:0ol/17:0 wax ester was used. All homozygous mutant lines were measured. The intensities of the product ions of most of the measured WE species were very low, often < 10 counts per scan, which is lower than the low intensities found for the product ions of most stem and silique WEs. These low intensities did not differ from background signals and hindered therefore a clear identification of these WE species. Higher intensities were found for the product ions of the WE species 22:0ol/16:0, 24:0ol/16:0, 26:0ol/16:0, 28:0ol/16:0, 30:0ol/16:0, 28:0ol/18:0 and 26:0ol/20:0 which were identified to occur in flower wax in this study. However, the intensities of these species were in most cases < 100 counts per scan. Due to the little occurrence of these WE species, their product ions were also not found in each scan for these product ions (the average of the intensities of five scans per sample was calculated). Significant differences between the mutant line(s) and the WT control are indicated for the clearly identified WE species mentioned above.

Below only the results which show differences between the WT and the mutant line(s) are depicted. When two mutant lines of one gene were analyzed, the results were only presented when the differences between WT and mutant lines were present in both mutant lines. Furthermore the results of *wsd11* are shown because Takeda and coworkers showed that this mutant is characterized by a folded petal phenotype, but wax esters have not been measured (Takeda *et al*., 2013). All other results are found in the Appendix (see Figures 58 to 64).

As depicted in Figure 30, wax ester chain lengths of C_{46}, C_{38}, C_{42}, C_{44} and C_{40} are most prominent in flowers of Col-0 WT with total wax ester amounts of approximately 5 ng/flower for the C_{46} chain length.

Other less abundant wax ester chain lengths are C_{48}, C_{50} and C_{52}. As shown in Figure 31, very abundant wax ester species measured in flowers of Col-0 WT are those with a 16:0 fatty acid moiety (22:0ol/16:0, 26:0ol/16:0, 28:0ol/16:0, 30:0ol/16:0, 24:0ol/16:0). Interestingly, several wax ester species of the chain length C_{46} are present in higher amounts (additionally to the above mentioned 30:0ol/16:0 also 28:0ol /18:0, 26:0ol /20:0 and 32:0ol/14:0).

As depicted in Figure 31, the flower wax esters of the *wsd1* mutant line are highly reduced compared to the wild type control. The strongest reduction can be observed for the wax esters harboring a 16:0 acyl moiety (22:0ol/16:0, 26:0ol/16:0, 28:0ol/16:0, 24:0ol/16:0). Other WE species like 28:0ol/18:0, 22:0ol /18:0 and 24:0ol /18:0 are slightly reduced. A slight increase in WEs could be observed for the species 30:0ol/16:0 and 32:0ol/16:0 in the mutant.

The mutant lines *wsd2-1* and *wsd2-2* are distinguished by their different ecotypes: *wsd2-1* has a Columbia background while *wsd2-2* has a Landsberg background. Therefore, two diagrams depict the results of the wax ester measurements: *wsd2-1* compared with the WT Col-0 (Figure 32), *wsd2-2* compared with the WT Ler (Figure 33). In the two mutant lines, the amount of the wax ester species 28:0ol/18:0 is reduced compared to wild type. Other wax ester species whose amounts are reduced in *wsd2-1* (22:0ol/16:0, 26:0ol/16:0) show slightly increased amounts in *wsd2-2*.

In Figure 34, the result of measuring flower wax of the mutant line *wsd5* is presented. Compared to the WT control, flower wax of *wsd5* contained lesser amounts of the WE species 22:0ol/16:0. The WE species 26:0ol/20:0 and 32:0ol /14:0 were slightly reduced in the mutant. The amounts of other WE species were similar between mutant and WT control.

Similar to the mutant *wsd5*, the mutant lines *wsd9-1* and *wsd9-2* showed a reduction of the WE species 22:0ol/16:0 (Figure 35). The amounts of other WE species were similar to those of the WT control.

The measurement of wax esters in flower wax of the *wsd11* mutant line, which was designated *fop1* by Takeda *et al*., 2013, revealed no obvious differences compared to the wild type (Figure 36). Also the folded phenotype could not be observed although the same mutant line (SALK_137481) as described by Takeda and coworkers was analyzed.

The measurement of the double mutant line *wsd1* x *wsd4-2* showed a similar reduction of the same WE species compared to the WT control like the mutant *wsd1* (Figure 31). Therefore, the results of *wsd1* x *wsd4-2* are presented in the Appendix (Figure 64).

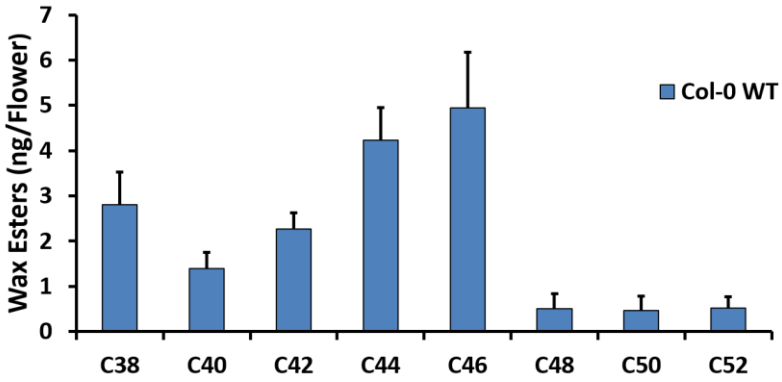

Figure 30: Flower Wax Esters from *A. thaliana* WT Col-0.

Wax from flowers was extracted with chloroform. The wax extract was fractionated by SPE (hexane/diethyl ether 99/1 (v/v)) and the wax ester fraction analyzed by Q-TOF MS/MS. The wax ester species with the same total chain length (alcohol + fatty acid) were summed up for each replicate. Five replicates were averaged and a standard deviation was calculated.

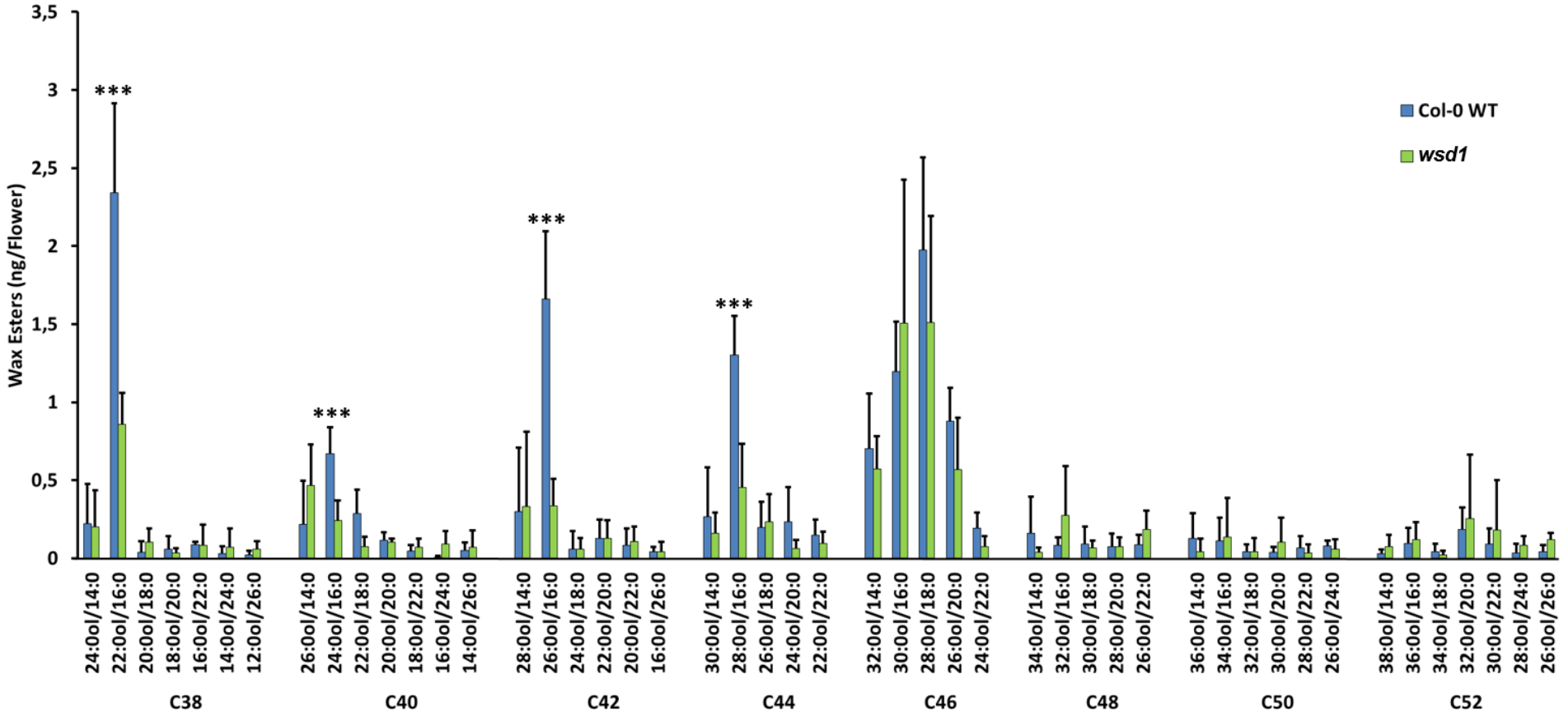

Figure 31: Flower Wax Esters from *A. thaliana* WT and Mutant Line *wsd1*.

Wax from 10 open flowers was extracted by chloroform. The wax extract was fractionated by SPE (hexane/diethyl ether 99/1 (v/v)) and the wax ester fraction analyzed by Q-TOF MS/MS. Data represent mean and standard deviation of 5 measurements for WT and of 4 measurements for *wsd1*. Asterisks indicate values that differ significantly from the wild type control (Student's *t* test, Welch correction, $P<0.01$ (***)).

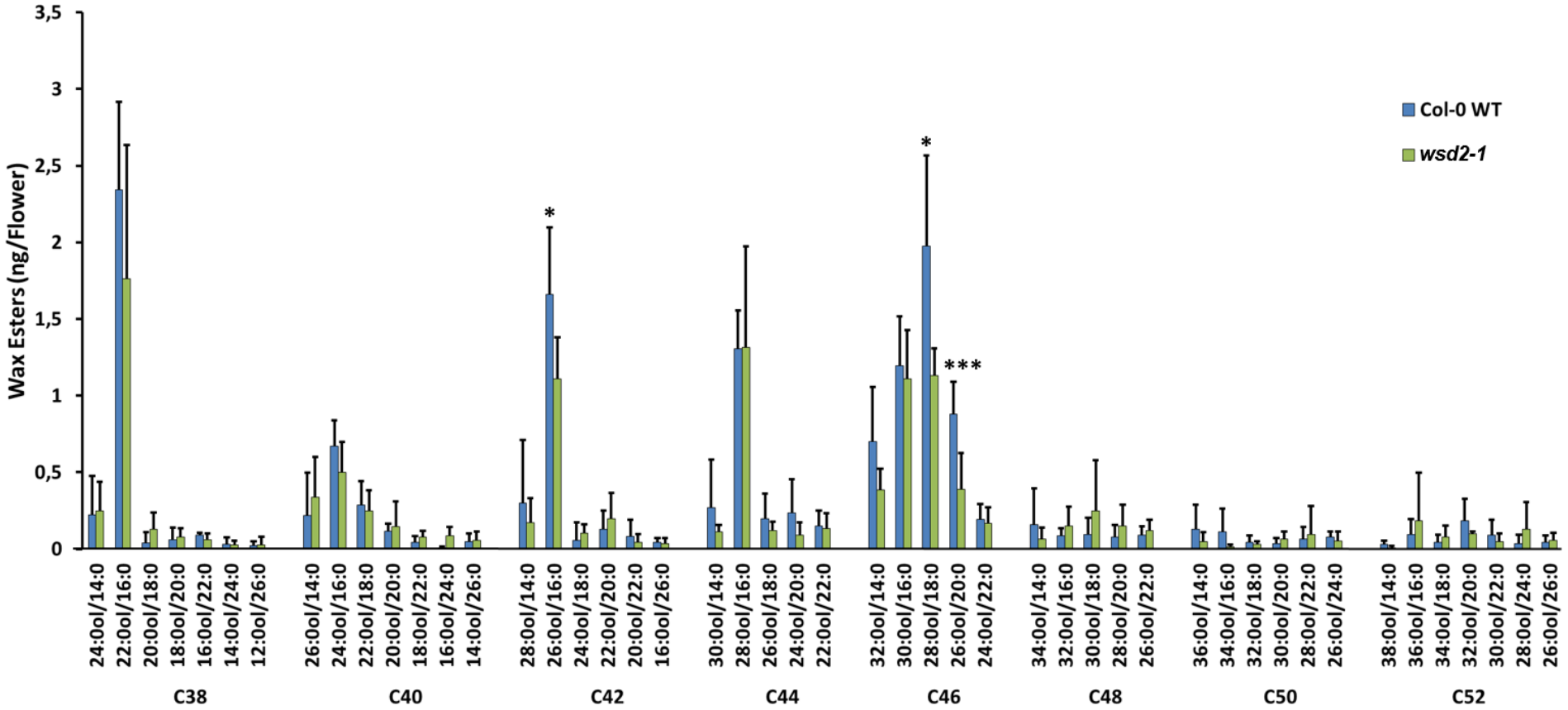

Figure 32: Flower Wax Esters from *A. thaliana* WT and Mutant Line *wsd2-1*.

Wax from 10 open flowers was extracted by chloroform. The wax extract was fractionated by SPE (hexane/diethyl ether 99/1 (v/v)) and the wax ester fraction analyzed by Q-TOF MS/MS. Data represent mean and standard deviation of 5 measurements. Asterisks indicate values that differ significantly from the wild type control (Student's *t* test, Welch correction, $P<0.05$ (*); $P<0.01$ (***)).

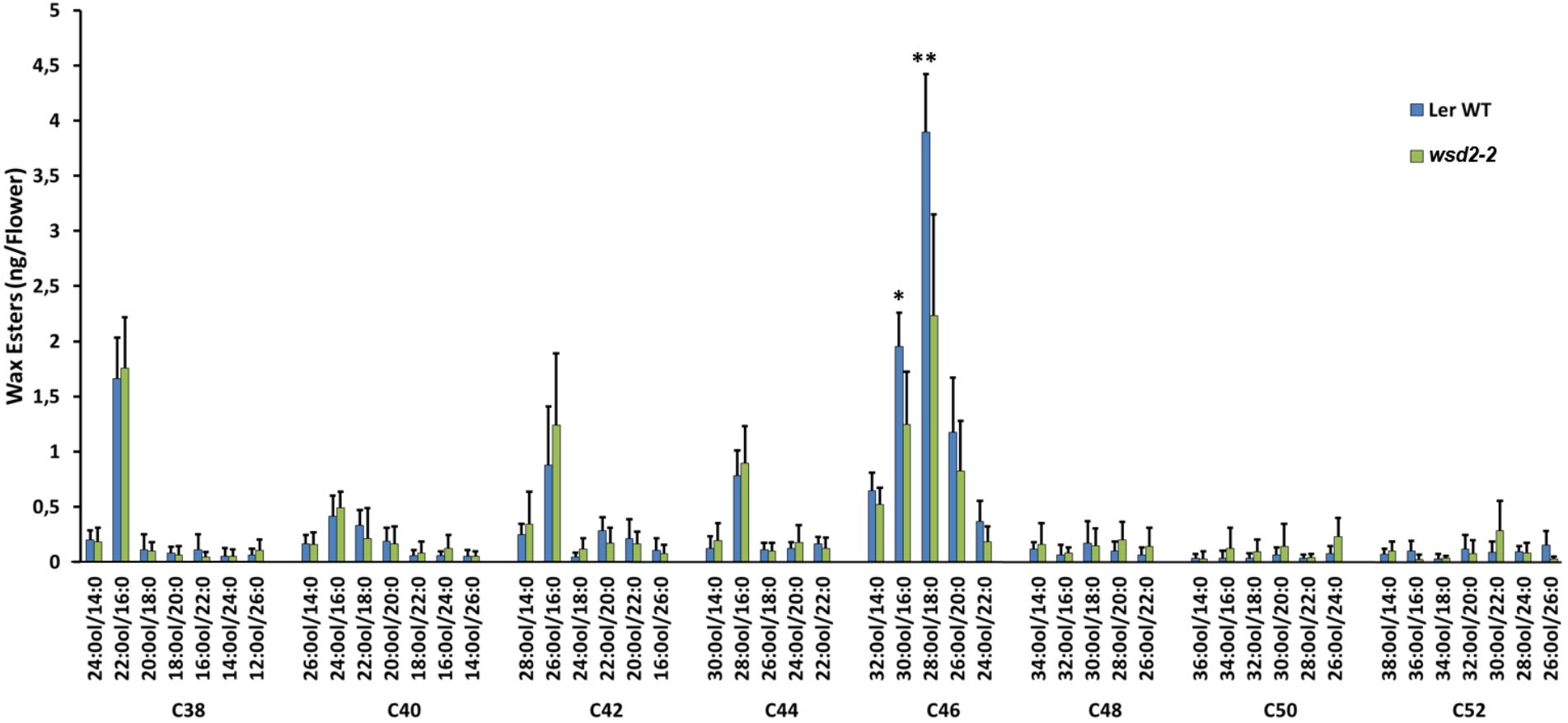

Figure 33: Flower Wax Esters from *A. thaliana* WT and Mutant Line *wsd2-2*.

Wax from 10 open flowers was extracted by chloroform. The wax extract was fractionated by SPE (hexane/diethyl ether 99/1 (v/v)) and the wax ester fraction analyzed by Q-TOF MS/MS. Data represent mean and standard deviation of 5 measurements. Asterisks indicate values that differ significantly from the wild type control (Student's *t* test, Welch correction, $P<0.05$ (*); $P<0.02$ (**)).

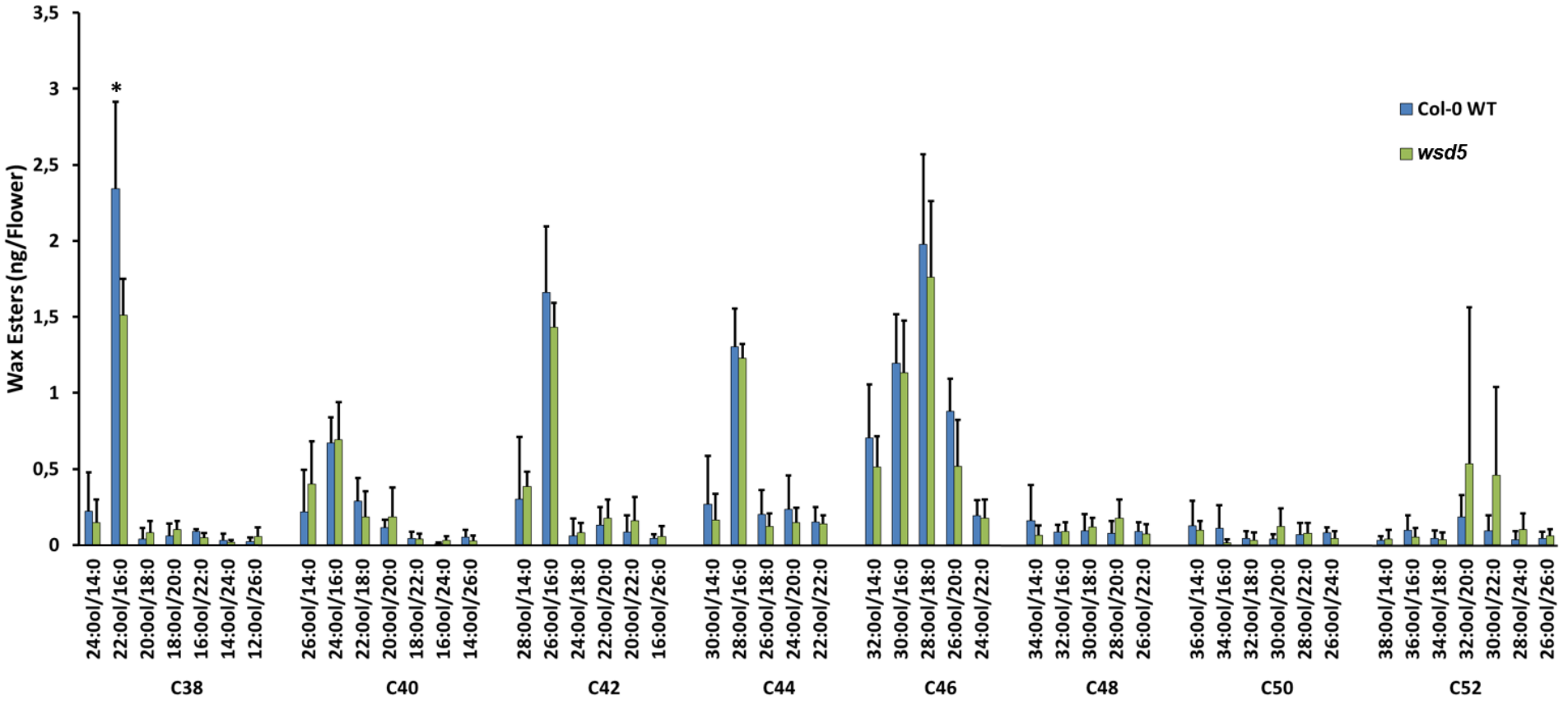

Figure 34: Flower Wax Esters from *A. thaliana* WT and Mutant Line *wsd5*.

Wax from 10 open flowers was extracted by chloroform. The wax extract was fractionated by SPE (hexane/diethyl ether 99/1 (v/v)) and the wax ester fraction analyzed by Q-TOF MS/MS. Data represent mean and standard deviation of 5 measurements. Asterisks indicate values that differ significantly from the wild type control (Student's *t* test, Welch correction, $P<0.05$ (*)).

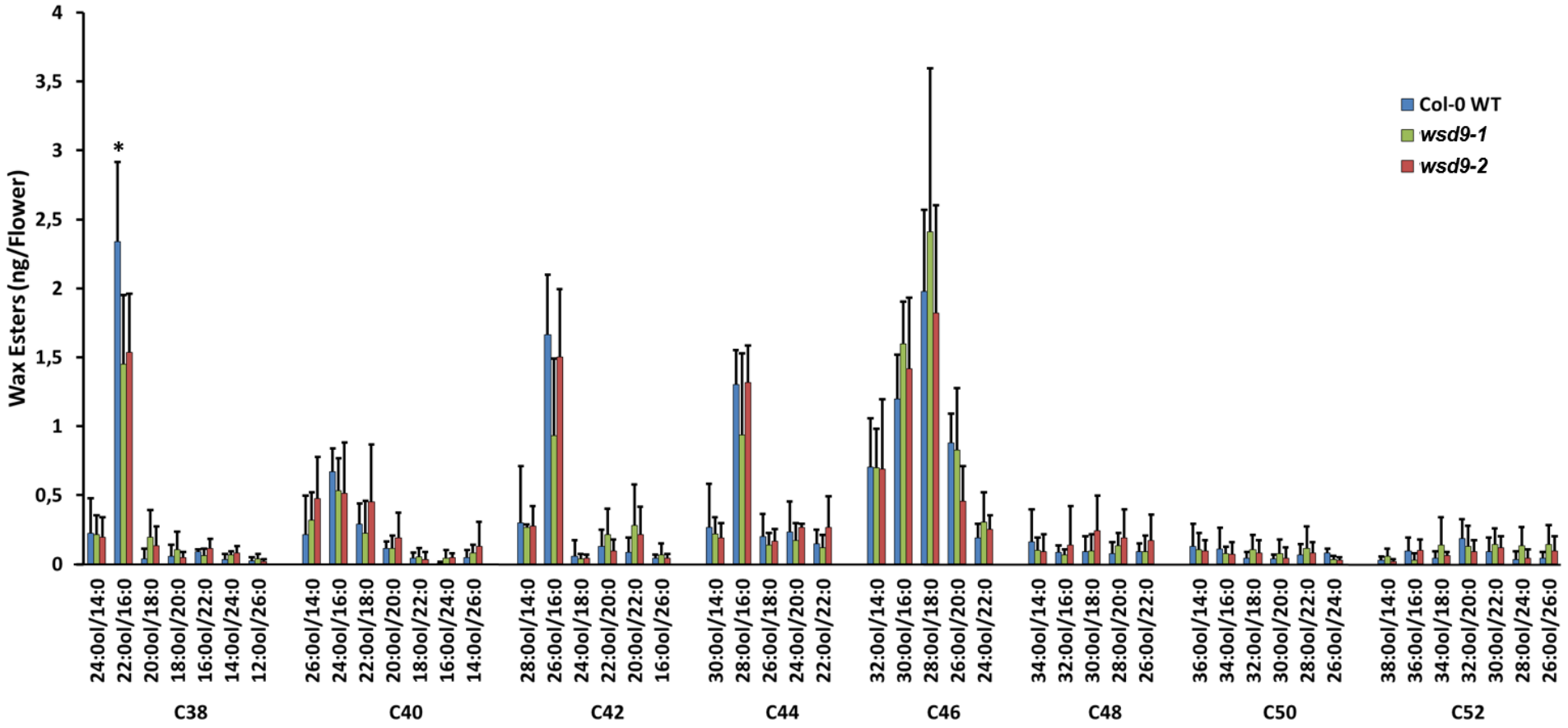

Figure 35: Flower Wax Esters from *A. thaliana* WT and Mutant Lines *wsd9-1* and *wsd9-2*.

Wax from 10 open flowers was extracted by chloroform. The wax extract was fractionated by SPE (hexane/diethyl ether 99/1 (v/v)) and the wax ester fraction analyzed by Q-TOF MS/MS. Data represent mean and standard deviation of 5 measurements. Asterisks indicate values that differ significantly from the wild type control (Student's *t* test, Welch correction, $P<0.05$ (*)).

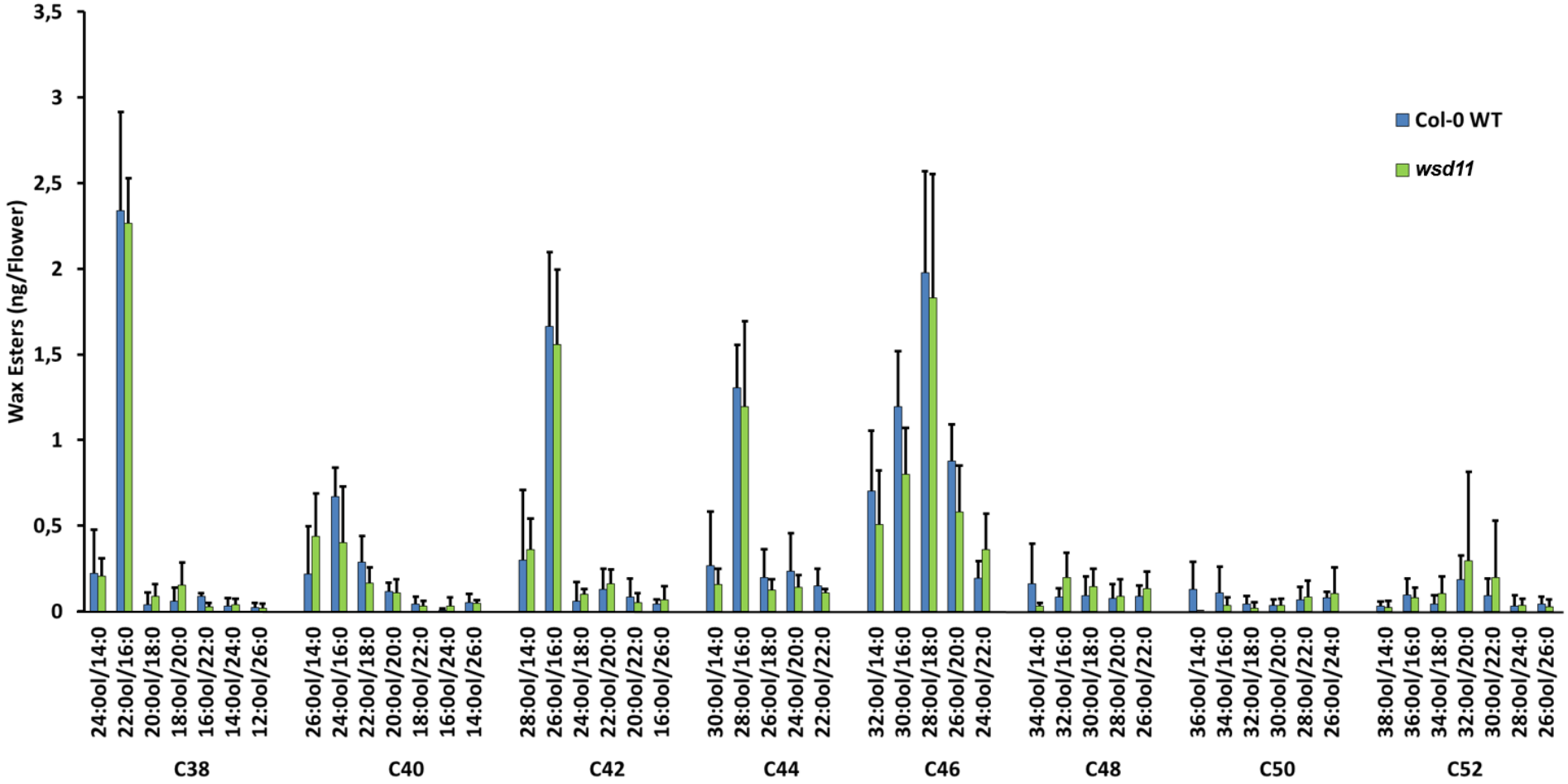

Figure 36: Flower Wax Esters from *A. thaliana* WT and Mutant Line *wsd11*.

The *wsd11* mutant was previously designated *fop1* by Takeda *et al*. (2013). Wax from 10 open flowers was extracted by chloroform. The wax extract was fractionated by SPE (hexane/diethyl ether 99/1 (v/v)) and the wax ester fraction analyzed by Q-TOF MS/MS. Data represent mean and standard deviation of 5 measurements for WT and of 4 measurements for *wsd11*.

WE species with methyl, isoamyl and short-to-medium alcohol moieties and very long chain fatty acyl moieties have been described to occur in the petal wax of *Petunia hydrida* (King *et al*., 2007). The WS/DGAT homolog *Ph*WS1 was speculated to contribute to the synthesis of these wax esters with most abundant chain lengths ranging from C_{23} to C_{30}, as the enzyme catalyzes the synthesis of wax esters consisting of medium chain alcohol moieties and long to very long-chain acyl moieties in-vitro (King *et al*., 2007). Therefore, flower wax of *Arabidopsis* might also contain WE species with short-to-medium alcohol moieties and a WSD might be involved in their synthesis. Thus, purified flower wax of *A. thaliana* WT and *wsd* mutants was analyzed with regard to WE species with short-to-medium alcohol moieties and also with longer alcohol moieties (C_1 to C_{23}) which were esterified to C_{14} to C_{26} fatty acyl moieties. The alcohol and fatty acyl residues of these WE species searched for were saturated and even-numbered, furthermore the alcohol moieties could also be odd-numbered. The targeted list of the WE species searched for is found in the Appendix (Table 13). For most WE species searched for the intensities were very low (very often < 10 counts per scan) which is similar to most of the flower WE species with longer alcohol moieties as described above. Below (Figures 37 and 38), WE species in *A. thaliana* WT occurring with amounts > 0.001 nmol per flower (with intensities ranging between 10 and approximately 200 counts per scan) are presented. Hereof, the WE species 8:0ol/18:0, 8:0ol/16:0, 18:0ol/16:0 and 22:0ol/14:0 were clearly identified. The clear identification of the residual WE species was hindered due to the low intensities of the product ions which did not differ from background signals. Differences between WT and mutants are only presented in the results if a significant difference between the WT and the mutant was measured for a clearly identified WE species. If two mutant lines per *WSD* gene were analyzed, the results were only presented below when both mutant lines were significant different from the WT. Furthermore, the results of the mutant *wsd11* which is also designated *fop1* by Takeda *et al*., 2013, are presented below although no obvious differences could be observed for the mutant compared to the WT control (Figure 38). The other results are found in the Appendix (see Figure 57).

In *Arabidopsis* WT, the WE species 8:0ol/18:0, 8:0ol/16:0 and 22:0ol/14:0 were most abundant. Other less abundant WE species were 12:0ol/16:0, 18:0ol/16:0, 8:0ol/20:0, 16:0ol/16:0, 4:0ol/24:0 and 21:0ol/16:0.

A significant reduction in both *wsd2-1* and *wsd2-2* mutants compared to the WT control was measured for the WE species 8:0ol/16:0 and 4:0ol/24:0ol (Figure 37). The mutants *wsd3-1* and *wsd3-2* showed reduced amounts of the WE species 22:0ol/14:0 compared to the WT control (Figure 37). The mutant *wsd5* showed an increase in the WE species 8:0ol/16:0 in flower wax compared to the WT control. In both mutants, *wsd8-1* and *wsd8-2*, the amounts of the WE species 8:0ol/16:0ol and 8:0ol/18:0 were significantly reduced compared to the WT control (Figure 38). The flower wax of the mutants *wsd9-1* and *wsd9-2* contained reduced amounts of the WE species 8:0ol/18:0, 12:0ol/16:0 and 4:0ol/24:0 compared to the WT control (Figure 38).

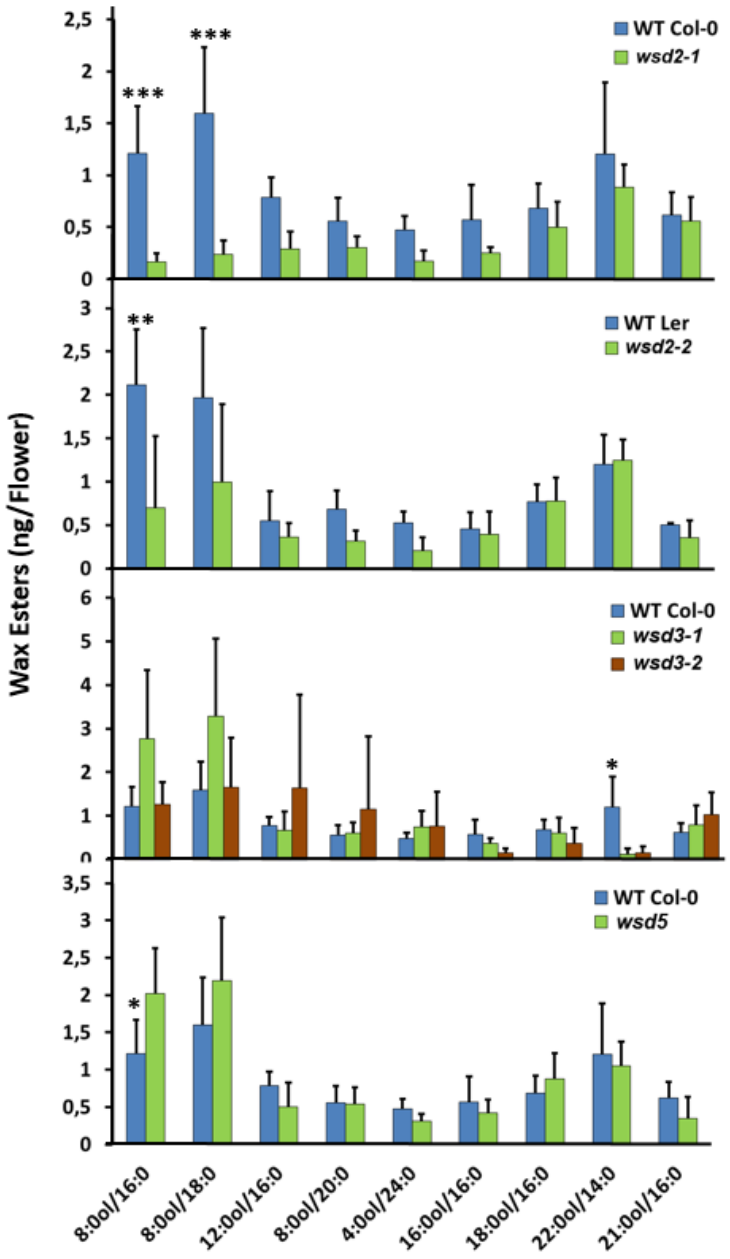

Figure 37: Abundant WE Species within the Chain Lengths of C_{17} to C_{37} Containing Short-to-Very-Long Chain Alcohol Moieties in Flowers of *A. thaliana* Col-0 WT and Ler WT and *wsd* Mutant Lines.

Wax from 10 open flowers was extracted by chloroform. The wax extract was fractionated by SPE (hexane/diethyl ether 99/1 (v/v)) and the wax ester fraction analyzed by Q-TOF MS/MS.
Data represent mean and standard deviation of 5 measurements for WT Col-0, WT Ler, *wsd2-1*, *wsd2-2* and *wsd3-1* and of 4 measurements for w*sd3-2*. Asterisks indicate values that differ significantly from the wild type control (Student's *t* test, Welch correction, $P<0.05$ (*); $P<0.02$ (**) and $P<0.01$ (***)).

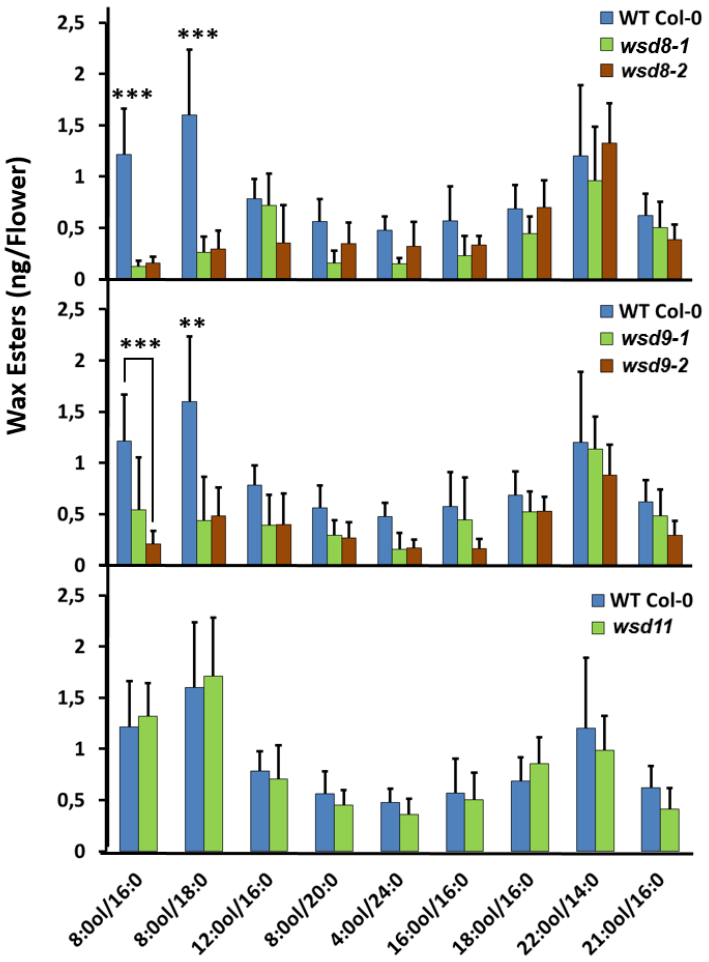

Figure 38: Abundant WE Species within the Chain Lengths of C_{17} to C_{37} Containing Short-to-Very-Long Chain Alcohol Moieties in Flowers of *A. thaliana* Col-0 WT and *wsd* Mutant Lines.

Wax from 10 open flowers was extracted by chloroform. The wax extract was fractionated by SPE (hexane/diethyl ether 99/1 (v/v)) and the wax ester fraction analyzed by Q-TOF MS/MS.
Data represent mean and standard deviation of 5 measurements for WT Col-0, *wsd8-2, wsd9-1, wsd9-2* and *wsd11* and of 4 measurements for *wsd8-1*. Asterisks indicate values that differ significantly from the wild type control (Student's *t* test, Welch correction, $P<0.05$ (*) and $P<0.02$ (**)).

3.11 Wax Esters from Silique Surface Wax of the *wsd* Mutant Lines

For the analysis of silique wax esters, homozygous mutant lines and the corresponding wild type ecotypes were used. Silique wax was extracted from green siliques with mature sizes, using 5 siliques per replicate, and the wax esters were isolated by SPE. The solvent of the purified wax ester fraction was evaporated and the dried lipids were dissolved in Q-TOF running buffer and analyzed by Q-TOF MS/MS. For quantification, 1 nmol of the standard 18:0ol/17:0 wax ester was used. The homozygous mutant lines (except *wsd10-1* and *wsd10-2*) were measured. Similar to stem wax ester, the intensities of the product ions of most WE species searched for were low (often < 100 counts per scan) with similar intensities than background signals. However, a few WE species could be clearly identified, namely 24:0ol/14:0, 22:0ol/16:0, 26:0ol/14:0, 24:0ol/16:0, 26:0ol/16:0, 28:0ol/16:0 and 30:0ol/16:0.

Below only the results which show significant differences between the WT control and the mutant line(s) are depicted. All other results are found in the Appendix (Figures 65 to 74). As shown in Figure 39, wax ester chain lengths of C_{42}, C_{40} and C_{44} are most prominent in siliques of Col-0 WT with amounts higher than approx. 2.6 ng/mg for the most abundant chain length C_{42}. Other less abundant wax ester chain lengths are C_{38}, C_{54}, C_{46}, C_{48}, C_{50} and C_{52}. As shown in Figure 40, very abundant wax ester species measured in siliques of Col-0 WT are those with a 16:0 fatty acid moiety (26:0ol/16:0 > 24:0ol/16:0 > 28:0ol/16:0 > 22:0ol/16:0 > 30:0ol/16:0). With these most abundant WE species harboring a 16:0 fatty acyl moiety, the silique wax ester pattern is similar to the wax ester pattern of stem and flower.

The amounts of the wax esters from siliques were strongly reduced in the *wsd1* mutant line compared to the WT control (Figure 40), like in stem and flowers, this is caused by the strong reduction of WEs with the 16:0 fatty acyl residue. While the amounts of most of the other less abundant wax ester species were hardly affected in the *wsd1* mutant, a few species like 24:0ol/18:0, 28:0ol/18:0 and 26:0ol/20:0 were slightly decreased in *wsd1*.

The mutant *wsd5* (Figure 41) showed a decrease in the abundant 26:0ol/16:0, a slighter decrease in 24:0ol/16:0, 28:0ol/16:0, 30:0ol/16:0 and 38:0ol/16:0 wax ester species. The other wax ester species had no reduced amounts in the mutant compared to the control. A few WE species showed a slight increase in the mutant line (like 22:0ol/16:0, 22:0ol/18:0, 26:0ol/18:0, 24:0ol/22:0).

Similar to stem and flower, the double mutant line *wsd1* x *wsd4-2* showed a high reduction of those WE species which were already decreased in the *wsd1* mutant (Figure 40) alone. Since no difference could be observed between the results of *wsd1* and *wsd1* x *wsd4-2* compared to the WT control, the results of the double mutant *wsd1* x *wsd4-2* are found in the Appendix (Figure 74).

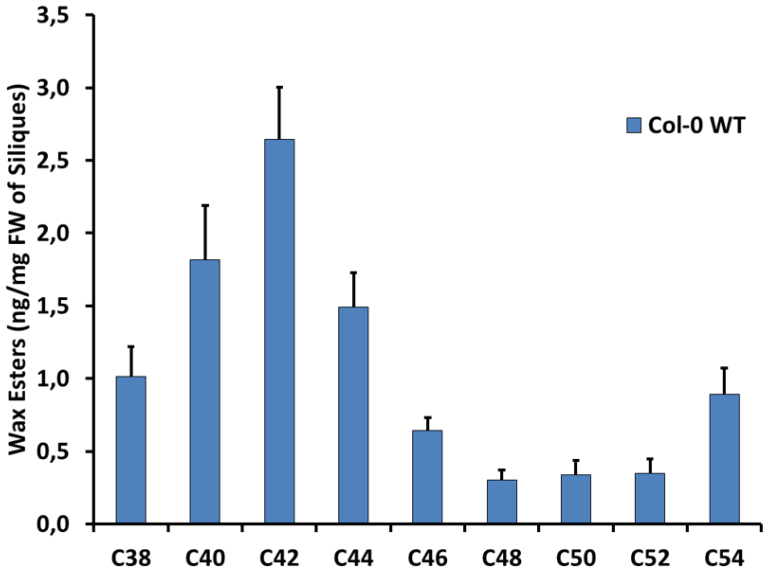

Figure 39: Silique Wax Esters from *A. thaliana* WT Col-0.

Wax from siliques was extracted with chloroform. The wax extract was fractionated by SPE (hexane/diethyl ether 99/1 (v/v)) and the wax ester fraction analyzed by Q-TOF MS/MS. The wax ester species with the same total chain length (alcohol + fatty acid) were summed up for each replicate. Five replicates were averaged and a standard deviation was calculated.

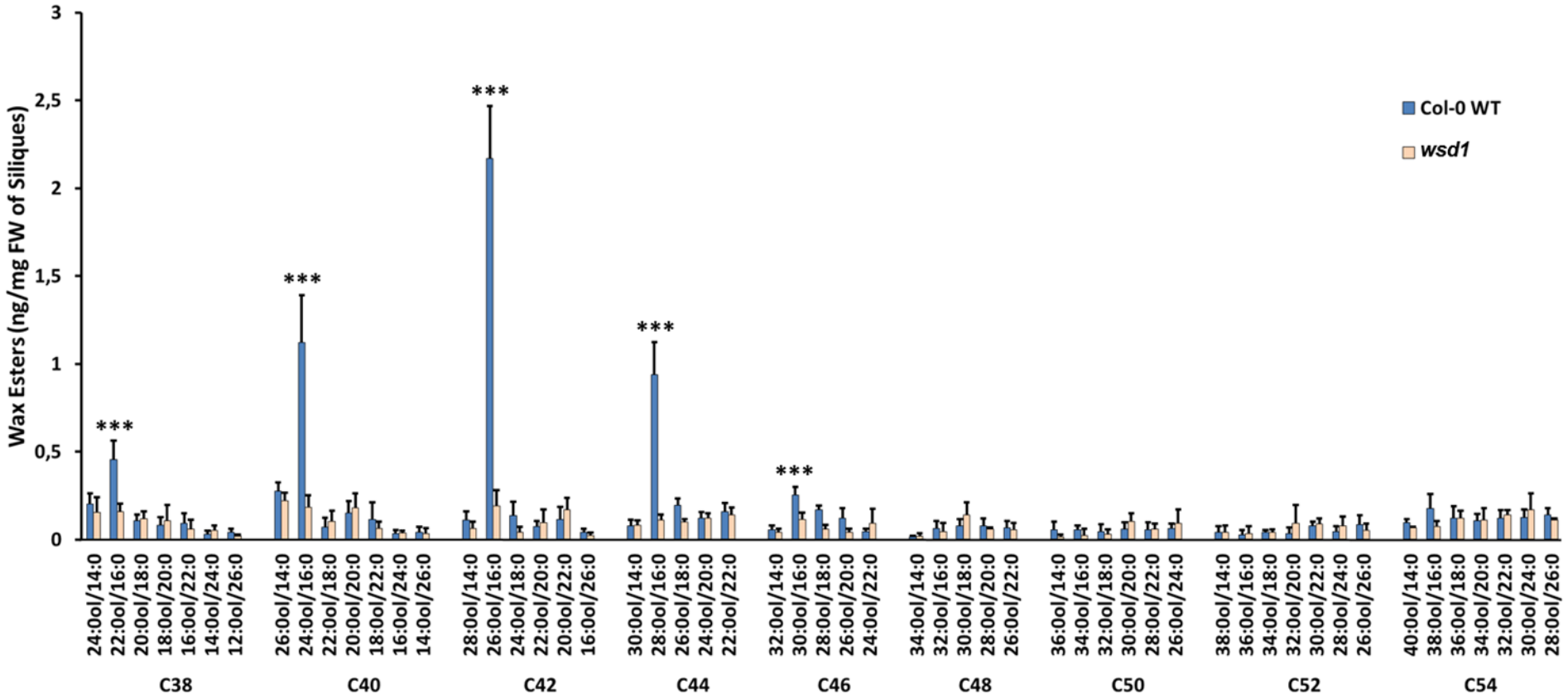

Figure 40: Silique Wax Esters from *A. thaliana* WT and Mutant Line *wsd1*.

Wax from 5 siliques, still green but in mature size, was extracted by chloroform. The wax extract was fractionated by SPE (hexane/diethyl ether 99/1 (v/v)) and the wax ester fraction analyzed by Q-TOF MS/MS. Data represent mean and standard deviation of 5 measurements. Asterisks are indicated for the values that are significantly different (Student's *t* test, Welch correction, $P<0.01$ (***)).

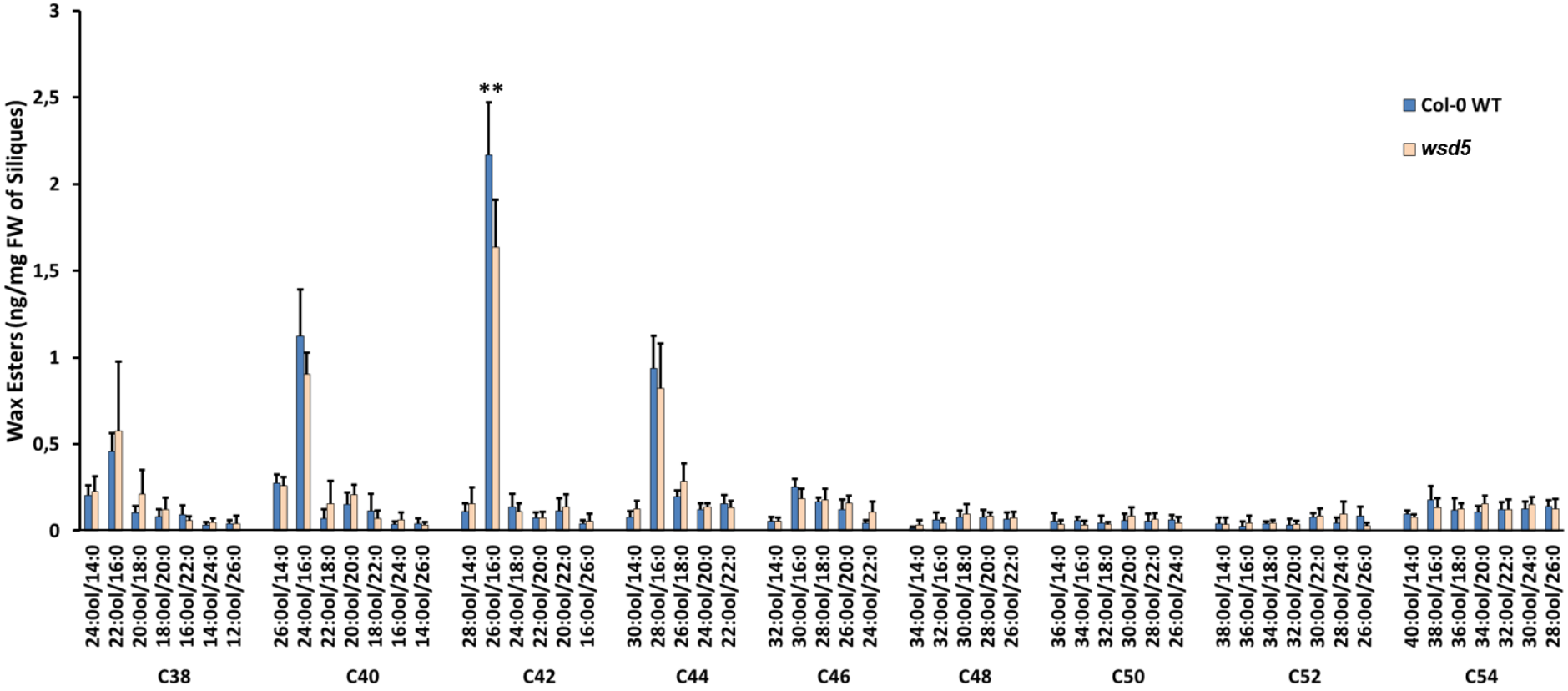

Figure 41: Silique Wax Esters from *A. thaliana* WT and Mutant Line *wsd5*.

Wax from 5 siliques, still green but in mature size, was extracted by chloroform. The wax extract was fractionated by SPE (hexane/diethyl ether 99/1 (v/v)) and the wax ester fraction analyzed by Q-TOF MS/MS. Data represent mean and standard deviation of 5 measurements. Asterisks are indicated for the values that are significantly different (Student's *t* test, Welch correction, $P<0.02$ (**)).

3.12 Analysis of Wax Esters in Leaf Cuticles from *Hordeum vulgare* after Exposure to Drought Stress

After the exposure to drought for two weeks, wilted leaves from *Hordeum vulgare* cv. Barke wild type and leaves from watered control plants were harvested and the wax extracted with chloroform. The wax extracts were purified by solid phase extraction and the wax ester composition analyzed by Q-TOF MS/MS and related to the surface area of the extracted leaves.

The intensities of the product ions of many WE species searched for were clearly higher than those of background signals which enabled the clear identification of these species. The clearly identified WE species with a chain length of C_{36} are 22:0ol/14:0, 20:0ol/16:0, 18:0ol/18:0, 16:0ol/20:0, with chain length of C_{38} are 24:0ol/14:0, 22:0ol/16:0, 20:0ol/18:0, 18:0ol/20:0, 16:0ol/22:0, with a chain length of C_{40} are 26:0ol/14:0, 24:0ol/16:0, 22:0ol/18:0, 20:0ol/20:0, with a chain length of C_{42} are 26:0ol/16:0, 24:0ol/18:0, 22:0ol/20:0, with a chain length of C_{44} is 26:0ol/18:0, with a chain length of C_{46} are 30:0ol/16:0, 26:0ol/20:0, with a chain length of C_{50} is 34:0ol/16:0. For the residual presented WE species, a clear identification was hindered due to low intensities which were similar to that of background signals.

As depicted in Figure 42, the exposure to drought stress led to a general increase in wax esters in the leaves from approx. 16.025 ng/cm^2 in the unstressed plants to approx. 19.428 ng/cm^2 in the drought stressed plants. The analyzed wax ester species are depicted in Figure 43. Especially the amounts of the wax ester species 22:0ol/16:0 and 20:0ol/16:0 which were both abundant in leaves were highly increased after exposure to drought. Other abundant wax ester species like 26:0ol/16:0, 24:0ol/16:0, 26:0ol/14:0 and 24:0ol/18:0 had slightly reduced levels in the stressed leaves compared to the control leaves.

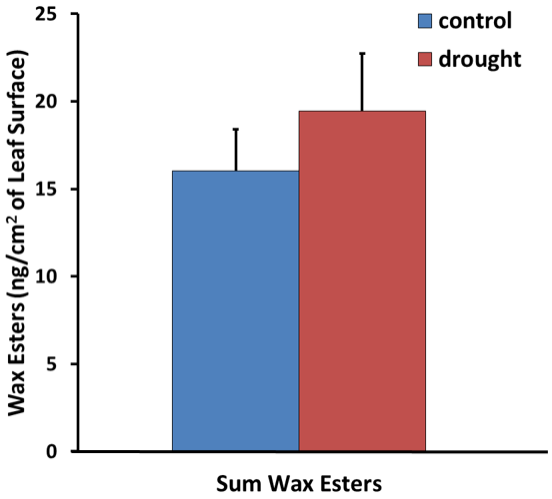

Figure 42: Increase in Sum of Wax Esters in *H. vulgare* cv. Barke Leaves after Exposure to Drought Stress.

Leaf wax from barley exposed to drought stress or normally watered was extracted by chloroform. The wax extract was fractionated by SPE (hexane/diethyl ether 99/1 (v/v)) and the wax ester fraction analyzed by Q-TOF MS/MS. Data represent mean and standard deviation of 5 measurements

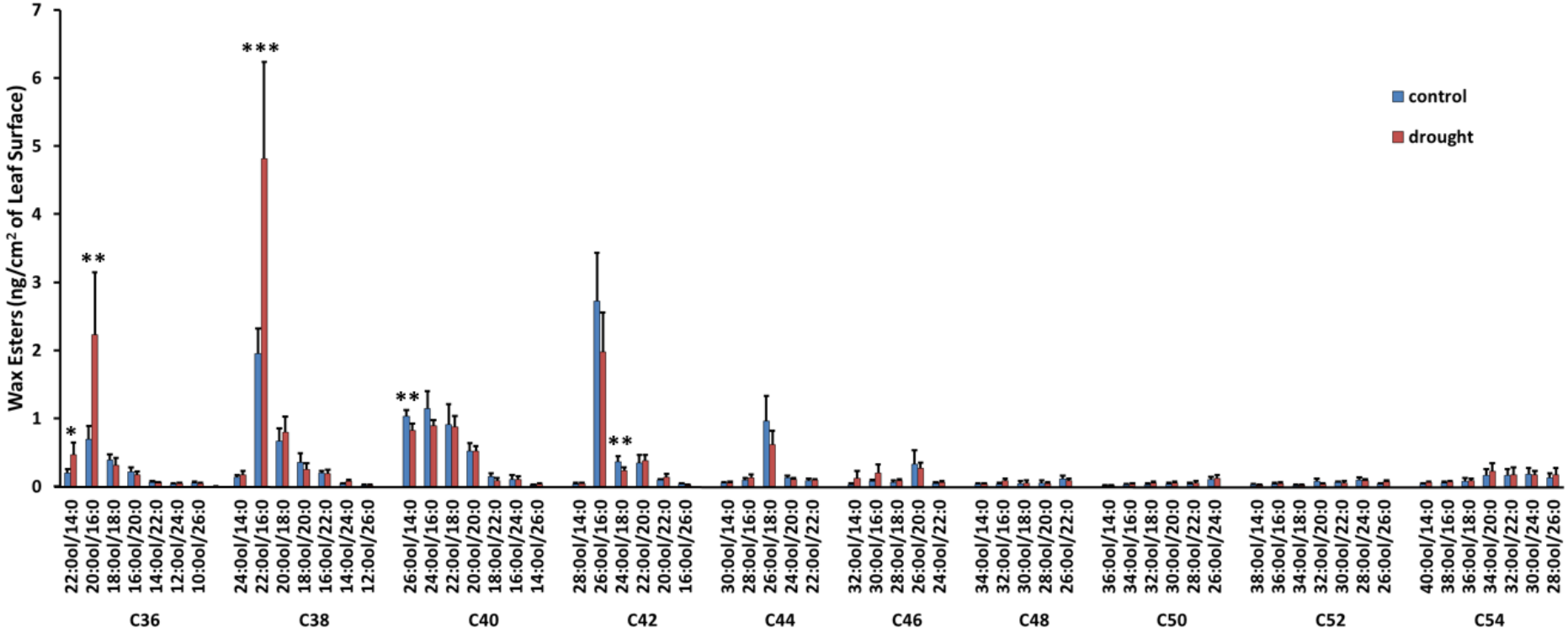

Figure 43: Increase in Wax Esters in *H. vulgare* cv. Barke Leaves after Exposure to Drought Stress.

Leaf wax from barley exposed to drought stress or normally watered was extracted by chloroform. The wax extract was fractionated by SPE (hexane/diethyl ether 99/1 (v/v)) and the wax ester fraction analyzed by Q-TOF MS/MS. Data represent mean and standard deviation of 5 measurements. Asterisks are indicated for those values that are significantly different (Student's *t* test, Welch correction, $P<0.05$ (*), $P<0.02$ (**), $P<0.01$ (***)).

4 Discussion

In this study, the function of *WSD* genes was investigated. To this end, the 11 *WSD* genes (*WSD1* - *WSD11*) occurring in *Arabidopsis thaliana* were analyzed regarding their gene expression in different plant organs of *A. thaliana* grown under optimal conditions or drought stress conditions. Furthermore, for heterologous expression in yeast, expression constructs of all *WSD* genes were cloned by using the pDR196 vector except for *WSD3* and *WSD10* whose cDNAs were gained by RT-PCR from inflorescence and root tissues from *A. thaliana*. The heterologous expression of WSD1 in *Saccharomyces cerevisiae* led to the production of an unknown lipid UL1. For subcellular localization of the WSD proteins *in planta*, cloning of expression constructs for all *WSD* genes was pursued by using the pLHGCSAtRNAi vector resulting in the fusion constructs *WSD3-eGFP,* pL-35S-*eGFP*-*WSD4* and pL-35S-*eGFP*-*WSD9* and subcellular localization studies of these WSD proteins. For wax ester analysis in *Arabidopsis*, T-DNA insertion and transposon mutant lines were genotyped resulting in homozygous mutant line(s) for each *WSD* gene. Wax esters which were extracted from cuticular wax from stem, flower and siliques of *A. thaliana* WT and *wsd* mutant lines were measured by Q-TOF MS/MS. The question if drought stress lead to an increase in wax esters in cuticular leaf wax of *Hordeum vulgare* was addressed.

4.1 Expression of *WSD* Genes in Different Plant Tissues

The analysis of *WSD* gene expression revealed very different expression patterns for the individual genes and also facilitated the comparison of the expression levels of the genes between the analyzed plant organs root, stem, leaf, inflorescence and silique (see Figure 14). While some genes like *WSD6* and *WSD7* are expressed with similar expression levels in all analyzed tissues, the expression of other *WSD* genes was limited to some specific plant organs, as, for instance, *WSD11* was only expressed in inflorescence.

The obtained gene expression data were compared with expression data found on the *Arabidopsis* eFP browser (http://bar.utoronto.ca/efp/cgi-bin/efpWeb.cgi) (data were provided by Schmid *et al*., 2005, therefore if expression data found on the eFP browser were used for comparison with data of this study, Schmid *et al*., 2005, was cited) and other published expression data.

The present study reveals for the first time a comprehensive data set for expression of the different *WSD* genes from *Arabidopsis* in different organs and during stress conditions (see Figure 14 and Figure 15). This is in particular important since only 5 *WSD* genes were included in previous expression studies (*WSD1*, *WSD2*, *WSD4*, *WSD6*, *WSD7*), while 6 genes (*WSD3*, *WSD5*, *WSD8*, *WSD9*, *WSD10*, *WSD11*) are absent from the Affymetrix ATH1 gene chip and were therefore not considered in expression experiments (Schmidt *et al*., 2005).

The expression data for *WSD1* generated in this study partly confirm the published expression data. In the present study, *WSD1* expression was observed in inflorescence and siliques while no

expression was detectable in roots, stem and leaf tissue (Figure 14). These expression data partly confirm the data published by Li *et al*., 2008, and Schmid *et al*., 2005: While Li *et al*., 2008, found expression of *WSD1* especially in flower buds, stems and leaves, Schmid *et al*., 2005, published high expression of *WSD1* in flower carpels, whole flower and immature siliques/seeds in stage "mid globular to early heart embryo". Furthermore, Schmid *et al*., 2005, found expression of *WSD1* in stem and with a lower expression level in rosette and cauline leaves. The differences of *WSD1* expression in this study compared to the published expression data might be explained by the use of different sampling: Li *et al*., 2008, used the upper 3 cm of inflorescence stem to analyze the gene expression in stem, while in this study, *WSD1* expression was examined in the lower part of the stem. Li *et al*., 2008, further confirmed the expression of *WSD1* in the top 3 cm of the stem by a GUS activity assay with a clearly visible decrease in *WDS1* expression in direction to the lower part of the stem. Schmid *et al*., 2005, found expression of *WSD1* in leaves by analyzing rosette leaf whorls, senescent leaves and cauline leaves, however only low to very low expression levels were detected in single full-grown rosette leaves. This might explain the missing *WSD1* expression in leaves in this study in which full-grown rosette leaves were used for RNA extraction. While Li *et al*., 2008, did not analyze siliques at all, Schmid *et al*., 2005, found a high expression at least in early developmental stages of siliques although full-grown green siliques were not analyzed. In this study, *WSD1* expression was detected in full-grown green siliques (Figure14). The absence of *WSD1* expression in lower parts of the inflorescence stem might be explained by growth under optimal conditions (for instance, the plants did not face drought). Furthermore, wax ester biosynthesis might occur predominantly in the upper parts of growing stems. This assumption is supported by the GUS activity assay performed by Li and coworkers which revealed a decrease in *WSD1* expression in direction of lower parts of the stem. The expression of *WSD1* in full-grown green wild type siliques is accompanied by the presence of a variety of wax ester species in the silique cuticle, while the amount of wax esters in silique cuticles of the *wsd1* mutant is significantly reduced (Figure 40). The expression of *WSD1* in flowers is accompanied by the presence of wax esters in flowers of the wild type and the significantly reduced wax ester amount in flowers of the *wsd1* mutant line (Figure 31) indicates that *WDS1* also contributes wax ester synthesis in flowers. Schmid *et al*., 2005, analyzed single organs of the flower and found by far the highest expression of *WSD1* in the carpels, therefore wax esters might accumulate at the carpels as well.

The expression data obtained for *WSD2* (Figure 14) confirm those published by Schmid *et al*., 2005. Schmid *et al*., 2005, published *WSD2* being mainly expressed in siliques/seeds in stage globular and in carpels and pedicels of flowers. In the present study, *WSD2* expression was detected in inflorescence and siliques which is in agreement with the published data.

Very little expression data exist for *WSD3*. Obularredy *et al*., 2013, measured *WSD3* expression by qPCR in guard cells. Other cells or plant tissues were not analyzed by Obularredy *et al*., 2013. In the present study, *WSD3* expression was detected in inflorescences and siliques (Figure 14).

The expression data available for *WSD4* reveal the highest gene expression in roots (Schmid *et al*., 2005). Lower gene expression levels were detected in seeds of the stage "walking-stick to early curled-cotyledons", flowers and leaves. Very weak expression was detected for leaves and stem. The present study confirms the expression of *WSD4* in roots and inflorescence (Figure 14). Furthermore, in this study, *WSD4* expression was detected in full-grown green siliques containing seeds (Figure 14). This expression might be localized in the developing seeds as it was described by Schmid *et al*., 2005, but *WSD4* might be expressed also in parts of siliques without seeds.

No data were available for the expression of *WSD5*. In the present study, expression was detected in inflorescences and siliques (Figure 14).

The *WSD6* expression data obtained in the present study confirm the expression data published by Schmid *et al*., 2005: *WSD6* is expressed widely in different plant tissues. By Schmid *et al*., 2005, the highest expression of *WSD6* was detected in senescent leaves and in flowers (here especially the sepals) but expression was also present in all other tissues analyzed. Expression of *WSD6* was further detected in guard cells (Obularredy *et al*., 2013). The expression data generated in the present study (Figure 14) confirm the published data by revealing *WDS6* expression in each analyzed plant tissue.

In the present study, *WSD7* was also found to be expressed in all analyzed plant tissues (Figure 14). High expression was noted in late stages of seed development with increasing expression in the seed stage "mid to late torpedo embryo", highest expression in the following seed stage "late torpedo to early walking-stick embryo" and the expression of *WSD7* remains still high in the subsequent seed developmental stages until the mature seed stage "green cotyledons embryo" (Schmid *et al*., 2005). High expression of *WSD7* was also observed in roots. Beside these tissues harboring high *WSD7* expression, the gene was widely expressed in lower amounts in all analyzed tissues, among those in guard cells (Schmid *et al*., 2005; Obularredy *et al*., 2013). While wax esters are widely found in aerial tissues (albeit with extremely low amount on leaf surfaces), the occurrence of wax esters in roots is nowhere described and also could not be detected in this work. However, after the experimental part of this work, Patwari *et al*. (2019) described wax ester synthase activity for both WSD6 and WSD7 in an enzymatic assay in insect cells, therefore, the contribution to root wax ester synthesis by WSD7 and also WSD6 might be extremely low or both WSD proteins might harbor a further enzymatic activity. It might also be that WEs are produced in roots only during specific conditions like stress or pathogen attack or that the WEs are not secreted to the roots surface. The WSD proteins might further act as DGAT or harbor other activities.

For several other annotated WS/DGATs, DGAT activities have been described, as for instance, WSD1 harbors both enzymatic activities with an approximately 10-fold lower DGAT activity than WS activity (Li *et al*., 2008). The same was published for the WS/DGAT from *Acinetobacter baylyi* strain ADP1 (formely *Acinetobacter calcoaceticus* strain ADP1, Vaneechoutte *et al*., 2006)

(Kalscheuer and Steinbüchel, 2003). Four WS/DGAT homologues from *Mycobacterium tuberculosis* H37Rv exhibit significant DGAT activities but no significant WS activity (Daniel *et al.*, 2004), while other WS/DGATs like the WS/DGAT from *Petunia hybrida* W115 harbor only a WS activity (King *et al*., 2007). Therefore, in addition to the wax ester synthase activity, WSD7 might function as DGAT contributing TAG to the seeds. This assumption is supported by the fact that the synthesis of triacylglycerol in developing seeds occurs in late stages of seed development. The biosynthesis of TAGs in developing seeds starts about 8 days after flowering when the developing seeds are in the stage "torpedo" and goes on until the seeds desiccate (Gómez *et al*., 2006; Focks and Benning, 1998; Siloto *et al*., 2006). As described above, the expression of *WSD7* also increases in the developmental stage "torpedo" and the expression continues to be high until the seed reached the developmental stage "green cotyledons embryo" (Schmid *et al*., 2005). However, DGAT1 and PDAT were described to be the major players for seed TAG synthesis in *Arabidopsis* (Zhang *et al*., 2009). Therefore, it is also possible that WSD7 is involved in wax ester synthesis in seeds. While wax esters presumably do not occur on the surface of *Arabidopsis* roots, TAGs are present in minor amounts in roots, but also in leaves and other vegetative tissues in *Arabidopsis* (Kelly *et al*., 2013). This goes along with the expression of *WSD7* in all analyzed tissues (Figure 14). Furthermore, as described in more detail below (see 4.2), the increase in *WSD7* expression upon exposure to drought stress going along with the accumulation of TAGs further supports the assumption that WSD7 harbors DGAT activity.

Little expression data are available of *WSD8*. Obularredy *et al*., 2013, published that *WSD8* expression was detected in guard cells. In the present study, *WSD8* was expressed highest in siliques (Figure 14), and with lower level in inflorescence. Very low expression of *WSD8* was found in stem.

For the genes *WSD9* and *WSD10*, no expression data were published. In the present study, *WSD9* expression was highest in stem and to a lower level in siliques. *WSD10* was found to be expressed very low in roots (Figure 14).

Expression of *WSD11* was detected only in inflorescences (Figure 14). This confirms expression data published by Takeda *et al.*, 2013, where *WSD11* (designated *FOP1*) expression was observed only in inflorescence and flowers but not in any other plant tissue. While Takeda *et al.*, 2013, focused on expression in aerial plant tissues, in this work also root tissue was analyzed and no expression of *WSD11* was detected in roots (Figure 14). Takeda *et al.*, 2013, analyzed *WSD11* expression in different floral developmental stages by a GUS activity assay and found *WSD11* being mainly expressed in the petal primordia in stage 9. After this developmental stage, the petals elongate through a narrow gap between sepals and anthers (Takeda *et al*., 2013).

4.2 Expression of *WSD* Genes in Leaves and Roots after Exposure to Stress

The exposure of *A. thaliana* WT to the stresses, ABA, NaCl or drought, resulted in elevated gene expression levels for some members of the *WSD* gene family (Figure 15). Especially *WSD6* and *WSD7* which were also expressed under control conditions exhibited a strong increase in gene expression in leaves and roots upon exposure to all applied stresses. For *WSD1* which was not expressed in leaves of the unstressed control, an induction of the gene expression after the exposure to the stresses was observed. Expression levels of *WSD5* could only be detected after exposure to 24 h of drought, in leaf and root tissue.

For some members of the *WSD* gene family, also a decrease in gene expression was observed in stressed root tissue (Figure 15 B), but not in stressed leaf tissue. Especially for *WSD10* that was strongly expressed in the control, no gene expression after exposure to ABA as well as only a reduced gene expression after exposure to salt stress and drought could be detected. Additionally for *WSD4*, a reduction of gene expression could be observed in roots after exposure to the applied stresses, but only after 24 h.

The obtained gene expression data were again compared with data provided by the *Arabidopsis* eFP browser (Goda *et al*., 2008 and Kilian *et al*., 2007). The experimental setting is different from the one of the present study by the age of the plants (18-days-old and 7-days-old plants, vs. 28-days-old plants in this study), by the concentration of ABA (10 µM vs. 100 µM) and drought exposure (air stream for 15 min vs. aeroponic growth for up to 24 h), and by the method of gene expression analysis (RNA hybridized to ATH1 Affymetrix GeneChip vs. semiquantitative RT-PCR with analysis in agarose gels). While the gene expression data published on the eFP browser were obtained by analyzing seedlings with roots (ABA stress) or by analyzing root and shoot tissue separately (NaCl and drought stress), in this project, the gene expression data were generated by analyzing root or leaf tissue separately. Despite the differences in the experimental setting, the *WSD1* gene expression data found on the eFP browser confirm the expression data generated in this study: the gene expression level of *WSD1* is elevated after exposure to all applied stresses compared to the unstressed control. Furthermore, eFP browser results for NaCl and drought stress show that *WSD1* expression increased in the shoot and not in the root which goes along with the results obtained in this study (Figure 15 A and 13 B) where *WSD1* gene expression could only be observed in stressed leaf tissue but not in stressed root tissue. The increase in *WSD1* gene expression upon exposure to drought, ABA, NaCl and furthermore cold was also described by Seo *et al*., 2011. In this publication, it was not distinguished between different plant tissues but two-week-old plants were analyzed, while in the present study, the expression of *WSD1* was analyzed in the two plant organs rosette leaves and roots (Figure 15).

The gene expression data of *WSD2* provided by the eFP browser is consistent with the data obtained in the present study (Figure 15): the level of gene expression was undetectable after

exposure to the stresses (eFP browser) while in the present study, no gene expression of *WSD2* was detectable on the gel.

Also the gene expression data for *WSD4* provided by the eFP browser confirmed some of the results obtained in the present study: the roots of plants exposed to drought or salt stress revealed a decrease in *WSD4* gene expression after 12 h of stress treatment (data on the eFP browser). After 24 h of stress treatment, the *WSD4* expression level were similar to the untreated control. There, the treatment with ABA resulted in no changes in gene expression compared to the control. In the present study, a reduction of gene expression in roots was observed after exposure to all applied stresses (Figure 15 B).

WSD6 and *WSD7* showed a clear increase in gene expression in all stressed tissues in this study (Figure 15). These results partly confirm the data provided by the eFP browser as there, for both genes a strong increase in gene expression was observed after ABA treatment which goes in line with the results obtained in the present study. For drought stress and salt stress, the gene expression was only slightly increased, remained equal or was even reduced compared to the control.

No expression data were published for the genes *WSD3*, *WSD5*, *WSD8*, *WSD9*, *WSD10* and *WSD11* concerning the applied stresses.

Different experimental settings used in this study and described on the eFP browser might explain the different expression results of the *WSD* genes. However, many gene expression data provided on the eFP browser are similar to those obtained in this study as described above. The increase in gene expression especially for *WSD1*, *WSD6* and *WSD7* upon the applied stresses indicates an involvement of these proteins in the response to drought, maybe by contributing wax esters to the cuticle.

WSD1 was already characterized as wax ester synthase contributing wax esters to the stem cuticle under optimal growth conditions (Li *et al*., 2008). In this study, *WSD1* expression could not be detected in rosette leaves under optimal growth conditions (see Figure 14 and Figure 15A "control") instead the expression was induced upon exposure to all applied stresses in rosette leaves (Figure 15 A). In plants grown under optimal growth conditions, wax esters occur only in minor amounts in leaf cuticles with levels of 0.2 µg/dm^2 in the Wassilewskija and Landsberg *erecta* ecotypes (Jenks *et al*., 1995). However, as a response to drought stress, the amount of wax esters might increase in leaf wax as a result of induced expression of *WSD1* upon drought stress. This assumption is supported by the *shn* mutant which features both, an increased load of cuticular waxes, including wax esters, and an increased resistance to drought (Aharoni *et al*., 2004).

Drought, osmotic stress and ABA lead to a general accumulation of cuticular waxes in leaves of *Arabidopsis* (Kosma *et al*., 2009; Seo *et al*., 2011), therefore, it is possible that also wax esters accumulate in leaf cuticles as a response to drought, presumably contributed by WSD1. However,

the proportion of wax esters in total leaf waxes is very low. Therefore, the contribution of wax esters to overall protection of the leaf against water loss of *Arabidopsis* plants might be rather limited, even under stress conditions. The induction of the *WSD1* gene expression as response to drought, ABA and salt stress (150 mM NaCl) was also published by Seo *et al*., 2011. Seo and coworkers focused on MYB96, a transcription factor promoting drought resistance in an ABA dependent signaling pathway. In the publication, the author describes that MYB96 induces the expression of *WSD1*. While Seo and coworkers did not discriminate plant organs but analyzed whole plant material, in this study, it could be shown that *WSD1* expression is induced in leaves but not in roots after the stress treatment (Figure 15). Seo and coworkers found putative MYB-binding consensus sequences in the promoter of *WSD1* and verified them experimentally as direct binding sites (Seo *et al*., 2011).

Since it is likely that also other members of the *WSD* gene family are involved in the response to drought, it was searched for putative MYB-binding consensus sequences in the promoters of other *WSD* genes. The sequences of the *cis*-elements which are characterized as putative MYB binding sequences, not only for MYB96 but also for another drought-inducible MYB homolog, MYB2 (Urao *et al*., 1993), were published by Abe *et al.*, 2003, and Urao *et al*., 1993. These sequences were used as queries in the present study. As depicted in Table 5, the promoters of all *WSD* genes except *WSD10* contain putative MYB-binding consensus sequences (*cis*-elements). Therefore, not only the expression of *WSD1*, but also of *WSD5*, *WSD6* and *WSD7* might be induced by a MYB transcription factor as a response to drought, but this assumption needs to be further examined. The expression of other *WSD* genes which are not highly expressed after the stress treatment might be regulated by other factors.

WSD6 and *WSD7* are already expressed under optimal growth conditions (also in all other plant tissues which have been analyzed, see Figure 14). The expression levels of the two genes increased strongly after the stress treatments in leaf and root tissue (see Figure 15). As mentioned above, extremely low amounts of wax esters occur in the leaf cuticle of *Arabidopsis* (Jenks *et al*., 1995) and it is possible that the amount might be increased in response to drought stress. *Arabidopsis* roots respond to drought by suberization of the root endodermis (younger primary roots) and the periderm (older primary roots) (Franke and Schreiber, 2007; Franke *et al*., 2009). While there are numerous publications on suberin and its associated waxes (Vishwanath *et al*., 2013; Delude *et al*., 2016), nowhere the occurrence of wax esters in *Arabidopsis* roots is noted. Even so, it might be possible that one or both genes contribute wax esters in minor amounts to root waxes. However, as discussed already above (see 4.1), it is also likely that WSD6 and WSD7 harbor further enzymatic activities in addition to wax ester synthase activity, for instance DGAT activity. This assumption is supported by the fact that the biosynthesis of TAG is increased in response to drought and salt stress in *Arabidopsis* (Gasulla *et al*., 2013; Mueller *et al*., 2015) which is consistent with the increased expression level of both genes. The accumulation of the polyunsaturated TAG

species is described for several abiotic stresses like heat, drought and salt stress (Mueller *et al*., 2015). Mueller and coworkers analyzed the effects of heat stress in-depth and found a similar extra-chloroplastic accumulation of the polyunsaturated TAGs in roots and shoots. *WSD6* and *WSD7* are expressed in both plant tissues, roots and shoots, and in both plant tissues, the expression levels are increased upon the stresses (Figure 15). Therefore, if the two genes encode DGATs, it is possible that they contribute to TAG synthesis in extraplastidial oil bodies. The polyunsaturated TAG species which are synthesized after drought stress might accumulate in oil bodies of the cytosol in similar amounts in roots and shoots as it occurred after heat treatment (see Mueller *et al*., 2015). As mentioned above, *WSD6* and *WSD7* are expressed in all analyzed tissues (Figure 14) of *Arabidopsis* plants grown under optimal conditions. Also TAGs occur in minor amounts in roots, leaves and also other vegetative tissue in plants grown under optimal conditions (Kelly *et al*., 2013). *WSD6* and *WSD7* might contribute to these TAGs.

Table 5: Sites of Putative MYB-binding Consensus Sequences in the Promoters of *WSD* Genes.

Promoter sequences were queried for putative MYB-binding consensus sequences within 1000 bps upstream from the translation start site of the respective genes. The following sequences were used as queries: (tggttt), (aaacca) (both sequences were found in the promoter of *WSD1* as described by Seo *et al*., 2011) and (taactg). (taactg) is known as recognition site of the MYB homolog *At*MYB2 whose expression is induced by exposure to drought, salt and ABA (Urao *et al*., 1993). Numbers represent the distance of the putative MYB-binding consensus sequence upstream from the respective translation start site.

Gene	Putative MYB-binding Consensus Sequence
WSD1	-774 (tggttt), -748 (aaacca) (as described by Seo *et al*., 2011)
WSD2	-70 (aaacca)
WSD3	-1100 (tggttt), -1082 (tggttt), -906 (aaacca), -209 (taactg)
WSD4	-653 (aaacca)
WSD5	-337 (aaacca), -317 (aaacca), -10 (aaacca)
WSD6	-827 (aaacca), -330 (taactg)
WSD7	-865 (aaacca), -313 (aaacca), -282 (aaacca)
WSD8	-959 (tggttt), -791 (aaacca), -697 (aaacca), -536 (taactg), -333 (tggttt), -76 (aaacca)
WSD9	-496 (tggttt)
WSD10	not found
WSD11	-175 (aaacca), -63 (taactg), -48 (aaacca)

The expression of *WSD5* could be observed only after 24 h of exposition to drought, none of the other applied stresses, ABA and NaCl, resulted in detectable gene expression of *WSD5*. *MYB96* and *MYB2* expression are induced by ABA and salt stress (Seo *et al*., 2009; Urao *et al*., 1993), therefore *WSD5* gene expression should be induced also by both ABA and salt, if it was mediated by one of these transcription factors. Due to the missing expression of *WSD5* after exposition to ABA and salt stress, it is unlikely that MYB2 or MYB96 induce the expression of *WSD5*. Therefore, the induction of *WSD5* expression by long-time exposure to drought is likely regulated otherwise. Furthermore, *WSD5* is only expressed after a long time of deprivation of water which means that

WSD5 is not involved in an early response to drought. Additionally, *WSD5* expression is not only induced in aerial parts of the plant but also in roots leading to the assumption that WSD5 might not function as a wax ester synthase. However, WSD5 might harbor DGAT activity which was already discussed above as further enzymatic activity of WSD6 and WSD7, induced in a late stage of drought response.

4.3 Transcripts of *WSD3* and of *WSD10*

The two different splice variants of *WSD3* found in inflorescences (Figure 16 A) confirm the sequences of splice variants deposited at the ARAPORT project, where *WSD3* splice variant 1 is referred to as At2g38995.2 (https://apps.araport.org/thalemine/portal.do?externalids=AT2G38995.2) and *WSD3* splice variant 2 is referred to as At2g38995.1 (https://apps.araport.org/thalemine/portal.do?externalids=AT2G38995.1). For both variants, expression in the inflorescence tissue was measured which is in line with these data. The function of these different splice variants is not known, however, splice variant 2 lacks the sequence HH*XXX*DG which resides in the second annotated exon and is spliced out in this variant (Figure 16 A). This sequence is highly conserved in WS/DGAT sequences and represents the putative active site of the enzyme (Kalscheuer and Steinbüchel, 2003). *WSD3* splice variant 2 might be inactive, in contrast to splice variant 1, because the putative active site of WS/DGATs is absent.

The sequence of the cDNA of *WSD10* generated from root mRNA (Figure 16 B) is identical to the sequence deposited at ARAPORT project. This sequence is referred to as At5g53380.1 (https://apps.araport.org/thalemine/portal.do?externalids=AT5g53380.1). The 18 bps missing in the two cDNAs (the one of this study and the one found at ARAPORT project) are annotated to contribute to the end of the first exon at TAIR. Splice variants were not found for *WSD10*, but it is possible that another up to now unknown splice variant of *WSD10* might be identical with this annotation.

4.4 Subcellular Localization of WSD Proteins

For subcellular localization of WSD proteins, it was the aim to clone two cDNA constructs for each WSD protein: one leading to the expression of the WSD protein in N-terminal fusion with eGFP, the other with C-terminal fusion to eGFP. By the generation of two fusion constructs per WSD protein, the risk that eGFP influences the localization of the WSD protein should be minimized. At the end of the present study, three different fusion constructs (WSD3 fused C-terminally to eGFP, WSD4 and WSD9 fused N-terminally to eGFP) were generated and the subcellular localization of these fusion proteins were examined in *N. benthamiana*.

The fluorescing overlays of the respective WSD proteins WSD3, WSD4 and WSD9 suggested that all three proteins reside at the ER (Figure 17). The three proteins lack C-terminal ER retention sequences like HDEL or KDEL, also the residual WSD proteins lack these ER retention signals. Besides the supposed localization of WSD3, WSD4 and WSD9 at the ER detected in the present study, WSD1 is also localized at the ER (Li *et al.*, 2008). Furthermore, WSD6 and WSD7 are localized at the ER and Golgi apparatus (Patwari *et al*., 2019). However, WSD11 (designated FOP1) resides at the plasma membrane (Takeda *et al*., 2013). The subcellular localization of the putative WS/DGATs in membranes is in line with the subcellular localization of characterized WS/DGATs in other species: *Ph*WS1 of *Petunia hydrida* W115 is membrane-bound (King *et al*., 2007), WS/DGAT of *Acinetobacter baylyi* ADP1 is located mainly in the plasma membrane (Stöveken *et al*., 2005). Furthermore, other enzymes involved in wax ester biosynthesis reside at the ER, for instance the fatty acyl-CoA reductase CER4 which catalyzes the biosynthesis of primary fatty alcohols which are used as substrates by WSD1 (Rowland *et al*., 2006; Lai *et al*., 2007). Also the fatty acyl-CoA elongation yielding substrates for CER4 is localized at the ER (Lessire *et al*., 1995). Therefore, if WSD3, WSD4 and WSD9 are wax ester synthases using primary alcohols synthesized by CER4 similar to WSD1, the close localization of the involved enzymes might result in an efficient biosynthesis of wax esters. Furthermore, if WSD3, WSD4 and WSD9 are active as DGATs, the substrate diacylglycerol (DAG) occurs in the ER and is therefore available for TAG biosynthesis possibly catalyzed by WSD3, WSD4 and WSD9. However, the enzymatic activity of the putative WS/DGATs WSD3, WSD4 and WSD9 is unclear and still needs to be characterized.

4.5 Heterologous Expression of WSD1 in *Saccharomyces cerevisiae*

Li *et al*., 2008, published that WSD1 synthesizes wax esters when expressed in *S. cerevisiae* H1246 supplemented with suitable substrates. Therefore, heterologous expression in yeast appeared to be an appropriate approach to characterize the enzymatic activities of the other WSD enzymes, WSD2 – WSD11 with WSD1 being a positive control. Expression constructs of the *WSD* gene members (except *WSD3* and *WSD10*) were cloned by inserting the cDNAs into the yeast expression vector pDR196. The protocol published for *WSD1* (Li *et al*., 2008) should be used for the expression of the other *WSD* cDNAs. To achieve a functional heterologous expression of WSD1 in yeast, several experiments were undertaken. Among others, different clones of the yeast strain H1246 were used (glycerol stocks bn31 and bn508, kindly provided from Prof Dr. Sten Stymne, Swedish University of Agricultural Sciences, Alnarp, Sweden). DNA constructs in different vectors (pDR196-*WSD1*, pESC-URA-*WSD1*, pYES2-*WSD1*) with the construct pESC-URA-*WSD1* being the one used by Li *et al*., 2008 (both, cDNA of *WSD1* and vector pESC-URA were kindly provided by Prof Dr. Ljerka Kunst, University of British Columbia, Vancouver, Canada, *WSD1* was inserted in pESC-URA in this study) were employed. The experimental protocol as described by Li *et al*., 2008,

but also several variations of this protocol were followed. For the detection of wax esters, a highly sensitive Q-TOF mass spectrometer was used but also thin layer chromatography was performed. The functional expression of WSD1 in yeast as published by Li *et al*., 2008, could not be reproduced in any of these experiments. This finding was also confirmed by other members the laboratory as well as members of another laboratory who conducted heterologous expression of WSD1 in yeast.

In this work, different yeast clones were cultivated with palmitic acid (16:0) and octadecanol (18:0ol) or grew without these supplements (see 3.6). The cultivated yeast clones carried either pDR196-*WSD1*, pESC-URA-*WSD1*, pYES2-*WSD1* or the empty vector pDR196. The supplements were added after the inoculation of the main cultures with overnight cultures to an OD_{600} of 0.02. After 24 h of cultivation, the cultures were harvested, the lipids extracted, the extracts purified and subsequently analyzed by TLC or Q-TOF MS/MS (see 3.6).
The analysis by Q-TOF MS/MS revealed that low amounts of WEs occurred in all samples supplemented with palmitic acid (16:0) and octadecanol (18:0ol), also in the empty vector control. In fact, the empty vector control contained the highest amount of wax esters (Figure 20).
On the TLC plate, no wax esters were visible on the lanes of all samples (Figure 18). Thus, WSD1 was not active as wax ester synthase in yeast. The low amounts of wax esters measured by Q-TOF MS/MS found in all samples supplemented with palmitic acid (16:0) and octadecanol (18:0ol) might be synthesized by a further unknown acyltransferase in H1246. Sandager *et al.*, 2002, described the occurrence of minor amounts of steryl esters and triacylglycerols in H1246 during stationary phase. In the publication of Li *et al*., 2008, WSD1 was presumed to be active in yeast because 18:0ol/16:0 wax ester and also wax esters with the longer chain lengths of 24:0ol/16:0 and 28:0ol/16:0 accumulated after supplementation of palmitic acid (16:0) together with octadecanol (18:0ol), tetracosanol (24:0) or octacosanol (28:0ol). However, the experiment lacked a suitable control. Yeast H1246 cells harboring the empty vector were only supplied with the fatty acid palmitic acid (16:0) but not with alcohols, in contrast to the WSD1 expressing cultures which were incubated with fatty acid and alcohol. Therefore, cells with the empty vector were not able to produce wax esters because of the lack of fatty alcohols, which might explain the absence of wax esters in the control.
While the heterologous expression of WSD1 in yeast did not result in any detectable wax ester synthase activity in the present study, an unknown lipid spot (unknown lipid 1, UL1) was detected on the TLC plate in the lanes of all WSD1 expressing samples but not in the lane of the control (Figure 18). UL1 was further investigated. Another unknown lipid 2 (UL2) which also occurred in the control was therefore not further examined. The spots of UL1 were more intense when the plate was incubated in iodine vapor and less intense after the plate was charred. Furthermore, the UL1 spots were found in higher amounts in the cultures which were not supplemented with palmitic acid (16:0) and octadecanol (18:0ol) and in less amounts in the cultures supplemented

with octadecanol and palmitic acid. The UL1 spots were scraped out from a preparative TLC plate and analyzed by Q-TOF MS/MS where ions with m/z of 300 - 1000 were selected and fragmented. In the total ion chromatogram (TIC) of the WSD1 expressing samples, a parental ion with m/z of 376.3265 yielded the highest peak (Figure 19), while in the TIC of the control, parental ions with a very similar m/z of 376.3449 or 376.3457 were present, but occurred in clearly lower abundance. The m/z's of the parental ions in the WSD1 and in the control sample differed by m/z of 0.02, however, the fragmentation of m/z around 376.5 resulted in very different pattern (Figure 19 B). Therefore, the parental ion derived from the WSD1 sample might represent UL1. The fragmentation of m/z around 376.5 yielded as main fragment a product ion with m/z of 105.0704 in the WSD1 sample while this product ion occurred only in trace amounts in the control (Figure 19 B). In the WSD1 sample, the fragmentation of m/z of 376.3265 might result in a neutral loss of an unsaturated fatty acid, $C_{16:1}$ as an ammonia adduct ($C_{16}H_{30}O_2$ NH_3; calculated mass, 271.251129). Such a neutral loss is observed in MS/MS spectra of DAG and TAG which show a loss of C16:1-NH_3 (Murphy *et al*., 2007). $C_{16:1}$ is one of the major fatty acids synthesized by *S. cerevisiae* and might be esterified by WSD1 to an alcohol. The product ion with m/z of 105.07 might represent a C_8H_9 fragment as it is found upon fragmentation of oxysterols (Griffiths *et al*., 2006). Besides the by far highest peak with m/z of 376.3265 in the TIC of the WSD1 sample (Figure 19 A), also other less abundant ions that fragment among others to the product ion with m/z of 105.07 occur in the TIC of the WSD1 sample. These less abundant parental ions have m/z of around 277, 294, 308, 310, 326, 350, 359, 362, 376, 392, 404 and several m/z ratios between 1000 and 1058. Parental ions with m/z of around 322 and 326 with a distinct peak of m/z of 105.07 occur in both, the control and WSD1 samples. The presence of the unknown lipid in all WSD1 expressing cultures indicates a catalytic active WSD1 enzyme, though no wax ester synthase activity of WSD1 could be detected in yeast. For the identification of the unknown lipid and also to identify the role of this lipid in *Arabidopsis*, further investigations need to be performed.

Another approach to demonstrate a wax ester synthase activity of WSD1 in yeast was to omit substrate supplementation into the medium. As fatty acids and long-chain fatty alcohols are lipophilic, while the medium is aqueous, the uptake of the substrates by the yeast might be impaired. Therefore, cDNA constructs carrying a fatty acyl-coenzyme A reductase from *Marinobacter aquaeolei* VT8 (*Ma*FAR) (Hofvander *et al*., 2011) either alone, or together with WSD1, or carrying exclusively WSD1 were cloned (see 2.3.1.6). While *Ma*FAR catalyzes the synthesis of diverse long-chain fatty alcohols in yeast (Hofvander *et al*., 2011), the fatty acyl-CoA substrates necessary for WSD1 activity are endogenous compounds of yeast metabolism. Thus, the two substrates were synthesized endogenously in the yeast and substrate supplementation could be avoided. As depicted in Figure 21, wax esters were present in the samples of the cultures expressing the *Ma*FAR alone or together with WSD1, but not in the empty vector control and to a very low level in the cultures expressing WSD1 alone. In fact, the culture expressing *Ma*FAR alone

contained the by far highest amount of wax esters, indicating the absence of a wax ester synthase activity in the *Ma*FAR + WSD1 expressing cultures and the presence of long-chain fatty alcohols synthesized by an active *Ma*FAR. Sandager *et al.*, 2002, described the occurrence of minor amounts of steryl esters and triacylglycerols in *S. cerevisiae* H1246 during stationary phase. The enzyme responsible for the minor amounts of steryl esters and triacylglycerols might also be responsible for the low amounts of WEs found in the samples.
Altogether, wax ester synthase activity of WSD1 in yeast could not be detected, however WSD1 might harbor a further enzymatic activity leading to the synthesis of an unknown lipid UL1.

4.6 Analysis of Wax Esters by Q-TOF MS/MS

All wax ester extracts were purified by solid phase extraction (SPE) prior to the measurement of wax esters by Q-TOF MS/MS. As wax esters occur only in minor amounts in *Arabidopsis thaliana* cuticular wax (for example approx. 0.7 - 2.9 % in total stem wax (Jenks *et al.*, 1995)) and as yeast crude cell extracts contained huge amounts of supplemented free alcohols and free fatty acids, the purification of the extracts led to a reduced lipid complexity and amount and reduced the occurrence of unknown isobaric contaminants. The purified samples contained still wax esters and steryl esters which could not be separated by SPE (or by TLC, see also Iven *et al.*, 2013). Therefore, wax ester data presented in this work do not contain wax ester species which have almost identical m/z's as their isobaric steryl esters. A problem regarding the clear identification of most WE species searched for in *Arabidopsis* wax was the very low intensity of their product ions. This led to signals which did not differ in their intensities from intensities of background signals. The problem might be solved by extracting wax from more plant material. However, a few WE species which were most abundant in the analyzed wax sample could be clearly identified. The problem of very low intensities was present for *Arabidopsis* wax samples (here especially for *Arabidopsis* flower wax) but not for barley wax where many WE species could be clearly identified.

The use of the standard mixture containing 1 nmol of 18:0ol/17:0 and 3 nmol of 18:0ol/27:0 should facilitate to correct the signal intensities according to the different signal responses of short vs. long wax esters. Although a threefold amount of the longer chain length C_{45} wax ester standard was employed, the signal intensity of the product ion $[C_{27}H_{54}O_2H]^+$ was low compared to that of the C_{35} wax ester product ion $[C_{17}H_{34}O_2H]^+$. This might be explained by the higher hydrophobicity due to the longer chain length of the C_{45} wax ester. Furthermore, the infusion of the 18:0ol/27:0 wax ester into the mass spectrometer was delayed, probably caused by an absorption to the injection loop or ion source. Therefore, the 18:0ol/27:0 wax ester was not used as standard for the analysis of wax esters. Therefore, only the 18:0ol/17:0 wax ester (1 nmol of 18:0ol/17:0) was used for the quantification. The quantification of wax esters based on the

18:0ol/17:0 internal standard might have led to an underestimation of very long chain wax esters. This problem might be eliminated by establishing correction factors for different chain lengths. The establishment of a correction factor was described in Iven *et al*., 2013, where wax esters with chain lengths of C_{32}-C_{36} and of C_{38}-C_{64} were quantified by using different correction factors and also only one internal standard, 17:0ol/17:0, was used. To increase the accuracy of the data presented in this work, a correction factor might be applied also for the present data. However, the method presented here is suitable for the comparison between different samples sets.

4.7 Wax Esters from Stem Surface Wax of the *wsd* Mutant Lines

Wax esters prepared from stem wax of the *wsd* mutant lines and wild type controls were analyzed as described in 2.3.11.6 and 2.3.11.7. In Figure 25, the distribution of even-numbered wax ester chain lengths in WT stem varying from C_{38} to C_{54} is presented. Most abundant chain lengths are C_{42} and C_{40} chain lengths followed by C_{44} and C_{38} chain lengths, with amounts of around 0.023 µg/cm² for C_{40} and C_{42} chain lengths. C_{44} chain length was described to be the most abundant, followed by C_{42} and C_{46} wax ester chain lengths with amounts of around 0.25 to 0.35 µg/cm² (Li *et al*., 2008) or 0.03 to 0.08 µg/cm² (Lai *et al*., 2007) for each the C_{44}, C_{42} and C_{46} chain lengths. The chain lengths C_{44}, C_{42} and C_{46} are most abundant in stem wax esters as published previously (Lai *et al.* 2007; Li *et al*., 2008). The sum of wax esters with the same total chain length (alcohol + fatty acid) in this work are somewhat lower than those published by Lai *et al*., 2007. The distribution of wax esters was different between the present study and published data. In the present study, chain lengths with C_{42} and C_{40} are most abundant, in contrast to the published data, where C_{44}>C_{46}>C_{48} wax ester chain lengths are most abundant in stem wax (Li *et al*., 2008; Lai *et al*., 2007; Rowland *et al*., 2006). This difference might be caused by the measuring method used in this work which shifts wax ester amounts in favor of shorter chain lengths as mentioned in 4.6. However, also the analysis of different parts of the stem might have contributed to different results as wax ester data published by Lai *et al*., 2007; Li *et al*., 2008, and Rowland *et al*., 2006, were obtained by analyzing whole stems while in this work, the wax was extracted from a 2-3 cm piece cut from the lower part of the stem (see 2.3.11.6).

The molecular species composition measured in WT stem wax is presented in Figure 26. The WE species which were clearly identified were 22:0ol/16:0, 24:0ol/16:0, 26:0ol/16:0 and 28:0ol/16:0. The 16:0 acyl moiety was by far the most abundant acyl moiety incorporated in wax esters which confirms the data published by Lai *et al*., 2007. Thus, the wax ester species 26:0ol/16:0, 24:0ol/16:0 and 28:0ol/16:0 were most abundant in WT stem wax (Figure 26). The wax ester composition of the *wsd1* mutant is presented in Figure 26 as well. Compared to the wild type, the amount of wax esters in stem wax is strongly reduced in *wsd1*. This reduction affects especially the amount of the main wax ester species occurring in wild type stem, 26:0ol/16:0,

24:0ol/16:0 and 28:0ol/16:0, which are only detected in low amounts in the *wsd1* mutant. The data obtained in this work are in agreement with Li *et al*., 2008, who published a severe reduction of wax esters in *wsd1* mutants.

Furthermore, in the present work, it was shown that the WE species 22:0ol/16:0 which occurs only in low amounts in wild type stem wax is only slightly affected by the reduction.

Therefore, another wax ester synthase might also contribute wax esters to stem wax while the reduction of main abundant wax ester species in stem indicates the involvement of WSD1 in wax ester synthesis as published by Li *et al*., 2008.

The mutants *wsd5*, *wsd7* (both *wsd7-1* and *wsd7-2*) and *wsd11* showed also a reduction of several wax ester species in stem (Figure 27, 28 and 29). The reduction affects especially the most abundant wax ester species with the 16:0 acyl moieties, but not as strongly as the reduction was observed for *wsd1*. Since in the *wsd1* mutant the most abundant wax ester species are severely reduced and only trace amounts could be detected (Li *et al*., 2008; Figure 26), it appears unlikely that WSD5, WSD7 and WSD11 contribute to these wax ester species in stem as well. For the *wsd7* mutant, Patwari *et al*., 2019, analyzed wax ester amount and species composition in stem and found similar amounts of the above mentioned WE species with 16:0 acyl moieties compared to the WT control. These results differ from the results obtained in this study where 24:0ol/16:0, 26:0ol/16:0 and 28:0ol/16:0 WEs were reduced compared to the WT control. Patwari and coworkers analyzed total stem sections of 10 cm while in this study, shorter stem sections of 2 – 3 cm were extracted. Enzymatic activity assays in Sf9 insect cells revealed a substrate preference of WSD7 for 16:0 alcohol while longer alcohols were only little or not accepted as substrate by WSD7 (Patwari *et al.*, 2019). This substrate preference is not in line with the reduction of the WE species 24:0ol/16:0, 26:0ol/16:0 and 28:0ol/16:0 in *wsd7* with their long chain alcohol moieties found in this study. Therefore, a repeat of the measurement of WEs extracted from wax of longer stem sections than 2 - 3 cm seems reasonable for *wsd7*.

For further examinations of WSD5 and WSD11, second mutant lines for *wsd5* and *wsd11* should be analyzed. For WSD5, the mutant line SAIL_695_H02C might be a candidate for further analysis and for WSD11, the mutant line SALK_093141 could be used for further studies. Both T-DNA insertion lines are available at *The European Arabidopsis Stock Centre*.

4.8 Wax Esters from Flower Surface Wax of the *wsd* Mutant Lines

Wax esters isolated from flower wax of the *wsd* mutant lines and wild types were analyzed as described in 2.3.11.6 and 2.3.11.7. In Figure 30, the distribution of wax esters with even-numbered chain lengths in WT flower varying from C_{38} to C_{52} is presented. The most abundant chain lengths are C_{46} followed by C_{38}, C_{42} and C_{44} with amounts of around 2.2 to 4.9 ng/flower (Figure 30). Bernard and Joubès, 2013, described wax ester chain lengths in *Arabidopsis* flowers

ranging from C_{38} to C_{46} with C_{44} and C_{46} being the most abundant chain lengths. The high amounts of WEs of the chain length C_{46} relative to the other measured chain lengths could be confirmed in this study. However, the C_{38} chain length was not described to also occur in high amounts while in this study, WEs of the chain length C_{38} constituted the second highest amount. The comparison of absolute amounts of wax esters is difficult due to the different scale types since in this study, the wax ester amount per flower was determined while in Bernard and Joubès, 2013, the amount per flower fresh weight was calculated.

The wax ester species composition in flower wax of *Arabidopsis* WT is similar to that measured in stem wax. Again, wax esters with a 16:0 acyl moiety predominate (Figure 31) though in C_{46} wax esters, the most abundant molecular species is 28:0ol/18:0 harboring an 18:0 acyl moiety. Regarding the WE species with chain lengths from C_{38} to C_{52}, the WE species 22:0ol/16:0, 24:0ol/16:0, 26:0ol/16:0, 28:0ol/16:0, 30:0ol/16:0, 28:0ol/18:0 and 26:0ol/20:0 were clearly identified to occur in flower wax in this study (Figure 31).

In addition to WE species ranging from the chain lengths C_{38} to C_{52}, it was also searched for WE species with shorter chain lengths (C_{17} to C_{37}) in which short-to-long and odd-numbered alcohol moieties (C_1 to C_{23}) were incorporated. The search for these WE species in flower wax of *Arabidopsis* was motivated by the results of King and coworkers, 2007, who found WE species with methyl, isoamyl and short-to-medium chain alcohol moieties esterified to very long chain fatty acyl moieties in the petal wax of the *Solanaceae* species *Petunia hydrida*. The WS/DGAT homolog *Ph*WS1 was speculated to be involved in the synthesis of these WE species, since the enzyme catalyzes the synthesis of wax esters consisting of medium chain alcohol moieties and long to very long-chain acyl moieties in vitro (King *et al*., 2007). In *Arabidopsis* WT, WE species with amounts > 0.001 nmol were 8:0ol/18:0, 8:0ol/16:0, 22:0ol/14:0, 12:0ol/16:0, 18:0ol/16:0, 8:0ol/20:0, 16:0ol/16:0, 4:0ol/24:0 and 21:0ol/16:0 (Figure 37). From these WE species, 8:0ol/16:0, 8:0ol/18:0, 18:0ol/16:0 and 22:0ol/14:0 could be clearly identified while the clear identification of the other WE species displayed in Figure 37 was hindered due to low intensities of the product ions. Therefore, these species might not occur in *Arabidopsis* flower wax.

King *et al*., 2007, described WE species with octanol, hexanol and isoamyl alcohol moieties as well as with 24:0, 22:0 and 26:0 fatty acyl moieties to be most abundant in petunia petal wax. WEs with dodecanol, decanol and butanol moieties were also present but less abundant. Furthermore King *et al*., 2007, detected WE species with very-long-chain alcohols (C_{22}-C_{28}) in petunia petal wax. Similarly, WE species with octanol moieties could be identified in *Arabidopsis* flower wax (Figure 37). Furthermore, a WE species with 18:0ol moiety which was not mentioned to occur in petunia petals by King *et al.*, 2007, was present in *Arabidopsis* flower wax (Figure 37).

The comparison of the amounts of the above described WE species between the WT and the *wsd* mutant line(s) resulted in many differences which were often significant (Figure 37 and 38, also Appendix Figure 48). In some cases where two mutant alleles were available for one *wsd* mutation,

a significant difference of the amounts of several WE species was observed between WT and one *wsd* mutant allele, but not the other. This shows the necessity to analyze at least two different mutant lines per *WSD* gene. In *Arabidopsis*, the amount of WEs occurring in the wax extract of 10 flowers was very low. It might be reasonable to analyze WE amounts extracted from considerably more flowers to obtain higher amounts of WEs. Regarding the significant differences between mutant lines and WT, only the WE species are discussed below which showed significant differences for both lines if two mutant alleles were investigated. When only one mutant allele was investigated, significant differences were also discussed.

Again, in the *wsd1* mutant, wax ester species harboring a 16:0 acyl moiety were severely reduced in the flower wax, here in C_{38} to C_{44} chain lengths while this reduction was not or only to a minor extent detected in shorter or longer chain lengths (Figure 31). Wax ester species with other acyl moieties as for instance the highly abundant 28:0ol/18:0 wax esters were not affected by this strong reduction in flower wax of the *wsd1* mutant. The results obtained for *wsd1* mutant led to the conclusion that WSD1 contributes wax esters harboring 16:0 acyl moieties to flower wax, at least for the chain lengths C_{38} to C_{44}. Other wax ester species occurring in flower wax (see Figure 31) might be synthesized by other wax ester synthases.

The flower wax of the two analyzed *wsd2* mutants, *wsd2-1* and *wsd2-2* (presented in different diagrams due to their different ecotypes, Ler and Col-0), revealed a significant reduction of the WE species 8:0ol/16:0 (Figure 37) and 28:0ol/18:0 (Figure 32 and Figure 33) compared to the WT control. Since the WE species are very different from each other regarding the chain lengths of the alcohol moiety, WSD2 might have a broad substrate specificity accepting both very-long and short chain alcohols. Investigations of the two mutant alleles including WE measurements of wax extracted from more plant material might give further hints on the function of WSD2.

Both *wsd3* mutant lines, *wsd3-1* and *wsd3-2*, showed a significant reduction in the C_{36} WE species 22:0ol/14:0 (Figure 37). Therefore, WSD3 might be involved in the synthesis of this WE species in flower wax. However, further investigations with both mutant lines including WE measurements of wax extracted from more plant material might be necessary as described above.

For the mutant *wsd5*, a slight reduction of 22:0ol/16:0 and a slight increase in 8:0ol/16:0 was measured (Figure 34 and Figure 38). Therefore, WSD5 might be involved in the synthesis of 22:0ol/16:0 in flower wax and its reduction might cause a compensatory increase in 8:0ol/16:0. However, a second mutant line needs to be analyzed, a candidate might be the T-DNA insertion line SAIL_695_H02C. Furthermore, WE measurements basing on flower wax extracted from more plant material might be necessary.

Both *wsd8* mutant lines, *wsd8-1* and *wsd8-2*, showed a strong reduction of the WE species 8:0ol/16:0 and 8:0ol/18:0 (Figure 38). Therefore, WSD8 might contribute these WE species to *Arabidopsis* flower wax. Since octanol is incorporated in both WE species, WSD8 might be specific for this alcohol or might favor shorter alcohols over long to very-long chain alcohols. However,

further investigations needs to be performed including WE measurements of wax extracted from more plant material.

Both *wsd9* mutant lines, *wsd9-1* and *wsd9-2*, showed a slight reduction of 8:0ol/18:0 (Figure 38) and 22:0ol/16:0 (Figure 35) in flower wax. WSD9 might have a broad substrate specificity accepting both very-long and short chain alcohols. However, further WE analysis including wax extracted from more plant material might be necessary.

The *wsd11* mutant was characterized by a folded petal phenotype, therefore also designated as *fop1* (folded petals1) by Takeda *et al.*, 2013, and scanning electron microscopy revealed flattened petal epidermal cells in the *fop1* mutant. As WSD11 is annotated as putative wax ester synthase, it was speculated if the enzyme contributes wax esters to the petal wax and by this allows a smooth elongation through the narrow space between anthers and sepals during petal development. As presented in Figure 36 and Figure 38, the wax ester composition and amount of *wsd11* flowers compared to the control are similar, no reduction of wax esters could be detected. Therefore, WSD11 might harbor another function than contributing wax esters to flower wax.

4.9 Wax Esters from Silique Surface Wax of the *wsd* Mutant Lines

Wax esters isolated from silique wax of the *wsd* mutant lines (except *wsd10* mutant lines) and wild type controls were analyzed as described in 2.3.11.6 and 2.3.11.7. In Figure 39, the distribution of even-numbered wax ester chain lengths in WT siliques varying from C_{38} to C_{54} is presented. The most abundant chain lengths are C_{42} followed by C_{40} and C_{44} with amounts of around 1.49 to 2.65 ng/mg fresh weight (Figure 39). The composition of wax esters in siliques of the wild type presented in Figure 40 is similar to that measured in wax of the wild type stem. The WE species 24:0ol/14:0, 22:0ol/16:0, 26:0ol/14:0, 24:0ol/16:0, 26:0ol/16:0, 28:0ol/16:0 and 30:0ol/16:0 were clearly identified to occur in silique surface wax.

Most abundant wax ester species harbor a 16:0 acyl moiety. The analysis of the *wsd1* mutant revealed a severe reduction of these wax esters in silique wax (Figure 40) leading to the assumption that WSD1 might contribute these wax ester species not only to flower wax and stem wax but also to silique wax.

The *wsd5* mutant revealed a slight decrease in the WE species 26:0ol/16:0 (Figure 41). Since only trace amounts of both wax esters remain in silique wax of the *wsd1* mutant, it seems unlikely that WSD5 contribute this wax ester species to silique wax. Therefore, the analysis of another *wsd5* mutant line which might be the T-DNA insertion line SAIL_695_H02C is necessary to interpret further the results obtained for *wsd5*.

4.10 Wax Esters in Leaf Cuticles from *Hordeum vulgare* after Exposure to Drought Stress

As presented in Figures 42 and 43, the amount of wax esters in leaf wax of *Hordeum vulgare* cv. Barke increased after drought stress treatment from 16.025 ng /cm^2 in the unstressed plant to 19.428 ng /cm^2 in the stressed plant (Figure 37). This increase in the total wax ester amount is mainly caused by the strong increase in the two very abundant wax ester species, 22:0ol/16:0 and 20:0ol/16:0. The WE species 22:0ol/16:0 and 20:0ol/16:0 increase from 1.949 and 0.693 ng/cm^2 in leaves of the unstressed plant to 4.818 and 2.230 ng/cm^2 in leaves of the stressed plant (Figure 43). The increase in wax esters in drought stressed barley leaves in this study are in line with data published by Larsson and Svenningsson, 1986. Larsson and Svenningsson, 1986, imposed water deficit on seedlings of 20 different cultivars of *Hordeum vulgare* by lowering the root temperature ("chilling shock", see also Ameglio *et al*., 1990) and thereby lowering the plant water potential. After the chilling shock, they observed a strong increase in wax esters in primary leaves compared to leaves of the unstressed controls. Interestingly, only the wax esters were increased after the stress treatment, while other lipids were generally not affected or were, like alcohols, even reduced after the stress treatment. Furthermore, the relative amounts of wax esters of the total lipids in primary barley leaves are 4.2 – 9.3 % in the unstressed plants while the amounts are 6.3 – 17.2 % in the stressed plants (Larsson and Svenningsson, 1986). These high amounts of wax esters in barley leaves (for comparison: *Arabidopsis thaliana* has approx. 0.1 - 0.2 % wax esters in total leaf wax and approx. 0.7 - 2.9 % in total stem wax (Jenks *et al*., 1995)) and the strong increase in wax esters after the stress treatment lead to the assumption that wax esters play a major role in the cuticle and are involved in the response to drought stress of barley. Furthermore, in the present study, the molecular species composition of wax esters with chain lengths varying from C_{36} – C_{54} were analyzed (Figure 43) and for C_{36} - C_{42}, the main fatty acyl residue contributing to the respective wax ester chain length is the palmitoyl 16:0 residue which is similar to *Arabidopsis*. C_{40} represents the most abundant wax ester chain length and further, wax esters of the chain lengths C_{42}, C_{38}, C_{36} and C_{44} are highly abundant (Figure 43). These results are different from results published by Hansjakob *et al*., 2010, and by Larsson and Svenningsson, 1986, who described the highest abundance of wax esters for the C_{46}, C_{48} and C_{44} chain lengths. The differences in published wax ester chain lengths in barley leaves compared to those in the present work might be explained by the measuring method used in the present work which shifts wax ester amounts in favor of shorter chain lengths as described above.

5 Summary

Wax esters (WEs) occur mainly in the cuticular waxes of plants. Thus, WEs are part of the barrier between the plant and its aerial environment and are involved in responses of the plant to changing environmental conditions. The gene family wax ester synthase/ diacylglycerol:acyl-CoA acyltransferase (*WS/DGAT*) is widely distributed with homologs occurring in prokaryotes and eukaryotes. One of the 11 WS/DGAT homologs occurring in the model plant *Arabidopsis thaliana*, namely WSD1, was previously characterized to contribute WEs to the stem surface wax (Li *et al*., 2008). The functions of the other homologs, WSD2 – WSD11, remained unclear over the experimental period of this work. In the present work, experiments were performed to characterize the WSDs from *A. thaliana*. Furthermore, WEs from surface wax of leaves from drought-stressed *Hordeum vulgare* were measured.

First, genotyping of T-DNA and transposon *wsd* mutant lines of *A. thaliana* were performed resulting in the isolation of 19 homozygous *wsd* mutant lines and one double homozygous mutant line. Of these *wsd* mutants, WE amount and species composition extracted from surface wax of stems, siliques and flowers were measured and compared to the WT control. WEs were measured by Q-TOF MS/MS. Few abundant WE species could be clearly identified while for other WE species, no higher intensities than those of background signals were detected.

In *Arabidopsis* WT, those WE species with a 16:0 fatty acyl moiety were most abundant in all three organs, stems, flowers and siliques.

The WE species pattern of the *wsd* mutants compared to the WT control revealed many differences. Especially the differences between the *wsd1* mutant and the WT were striking, suggesting an involvement of WSD1 in the synthesis of abundant WE species with a 16:0 fatty acyl moiety not only in stem, but also in silique and flower surface wax in *A. thaliana*.

In addition, expression studies of the *WSD* genes were performed. Under normal growth conditions, *WSD6* and *WSD7* were expressed in all five analyzed plant organs root, stem, leaf, inflorescence, and silique, while the other *WSD* genes were expressed only in one or a few plant organs. Furthermore, it was shown that drought stress, salt stress and abscisic acid (ABA) affects the expression of some *WSD* genes compared to the control: the increase in gene expression of *WSD6* and *WSD7* in root and leaf, as well as the induction of *WSD1* expression in leaf tissue after the stress treatments were most striking and suggests an involvement of these WSD proteins in the response to drought and salt stress and the regulation by ABA. In addition, subcellular localization studies of WSD proteins were performed in *Nicotiana benthamiana* suggesting WSD3, WSD4 and WSD9 reside at the endoplasmic reticulum (ER). Furthermore, heterologous expression studies of WSD1 in *Saccharomyces cerevisiae* were performed. These studies resulted in the detection of an unknown lipid (Unknown Lipid 1, UL1). This led to the assumption that WSD1 might harbor another enzymatic activity than WS and DGAT activity. However, the

expression of WSD1 in yeast did not lead to the synthesis of WEs, neither if WSD1 was expressed alone nor if WSD1 was coexpressed with the acyl-coenzyme A reductase from *Marinobacter aquaeolei* leading to the production of endogenous fatty alcohols. Lack of wax ester synthase activity after expression of WSD1 in yeast was in contrast to the results of Li *et al.*, 2008.

In conclusion, it could be shown that WEs occur in the surface wax of different plant organs of *A. thaliana* with WE species harboring a 16:0 fatty acyl moiety being most abundant. The investigation of *wsd* mutants suggested the contribution of WEs to stem, silique and inflorescence surface wax by WSD1. Gene expression studies indicated an involvement of different WSD proteins in the response to drought and salt stress. In barley, WEs increased in surface wax of leaves after exposure to drought.

6 References

Abe H, Urao T, Ito T, Seki M, Shinozaki K, Yamaguchi-Shinozaki K (2003) Arabidopsis *At*MYC2 (bHLH) and *At*MYB2 (MYB) function as transcriptional activators in abscisic acid signaling. The Plant Cell **15**: 63-78.

Aharoni A, Dixit S, Jetter R, Thoenes E, van Arkel G, Pereira A (2004) The SHINE clade of AP2 domain transcription factors activates wax biosynthesis, alters cuticle properties, and confers drought tolerance when overexpressed in Arabidopsis. The Plant Cell **16**: 2463-2480.

Alvarez AMR, Rodríguez MLG (2000) Lipids in pharmaceutical and cosmetic preparations. Grasas y Aceites **51**: 74-96.

Alvarez HM, Souto MF, Viale A, Pucci OH (2001) Biosynthesis of fatty acids and triacylglycerols by 2, 6, 10, 14-tetramethyl pentadecane-grown cells of *Nocardia globerula* 432. FEMS Microbiology Letters **200**: 195-200.

Ameglio T, Morizet J, Cruiziat P, Martignac M, Bodet C, Raynaud H (1990) The effects of root temperature on water flux, potential and root resistance in sunflower. Agronomie **10**: 331-340.

Antia NJ, Lee RF, Nevenzel JC, Cheng JY (1974) Wax ester production by the marine cryptomonad *Chroomonas salina* grown photoheterotrophically on glycerol. Journal of Eukaryotic Microbiology **21**: 768-771.

Bacon J, Dover LG, Hatch KA, Zhang Y, Gomes JM, Kendall S, Wernisch L, Stoker NG, Butcher PD, Besra GS, Marsh PD (2007) Lipid composition and transcriptional response of *Mycobacterium tuberculosis* grown under iron-limitation in continuous culture: identification of a novel wax ester. Microbiology **153**: 1435-1444.

Barthlott W, Neinhuis C (1997) Purity of the sacred lotus, or escape from contamination in biological surfaces. Planta **202**: 1-8.

Bernard A, Domergue F, Pascal S, Jetter R, Renne C, Faure JD, Haslam RP, Napier JA, Lessire R, Joubès J (2012) Reconstitution of plant alkane biosynthesis in yeast demonstrates that Arabidopsis ECERIFERUM1 and ECERIFERUM3 are core components of a very-long-chain alkane synthesis complex. The Plant Cell **24**: 3106-3118

Bernard A, Joubès J (2013) Arabidopsis cuticular waxes: advances in synthesis, export and regulation. Progress in Lipid Research **52:** 110-129.

Biester EM, Hellenbrand J, Gruber J, Frentzen M, Hamberg M (2012) Identification of avian wax synthases. BMC Biochemistry **13**: 4.

Bonaventure G, Beisson F, Ohlrogge J, Pollard M. (2004) Analysis of the aliphatic monomer composition of polyesters associated with Arabidopsis epidermis: occurrence of octadeca-cis-6, cis-9-diene-1, 18-dioate as the major component. The Plant Journal **40**: 920-930.

Camera E, Ludovici M, Galante M, Sinagra JL, Picardo M (2010) Comprehensive analysis of the major lipid classes in sebum by rapid resolution high-performance liquid chromatography and electrospray mass spectrometry. Journal of Lipid Research **51**: 3377-3388.

Chapman KD, Ohlrogge JB (2012) Compartmentation of triacylglycerol accumulation in plants. Journal of Biological Chemistry **287**: 2288-2294.

Cheng D, Nikolau BJ (2013) CHAPTER II. HETEROLOGOUS EXPRESSION OF WS GENES IN MICROBIAL SYSTEMS. Wax Ester Biosynthetic Pathway **2013**: 14

Cheng JB, Russell DW (2004) Mammalian wax biosynthesis II. Expression cloning of wax synthase cDNAs encoding a member of the acyltransferase enzyme family. Journal of Biological Chemistry **279**: 37798-37807.

Coleman RA, Lee DP (2004) Enzymes of triacylglycerol synthesis and their regulation. Progress in Lipid Research **43**: 134-176.

Daniel J, Deb C, Dubey VS, Sirakova TD, Abomoelak B, Morbidoni HR, Kolattukudy PE (2004) Induction of a novel class of diacylglycerol acyltransferases and triacylglycerol accumulation in Mycobacterium tuberculosis as it goes into a dormancy-like state in culture. Journal of Bacteriology **186:** 5017-5030.

Delude C, Fouillen L, Bhar P, Cardinal MJ, Pascal S, Santos P, Kosma DK, Joubès Jé, Rowland O, Domergue F (2016) Primary fatty alcohols are major components of suberized root tissues of Arabidopsis in the form of alkyl hydroxycinnamates. Plant Physiology **171:** 1934-1950.

Estelle MA, Somerville C (1987) Auxin-resistant mutants of *Arabidopsis thaliana* with an altered morphology. Molecular and General Genetics MGG **206**: 200-206.

Fitzgerald M, Murphy RC (2007) Electrospray mass spectrometry of human hair wax esters. Journal of Lipid Research **48:** 1231-1246.

Focks N, Benning C (1998) wrinkled1: a novel, low-seed-oil mutant of Arabidopsis with a deficiency in the seed-specific regulation of carbohydrate metabolism. Plant Physiology **118:** 91-101.

Franke R, Höfer R, Briesen I, Emsermann M, Efremova N, Yephremov A, Schreiber L (2009) The DAISY gene from Arabidopsis encodes a fatty acid elongase condensing enzyme involved in the biosynthesis of aliphatic suberin in roots and the chalaza-micropyle region of seeds. The Plant Journal **57:** 80-95.

Franke R, Schreiber L (2007) Suberin—a biopolyester forming apoplastic plant interfaces. Current Opinion in Plant Biology **10:** 252-259.

Fuchs B, Süß R, Teuber K, Eibisch M, Schiller J (2011) Lipid analysis by thin-layer chromatography—a review of the current state. Journal of Chromatography A **1218**: 2754-2774.

Gasulla F, Dorp K, Dombrink I, Zähringer U, Gisch N, Dörmann P, Bartels D (2013) The role of lipid metabolism in the acquisition of desiccation tolerance in *Craterostigma plantagineum*: a comparative approach. The Plant Journal **75:** 726-741.

Gellerman JL, Anderson WH, Schlenk H (1975). Synthesis and analysis of phytyl and phytenoyl wax esters. Lipids **10**: 656-661.

Griffiths WJ, Wang Y, Alvelius G, Liu S, Bodin K, Sjövall J (2006) Analysis of oxysterols by electrospray tandem mass spectrometry. Journal of the American Society for Mass Spectrometry **17**: 341-362.

Goda H, Sasaki E, Akiyama K, Maruyama-Nakashita A, Nakabayashi K, Li W, Ogawa M, Yamauchi Y, Preston J, Aoki K, Kiba T, Takatsuto S, Fujioka S, Asami T, Nakano T, Kato H, Mizuno T, Sakakibara H, Yamaguchi S, Nambara E, Kamiya Y, Takahashi H, Yokota Hirai M, Sakura T, Shinozaki K, Saito K, Yoshida S, Shimada Y (2008) The AtGenExpress hormone and chemical treatment data set: experimental design, data evaluation, model data analysis and data access. The Plant Journal **55**: 526-542.

Gómez LD, Baud S, Gilday A, Li Y, Graham IA (2006) Delayed embryo development in the ARABIDOPSIS TREHALOSE-6-PHOSPHATE SYNTHASE 1 mutant is associated with altered cell wall structure, decreased cell division and starch accumulation. The Plant Journal **46:** 69-84.

González A, Ayerbe L (2010) Effect of terminal water stress on leaf epicuticular wax load, residual transpiration and grain yield in barley. Euphytica **172**: 341-349.

Hansjakob A, Bischof S, Bringmann G, Riederer M, Hildebrandt U (2010) Very-long-chain aldehydes promote in vitro prepenetration processes of Blumeria graminis in a dose-and chain length-dependent manner. New Phytologist **188:** 1039-1054.

Hegebarth D, Jetter R (2017) Cuticular Waxes of *Arabidopsis thaliana* Shoots: Cell-Type-Specific Composition and Biosynthesis. Plants **6**: 27.

Hobbs DH, Lu C, Hills MJ (1999) Cloning of a cDNA encoding diacylglycerol acyltransferase from *Arabidopsis thaliana* and its functional expression. FEBS Letters **452**: 145-149.

Höper AC, Salma W, Sollie SJ, Hafstad AD, Lund J, Khalid AM, Raa J, Aasum E, Larsen TS (2014) Wax esters from the marine copepod *Calanus finmarchicus* reduce diet-induced obesity and obesity-related metabolic disorders in mice. The Journal of Nutrition **144**: 164-169.

Hofvander P, Doan TT, Hamberg M (2011) A prokaryotic acyl-CoA reductase performing reduction of fatty acyl-CoA to fatty alcohol. FEBS Letters **585:** 3538-3543.

Holmes MG, Keiller DR (2002) Effects of pubescence and waxes on the reflectance of leaves in the ultraviolet and photosynthetic wavebands: a comparison of a range of species. Plant, Cell & Environment **25**: 85-93.

Iven T, Herrfurth C, Hornung E, Heilmann M, Hofvander P, Stymne S, Zhu L-H, Feussner I (2013) Wax ester profiling of seed oil by nano-electrospray ionization tandem mass spectrometry. Plant Methods **9:** 24.

Jenks MA, Tuttle HA, Eigenbrode SD, Feldmann KA (1995) Leaf epicuticular waxes of the eceriferum mutants in *Arabidopsis*. Plant Physiology **108:** 369-377.

Kalscheuer R, Luftmann H, Steinbüchel A (2004) Synthesis of novel lipids in *Saccharomyces cerevisiae* by heterologous expression of an unspecific bacterial acyltransferase. Applied and environmental microbiology **70**(12): 7119-7125.

Kalscheuer R, Steinbüchel A (2003) A novel bifunctional wax ester synthase/acyl-CoA: diacylglycerol acyltransferase mediates wax ester and triacylglycerol biosynthesis in *Acinetobacter calcoaceticus* ADP1. Journal of Biological Chemistry **278:** 8075-8082.

Kalscheuer R, Stölting T, Steinbüchel A (2006) Microdiesel: *Escherichia coli* engineered for fuel production. Microbiology **152**: 2529-2536.

Kalscheuer R, Uthoff S, Luftmann H, Steinbüchel A (2003) In vitro and in vivo biosynthesis of wax diesters by an unspecific bifunctional wax ester synthase/acyl-CoA: diacylglycerol acyltransferase from *Acinetobacter calcoaceticus* ADP1. European Journal of Lipid Science and Technology **105**: 578-584.

Kelly AA, van Erp H, Quettier AL, Shaw E, Menard G, Kurup S, Eastmond PJ (2013) The sugar-dependent1 lipase limits triacylglycerol accumulation in vegetative tissues of *Arabidopsis*. Plant Physiology **162:** 1282-1289.

Kilian J, Whitehead D, Horak J, Wanke D, Weinl S, Batistic O, D'Angelo C, Bornberg-Bauer E, Kudla Jö, Harter K (2007) The AtGenExpress global stress expression data set: protocols, evaluation and model data analysis of UV-B light, drought and cold stress responses. The Plant Journal **50:** 347-363.

Kim HU, Li Y, Huang AH (2005) Ubiquitous and endoplasmic reticulum–located lysophosphatidyl acyltransferase, LPAT2, is essential for female but not male gametophyte development in *Arabidopsis*. The Plant Cell **17**: 1073-1089.

King A, Nam JW, Han J, Hilliard J, Jaworski JG (2007) Cuticular wax biosynthesis in petunia petals: cloning and characterization of an alcohol-acyltransferase that synthesizes wax-esters. Planta **226:** 381-394.

Kosma DK, Bourdenx B, Bernard A, Parsons EP, Lü S, Joubès J, Jenks MA (2009) The impact of water deficiency on leaf cuticle lipids of *Arabidopsis*. Plant Physiology **151:** 1918-1929.

Kunst L, Samuels AL (2003) Biosynthesis and secretion of plant cuticular wax. Progress in Lipid Research **42**: 51-80.

Lai C, Kunst L, Jetter R (2007) Composition of alkyl esters in the cuticular wax on inflorescence stems of *Arabidopsis thaliana cer* mutants. The Plant Journal **50:** 189-196.

Lardizabal KD, Metz JG, Sakamoto T, Hutton WC, Pollard MR, Lassner MW (2000) Purification of a jojoba embryo wax synthase, cloning of its cDNA, and production of high levels of wax in seeds of transgenic *Arabidopsis*. Plant Physiology **122**: 645-656.

Larsson S, Svenningsson M (1986) Cuticular transpiration and epicuticular lipids of primary leaves of barley (*Hordeum vulgare*). Physiologia Plantarum **68:** 13-19.

Lee RF, Hagen W, Kattner G (2006) Lipid storage in marine zooplankton. Marine Ecology Progress Series **307**: 273-306.

Lee SB, Suh MC (2013) Recent advances in cuticular wax biosynthesis and its regulation in *Arabidopsis*. Molecular Plant **6**: 246-249.

Lessire R, Juguelin H, Moreau P, Cassagne C (1985) Elongation of acyl-CoAs by microsomes from etiolated leek seedlings. Phytochemistry **24:** 1187-1192.

Li F, Wu X, Lam P, Bird D, Zheng H, Samuels L, Jetter R, Kunst L (2008) Identification of the wax ester synthase/acyl-coenzyme A: diacylglycerol acyltransferase WSD1 required for stem wax ester biosynthesis in *Arabidopsis*. Plant Physiology **148:** 97-107.

Lundqvist U, Wettstein DV (1962) Induction of eceriferum mutants in barley by ionizing radiations and chemical mutagens. Hereditas **48**: 342-362.

Moreau RA, Huang AH (1977) Gluconeogenesis from storage wax in the cotyledons of jojoba seedlings. Plant Physiology **60**: 329-333.

Morris RJ (1973) The lipid structure of the spermaceti organ of the sperm whale (*Physeter catodon*). Deep Sea Research and Oceanographic Abstracts **20**: 911-912, 913-916.

Mueller SP, Krause DM, Mueller MJ, Fekete A (2015) Accumulation of extra-chloroplastic triacylglycerols in *Arabidopsis* seedlings during heat acclimation. Journal of Experimental Botany **66:** 4517-4526.

Murphy RC, James PF, McAnoy AM, Krank J, Duchoslav E, Barkley RM (2007) Detection of the abundance of diacylglycerol and triacylglycerol molecular species in cells using neutral loss mass spectrometry. Analytical Biochemistry **366:** 59-70.

Napier JA, Stobart AK, Shewry PR (1996) The structure and biogenesis of plant oil bodies: the role of the ER membrane and the oleosin class of proteins. Plant Molecular Biology **31**: 945-956.

Nicolaides N, Kaitaranta JK, Rawdah TN, Macy JI, Boswell FM, Smith RE (1981) Meibomian gland studies: comparison of steer and human lipids. Investigative Ophthalmology & Visual Science **20**: 522-536.

Obulareddy N, Panchal S, Melotto M. (2013) Guard cell purification and RNA isolation suitable for high-throughput transcriptional analysis of cell-type responses to biotic stresses. Molecular Plant-Microbe Interactions **26:** 844-849.

Olukoshi ER, Packter NM (1994) Importance of stored triacylglycerols in Streptomyces: possible carbon source for antibiotics. Microbiology **140**: 931-943.

Patwari P, Salewski V, Gutbrod K, Kreszies T, Dresen-Scholz B, Peisker H, Steiner U, Meyer AJ, Schreiber L, Dörmann P (2019) Surface wax esters contribute to drought tolerance in *Arabidopsis*. The Plant Journal **98** (4): 727-744.

Piffanelli P, Ross JH, Murphy DJ (1998) Biogenesis and function of the lipidic structures of pollen grains. Sexual Plant Reproduction **11**: 65-80.

Pollard M, Beisson F, Li Y, Ohlrogge JB (2008) Building lipid barriers: biosynthesis of cutin and suberin. Trends in Plant Science **13**: 236-246.

Reina-Pinto JJ, Yephremov A (2009) Surface lipids and plant defenses. Plant Physiology and Biochemistry **47**: 540-549.

Riederer M, Schreiber L (2001) Protecting against water loss: analysis of the barrier properties of plant cuticles. Journal of Experimental Botany **52:** 2023-2032.

Routaboul JM, Benning C, Bechtold N, Caboche M, Lepiniec L (1999) The TAG1 locus of *Arabidopsis* encodes for a diacylglycerol acyltransferase. Plant Physiology and Biochemistry **37**: 831-840.

Rowland O, Zheng H, Hepworth SR, Lam P, Jetter R, Kunst L (2006) CER4 encodes an alcohol-forming fatty acyl-coenzyme A reductase involved in cuticular wax production in *Arabidopsis*. Plant Physiology **142:** 866-877.

Sánchez J, Harwood JL (2002) Biosynthesis of triacylglycerols and volatiles in olives. European Journal of Lipid Science and Technology **104**: 564-573.

Sandager L, Gustavsson MH, Ståhl U, Dahlqvist A, Wiberg E, Banas A, Lenman M, Ronne H, & Stymne S (2002) Storage lipid synthesis is non-essential in yeast. Journal of Biological Chemistry **277:** 6478-6482.

Shepherd T, Wynne Griffiths D (2006) The effects of stress on plant cuticular waxes. New Phytologist **171**: 469-499.

Schmid M, Davison TS, Henz SR, Pape UJ, Demar M, Vingron M, Schölkopf B, Weigel D, Lohmann JU (2005) A gene expression map of *Arabidopsis thaliana* development. Nature Genetics **37:** 501-506.

Seo PJ, Lee SB, Suh MC, Park MJ, Go YS, Park CM (2011) The MYB96 transcription factor regulates cuticular wax biosynthesis under drought conditions in *Arabidopsis*. The Plant Cell **23:** 1138-1152.

Seo PJ, Xiang F, Qiao M, Park JY, Lee YN, Kim SG, Lee Y-H, Park WJ, Park CM (2009) The MYB96 transcription factor mediates abscisic acid signaling during drought stress response in *Arabidopsis*. Plant Physiology **151:** 275-289.

Sieber P, Schorderet M, Ryser U, Buchala A, Kolattukudy P, Métraux JP, Nawrath C (2000) Transgenic *Arabidopsis* plants expressing a fungal cutinase show alterations in the structure and properties of the cuticle and postgenital organ fusions. The Plant Cell **12**: 721-737.

Siloto RM, Findlay K, Lopez-Villalobos A, Yeung EC, Nykiforuk CL, Moloney MM (2006) The accumulation of oleosins determines the size of seed oilbodies in *Arabidopsis*. The Plant Cell **18:** 1961-1974.

Singer SD, Chen G, Mietkiewska E, Tomasi P, Jayawardhane K, Dyer JM, Weselake RJ (2016) *Arabidopsis* GPAT9 contributes to synthesis of intracellular glycerolipids but not surface lipids. Journal of Experimental Botany **67**: 4627-4638.

Sievers F, Wilm A, Dineen D, Gibson TJ, Karplus K, Li W, Lopez R, McWilliam H, Remmert M, Söding J, Thompson JD, Higgins DG (2011) Fast, scalable generation of high-quality protein multiple sequence alignments using Clustal Omega. Molecular systems biology **7**(1): 539.

Sievers F, Higgins DG (2018) Clustal Omega for making accurate alignments of many protein sequences. Protein Science **27**(1): 135-145.

Smith KR, Thiboutot DM (2008) Thematic review series: skin lipids. Sebaceous gland lipids: friend or foe? Journal of Lipid Research **49**: 271-281.

Stachelhaus T, Mootz HD, Bergendahl V, Marahiel MA (1998) Peptide bond formation in nonribosomal peptide biosynthesis catalytic role of the condensation domain. Journal of Biological Chemistry **273**: 22773-22781.

Stewart ME, Quinn MA, Downing DT (1982) Variability in the fatty acid composition of wax esters from *vernix caseosa* and its possible relation to sebaceous gland activity. Journal of Investigative Dermatology **78**: 291-295.

Stöveken T, Kalscheuer R, Malkus U, Reichelt R, Steinbüchel A (2005) The wax ester synthase/acyl coenzyme A: diacylglycerol acyltransferase from Acinetobacter sp. strain ADP1: characterization of a novel type of acyltransferase. Journal of Bacteriology **187:** 1369-1376.

Stöveken T, Kalscheuer R, Steinbüchel A (2009) Both histidine residues of the conserved HHXXXDG motif are essential for wax ester synthase/acyl-CoA: diacylglycerol acyltransferase catalysis. European journal of lipid science and technology, **111**(2): 112-119.

Studier FW (1991) Use of bacteriophage T7 lysozyme to improve an inducible T7 expression system. Journal of Molecular Biology **219:** 37-44.

Sundram K, Sambanthamurthi R, Tan YA (2003) Palm fruit chemistry and nutrition. Asia Pacific Journal of Clinical Nutrition **12**.

Suutari, M., Liukkonen, K., & Laakso, S. (1990). Temperature adaptation in yeasts: the role of fatty acids. Microbiology **136:** 1469-1474.

Takeda S, Iwasaki A, Matsumoto N, Uemura T, Tatematsu, K, Okada K (2013) Physical interaction of floral organs controls petal morphogenesis in *Arabidopsis*. Plant Physiology **161:** 1242-1250.

Teerawanichpan P, Qiu X (2010) Fatty acyl-CoA reductase and wax synthase from *Euglena gracilis* in the biosynthesis of medium-chain wax esters. Lipids **45**: 263-273.

Tomiyama T, Kurihara K, Ogawa T, Maruta T, Ogawa T, Ohta D, Sawa Y, Ishikawa T (2017) Wax ester synthase/diacylglycerol acyltransferase isoenzymes play a pivotal role in wax ester biosynthesis in *Euglena gracilis*. Scientific reports **7**(1): 1-13.

Tsujita T, Sumiyoshi M, Okuda H (1999) Wax ester-synthesizing activity of lipases. Lipids **34**: 1159-1166.

Tulloch AP (1970) The composition of beeswax and other waxes secreted by insects. Lipids **5**: 247-258.

Turkish AR, Henneberry AL, Cromley D, Padamsee M, Oelkers P, Bazzi H, Christiano AM, Billheimer JT, Sturley SL (2005) Identification of Two Novel Human Acyl-CoA Wax Alcohol Acyltransferases MEMBERS OF THE DIACYLGLYCEROL ACYLTRANSFERASE 2 (DGAT2) GENE SUPERFAMILY. Journal of Biological Chemistry **280**: 14755-14764.

Urao T, Yamaguchi-Shinozaki K, Urao S, Shinozaki K (1993) An *Arabidopsis* myb homolog is induced by dehydration stress and its gene product binds to the conserved MYB recognition sequence. The Plant Cell **5:** 1529-1539.

Uthoff S, Stöveken T, Weber N, Vosmann K, Klein E, Kalscheuer R, Steinbüchel A (2005) Thio wax ester biosynthesis utilizing the unspecific bifunctional wax ester synthase/acyl coenzyme A: diacylglycerol acyltransferase of Acinetobacter sp. strain ADP1. Applied and Environmental Microbiology **71**: 790-796.

Vaneechoutte M, Young DM, Ornston LN, De Baere T, Nemec A, Van Der Reijden T, Carr E, Tjernberg I, Dijkshoorn L (2006) Naturally transformable *Acinetobacter* sp. strain ADP1 belongs to the newly described species *Acinetobacter baylyi*. Applied and environmental microbiology **72**(1): 932-936.

Vishwanath SJ, Kosma DK, Pulsifer IP, Scandola S, Pascal S, Joubès J, Dittrich-Domergue F, Lessire R, Rowland O, Domergue F (2013) Suberin-associated fatty alcohols in *Arabidopsis*: distributions in roots and contributions to seed coat barrier properties. Plant Physiology **163:** 1118-1132.

Voinnet O, Lederer C, Baulcombe DC (2000) A viral movement protein prevents spread of the gene silencing signal in *Nicotiana benthamiana*. Cell **103**: 157-167.

Vogg G, Fischer S, Leide J, Emmanuel E, Jetter R, Levy AA, Riederer M (2004) Tomato fruit cuticular waxes and their effects on transpiration barrier properties: functional characterization of a mutant deficient in a very-long-chain fatty acid β-ketoacyl-CoA synthase. Journal of Experimental Botany **55**: 1401-1410.

Vrkoslav V, Urbanová K, Cvačka J (2010) Analysis of wax ester molecular species by high performance liquid chromatography/atmospheric pressure chemical ionisation mass spectrometry. Journal of Chromatography A **1217**: 4184-4194.

Wang ZY, Xiong L, Li W, Zhu JK, Zhu J (2011) The plant cuticle is required for osmotic stress regulation of abscisic acid biosynthesis and osmotic stress tolerance in *Arabidopsis*. Plant Cell **23:** 1971-1984.

Wang Y, Wan L, Zhang L, Zhang Z, Zhang H, Quan R, Zhou S, Huang R (2012) An ethylene response factor *Os*WR1 responsive to drought stress transcriptionally activates wax synthesis related genes and increases wax production in rice. Plant Molecular Biology **78**: 275-288.

Wewer V, Dombrink I, vom Dorp K, Dörmann, P (2011) Quantification of sterol lipids in plants by quadrupole time-of-flight mass spectrometry. Journal of Lipid Research **52:** 1039-1054.

Xiong L, Schumaker KS, Zhu JK (2002) Cell signaling during cold, drought, and salt stress. The Plant Cell **14**: S165-S183.

Yeats TH, Rose JK (2013) The formation and function of plant cuticles. Plant Physiology **163**: 5-20.

Yamada Y, Nishida S, Graeve M, Kattner G (2016) Lipid and fatty acid/alcohol compositions of the subarctic copepods *Neocalanus cristatus* and *Eucalanus bungii* from various depths in the Oyashio region, western North Pacific. Comparative Biochemistry and Physiology Part B: Biochemistry and Molecular Biology **198**: 57-65.

Yamaguchi-Shinozaki K, Shinozaki K (1994) A novel cis-acting element in an *Arabidopsis* gene is involved in responsiveness to drought, low-temperature, or high-salt stress. The Plant Cell **6:** 251-264.

Yen CLE, Brown CH, Monetti M, Farese RV (2005) A human skin multifunctional O-acyltransferase that catalyzes the synthesis of acylglycerols, waxes, and retinyl esters. Journal of Lipid Research **46**: 2388-2397.

Yen CLE, Monetti M, Burri BJ, Farese RV (2005) The triacylglycerol synthesis enzyme DGAT1 also catalyzes the synthesis of diacylglycerols, waxes, and retinyl esters. Journal of Lipid Research **46**: 1502-1511.

Zhang M, Fan J, Taylor DC, Ohlrogge JB (2009) DGAT1 and PDAT1 acyltransferases have overlapping functions in *Arabidopsis* triacylglycerol biosynthesis and are essential for normal pollen and seed development. The Plant Cell **21**: 3885-3901.

Zhu JK (2002) Salt and drought stress signal transduction in plants. Annual Review of Plant Biology **53**: 247-273.

Zou J, Wei Y, Jako C, Kumar A, Selvaraj G, Taylor DC (1999) The *Arabidopsis thaliana* TAG1 mutant has a mutation in a diacylglycerol acyltransferase gene. The Plant Journal **19**: 645-653.

7 Appendix

7.1 Synthetic Oligonucleotides

Table 6: Oligonucleotides Used for Genotyping of T-DNA/Transposon Insertion Lines.

Primer	Sequence (5'-3')
wsd1 for (bn533)	TCAAAGAATTCACAAGTTCATTCTTC
wsd1 rev (bn532)	ATGGTACCATTTTGTGATGGG
wsd2-1 for (bn132)	TTTTCCTCTGTCTCTCCAACG
wsd2-1 rev (bn133)	ATATCCGGAACAATGACATGC
wsd2-2 for (bn1194)	AAACAAAGCGAAGAACGTTTG
wsd2-2 rev (bn1195)	GACACCAAAGGTACTTGCAGC
wsd3-1 for (bn285)	CGATTCATAAATTAATGTTCCAGG
wsd3-1 rev (bn286)	TAAGTGTTTCTCGCGAGATTG
wsd3-2 for (bn1770)	AATTTCATCATTCTCTTGGCG
wsd3-2 rev (bn1771)	CCTCGAGTTTTGTGTCTGCTC
wsd4-1 for (bn193)	ATCGTACCCAAAATCAAACCC
wsd4-1 rev (bn194)	TTCAAGATGTTCCAATGGGTC
wsd4-2 for (bn531)	TCAAATTGCTTGGAATCAAGG
wsd4-2 rev (bn530)	GTTGTTTCAGCAACAAGGCTC
wsd5 for (bn1795)	ACGAGGGCAAATAGCGGAAA
wsd5 rev (bn1796)	ATGGTCGACTTGGCTCTTCG
wsd6-1 for (bn261)	GACCAATAATCTTTAGGGCGG
wsd6-1 rev (bn262)	TTCAAAACCAACATAATCGCC
wsd6-2 for (bn137)	TCGGATTTCATTCCAAAAATG
wsd6-2 rev (bn136)	TCTAAACTGAAATCAAGCGTTG
wsd7-1 for (bn192)	TGGGGACAAATGTGAACCTAC
wsd7-1 rev (bn191)	TCCGTTTCATGGATGGAATAG
wsd7-2 for (bn526)	TGGGGACAAATGTGAACCTAC
wsd7-2 rev (bn527)	CAGCTTTTAGTGGCGTTTTTG
wsd8-1 for (bn1799)	GAGATTGGACTAGTGGCGGG
wsd8-1 rev (bn1800)	TACCGTACAACCTGCACGAA
wsd8-2 for (bn528)	TCGGAATTACACAAGCTGCTC
wsd8-2 rev (bn529)	CCCAGAGAACAGCTTTCATTG
wsd9-1 for (bn139)	CTCTGACGCCGAAGCTATATG
wsd9-1 rev (bn138)	ATGACGAACTCCGAAAATGTG
wsd9-2 for (bn139)	CTCTGACGCCGAAGCTATATG
wsd9-2 rev (bn138)	ATGACGAACTCCGAAAATGTG
wsd10-1 for (bn1192)	TGAAGCATAACGTTTCCAAGC
wsd10-1 rev (bn1193)	TAGATTTACCGCAACACCTGC
wsd10-2 for (bn1190)	ACCGAACCGTCTCATTGGA
wsd10-2 rev (bn1191)	CCATGGATTCCAACAAATCAG
wsd11 for (bn195)	TTGCCATGATGAATTCAGGAG
wsd11 rev (bn196)	TAGAGGATCGGTCTCTAGCCC
Border primer SALK lines LBb1.3 (bn78)	ATTTTGCCGATTTCGGAAC
Border primer GABI KAT (bn142)	CCCATTTGGACGTGAATGTAGACAC
Border primer Ds5-4 (bn278)	TACGATAACGGTCGGTACGG
Border primer SAIL LB1 (bn1474)	GCCTTTTCAGAAATGGATAAATAGCCTTGCTTCC
Border primer SPM (bn131)	TACGAATAAGAGCGTCCATTTTAGAGTGA

Border primer RIKEN LB (bn126)	TACCTCGGGTTCGAAATC

The sequences of the primers listed above were recommended for genotyping by SIGnAL. (http://signal.salk.edu/tdnaprimers.2.html)

Table 7: Oligonucleotides Used for RT-PCR.

Primer	Sequence (5'-3')	Annealing Temperature
WSD1 for (bn1809) *WSD1* rev (bn1810)	ATGAAAGCGGAAAAAGTTATGG TATTTCCCCTTGTGTGGCAGA	58 °C
WSD2 for (bn1392) *WSD2* rev (bn1393)	GGGATGAAGCCACAGG CGTCTACATCAACCCCAATG	64 °C
WSD3 for (bn1801) *WSD3* rev (bn1771)	AAAGCGTCTTGGGTTCCTGT CCTCGAGTTTTGTGTCTGCTC	64 °C
WSD4 for (bn2000) *WSD4* rev (bn2001)	CCGGTCGTCATCAAGGTCAT TTCAACGGGACCAACCATGT	64 °C
WSD5 for (bn1388) *WSD5* rev (bn1389)	GGGAAAATACTTCTCAACACGC GCTAAATCTACTGAGTAGAAGTTC	58 °C
WSD6 for (bn1386) *WSD6* rev (bn1387)	GCTGCCCTAACGTTCGTCGC TTCAATCTAATGAGCGGGAGTC	64 °C
WSD7 for (bn1384) *WSD7* rev (bn1839)	TTGATCGACCGGTGAGGAAC GAGTAAACCTCTTTCACAGAGAGAAGC	64 °C
WSD8 for (bn1382) *WSD8* rev (bn1383)	CATCATTATTCAATCAACACTTG CGTCTTTAATTAAGGATTTAGACC	58 °C
WSD9 for (bn1380) *WSD9* rev (bn1381)	GGATCAATGTCGCAGTAGCG ACATGATTTGGTAATCCTTTCTC	58 °C
WSD10 for (bn1190) *WSD10* rev (bn1193)	ACCGAACCGTCTCATTGGA TAGATTTACCGCAACACCTGC	64 °C
WSD11 for (bn1373) *WSD11* rev (bn1374)	CTCTAGAAGCCGTATTCTCC TCAGCCGTTACCGATATTATG	58 °C
rd29A for (bn1994) *rd29A* rev (bn1995)	AGAGGAGCCAAAACAGAGCA AACAGTGGAGCCAAGTGATTG	64 °C
ACTII for (bn358) *ACTII* rev (bn359)	GCCATCCAAGCTGTTCTCTC GAACCACCGATCCAGACACT	68 °C

Table 8: Oligonucleotides Used for the Amplification of *WSD3* and *WSD10* by RT-PCR from Inflorescence (*WSD3*) and Root (*WSD10*) RNA.

The amplified genes were cloned into pJET1.2/blunt and subjected to sequencing using pJET1.2/blunt sequencing primers (Table 9).

RT-PCR Primer	Sequence (5'-3')
WSD3	ATGTATACTATGAAAAAGGGAAAAGACA TCAAACCTCCATTTTATGAACTCCT
WSD10	ATGACGAAGGAAGAAGTAGAGGA TCAGTCACTTTTACCGGAAAGA

Table 9: pJET1.2/blunt Sequencing Primers.

Sequencing Primer	Sequence (5'-3')
pJET1.2/blunt forward sequencing primer	CGACTCACTATAGGGAGAGCGGC
pJET1.2/blunt reverse sequencing primer	AAGAACATCGATTTTCCATGGCAG

Table 10: Oligonucleotides Used for the Amplification of *WSD* cDNAs and *eGFP.* Amplified DNA was Used for the Generation of the Fusion Constructs pL-35S-*WSD-eGFP* and pL-35S-*eGFP-WSD*.

Primer	Restriction Enzyme	Sequence (5'-3')
eGFP for without stop (bn1887)[a]	*Spe*I	CACTAGTATGGTGAGCAAGGGCGAGGA
eGFP rev without stop (bn1888)[a]	*Bam*HI	CGGATCCCTTGTACAGCTCGTCCATGC
eGFP for (bn1280)[a]	*Bam*HI	CGGATCCATGGTGAGCAAGGGCGAGGA
eGFP rev (bn1281)[a]	*Sal*I	CGTCGACTTACTTGTACAGCTCGTCCA
WSD2 for *WSD2-eGFP* for (bn 2077)	*Spe*I	CTACTAGTATGGCAATAGAAAGGCA
WSD2 for *WSD2-eGFP* rev (bn2078)	*Bam*HI	CAGGATCCAACCTTTGAAGCATGA
WSD2 for *eGFP-WSD2* for (bn2091)	*Bam*HI	TGGGATCCATGGCAATAGAAAGG
WSD2 for *eGFP-WSD2* rev (bn2092)	*Sal*I	CAGTCGACTTAAACCTTTGAAGCA
WSD3 for *WSD3-eGFP* for (bn2137)	SpeI	TGACTAGTATGTATACTATGAAAAAGG
WSD3 for *WSD3-eGFP* rev (bn2138)	*Bam*HI	ACGGATCCAACCTCCATTTTATGAAC
WSD3 for *eGFP-WSD3* for (bn2135)	*Bam*HI	TGGGATCCATGTATACTATGAAAAAGGG
WSD3 for *eGFP-WSD3* rev (bn2136)	*Sal*I	ACGTCGACTCAAACCTCCATTTTATGA
WSD4 for *WSD4-eGFP* for (bn1899)	*Spe*I	TGACTAGTATGGAGATTGAGACACGA
WSD4 for *WSD4-eGFP* rev (bn1900)	*Bam*HI	ACGGATCCTAGCATTCTGTAAAGTAG
WSD4 for *eGFP-WSD4* for (bn1897)	*Bam*HI	TGGGATCCATGGAGATTGAGACA
WSD4 for *eGFP-WSD4* rev (bn1898)	*Sal*I	ACGTCGACTCATAGCATTCTGTAAAG
WSD5 for *WSD5-eGFP* for (bn2079)	*Spe*I	TGACTAGTATGGAGATTAAGATACGA
WSD5 for *WSD5-eGFP* rev (bn2080)	*Bgl*II	ACAGATCTCTGAGTAGAAGTTCTTTCT
WSD5 for *eGFP-WSD5* for (bn2093)	*Bgl*II	TGAGATCTATGGAGATTAAGATACGA
WSD5 for *eGFP-WSD5* rev (bn2094)	*Xho*I	ACCTCGAGCTACTGAGTAGAAGT
WSD6 for *WSD6-eGFP* for (bn2081)	*Spe*I	TGACTAGTATGGAGATTAAGACACGA
WSD6 for *WSD6-eGFP* rev (bn2082)	*Bam*HI	CAGGATCCATCTAATGAGCGGGAGT
WSD6 for *eGFP-WSD6* for (bn2095)	*Bam*HI	TGGGATCCATGGAGATTAAGACACGA
WSD6 for *eGFP-WSD6* rev (bn2096)	*Sal*I	ACGTCGACTCAATCTAATGAGCGG
WSD7 for *WSD7-eGFP* for (bn2083)	*Spe*I	TGACTAGTATGACTTATGGGGAGGAG
WSD7 for *WSD7-eGFP* rev (bn2084)	*Bam*HI	CTGGATCCGAGTAAACCTCTTTCACA
WSD7 for *eGFP-WSD7* for (bn2097)	*Bam*HI	TGGGATCCATGACTTATGGGGAG
WSD7 for *eGFP-WSD7* rev (bn2098)	*Sal*I	ACGTCGACTTAGAGTAAACCTCTTTCA
WSD8 for *WSD8-eGFP* for (bn2085)	*Spe*I	TGACTAGTATGAAGAATGAGGAGGAG
WSD8 for *WSD8-eGFP* rev (bn2086)	*Bgl*II	AGAGATCTGACCTTATAGGCCTCT
WSD8 for *eGFP-WSD8* for (bn2099)	*Bgl*II	TGAGATCTATGAAGAATGAGGAGGA
WSD8 for *eGFP-WSD8* rev (bn2100)	*Sal*I	ACGTCGACTTAGACCTTATAGGCCT
WSD9 for *WSD9-eGFP* for (bn2087)	*Spe*I	TGACTAGTATGGAGAAGAAGATGAAAG A
WSD9 for *WSD9-eGFP* rev (bn2088)	*Bam*HI	CAGGATCCATTGACATGATTTGGTA
WSD9 for *eGFP-WSD9* for (bn2101)	*Bam*HI	TGGGATCCATGGAGAAGAAGATGAA
WSD9 for *eGFP-WSD9*rev (bn2102)	*Sal*I	ACGTCGACTTAATTGACATGATTTG
WSD10 for *WSD10-eGFP* for (bn2089)	*Nhe*I	TGGCTAGCATGACGAAGGAAGAAGTA
WSD10 for *WSD10-eGFP* rev (bn2090)	*Bgl*II	ACAGATCTGTCACTTTTACCGGAAAG
WSD10 for *eGFP-WSD10* for (bn2103)	*Bgl*II	TGAGATCTATGACGAAGGAAGAAGTA
WSD10 for *eGFP-WSD10* rev (bn2104)	*Sal*I	ACGTCGACTCAGTCACTTTTACCG

[a] Primers were designed by Dr. Meike Siebers, University of Bonn, now: Max Planck Institute for Plant Breeding Research, Cologne, Germany

Table 11: Oligonucleotides Used for Cloning of *WSD* and *MaFAR* cDNAs into Yeast Expression Vectors.

Construct	Restriction Enzyme	Sequence (5'-3')
pDR196-*WSD1*	*Pst*I	ctgcagATGAAAGCGGAAAAAGTTATG
	*Sal*I	gtcgacTCAAACTTCCGTTTTGTGAAAT
pESC-URA-*WSD1*[a]	*Bam*HI	agaggatccATGAAAGCGGAAAAAGTTATGG
	*Xho*I	agactcgagTCAAACTTCCGTTTTGTGAAA
pYES2-*WSD1*[b]	*Bam*HI	ggatccGATGAAAGCGGAAAAAGTTATG
	*Eco*RI	gaattcTCAAACTTCCGTTTTGTGAAAT
pDR196-*WSD2*	*Pst*I	ctgcagATGGCAATAGAAAGGCAAG
	*Sal*I	gtcgacTTAAACCTTTGAAGCATGA
pDR196-*WSD4*	*Spe*I	actagtATGGAGATTGAGACACG
	*Sal*I	gtcgacTCATAGCATTCTGTAAAG
pDR196-*WSD5*	*Spe*I	actagtATGGAGATTAAGATACGACGAAG
	*Pst*I	ctgcagCTACTGAGTAGAAGTTC
pDR196-*WSD6*	*Pst*I	ctgcagATGGAGATTAAGACACGACGAG
	*Sal*I	gtcgacTCAATCTAATGAGCGGGAGTCTC
pDR196-*WSD7*	*Pst*I	ctgcagATGACTTATGGGGAGGAGGAGC
	*Sal*I	gtcgacTTAGAGTAAACCTCTTTCACAG
pDR196-*WSD8*	*Pst*I	ctgcagATGAAGAATGAGGAGGAGGAG
	*Sal*I	gtcgacTTAGACCTTATAGGCCTCTTTG
pDR196-*WSD9*	*Spe*I	actagtATGGAGAAGAAGATGAAAGAGGAGGAGGAGG
	*Sal*I	gtcgacTTAATTGACATGATTTGGTAATCCTTTCTCT
pDR196-*WSD11*	*Spe*I	gcactagtATGGGTGAAGACA
	*Sal*I	gcgtcgacTTAGACCTCAATCTCATATAAC
pESC-URA-*MaFAR*	*Spe*I	atactagtATGGCAATCCAGCAGGTC
	*Pac*I	atttaattaaTCATGCCGCTTTTTTACG
pESC-URA-*MaFAR-WSD1*[c]		

[a]Primer sequences are identical as published in Li *et al.*, 2008. pESC-TRP-*WSD1* and an empty pESC-URA vector were obtained from Prof Dr. Ljerka Kunst, University of British Columbia, Vancouver, British Columbia, Canada. Then *WSD1* was moved from pESC-TRP into pESC-URA by restriction with *Xho*I and *Bam*HI.

[b] The construct was cloned by Dr. Antje Lohmann, MPI Golm, now: Merck KGaA, Darmstadt, Germany.

[c] *MaFAR* was inserted using *Spe*I and *Pac*I (see pESC-URA-*MaFAR*) into the pESC-URA-*WSD1*.

7.2 cDNA Sequences of *WSD3* and *WSD10*

```
                1                                                   50
genomic_seq_WSD3    ATGTATACTA TGAAAAAGGG AAAAGACATG GCGAAAGAGG AGCAAGAAAC
splice_variant_1    ATGTATACTA TGAAAAAGGG AAAAGACATG GCGAAAGAGG AGCAAGAAAC
splice_variant_2    ATGTATACTA TGAAAAAGGG AAAAGACATG GCGAAAGAGG AGCAAGAAAC

                51                                                  100
genomic_seq_WSD3    AGCGGCAATA GAGCCACTTA GCCCGGTTTC ACAGTTGTTT GTTTCGCCGA
splice_variant_1    AGCGGCAATA GAGCCACTTA GCCCGGTTTC ACAGTTGTTT GTTTCGCCGA
splice_variant_2    AGCGGCAATA GAGCCACTTA GCCCGGTTTC ACAGTTGTTT GTTTCGCCGA

               101                                                  150
genomic_seq_WSD3    GTCTCTACTG CTTCATTATT TTCACTTTAG GGTTCCAAAC TAGATGCAAC
splice_variant_1    GTCTCTACTG CTTCATTATT TTCACTTTAG GGTTCCAAAC TAGATGCAAC
splice_variant_2    GTCTCTACTG CTTCATTATT TTCACTTTAG GGTTCCAAAC TAGATGCAAC

               151                                                  200
genomic_seq_WSD3    CCATCCACCA TTGTTGAAGG TGTCAAGAAC ACATGGATCA AGCTCCCTCG
splice_variant_1    CCATCCACCA TTGTTGAAGG TGTCAAGAAC ACATGGATCA AGCTCCCTCG
splice_variant_2    CCATCCACCA TTGTTGAAGG TGTCAAGAAC ACATGGATCA AGCTCCCTCG
```

```
                    201                                                 250
genomic_seq_WSD3    CTTCTCTAGC AAAGTGGTAA AGCTTATATA TTTCCAATTG CTTTGATTGT
splice_variant_1    CTTCTCTAGC AAAGTG.... .......... .......... ..........
splice_variant_2    CTTCTCTAGC AAAGTG.... .......... .......... ..........

                    251                                                 300
genomic_seq_WSD3    TACATGTAAG AACGTTAAAC GTACAAGAGA ATCTTAAGAA TATCATAACT
splice_variant_1    .......... .......... .......... .......... ..........
splice_variant_2    .......... .......... .......... .......... ..........

                    301                                                 350
genomic_seq_WSD3    ATGATAAAAA AAAAATAGAC TTGAATATAC CTACCTAATA CAATATTTCC
splice_variant_1    .......... .......... .......... .......... ..........
splice_variant_2    .......... .......... .......... .......... ..........

                    351                                                 400
genomic_seq_WSD3    TTAATAATTC TCTTACTTTT GATGGTGATT GTTTTTTTTA ATTTTTCTGT
splice_variant_1    .......... .......... .......... .......... ..........
splice_variant_2    .......... .......... .......... .......... ..........

                    401                                                 450
genomic_seq_WSD3    CAACATTATA CATTATATAC CAGTTTTAAA TTTGAATTTT CTTTAGCTAT
splice_variant_1    .......... .......... .......... .......... ..........
splice_variant_2    .......... .......... .......... .......... ..........

                    451                                                 500
genomic_seq_WSD3    ATAACAATTT CTTTTATCAC GATTCATAAA TTAATGTTCC AGGAGATAAA
splice_variant_1    .......... .......... .......... .......... ..GAGATAAA
splice_variant_2    .......... .......... .......... .......... ..........

                    501                                                 550
genomic_seq_WSD3    GAAAAATGGA AAAGCGTCTT GGGTTCCTGT TAGTGTTCGA GTAGAAGATC
splice_variant_1    GAAAAATGGA AAAGCGTCTT GGGTTCCTGT TAGTGTTCGA GTAGAAGATC
splice_variant_2    .......... .......... .......... .......... ..........

                    551                                                 600
genomic_seq_WSD3    ATGTTGTTGT TCCAGATCTT GATTATTCCA ACATTGAAAA TCCTGATCAA
splice_variant_1    ATGTTGTTGT TCCAGATCTT GATTATTCCA ACATTGAAAA TCCTGATCAA
splice_variant_2    .......... .......... .......... .......... ..........

                    601                                                 650
genomic_seq_WSD3    TTTATAGAAG ACTATACTTC GAAATTAGCT AATACTCCGA TGGACATGTC
splice_variant_1    TTTATAGAAG ACTATACTTC GAAATTAGCT AATACTCCGA TGGACATGTC
splice_variant_2    .......... .......... .......... .......... ..........

                    651                                                 700
genomic_seq_WSD3    CCGACCTTTA TGGGAACTTC ATTTACTTAA TATAAAGACA TCAAATGCAG
splice_variant_1    CCGACCTTTA TGGGAACTTC ATTTACTTAA TATAAAGACA TCAAATGCAG
splice_variant_2    .......... .......... .......... .......... ..........

                    701                                                 750
genomic_seq_WSD3    AATCTTTAGC TATAGGAAAA TTTCATCATT CTCTTGGCGA TGGGATGTCT
splice_variant_1    AATCTTTAGC TATAGGAAAA TTTCATCATT CTCTTGGCGA TGGGATGTCT
splice_variant_2    .......... .......... .......... .......... ..........

                    751                                                 800
genomic_seq_WSD3    CTTATATCTC TTCTATTAGC TAGTTCACGG AAAACATCAG ATCCTGACGC
splice_variant_1    CTTATATCTC TTCTATTAGC TAGTTCACGG AAAACATCAG ATCCTGACGC
splice_variant_2    .......... .......... .......... .......... ..........

                    801                                                 850
genomic_seq_WSD3    TTTGCCTACT ACCGCGGCTA CAAGAAAGCA TGCCAGTTCC AATAAAAAGA
splice_variant_1    TTTGCCTACT ACCGCGGCTA CAAGAAAGCA TGCCAGTTCC AATAAAAAGA
splice_variant_2    .......... .......... .......... .......... ..........

                    851                                                 900
genomic_seq_WSD3    GTTGGTGGTT GGTTGGAAGA TTTTGGTTTA TGATAAGAAT CATTTTCACT
splice_variant_1    GTTGGTGGTT GGTTGGAAGA TTTTGGTTTA TGATAAGAAT CATTTTCACT
splice_variant_2    .......... .......... .......... .......... ..........

                    901                                                 950
genomic_seq_WSD3    ACTGTTGTTG AATTGTTTAA GTATTTGCTT ACACTATGTT TTATGCGGGA
splice_variant_1    ACTGTTGTTG AATTGTTTAA GTATTTGCTT ACACTATGTT TTATGCGGGA
splice_variant_2    .......... .......... .......... .......... ..........
```

```
                 951                                                 1000
genomic_seq_WSD3 CACTAAAACT CCCCTAATGG GTAAAACGGG TGATGCAATA CGATCTAGAA
splice_variant_1 CACTAAAACT CCCCTAATGG GTAAAACGGG TGATGCAATA CGATCTAGAA
splice_variant_2 .......... .......... .......... .......... ..........

                 1001                                                1050
genomic_seq_WSD3 AGGTTATACA TCGGATAGTA AGCTTTGATG ATGTCAAGTT GGTGAAGAAC
splice_variant_1 AGGTTATACA TCGGATAGTA AGCTTTGATG ATGTCAAGTT GGTGAAGAAC
splice_variant_2 .......... .......... .......... .......... ..........

                 1051                                                1100
genomic_seq_WSD3 AACATGGATA TGGTTCGCAT ATTTAATATT CATATAGGCA TTTTCTTTCT
splice_variant_1 AACATGGATA TG........ .......... .......... ..........
splice_variant_2 .......... .......... .......... .......... ..........

                 1101                                                1150
genomic_seq_WSD3 GTAATTCTGT TAGTCATTTT CTTTGTTTTA CTTATATCAA GAACTTTATA
splice_variant_1 .......... .......... .......... .......... ..........
splice_variant_2 .......... .......... .......... .......... ..........

                 1151                                                1200
genomic_seq_WSD3 ATTTGTTTTG TCTTTTGCTT TTGTAGAAAG TGAATGATGT TCTTCTTGGA
splice_variant_1 .......... .......... ......AAAG TGAATGATGT TCTTCTTGGA
splice_variant_2 .......... .......... ......AAAG TGAATGATGT TCTTCTTGGA

                 1201                                                1250
genomic_seq_WSD3 ATGACACAGG CAGGTCTCTC AAGATATTTG AGCAGGAAAT ATGGTAATTT
splice_variant_1 ATGACACAGG CAGGTCTCTC AAGATATTTG AGCAGGAAAT ATG.......
splice_variant_2 ATGACACAGG CAGGTCTCTC AAGATATTTG AGCAGGAAAT ATG.......

                 1251                                                1300
genomic_seq_WSD3 CAAATTCTTT CCCGATCTAA TTGTGTGTTA TTGACCTTGA TGTTGTTAAA
splice_variant_1 .......... .......... .......... .......... ..........
splice_variant_2 .......... .......... .......... .......... ..........

                 1301                                                1350
genomic_seq_WSD3 TGCATCTTAT GTTTTAAATA GATGAAAAAA TAAAGTGAAA AAAGAAATGA
splice_variant_1 .......... .......... .......... .......... ..........
splice_variant_2 .......... .......... .......... .......... ..........

                 1351                                                1400
genomic_seq_WSD3 GAAAGCAATT TCCTTGATAA AAAAATCCAT ATATGTTATA GTTTCTAAAA
splice_variant_1 .......... .......... .......... .......... ..........
splice_variant_2 .......... .......... .......... .......... ..........

                 1401                                                1450
genomic_seq_WSD3 ATTAATTATT ACTAGATAGA GTAGATTTTT ATTTTACAAT CTCGCGAGAA
splice_variant_1 .......... .......... .......... .......... ..........
splice_variant_2 .......... .......... .......... .......... ..........

                 1451                                                1500
genomic_seq_WSD3 ACACTTATGT TTTCTACAAC TTTTTAAATT TATCTGAATT CTAAAATAAT
splice_variant_1 .......... .......... .......... .......... ..........
splice_variant_2 .......... .......... .......... .......... ..........

                 1501                                                1550
genomic_seq_WSD3 TTTTAAATAT TTCAAAAACT CAAATAGTAT AAATTAGAAG ATACGGTTAC
splice_variant_1 .......... .......... .......... .......... ..........
splice_variant_2 .......... .......... .......... .......... ..........

                 1551                                                1600
genomic_seq_WSD3 ATTTGAACTT AAGTATAATA GATTTTGTTT TGTTTATGTT GACACAAAAG
splice_variant_1 .......... .......... .......... .......... ..........
splice_variant_2 .......... .......... .......... .......... ..........

                 1601                                                1650
genomic_seq_WSD3 AGAGAGAAAA AAATTGTTTT GTTACATACA TCATTGATTA TATCATAAAC
splice_variant_1 .......... .......... .......... .......... ..........
splice_variant_2 .......... .......... .......... .......... ..........

                 1651                                                1700
genomic_seq_WSD3 AAACTGTTTT CAGTTTTTAA CAATTTTTAA AGTAGATGAA GATATGGTGG
splice_variant_1 .......... .......... .......... .....ATGAA GATATGGTGG
splice_variant_2 .......... .......... .......... .....ATGAA GATATGGTGG
```

```
                    1701                                                1750
genomic_seq_WSD3    TCGAGAAGAA AAAAAACTTG GAGAAAATCC GTCTTCGTGG TACAGTATTC
splice_variant_1    TCGAGAAGAA AAAAAACTTG GAGAAAATCC GTCTTCGTGG TACAGTATTC
splice_variant_2    TCGAGAAGAA AAAAAACTTG GAGAAAATCC GTCTTCGTGG TACAGTATTC

                    1751                                                1800
genomic_seq_WSD3    GTAAATTTAA GAGCAGACAC AAAACTCGAG GTAAATCAAA GTAACTGTTA
splice_variant_1    GTAAATTTAA GAGCAGACAC AAAACTCGAG G......... ..........
splice_variant_2    GTAAATTTAA GAGCAGACAC AAAACTCGAG G......... ..........

                    1801                                                1850
genomic_seq_WSD3    TTGTCAGTTT TAATAAATGA GGATGCAAGC TGTTCATAAC ATATGTAAAT
splice_variant_1    .......... .......... .......... .......... ..........
splice_variant_2    .......... .......... .......... .......... ..........

                    1851                                                1900
genomic_seq_WSD3    AAATTTAGGA TTTGGCGAAT ATGATGGCAA AAGGTTCAAA GTGTAGATGG
splice_variant_1    .........A TTTGGCGAAT ATGATGGCAA AAGGTTCAAA GTGTAGATGG
splice_variant_2    .........A TTTGGCGAAT ATGATGGCAA AAGGTTCAAA GTGTAGATGG

                    1901                                                1950
genomic_seq_WSD3    GGAAACTTCG TAGGTGTTAT TATATTTCCT TTATGGGTGA GATCCGAAGA
splice_variant_1    GGAAACTTCG TAGGTGTTAT TATATTTCCT TTATGGGTGA GATCCGAAGA
splice_variant_2    GGAAACTTCG TAGGTGTTAT TATATTTCCT TTATGGGTGA GATCCGAAGA

                    1951                                                2000
genomic_seq_WSD3    TGATCCGTTG GAATACGTTC GACGAGCCAA ATCTACTATG GATATCAAAA
splice_variant_1    TGATCCGTTG GAATACGTTC GACGAGCCAA ATCTACTATG GATATCAAAA
splice_variant_2    TGATCCGTTG GAATACGTTC GACGAGCCAA ATCTACTATG GATATCAAAA

                    2001                                                2050
genomic_seq_WSD3    AACTGTCCAT AGAATCACTT ATTTGCTATG GACTCATCAA ACTTACCAGA
splice_variant_1    AACTGTCCAT AGAATCACTT ATTTGCTATG GACTCATCAA ACTTACCAGA
splice_variant_2    AACTGTCCAT AGAATCACTT ATTTGCTATG GACTCATCAA ACTTACCAGA

                    2051                                                2100
genomic_seq_WSD3    AAAATACTCG GGGGAAAGGT AAATTATAAA ATCACTATCA CCTAGTTGTC
splice_variant_1    AAAATACTCG GGGGAAAGGT A......... ..........  ..........
splice_variant_2    AAAATACTCG GGGGAAAGGT A......... ..........  ..........

                    2101                                                2150
genomic_seq_WSD3    CAATTATATA CGTATGTATG TGTAAAACTA TAAATTGTTA ATGCAGGTAG
splice_variant_1    .......... .......... .......... .......... .........G
splice_variant_2    .......... .......... .......... .......... .........G

                    2151                                                2200
genomic_seq_WSD3    TAGAAACTCT TGTTAGGAGA CTATTTGATC ATACGACATT GACATTTTCT
splice_variant_1    TAGAAACTCT TGTTAGGAGA CTATTTGATC ATACGACATT GACATTTTCT
splice_variant_2    TAGAAACTCT TGTTAGGAGA CTATTTGATC ATACGACATT GACATTTTCT

                    2201                                                2250
genomic_seq_WSD3    AATGTGATGG GTCCAGACGA AGATATAAGT TTTTTTGACC ATCCAATGTC
splice_variant_1    AATGTGATGG GTCCAGACGA AGATATAAGT TTTTTTGACC ATCCAATGTC
splice_variant_2    AATGTGATGG GTCCAGACGA AGATATAAGT TTTTTTGACC ATCCAATGTC

                    2251                                                2300
genomic_seq_WSD3    TTACGTAGCA GCAAGCGCAT TAGGTGGACC ACAAGTAAGT ATAGCTAATC
splice_variant_1    TTACGTAGCA GCAAGCGCAT TAGGTGGACC ACAAG..... ..........
splice_variant_2    TTACGTAGCA GCAAGCGCAT TAGGTGGACC ACAAG..... ..........

                    2301                                                2350
genomic_seq_WSD3    ATGTCATACT TGTATATCAA CTATTTTTTG TAGAAATCAC TAAAAACTGT
splice_variant_1    .......... .......... .......... .......... ..........
splice_variant_2    .......... .......... .......... .......... ..........

                    2351                                                2400
genomic_seq_WSD3    GGTGAAATCA AGTAACATGT TGTTTATGTT TGTTGTTGAA CAAGGCTCTT
splice_variant_1    .......... .......... .......... .......... .....CTCTT
splice_variant_2    .......... .......... .......... .......... .....CTCTT

                    2401                                                2450
genomic_seq_WSD3    ATTATCCATT ACGTAACCTA TGTAAACAAG ATTGTCATCA ATCTAGCAGT
splice_variant_1    ATTATCCATT ACGTAACCTA TGTAAACAAG ATTGTCATCA ATCTAGCAGT
splice_variant_2    ATTATCCATT ACGTAACCTA TGTAAACAAG ATTGTCATCA ATCTAGCAGT
```

```
                    2451                                                2500
genomic_seq_WSD3    AGACACATCA GTGATTCGAG ACCCTCATCT ACTATGTGAT GATTTGGTAG
splice_variant_1    AGACACATCA GTGATTCGAG ACCCTCATCT ACTATGTGAT GATTTGGTAG
splice_variant_2    AGACACATCA GTGATTCGAG ACCCTCATCT ACTATGTGAT GATTTGGTAG

                    2501                                                2550
genomic_seq_WSD3    AATCGCTCGA TATCATCAAA CTTGCTGCCA TGGAGAAAGG AGTTCATAAA
splice_variant_1    AATCGCTCGA TATCATCAAA CTTGCTGCCA TGGAGAAAGG AGTTCATAAA
splice_variant_2    AATCGCTCGA TATCATCAAA CTTGCTGCCA TGGAGAAAGG AGTTCATAAA

                    2551     2562
genomic_seq_WSD3    ATGGAGGTTT GA
splice_variant_1    ATGGAGGTTT GA
splice_variant_2    ATGGAGGTTT GA
```

Figure 44: cDNA Sequences of *WSD3*, Aligned to the Genomic Sequence from TAIR (TAIR Accession: Sequence 6530302237, GenBank Accession Number CP002685.1).

cDNAs from splice variants 1 and 2 were obtained by RT-PCR from inflorescence mRNA. Sequences were aligned using MultAlin (http://multalin.toulouse.inra.fr/multalin/). Grey letters indicate 100 % sequence identity. Splice variant 1 harbors a complete acyltransferase open reading frame and was therefore employed for further studies.

```
                    1                                                   50
genomic_seq_WSD10   ATGACGAAGG AAGAAGTAGA GGAGGAGCCT CTAAGCCCGA TGGCTCGGTT
       cDNA_WSD10   ATGACGAAGG AAGAAGTAGA GGAGGAGCCT CTAAGCCCGA TGGCTCGGTT

                    51                                                  100
genomic_seq_WSD10   ATTCCAGTCA CCGGGGATAG AAAATTGCAT TATCACGATG ATTGGTTTCA
       cDNA_WSD10   ATTCCAGTCA CCGGGGATAG AAAATTGCAT TATCACGATG ATTGGTTTCA

                    101                                                 150
genomic_seq_WSD10   AAGCCAAGAT TAATCCTGAC ATCATTCTAG ATGACTTGAA GCATAACGTT
       cDNA_WSD10   AAGCCAAGAT TAATCCTGAC ATCATTCTAG ATGACTTGAA GCATAACGTT

                    151                                                 200
genomic_seq_WSD10   TCCAAGCATC CTCGTTTCTG TAGTAAATTG GTAATTGCCA CACATACAAA
       cDNA_WSD10   TCCAAGCATC CTCGTTTCTG TAGTAAATTG .......... ..........

                    201                                                 250
genomic_seq_WSD10   TTGTACCTAG TTTTATTTAG GATTTAACAT TTTTTTTGTA TGCATTGTGT
       cDNA_WSD10   .......... .......... .......... .......... ..........

                    251                                                 300
genomic_seq_WSD10   AAAATTTTGA AGTCAGATGA TGGTGAGAGA TGGATGAAGA CCAAAGTCAA
       cDNA_WSD10   .......... ..TCAGATGA TGGTGAGAGA TGGATGAAGA CCAAAGTCAA

                    301                                                 350
genomic_seq_WSD10   TGTAGAAGAC CATGTATTTG TACCAGACAT AGACCTACAA GAGATTAACA
       cDNA_WSD10   TGTAGAAGAC CATGTATTTG TACCAGACAT AGACCTACAA GAGATTAACA

                    351                                                 400
genomic_seq_WSD10   AAGATGGAGA TGGCTTCGTC GATGACTATG TCTCGCGTCT AACATTGAGT
       cDNA_WSD10   AAGATGGAGA TGGCTTCGTC GATGACTATG TCTCGCGTCT AACATTGAGT

                    401                                                 450
genomic_seq_WSD10   CCTCTCGATA AATCGAAACC ATTGTGGGAT ATTCATATCC TCAATGTCAA
       cDNA_WSD10   CCTCTCGATA AATCGAAACC ATTGTGGGAT ATTCATATCC TCAATGTCAA

                    451                                                 500
genomic_seq_WSD10   AACATCTGAT GCAGAAGCGG TCGGTGTAAT GAGATGTCAT CATTCTTTGG
       cDNA_WSD10   AACATCTGAT GCAGAAGCGG TCGGTGTAAT GAGATGTCAT CATTCTTTGG

                    501                                                 550
genomic_seq_WSD10   CAGATGGAAT GTCCTTGATG TCACTCTTGG TGGCATGTAC CCGAAAAACA
       cDNA_WSD10   CAGATGGAAT GTCCTTGATG TCACTCTTGG TGGCATGTAC CCGAAAAACA

                    551                                                 600
genomic_seq_WSD10   TCAAATCTTG AGTCATTTCC TACCATTCCT GCCATAAAAC GGCGTGAACA
       cDNA_WSD10   TCAAATCTTG AGTCATTTCC TACCATTCCT GCCATAAAAC GGCGTGAACA
```

```
                    601                                                 650
genomic_seq_WSD10   AATGATGTCG CATCGCTTTG GAAACAAAGG CTGGTATTCA AGATCGATAA
       cDNA_WSD10   AATGATGTCG CATCGCTTTG GAAACAAAGG CTGGTATTCA AGATCGATAA

                   651                                                  700
genomic_seq_WSD10   ACGCAGTTTA TTATGCCGTG AGATTAATTT GGAATACAAT TGTGGATCTT
       cDNA_WSD10   ACGCAGTTTA TTATGCCGTG AGATTAATTT GGAATACAAT TGTGGATCTT

                    701                                                 750
genomic_seq_WSD10   CTACTGCTTT GGGCGACTAG TCTTTTTTTT AAGGATACAG AGACGCCTAT
       cDNA_WSD10   CTACTGCTTT GGGCGACTAG TCTTTTTTTT AAGGATACAG AGACGCCTAT

                    751                                                 800
genomic_seq_WSD10   TAGCGAGGGT ATTGGATCCG GGAATAATGC AAGGAGATTT TATCACCGAA
       cDNA_WSD10   TAGCGAGGGT ATTGGATCCG GGAATAATGC AAGGAGATTT TATCACCGAA

                    801                                                 850
genomic_seq_WSD10   CCGTCTCATT GGATGATATT AAACTGATAA AAAATGCTAT GAAGATGGTG
       cDNA_WSD10   CCGTCTCATT GGATGATATT AAACTGATAA AAAATGCTAT GAAGATG...

                    851                                                 900
genomic_seq_WSD10   AGTTACTTGT AAATAATTTT ATTTTCTCAA CCTATACTTC CTATAACATT
       cDNA_WSD10   .......... .......... .......... .......... ..........

                    901                                                 950
genomic_seq_WSD10   GTGGTATTTG TGTGTGTGGC TAGACTATCA ATGATGTTCT ACTTGGAGTT
       cDNA_WSD10   .......... .......... ...ACTATCA ATGATGTTCT ACTTGGAGTT

                    951                                                1000
genomic_seq_WSD10   ACACAAGACG CTCTCTCCCG CTATCTTAAC CAGCGATATG GTAAATATTG
       cDNA_WSD10   ACACAAGACG CTCTCTCCCG CTATCTTAAC CAGCGATATG G.........

                   1001                                                1050
genomic_seq_WSD10   AAATGAAATA TAAATCTAAG CAATACATTG GAACTAATTT ATTCTAATGT
       cDNA_WSD10   .......... .......... .......... .......... ..........

                   1051                                                1100
genomic_seq_WSD10   TTCGCTTATG TGTTCTGTTT CTTGACAAAC AAGGCGACAA AAATGGTGAG
       cDNA_WSD10   .......... .......... .......... ....CGACAA AAATGGTGAG

                   1101                                                1150
genomic_seq_WSD10   GGTGTAACAA CGACATCGAA TCTAAACAAT CTTCCAGGTA AAATACGAAT
       cDNA_WSD10   GGTGTAACAA CGACATCGAA TCTAAACAAT CTTCCAGGTA AAATACGAAT

                   1151                                                1200
genomic_seq_WSD10   TCGAGCAGGT GTTGCGGTAA ATCTAAGGCA GGATATTGGA ATTCAGGTTA
       cDNA_WSD10   TCGAGCAGGT GTTGCGGTAA ATCTAAGGCA GGATATTGGA ATTCAG....

                   1201                                                1250
genomic_seq_WSD10   GATATCTACA TCTACATCTT TATCTTAGTT GAAAAGAATT TAACACTAAC
       cDNA_WSD10   .......... .......... .......... .......... ..........

                   1251                                                1300
genomic_seq_WSD10   TTGATAAAAC AATTGTGTGA AGCCTTTGGA GGACATGTTG GCCAAGGATT
       cDNA_WSD10   .......... .......... ..CCTTTGGA GGACATGTTG GCCAAGGATT

                   1301                                                1350
genomic_seq_WSD10   CGAAATGTAG ATGGGGAAAT TATGATTCCT TAGTTTTTGT TCCATTCTCC
       cDNA_WSD10   CGAAATGTAG ATGGGGAAAT TATGATTCCT TAGTTTTTGT TCCATTCTCC

                   1351                                                1400
genomic_seq_WSD10   ATAAGTTTGG AAACCGATCC ATTGGTTCCT TTATTAAAAG CTAAATCAAT
       cDNA_WSD10   ATAAGTTTGG AAACCGATCC ATTGGTTCCT TTATTAAAAG CTAAATCAAT

                   1401                                                1450
genomic_seq_WSD10   AATGGATCGA AAGAAGCACT CTCTTGTCGC CCCTATGCAT TATTCAATCA
       cDNA_WSD10   AATGGATCGA AAGAAGCACT CTCTTGTCGC CCCTATGCAT TATTCAATCA

                   1451                                                1500
genomic_seq_WSD10   TCGAGTTTAT CATCAATACT TTCGGAACTA AGGTATAGAT TAGTGATAAT
       cDNA_WSD10   TCGAGTTTAT CATCAATACT TTCGGAACTA AGGTAT.... ..........

                   1501                                                1550
genomic_seq_WSD10   GGAACACAAG GATTGTTTAA TGTAGGGACA TCATATGAAA CTCATGTCAT
       cDNA_WSD10   .......... .......... .......... .......... ..........
```

```
                    1551                                                1600
genomic_seq_WSD10   TGTAGGTATT CAACCGAACA TGTTCGAACA CAACAACAAT CTTATCAAAC
       cDNA_WSD10   .........T CAACCGAACA TGTTCGAACA CAACAACAAT CTTATCAAAC

                    1601                                                1650
genomic_seq_WSD10   ATTGTTGGCC CCGTGGAAGA AGTTAGTTTA CACGGCAATT GTATCACTTA
       cDNA_WSD10   ATTGTTGGCC CCGTGGAAGA AGTTAGTTTA CACGGCAATT GTATCACTTA

                    1651                                                1700
genomic_seq_WSD10   CATTGCTCTA ACCGGCTATG GACACTCGCA AGTACGTGTT TTTCACTATT
       cDNA_WSD10   CATTGCTCTA ACCGGCTATG GACACTCGCA AG........ ..........

                    1701                                                1750
genomic_seq_WSD10   GAATTATATT GATAAGTTTG TAATATAGTA CTCGTAAAGA GATCTTTATA
       cDNA_WSD10   .......... .......... .......... .......... ..........

                    1751                                                1800
genomic_seq_WSD10   TCCTTCTAAT TTTCGTATAT GTTATGTGTT TGGTAGGCAC TGATGATACA
       cDNA_WSD10   .......... .......... .......... .......CAC TGATGATACA

                    1801                                                1850
genomic_seq_WSD10   TTTCATAAGT TACGCGAACA AGATGATAAT TACGATAGCC GTCGATCCTG
       cDNA_WSD10   TTTCATAAGT TACGCGAACA AGATGATAAT TACGATAGCC GTCGATCCTG

                    1851                                                1900
genomic_seq_WSD10   CGGTCATACC AGATCCTCAC AATATTTGTG ATGAAATGGA AAAGTCTTTG
       cDNA_WSD10   CGGTCATACC AGATCCTCAC AATATTTGTG ATGAAATGGA AAAGTCTTTG

                    1901                                  1939
genomic_seq_WSD10   AAAGCTATGA AAGACACTCT TTCCGGTAAA AGTGACTGA
       cDNA_WSD10   AAAGCTATGA AAGACACTCT TTCCGGTAAA AGTGACTGA
```

Figure 45: cDNA Sequence of *WSD10*, Aligned to the Genomic Sequence from TAIR (sequence 2154285, GenBank accession number CP002688.1).

The cDNA was obtained by RT-PCR from root mRNA. Sequences were aligned using MultAlin (http://multalin.toulouse.inra.fr/multalin/). Grey letters indicate 100 % sequence identity. The cDNA harbors a complete acyltransferase open reading frame which is 18 bps shorter than annotated by TAIR (see also Figure 16 in the Results).

7.3 Vector Maps

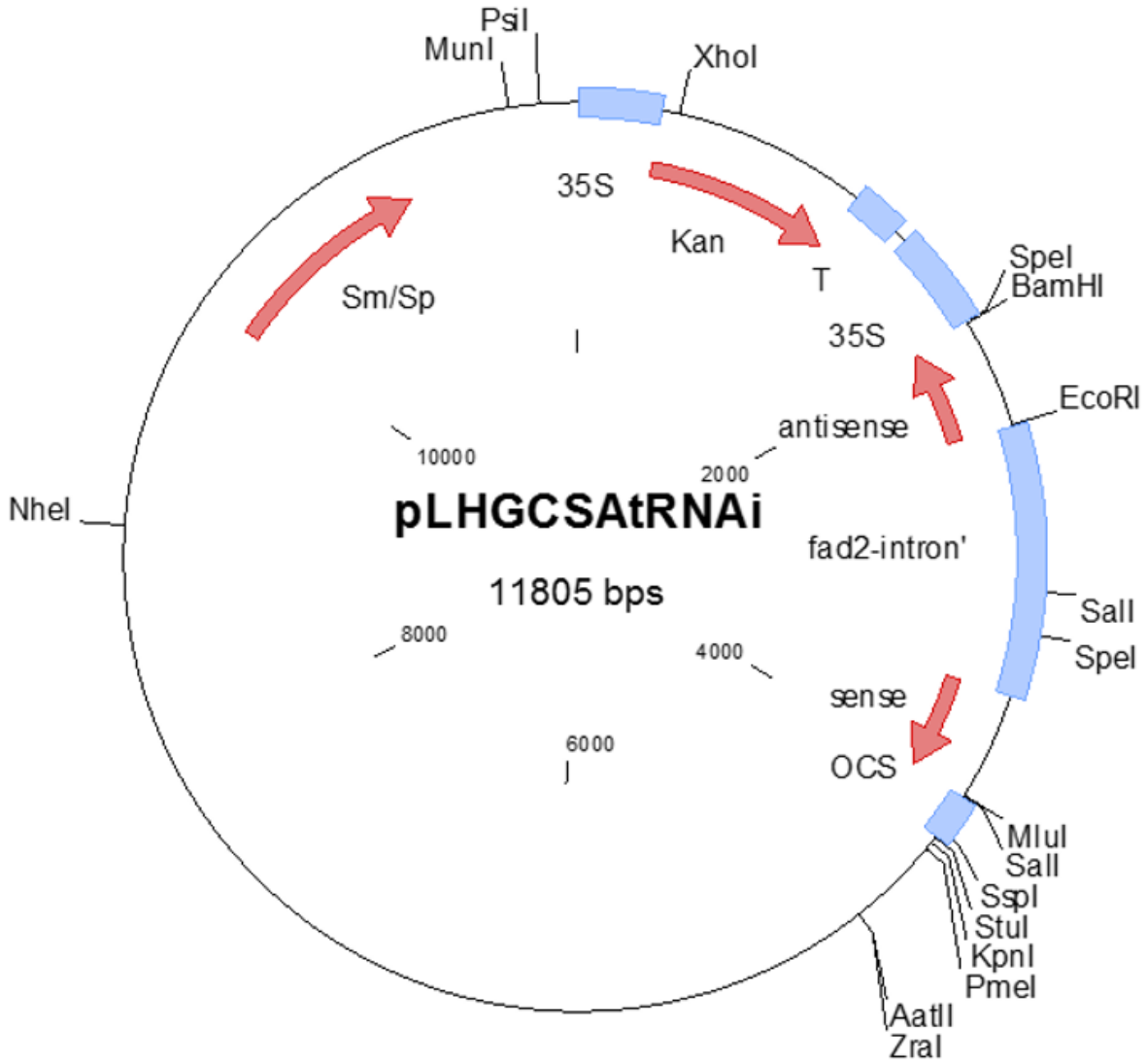

Figure 46: Cloning of *WSD* cDNA Sequences into the Vector pLHGCSAtRNAi for Subcellular Localization in Tobacco Leaves.

The vector pLHGCSAtRNAi (Dr. Georg Hölzl, IMBIO, University Bonn, Germany; vector map see at the top) was employed for N-terminal and C-terminal fusion constructs. The aim was to insert the cDNAs of all *WSD* genes (except *WSD1* and *WSD11* whose subcellular localizations were already characterized by Li *et al.*, 2008 and Takeda *et al.*, 2013) as WSD-eGFP or eGFP-WSD to obtain N-terminal and C-terminal fusion constructs for each *WSD* cDNA. As a result, *WSD3* was fused N-terminally to *eGFP* by using the restriction sites of *Spe*I and *Bam*HI yielding the fusion construct pL-35S-*WSD3-eGFP.* WSD4 and WSD9 were fused C-terminally to *eGFP* by using the restriction sites of *Bam*HI and *Sal*I which resulted in the fusion constructs pL-35S-*eGFP-WSD4* and pL-35S-*eGFP-WSD9* respectively. The other cDNAs of the *WSD* genes were amplified with primers listed in Table 6, inserted in pJET1.2/blunt and sequenced but not yet transferred into the vectors. The next experimental step would be fuse the other *WSD* sequences with the N-terminus and with the C-terminus to *eGFP* in pL-35S-*eGFP*.

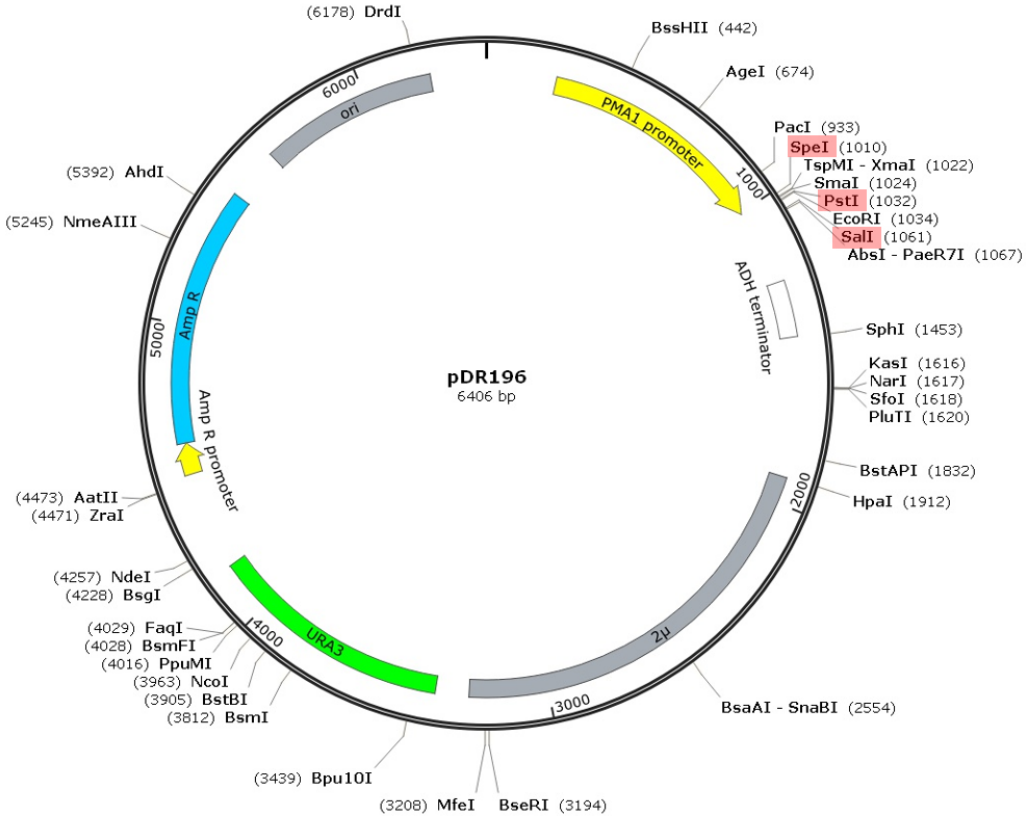
pDR196
6406 bp
(6178) DrdI
BssHII (442)
AgeI (674)
PacI (933)
SpeI (1010)
TspMI - XmaI (1022)
SmaI (1024)
PstI (1032)
EcoRI (1034)
SalI (1061)
AbsI - PaeR7I (1067)
SphI (1453)
KasI (1616)
NarI (1617)
SfoI (1618)
PluTI (1620)
BstAPI (1832)
HpaI (1912)
BsaAI - SnaBI (2554)
(3208) MfeI
BseRI (3194)
(3439) Bpu10I
(3812) BsmI
(3905) BstBI
(3963) NcoI
(4016) PpuMI
(4028) BsmFI
(4029) FaqI
(4228) BsgI
(4257) NdeI
(4471) ZraI
(4473) AatII
(5245) NmeAIII
(5392) AhdI
ori
PMA1 promoter
ADH terminator
Amp R
Amp R promoter
URA3
2µ
6000
1000
2000
3000
4000
5000

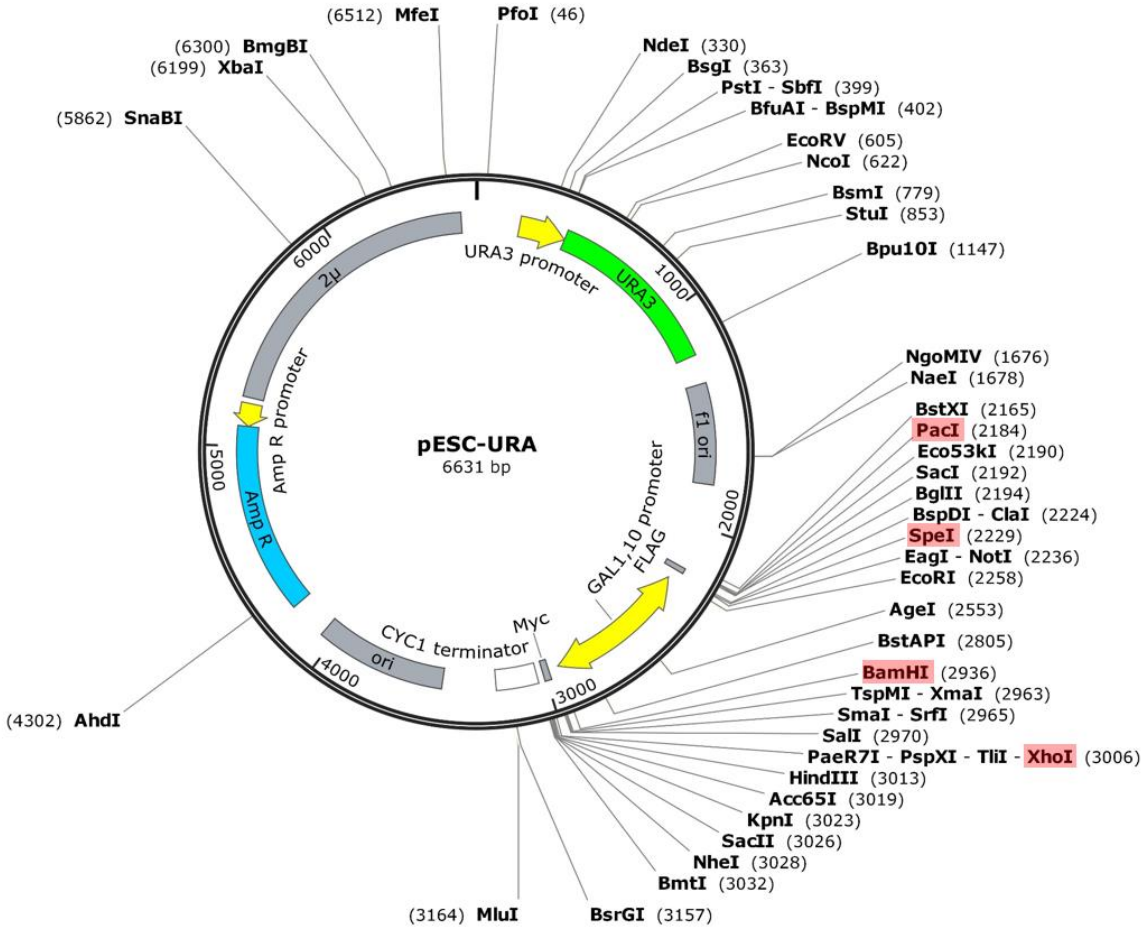
pESC-URA
6631 bp
(6512) MfeI
PfoI (46)
NdeI (330)
BsgI (363)
PstI - SbfI (399)
BfuAI - BspMI (402)
EcoRV (605)
NcoI (622)
BsmI (779)
StuI (853)
Bpu10I (1147)
NgoMIV (1676)
NaeI (1678)
BstXI (2165)
PacI (2184)
Eco53kI (2190)
SacI (2192)
BglII (2194)
BspDI - ClaI (2224)
SpeI (2229)
EagI - NotI (2236)
EcoRI (2258)
AgeI (2553)
BstAPI (2805)
BamHI (2936)
TspMI - XmaI (2963)
SmaI - SrfI (2965)
SalI (2970)
PaeR7I - PspXI - TliI - XhoI (3006)
HindIII (3013)
Acc65I (3019)
KpnI (3023)
SacII (3026)
NheI (3028)
BmtI (3032)
BsrGI (3157)
(3164) MluI
(4302) AhdI
(5862) SnaBI
(6199) XbaI
(6300) BmgBI
URA3 promoter
URA3
f1 ori
GAL1,10 promoter
FLAG
Myc
CYC1 terminator
ori
Amp R promoter
Amp R
2µ
6000
1000
2000
3000
4000
5000

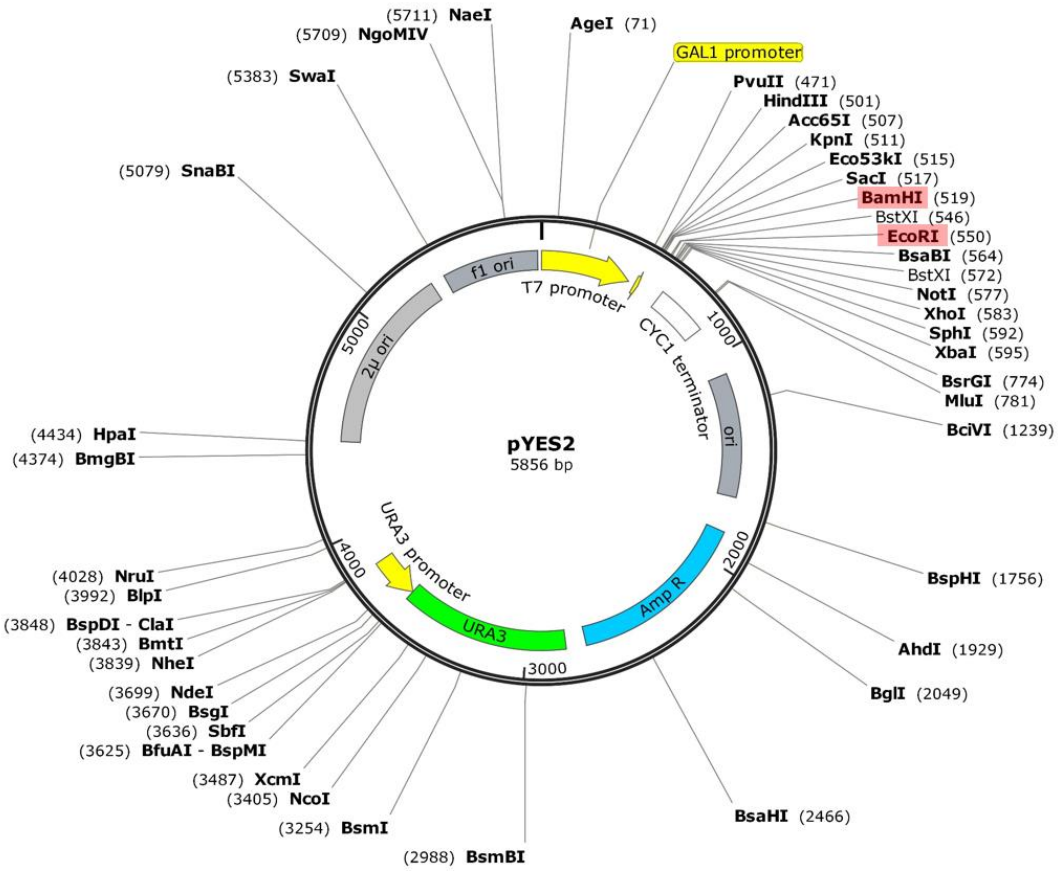

Figure 47: Vectors Used for Heterologous Expression of *WSD* cDNA in *S. cerevisiae* H1246.

In pDR196, the *WSD* cDNA was inserted downstream of the constitutive *PMA1* promoter. pESC-URA and pYES2 feature *GAL* promoters where the expression of the inserted *WSD* gene is repressed by glucose and induced by galactose. All three vectors contain the *URA3* gene for selection and cultivation of transformed yeast clones. Restriction sites that are highlighted in red were used for cloning (see Table 7). Vector maps were created with Snapgene.

7.4 Targeted Lists for Q-TOF MS/MS Analysis

Table 12: Isobaric Wax Ester and Steryl Ester Species.

Parental Ion Wax Ester / Steryl Ester [a] $[M+NH_4]^+$ m/z	Product Ion Wax Ester/ Steryl Ester [a] m/z	Wax Ester Species	Steryl Ester Species
638.681 / 638.5871	369.3727 / 369.3505	18:0ol/24:0	16:2-Cholesterol
666.7123 / 666.6184	369.3727 / 369.3505	20:0ol/24:0	18:2-Cholesterol
666.7123 / 666.6184	397.4051 / 397.3818	18:0ol/26:0	16:2-Sitosterol
694.7436 / 694.6497	369.3727 / 369.3505	22:0ol/24:0	20:2-Cholesterol
694.7436 / 694.6497	397.4051 / 397.3818	20:0ol/26:0	18:2-Sitosterol
722.7749 / 722.6810	397.4051 / 397.3818	22:0ol/26:0	20:2-Sitosterol
722.7749 / 722.6810	369.3727 / 369.3505	24:0ol/24:0	22:2-Cholesterol
750.8062 / 750.7123	397.4051 / 397.3818	24:0ol/26:0	22:2-Sitosterol

[a] The m/z's for steryl esters (parental ions and product ions) were taken from Wewer *et al.*, 2011

Table 13: Targeted List of Wax Esters with Chain Lengths of C_{17} to C_{37} Containing Short-to-Medium Alcohol Moieties Used for MS/MS Measurements in Plant Tissue.

Wax Ester Molecular Species	Molecular Formula [M]	$[M+NH_4]^+$ m/z	Product Ion $[FA+H]^+$ m/z
18:0ol/17:0 (I.S.)	$C_{35}H_{70}O_2$	540.5714	271.2632
3:0ol/14:0	$C_{17}H_{34}O_2$	288.2897	229.2162
1:0ol/16:0	$C_{17}H_{34}O_2$	288.2897	257.2475
4:0ol/14:0	$C_{18}H_{36}O_2$	302.3054	229.2162
2:0ol/16:0	$C_{18}H_{36}O_2$	302.3054	257.2475
5:0ol/14:0	$C_{19}H_{38}O_2$	316.321	229.2162
3:0ol/16:0	$C_{19}H_{38}O_2$	316.321	257.2475
1:0ol/18:0	$C_{19}H_{38}O_2$	316.321	285.2788
6:0ol/14:0	$C_{20}H_{40}O_2$	330.3367	229.2162
4:0ol/16:0	$C_{20}H_{40}O_2$	330.3367	257.2475
2:0ol/18:0	$C_{20}H_{40}O_2$	330.3367	285.2788
7:0ol/14:0	$C_{21}H_{42}O_2$	344.3523	229.2162
5:0ol/16:0	$C_{21}H_{42}O_2$	344.3523	257.2475
3:0ol/18:0	$C_{21}H_{42}O_2$	344.3523	285.2788
1:0ol/20:0	$C_{21}H_{42}O_2$	344.3523	313.3101
8:0ol/14:0	$C_{22}H_{44}O_2$	358.368	229.2162
6:0ol/16:0	$C_{22}H_{44}O_2$	358.368	257.2475
4:0ol/18:0	$C_{22}H_{44}O_2$	358.368	285.2788
2:0ol/20:0	$C_{22}H_{44}O_2$	358.368	313.3101
9:0ol/14:0	$C_{23}H_{46}O_2$	372.3836	229.2162
7:0ol/16:0	$C_{23}H_{46}O_2$	372.3836	257.2475
5:0ol/18:0	$C_{23}H_{46}O_2$	372.3836	285.2788
3:0ol/20:0	$C_{23}H_{46}O_2$	372.3836	313.3101
1:0ol/22:0	$C_{23}H_{46}O_2$	372.3836	341.3414
10:0ol/14:0	$C_{24}H_{48}O_2$	386.3993	229.2162
8:0ol/16:0	$C_{24}H_{48}O_2$	386.3993	257.2475
6:0ol/18:0	$C_{24}H_{48}O_2$	386.3993	285.2788
4:0ol/20:0	$C_{24}H_{48}O_2$	386.3993	313.3101
2:0ol/22:0	$C_{24}H_{48}O_2$	386.3993	341.3414
11:0ol/14:0	$C_{25}H_{50}O_2$	400.4149	229.2162
9:0ol/16:0	$C_{25}H_{50}O_2$	400.4149	257.2475
7:0ol/18:0	$C_{25}H_{50}O_2$	400.4149	285.2788
5:0ol/20:0	$C_{25}H_{50}O_2$	400.4149	313.3101
3:0ol/22:0	$C_{25}H_{50}O_2$	400.4149	341.3414
1:0ol/24:0	$C_{25}H_{50}O_2$	400.4149	369.3727
12:0ol/14:0	$C_{26}H_{52}O_2$	414.4306	229.2162
10:0ol/16:0	$C_{26}H_{52}O_2$	414.4306	257.2475
8:0ol/18:0	$C_{26}H_{52}O_2$	414.4306	285.2788
6:0ol/20:0	$C_{26}H_{52}O_2$	414.4306	313.3101
4:0ol/22:0	$C_{26}H_{52}O_2$	414.4306	341.3414
2:0ol/24:0	$C_{26}H_{52}O_2$	414.4306	369.3727

13:0ol/14:0	$C_{27}H_{54}O_2$	427.4384	229.2162
11:0ol/16:0	$C_{27}H_{54}O_2$	427.4384	257.2475
9:0ol/18:0	$C_{27}H_{54}O_2$	427.4384	285.2788
7:0ol/20:0	$C_{27}H_{54}O_2$	427.4384	313.3101
5:0ol/22:0	$C_{27}H_{54}O_2$	427.4384	341.3414
3:0ol/24:0	$C_{27}H_{54}O_2$	427.4384	369.3727
1:0ol/26:0	$C_{27}H_{54}O_2$	427.4384	397.4051
14:0ol/14:0	$C_{28}H_{56}O_2$	442.4619	229.2162
12:0ol/16:0	$C_{28}H_{56}O_2$	442.4619	257.2475
10:0ol/18:0	$C_{28}H_{56}O_2$	442.4619	285.2788
8:0ol/20:0	$C_{28}H_{56}O_2$	442.4619	313.3101
6:0ol/22:0	$C_{28}H_{56}O_2$	442.4619	341.3414
4:0ol/24:0	$C_{28}H_{56}O_2$	442.4619	369.3727
2:0ol/26:0	$C_{28}H_{56}O_2$	442.4619	397.4051
15:0ol/14:0	$C_{29}H_{58}O_2$	456.4775	229.2162
13:0ol/16:0	$C_{29}H_{58}O_2$	456.4775	257.2475
11:0ol/18:0	$C_{29}H_{58}O_2$	456.4775	285.2788
9:0ol/20:0	$C_{29}H_{58}O_2$	456.4775	313.3101
7:0ol/22:0	$C_{29}H_{58}O_2$	456.4775	341.3414
5:0ol/24:0	$C_{29}H_{58}O_2$	456.4775	369.3727
3:0ol/26:0	$C_{29}H_{58}O_2$	456.4775	397.4051
16:0ol/14:0	$C_{30}H_{60}O_2$	470.4932	229.2162
14:0ol/16:0	$C_{30}H_{60}O_2$	470.4932	257.2475
12:0ol/18:0	$C_{30}H_{60}O_2$	470.4932	285.2788
10:0ol/20:0	$C_{30}H_{60}O_2$	470.4932	313.3101
8:0ol/22:0	$C_{30}H_{60}O_2$	470.4932	341.3414
6:0ol/24:0	$C_{30}H_{60}O_2$	470.4932	369.3727
4:0ol/26:0	$C_{30}H_{60}O_2$	470.4932	397.4051
17:0ol/14:0	$C_{31}H_{62}O_2$	484.5088	229.2162
15:0ol/16:0	$C_{31}H_{62}O_2$	484.5088	257.2475
13:0ol/18:0	$C_{31}H_{62}O_2$	484.5088	285.2788
11:0ol/20:0	$C_{31}H_{62}O_2$	484.5088	313.3101
9:0ol/22:0	$C_{31}H_{62}O_2$	484.5088	341.3414
7:0ol/24:0	$C_{31}H_{62}O_2$	484.5088	369.3727
5:0ol/26:0	$C_{31}H_{62}O_2$	484.5088	397.4051
18:0ol/14:0	$C_{32}H_{64}O_2$	498.5245	229.2162
16:0ol/16:0	$C_{32}H_{64}O_2$	498.5245	257.2475
14:0ol/18:0	$C_{32}H_{64}O_2$	498.5245	285.2788
12:0ol/20:0	$C_{32}H_{64}O_2$	498.5245	313.3101
10:0ol/22:0	$C_{32}H_{64}O_2$	498.5245	341.3414
8:0ol/24:0	$C_{32}H_{64}O_2$	498.5245	369.3727
6:0ol/26:0	$C_{32}H_{64}O_2$	498.5245	397.4051
19:0ol/14:0	$C_{33}H_{66}O_2$	512.5401	229.2162
17:0ol/16:0	$C_{33}H_{66}O_2$	512.5401	257.2475
15:0ol/18:0	$C_{33}H_{66}O_2$	512.5401	285.2788

13:0ol/20:0	$C_{33}H_{66}O_2$	512.5401	313.3101
11:0ol/22:0	$C_{33}H_{66}O_2$	512.5401	341.3414
9:0ol/24:0	$C_{33}H_{66}O_2$	512.5401	369.3727
7:0ol/26:0	$C_{33}H_{66}O_2$	512.5401	397.4051
20:0ol/14:0	$C_{34}H_{68}O_2$	526.5558	229.2162
18:0ol/16:0	$C_{34}H_{68}O_2$	526.5558	257.2475
16:0ol/18:0	$C_{34}H_{68}O_2$	526.5558	285.2788
14:0ol/20:0	$C_{34}H_{68}O_2$	526.5558	313.3101
12:0ol/22:0	$C_{34}H_{68}O_2$	526.5558	341.3414
10:0ol/24:0	$C_{34}H_{68}O_2$	526.5558	369.3727
8:0ol/26:0	$C_{34}H_{68}O_2$	526.5558	397.4051
21:0ol/14:0	$C_{35}H_{70}O_2$	540.5714	229.2162
19:0ol/16:0	$C_{35}H_{70}O_2$	540.5714	257.2475
17:0ol/18:0	$C_{35}H_{70}O_2$	540.5714	285.2788
15:0ol/20:0	$C_{35}H_{70}O_2$	540.5714	313.3101
13:0ol/22:0	$C_{35}H_{70}O_2$	540.5714	341.3414
11:0ol/24:0	$C_{35}H_{70}O_2$	540.5714	369.3727
9:0ol/26:0	$C_{35}H_{70}O_2$	540.5714	397.4051
22:0ol/14:0	$C_{36}H_{72}O_2$	554.5871	229.2162
20:0ol/16:0	$C_{36}H_{72}O_2$	554.5871	257.2475
18:0ol/18:0	$C_{36}H_{72}O_2$	554.5871	285.2788
16:0ol/20:0	$C_{36}H_{72}O_2$	554.5871	313.3101
14:0ol/22:0	$C_{36}H_{72}O_2$	554.5871	341.3414
12:0ol/24:0	$C_{36}H_{72}O_2$	554.5871	369.3727
10:0ol/26:0	$C_{36}H_{72}O_2$	554.5871	397.4051
23:0ol/14:0	$C_{37}H_{74}O_2$	568.6027	229.2162
21:0ol/16:0	$C_{37}H_{74}O_2$	568.6027	257.2475
19:0ol/18:0	$C_{37}H_{74}O_2$	568.6027	285.2788
17:0ol/20:0	$C_{37}H_{74}O_2$	568.6027	313.3101
15:0ol/22:0	$C_{37}H_{74}O_2$	568.6027	341.3414
13:0ol/24:0	$C_{37}H_{74}O_2$	568.6027	369.3727
11:0ol/26:0	$C_{37}H_{74}O_2$	568.6027	397.4051

Table 14: Targeted List of Wax Esters with Chain Lengths of C_{38} to C_{54} Used for MS/MS Measurements in Plant Tissue.

Wax Ester Molecular Species	Molecular Formula [M]	$[M+NH_4]^+$ m/z	Product Ion $[FA+H]^+$ m/z
18:0ol/17:0 (I.S.)	$C_{35}H_{70}O_2$	540.5714	271.2632
24:0ol/14:0	$C_{38}H_{76}O_2$	582.6184	229.2162
22:0ol/16:0	$C_{38}H_{76}O_2$	582.6184	257.2475
20:0ol/18:0	$C_{38}H_{76}O_2$	582.6184	285.2788
18:0ol/20:0	$C_{38}H_{76}O_2$	582.6184	313.3101
16:0ol/22:0	$C_{38}H_{76}O_2$	582.6184	341.3414
14:0ol/24:0	$C_{38}H_{76}O_2$	582.6184	369.3727
12:0ol/26:0	$C_{38}H_{76}O_2$	582.6184	397.4051

26:0ol/14:0	$C_{40}H_{80}O_2$	610.6497	229.2162
24:0ol/16:0	$C_{40}H_{80}O_2$	610.6497	257.2475
22:0ol/18:0	$C_{40}H_{80}O_2$	610.6497	285.2788
20:0ol/20:0	$C_{40}H_{80}O_2$	610.6497	313.3101
18:0ol/22:0	$C_{40}H_{80}O_2$	610.6497	341.3414
16:0ol/24:0	$C_{40}H_{80}O_2$	610.6497	369.3727
14:0ol/26:0	$C_{40}H_{80}O_2$	610.6497	397.4051
28:0ol/14:0	$C_{42}H_{84}O_2$	638.6810	229.2162
26:0ol/16:0	$C_{42}H_{84}O_2$	638.6810	257.2475
24:0ol/18:0	$C_{42}H_{84}O_2$	638.6810	285.2788
22:0ol/20:0	$C_{42}H_{84}O_2$	638.6810	313.3101
20:0ol/22:0	$C_{42}H_{84}O_2$	638.6810	341.3414
16:0ol/26:0	$C_{42}H_{84}O_2$	638.6810	397.4051
30:0ol/14:0	$C_{44}H_{88}O_2$	666.7123	229.2162
28:0ol/16:0	$C_{44}H_{88}O_2$	666.7123	257.2475
26:0ol/18:0	$C_{44}H_{88}O_2$	666.7123	285.2788
24:0ol/20:0	$C_{44}H_{88}O_2$	666.7123	313.3101
22:0ol/22:0	$C_{44}H_{88}O_2$	666.7123	341.3414
18:0ol/27:0 (I.S.)	$C_{45}H_{90}O_2$	680.7279	411.4197
32:0ol/14:0	$C_{46}H_{92}O_2$	694.7436	229.2162
30:0ol/16:0	$C_{46}H_{92}O_2$	694.7436	257.2475
28:0ol/18:0	$C_{46}H_{92}O_2$	694.7436	285.2788
26:0ol/20:0	$C_{46}H_{92}O_2$	694.7436	313.3101
24:0ol/22:0	$C_{46}H_{92}O_2$	694.7436	341.3414
34:0ol/14:0	$C_{48}H_{96}O_2$	722.7749	229.2162
32:0ol/16:0	$C_{48}H_{96}O_2$	722.7749	257.2475
30:0ol/18:0	$C_{48}H_{96}O_2$	722.7749	285.2788
28:0ol/20:0	$C_{48}H_{96}O_2$	722.7749	313.3101
26:0ol/22:0	$C_{48}H_{96}O_2$	722.7749	341.3414
36:0ol/14:0	$C_{50}H_{100}O_2$	750.8062	229.2162
34:0ol/16:0	$C_{50}H_{100}O_2$	750.8062	257.2475
32:0ol/18:0	$C_{50}H_{100}O_2$	750.8062	285.2788
30:0ol/20:0	$C_{50}H_{100}O_2$	750.8062	313.3101
28:0ol/22:0	$C_{50}H_{100}O_2$	750.8062	341.3414
26:0ol/24:0	$C_{50}H_{100}O_2$	750.8062	369.3727
38:0ol/14:0	$C_{52}H_{104}O_2$	776.8218	229.2162
36:0ol/16:0	$C_{52}H_{104}O_2$	776.8218	257.2475
34:0ol/18:0	$C_{52}H_{104}O_2$	776.8218	285.2788
32:0ol/20:0	$C_{52}H_{104}O_2$	776.8218	313.3101
30:0ol/22:0	$C_{52}H_{104}O_2$	776.8218	341.3414
28:0ol/24:0	$C_{52}H_{104}O_2$	776.8218	369.3727
26:0ol/26:0	$C_{52}H_{104}O_2$	776.8218	397.4051
40:0ol/14:0	$C_{54}H_{108}O_2$	806.8688	229.2162
38:0ol/16:0	$C_{54}H_{108}O_2$	806.8688	257.2475
36:0ol/18:0	$C_{54}H_{108}O_2$	806.8688	285.2788

34:0ol/20:0	$C_{54}H_{108}O_2$	806.8688	313.3101
32:0ol/22:0	$C_{54}H_{108}O_2$	806.8688	341.3414
30:0ol/24:0	$C_{54}H_{108}O_2$	806.8688	369.3727
28:0ol/26:0	$C_{54}H_{108}O_2$	806.8688	397.4051

Table 15: Targeted List of Wax Esters Used for MS/MS Measurements in Yeast Cultures Expressing *WSD* cDNAs.

Wax Ester Molecular Species	Molecular Formula [M]	$[M+NH_4]^+$ m/z	Product Ion $[FA+H]^+$ m/z
16:0ol/16:1	$C_{32}H_{62}O_2$	496.5088	255.2319
16:1ol/16:0	$C_{32}H_{62}O_2$	496.5088	257.2475
16:0ol/16:0	$C_{32}H_{64}O_2$	498.5245	257.2475
18:1ol/16:1	$C_{34}H_{64}O_2$	522.5245	255.2319
16:1ol/18:1	$C_{34}H_{64}O_2$	522.5245	283.2632
16:0ol/18:1	$C_{34}H_{66}O_2$	524.5401	283.2632
16:1ol/18:0	$C_{34}H_{66}O_2$	524.5401	285.2788
18:0ol/16:1	$C_{34}H_{66}O_2$	524.5401	255.2319
18:1ol/16:0	$C_{34}H_{66}O_2$	524.5401	257.2475
18:0ol/16:0	$C_{34}H_{68}O_2$	526.5558	257.2475
16:0ol/18:0	$C_{34}H_{68}O_2$	526.5558	285.2788
18:0ol/17:0 (I.S.)	$C_{35}H_{70}O_2$	540.5714	271.2632
18:1ol/18:1	$C_{36}H_{68}O_2$	550.5558	283.2632
18:0ol/18:1	$C_{36}H_{70}O_2$	552.5714	283.2632
18:1ol/18:0	$C_{36}H_{70}O_2$	552.5714	285.2788
16:1ol/20:0	$C_{36}H_{70}O_2$	552.5714	313.3101
20:0ol/16:1	$C_{36}H_{70}O_2$	552.5714	255.2319
20:0ol/16:0	$C_{36}H_{72}O_2$	554.5871	257.2475
18:0ol/18:0	$C_{36}H_{72}O_2$	554.5871	285.2788
16:0ol/20:0	$C_{36}H_{72}O_2$	554.5871	313.3101
20:0ol/18:1	$C_{38}H_{76}O_2$	580.6027	283.2632
18:1ol/20:0	$C_{38}H_{74}O_2$	580.6027	313.3101
20:0ol/18:0	$C_{38}H_{76}O_2$	582.6184	285.2788
18:0ol/20:0	$C_{38}H_{76}O_2$	582.6184	313.3101
20:0ol/20:0	$C_{40}H_{80}O_2$	610.6497	313.3101
18:0ol/27:0 (I.S.)	$C_{45}H_{90}O_2$	680.7279	411.4197

7.5 Wax Esters from Stem Surface Wax of *wsd* Mutant Lines

Diagrams are presented on the following pages.

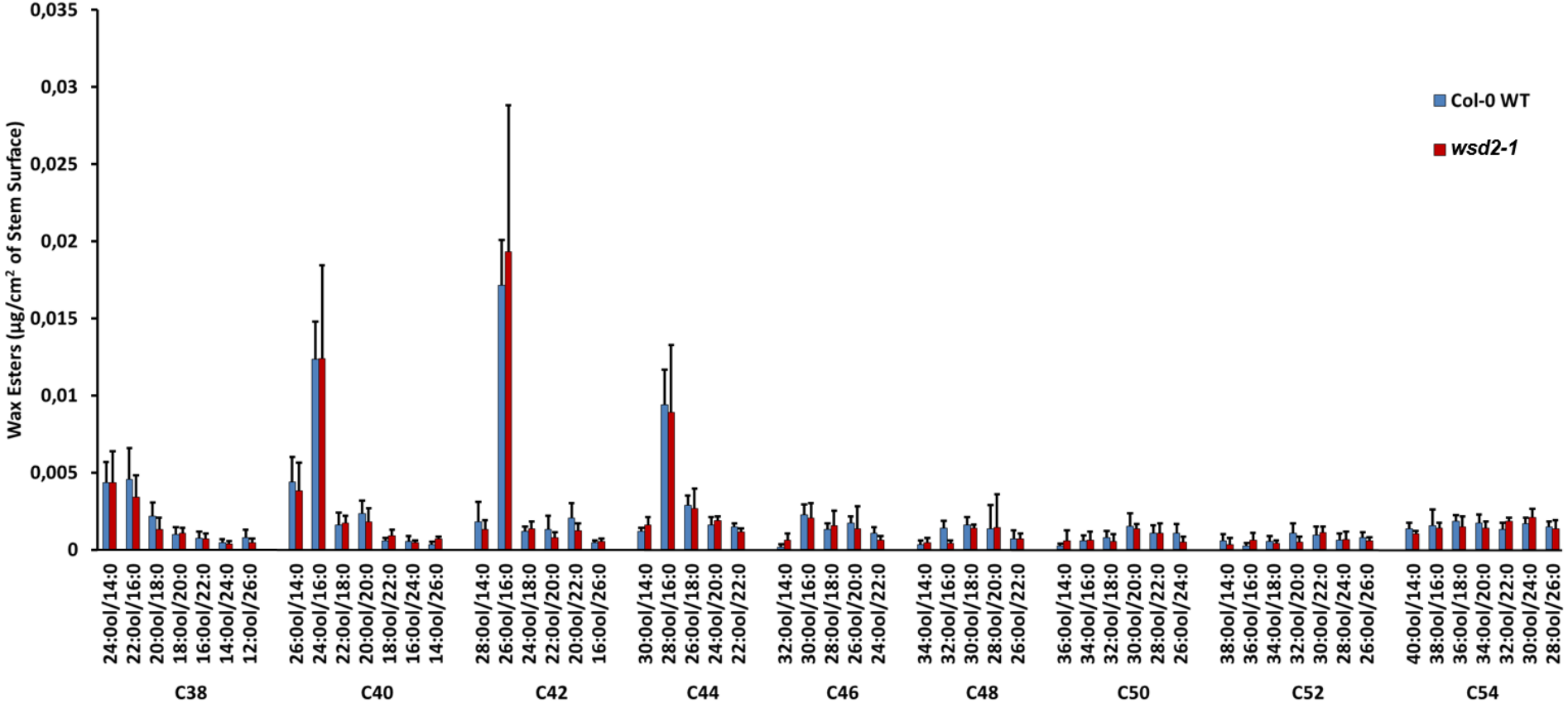

Figure 48: Stem Wax Esters from *A. thaliana* WT and Mutant Line *wsd2-1*.

Wax from inflorescence stems was extracted by chloroform. The wax extract was fractionated by SPE (hexane/diethyl ether 99/1 (v/v)) and the wax ester fraction analyzed by Q-TOF MS/MS. Data represent mean and standard deviation of 5 measurements.

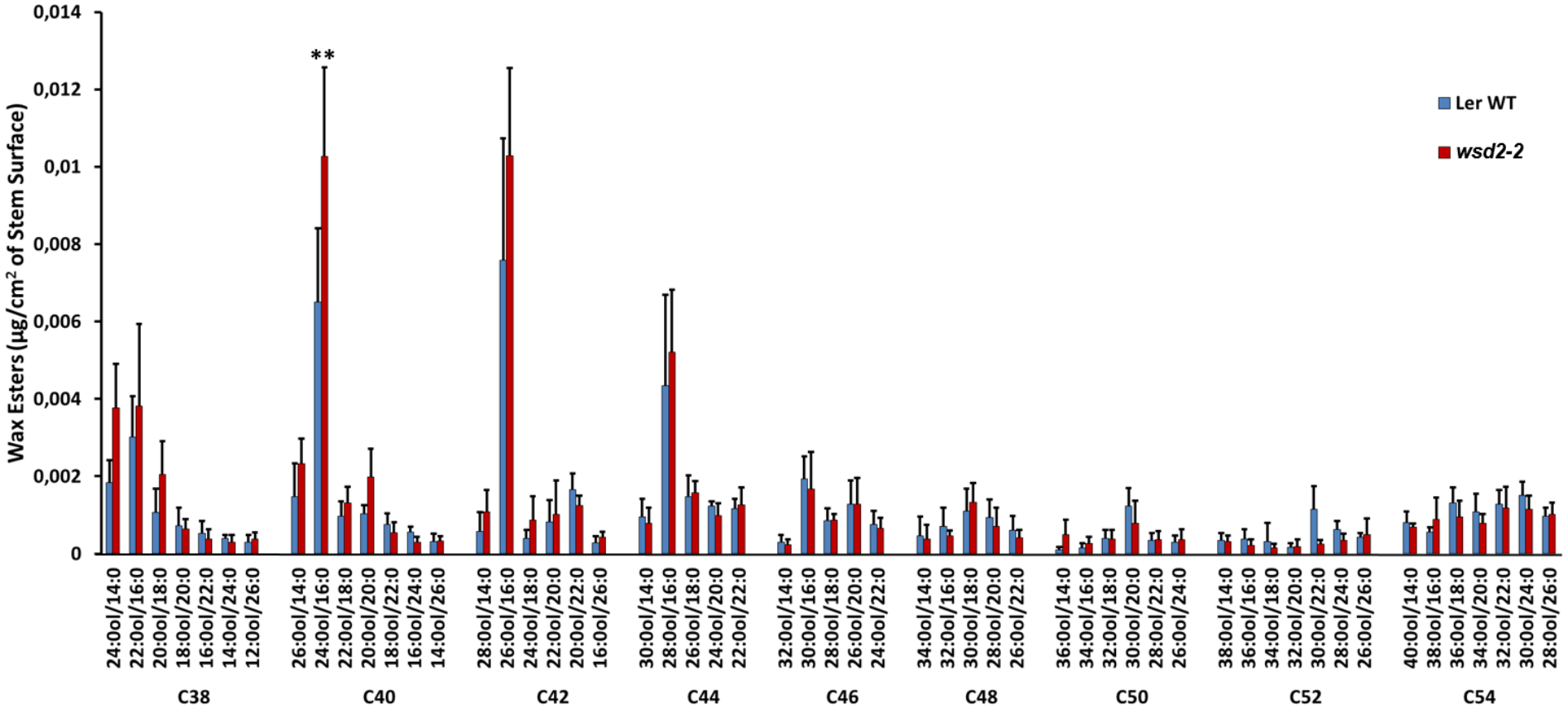

Figure 49: Stem Wax Esters from *A. thaliana* WT and Mutant Line *wsd2-2*.

Wax from inflorescence stems was extracted by chloroform. The wax extract was fractionated by SPE (hexane/diethyl ether 99/1 (v/v)) and the wax ester fraction analyzed by Q-TOF MS/MS. Data represent mean and standard deviation of 5 measurements. Asterisks indicate values that differ significantly from the wild type control (Student's *t* test, Welch correction, $P<0.02$ (**)).

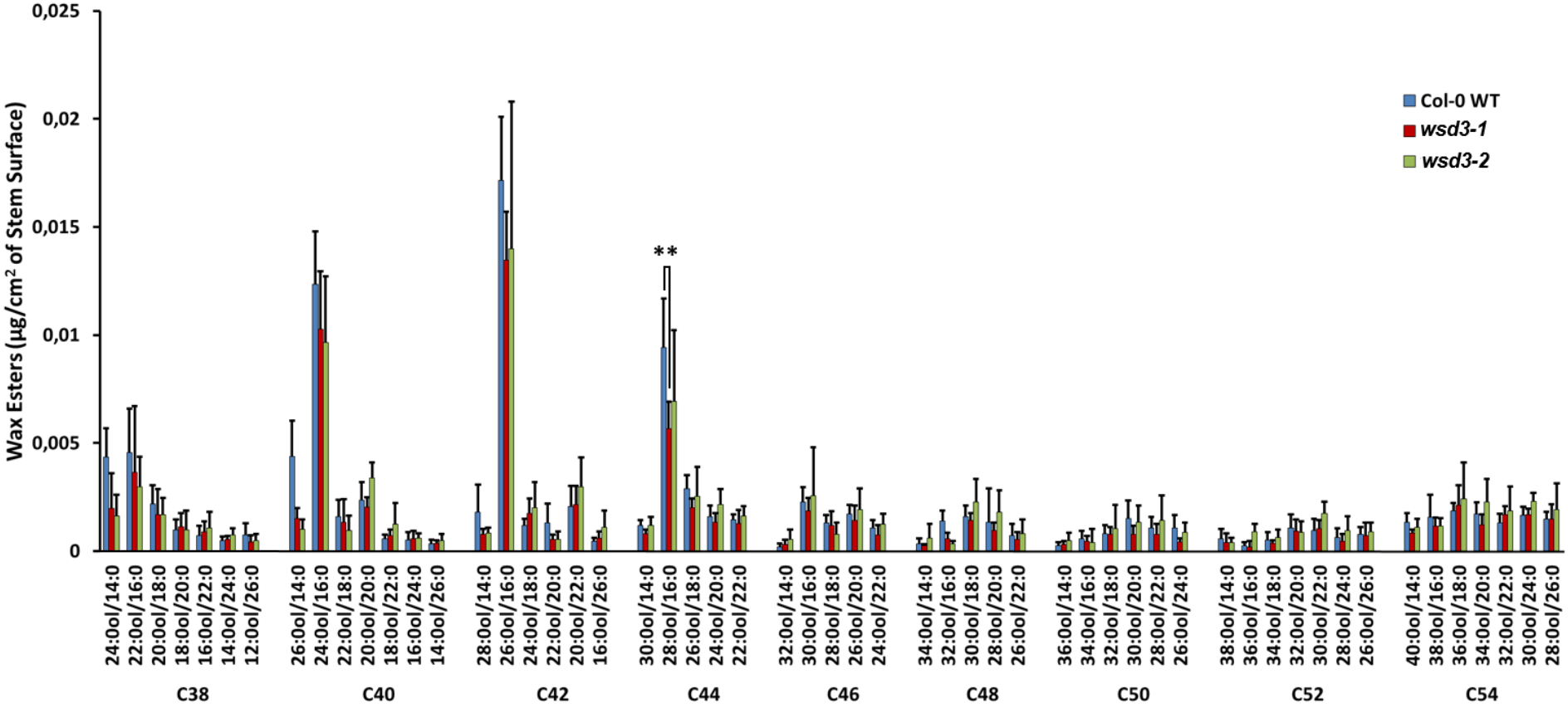

Figure 50: Stem Wax Esters from *A. thaliana* WT and Mutant Lines *wsd3-1* and *wsd3-2*.

Wax from inflorescence stems was extracted by chloroform. The wax extract was fractionated by SPE (hexane/diethyl ether 99/1 (v/v)) and the wax ester fraction analyzed by Q-TOF MS/MS. Data represent mean and standard deviation of 5 measurements. Asterisks indicate values that differ significantly from the wild type control (Student's *t* test, Welch correction, $P<0.02$ (**)).

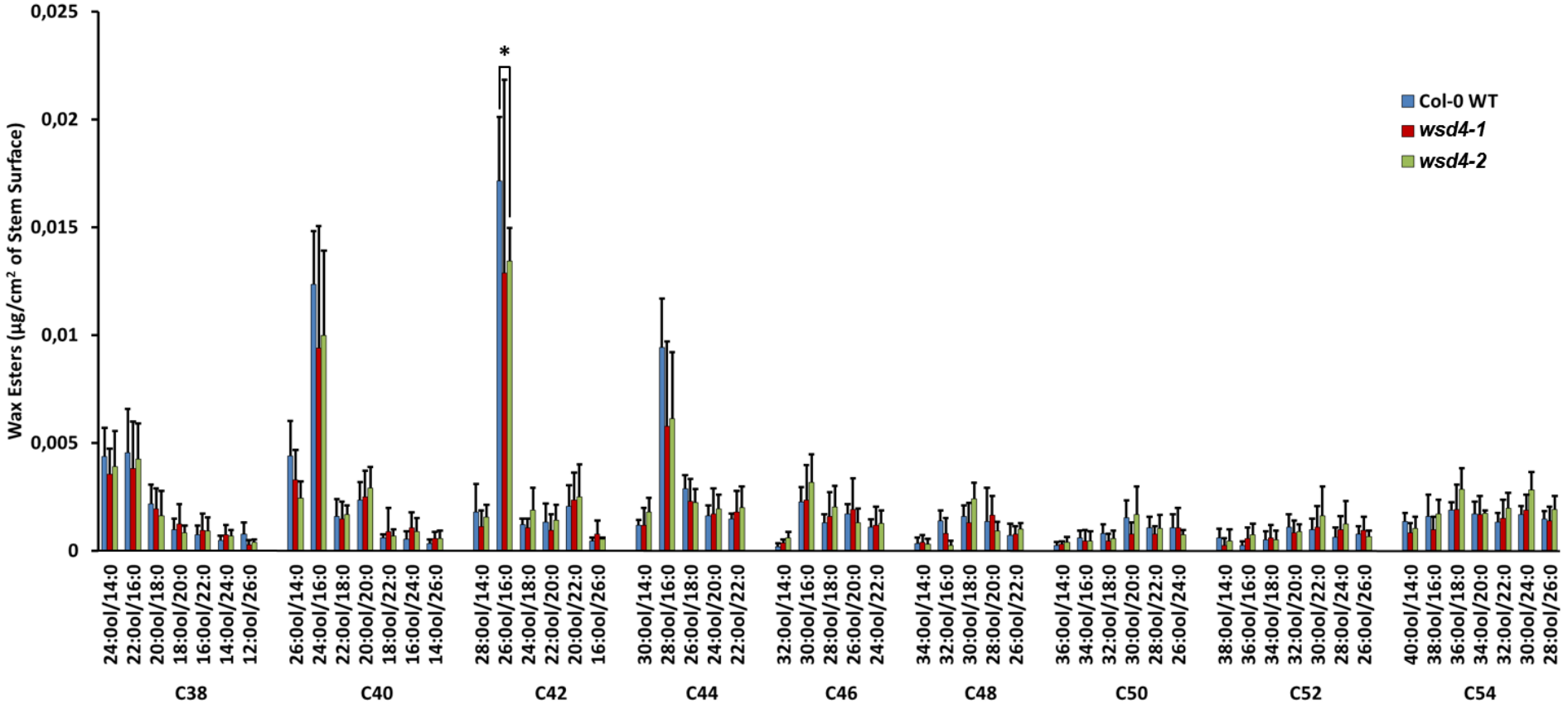

Figure 51: Stem Wax Esters from *A. thaliana* WT and Mutant Lines *wsd4-1* and *wsd4-2*.

Wax from inflorescence stems was extracted by chloroform. The wax extract was fractionated by SPE (hexane/diethyl ether 99/1 (v/v)) and the wax ester fraction analyzed by Q-TOF MS/MS. Data represent mean and standard deviation of 5 measurements. Asterisks indicate values that differ significantly from the wild type control (Student's *t* test, Welch correction, $P<0.05$ (*)).

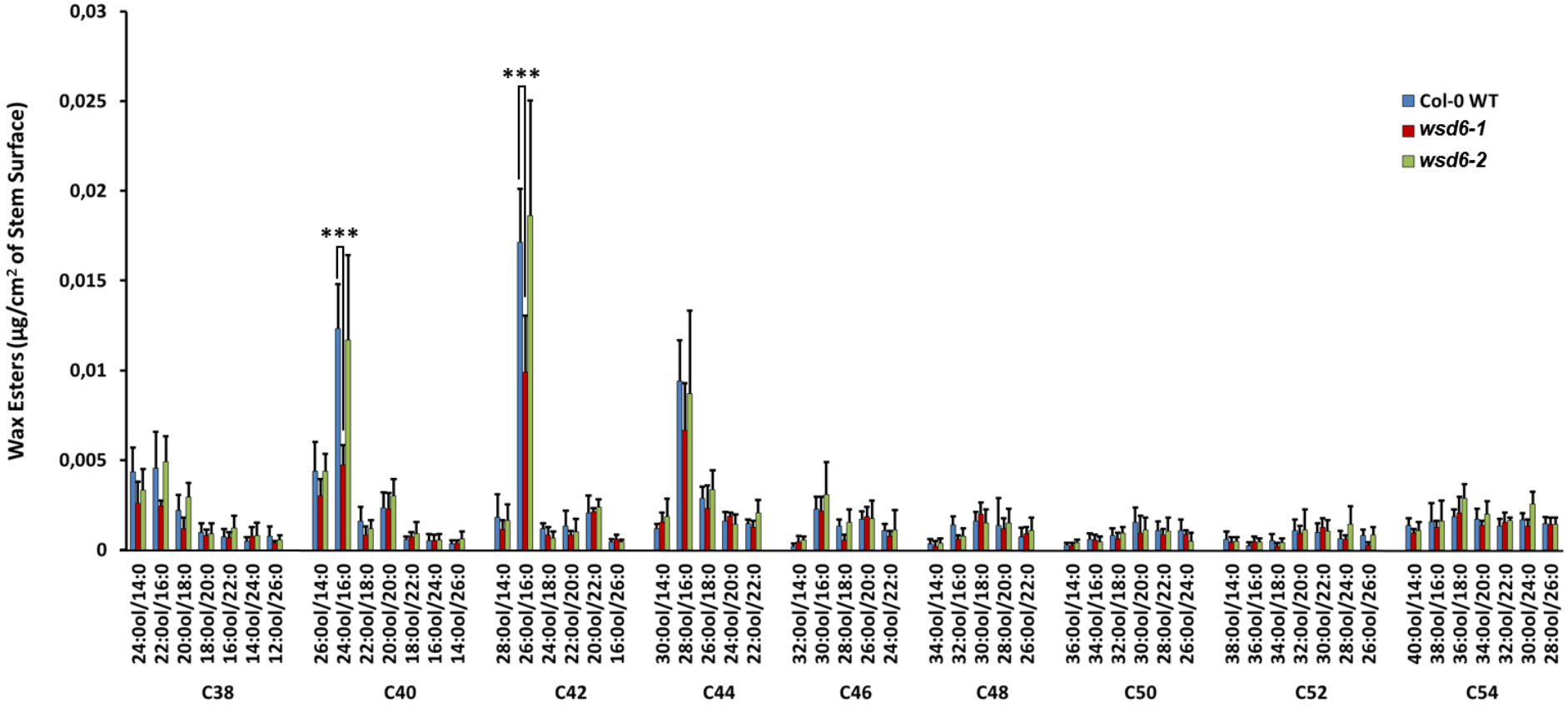

Figure 52: Stem Wax Esters from *A. thaliana* WT and Mutant Lines *wsd6-1* and *wsd6-2*.

Wax from inflorescence stems was extracted by chloroform. The wax extract was fractionated by SPE (hexane/diethyl ether 99/1 (v/v)) and the wax ester fraction analyzed by Q-TOF MS/MS. Data represent mean and standard deviation of 5 measurements. Asterisks indicate values that differ significantly from the wild type control (Student's *t* test, Welch correction, $P<0.01$ (***)).

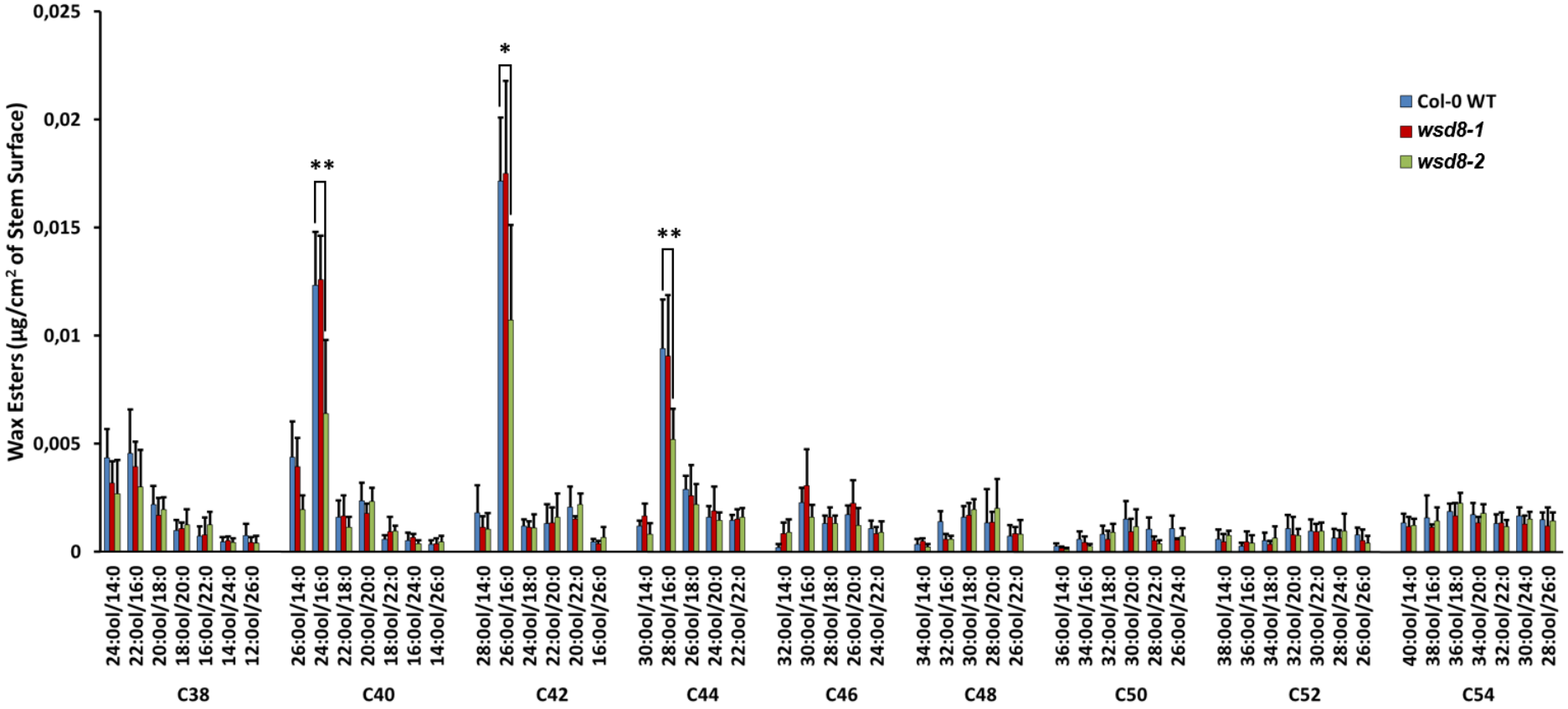

Figure 53: Stem Wax Esters from *A. thaliana* WT and Mutant Lines *wsd8-1* and *wsd8-2*.

Wax from inflorescence stems was extracted by chloroform. The wax extract was fractionated by SPE (hexane/diethyl ether 99/1 (v/v)) and the wax ester fraction analyzed by Q-TOF MS/MS. Data represent mean and standard deviation of 5 measurements. Asterisks indicate values that differ significantly from the wild type control (Student's *t* test, Welch correction, $P<0.05$ (*) and $P<0.02$ (**)).

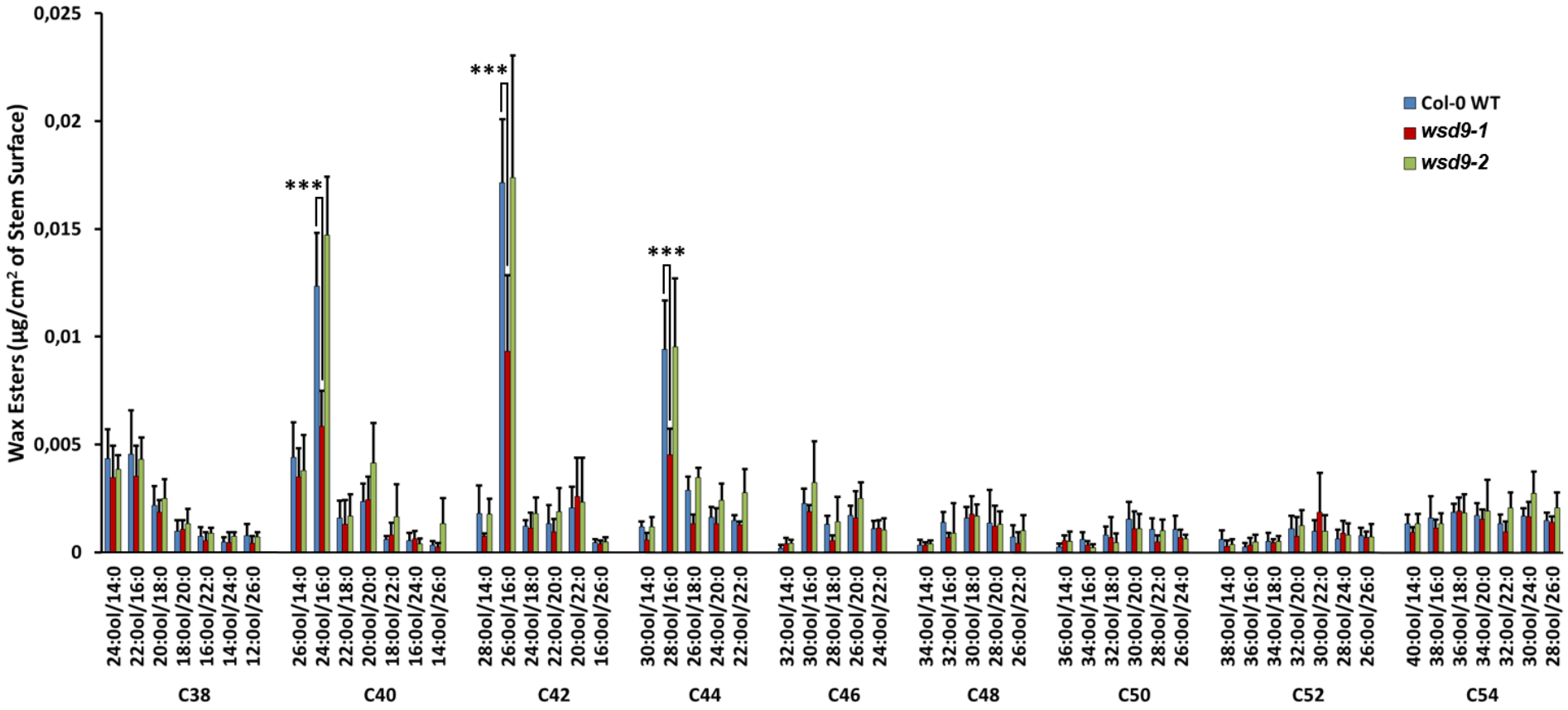

Figure 54: Stem Wax Esters from *A. thaliana* WT and Mutant Lines *wsd9-1* and *wsd9-2*.

Wax from inflorescence stems was extracted by chloroform. The wax extract was fractionated by SPE (hexane/diethyl ether 99/1 (v/v)) and the wax ester fraction analyzed by Q-TOF MS/MS. Data represent mean and standard deviation of 5 measurements. Asterisks indicate values that differ significantly from the wild type control (Student's *t* test, Welch correction, $P<0.01$ (***)).

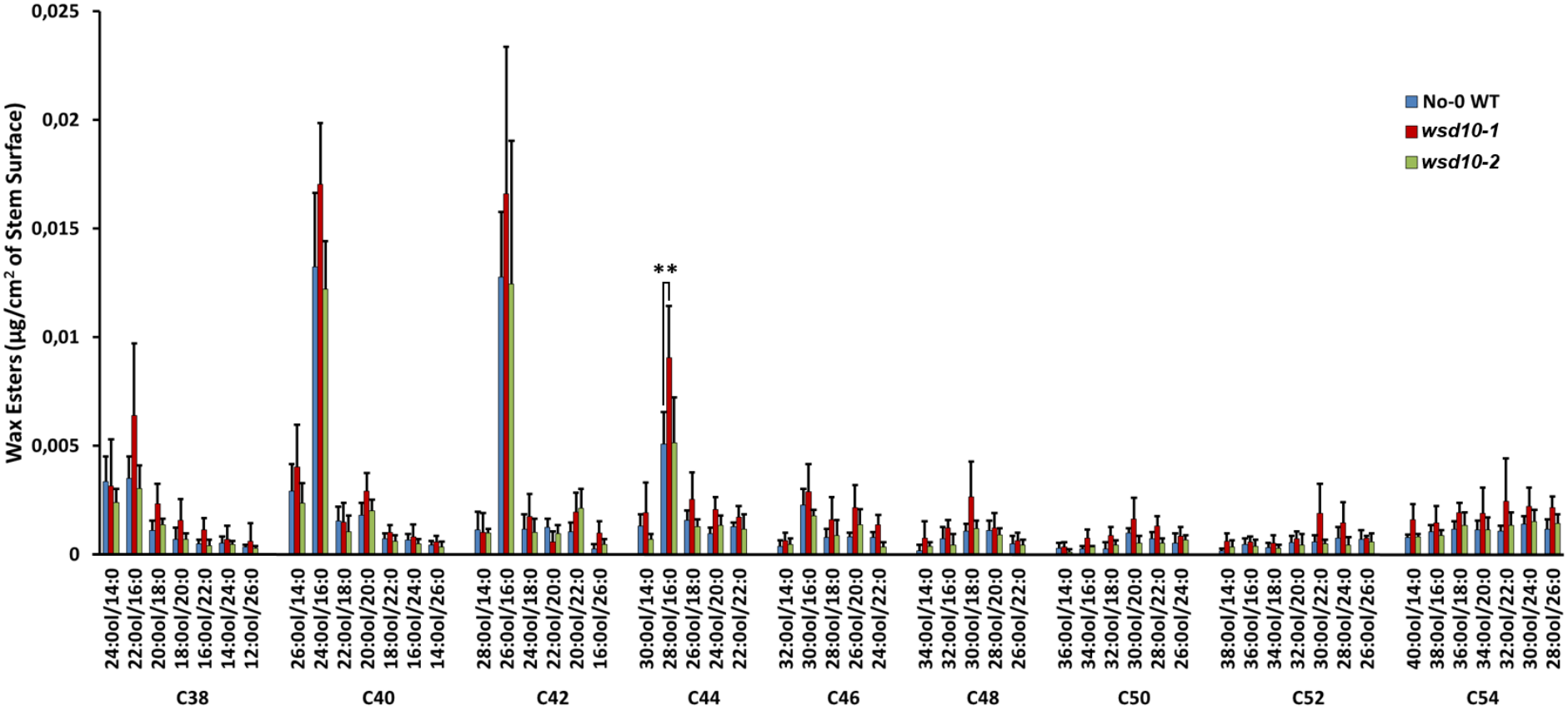

Figure 55: Stem Wax Esters from *A. thaliana* WT and Mutant Lines *wsd10-1* and *wsd10-2*.

Wax from inflorescence stems was extracted by chloroform. The wax extract was fractionated by SPE (hexane/diethyl ether 99/1 (v/v)) and the wax ester fraction analyzed by Q-TOF MS/MS. Data represent mean and standard deviation of 5 measurements. Asterisks indicate values that differ significantly from the wild type control (Student's *t* test, Welch correction, $P<0.02$ (**)).

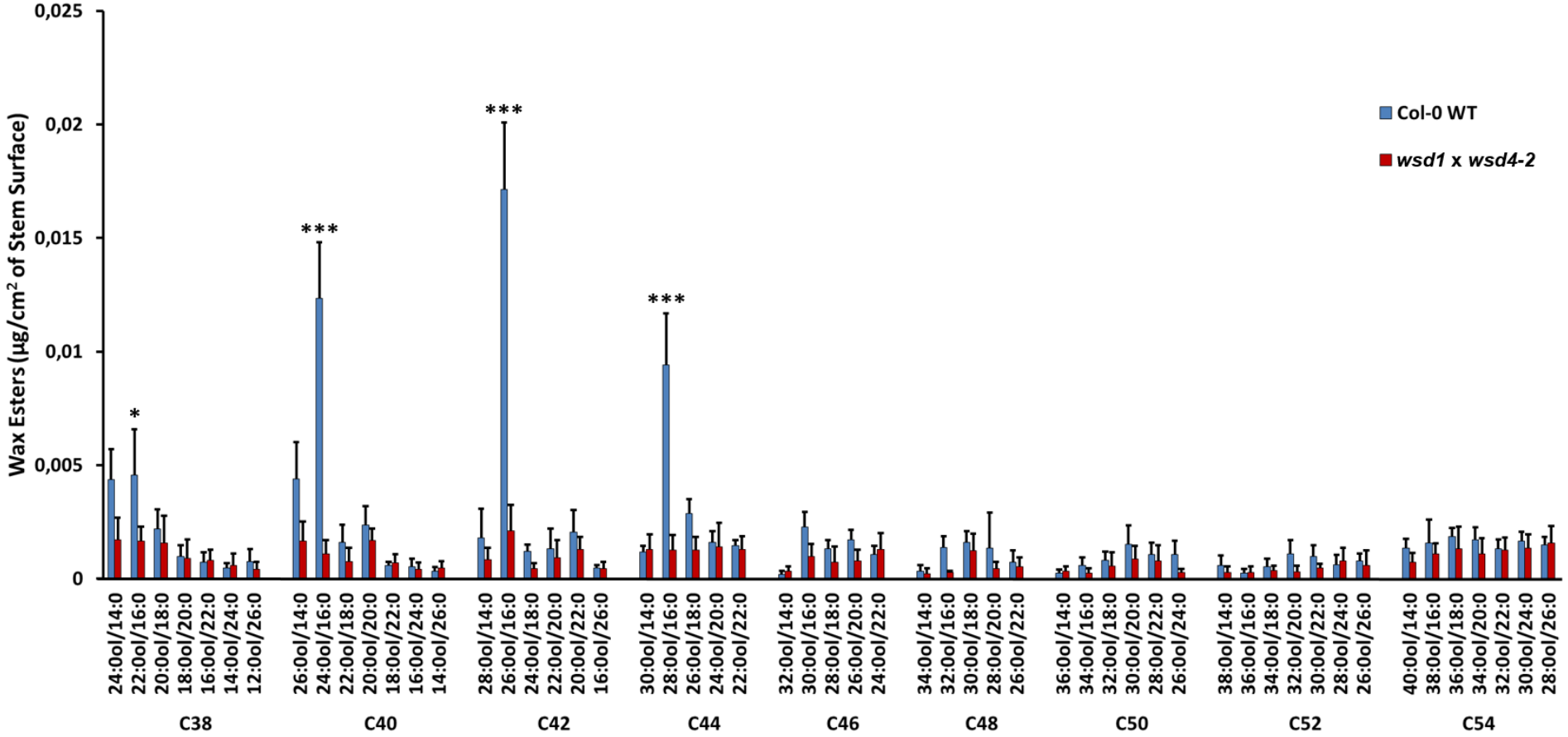

Figure 56: Stem Wax Esters from *A. thaliana* WT and Double Homozygous Mutant Line *wsd1* x *wsd4-2*.

Wax from inflorescence stems was extracted by chloroform. The wax extract was fractionated by SPE (hexane/diethyl ether 99/1 (v/v)) and the wax ester fraction analyzed by Q-TOF MS/MS. Data represent mean and standard deviation of 5 measurements. Asterisks indicate values that differ significantly from the wild type control (Student's *t* test, Welch correction, $P<0.05$ (*) and $P<0.01$ (***)).

7.6 Wax Esters from Flower Surface Wax of *wsd* Mutant Lines

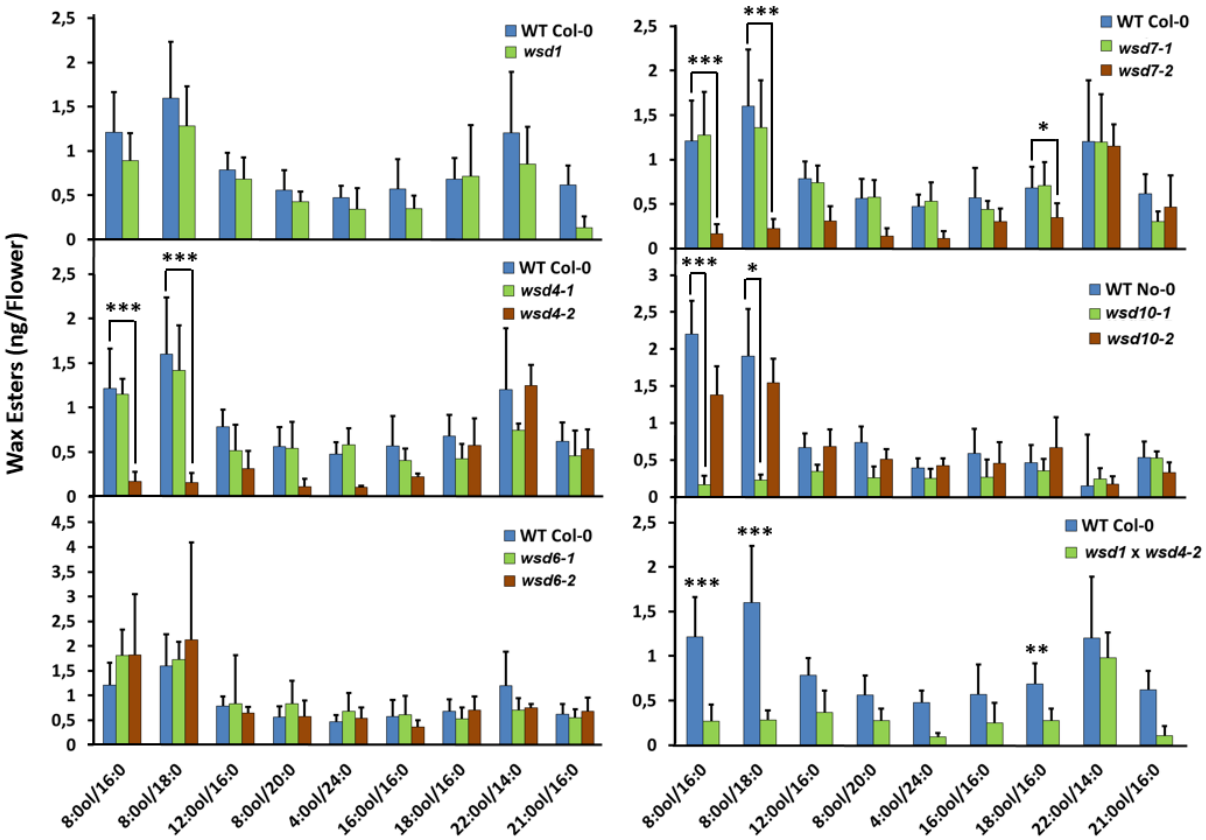

Figure 57: Abundant WE Species with the Total Chain Lengths of C_{17} to C_{37} Containing Short-to-Very-Long Chain Alcohol Moieties in Flowers of *A. thaliana* Col-0 WT and No-0 WT and *wsd* Mutant Lines.

Wax from 10 open flowers was extracted by chloroform. The wax extract was fractionated by SPE (hexane/diethyl ether 99/1 (v/v)) and the wax ester fraction analyzed by Q-TOF MS/MS. Data represent mean and standard deviation of 5 measurements for WT Col-0, WT No-0, *wsd1*, *wsd4-1*, *wsd4-2*, *wsd7-1*, *wsd7-2*, *wsd10-1*, *wsd10-2* and double homozygous mutant *wsd1* x *wsd4-2* and of 4 measurements for *wsd6-1* and *wsd6-2*. Asterisks indicate values that differ significantly from the wild type control (Student's *t* test, Welch correction, $P<0.05$ (*); $P<0.02$ (**) and $P<0.01$ (***)).

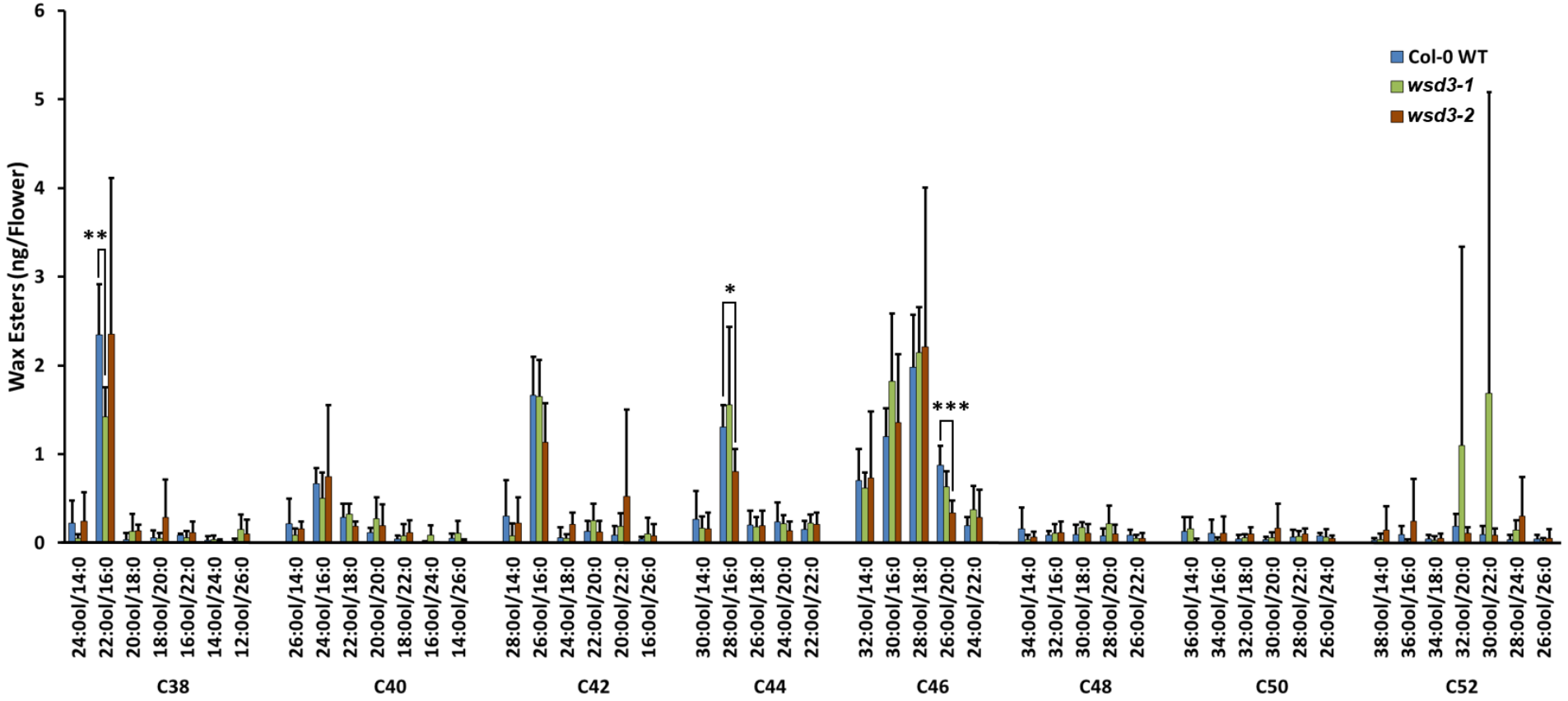

Figure 58: Flower Wax Esters from *A. thaliana* WT and Mutant Lines *wsd3-1* and *wsd3-2*.

Wax from 10 open flowers was extracted by chloroform. The wax extract was fractionated by SPE (hexane/diethyl ether 99/1 (v/v)) and the wax ester fraction analyzed by Q-TOF MS/MS. Data represent mean and standard deviation of 5 measurements for WT and *wsd3-1* and of 4 measurements for *wsd3-2*. Asterisks indicate values that differ significantly from the wild type control (Student's *t* test, Welch correction, $P<0.05$ (*) and $P<0.02$ (**) and $P<0.01$ (***)).

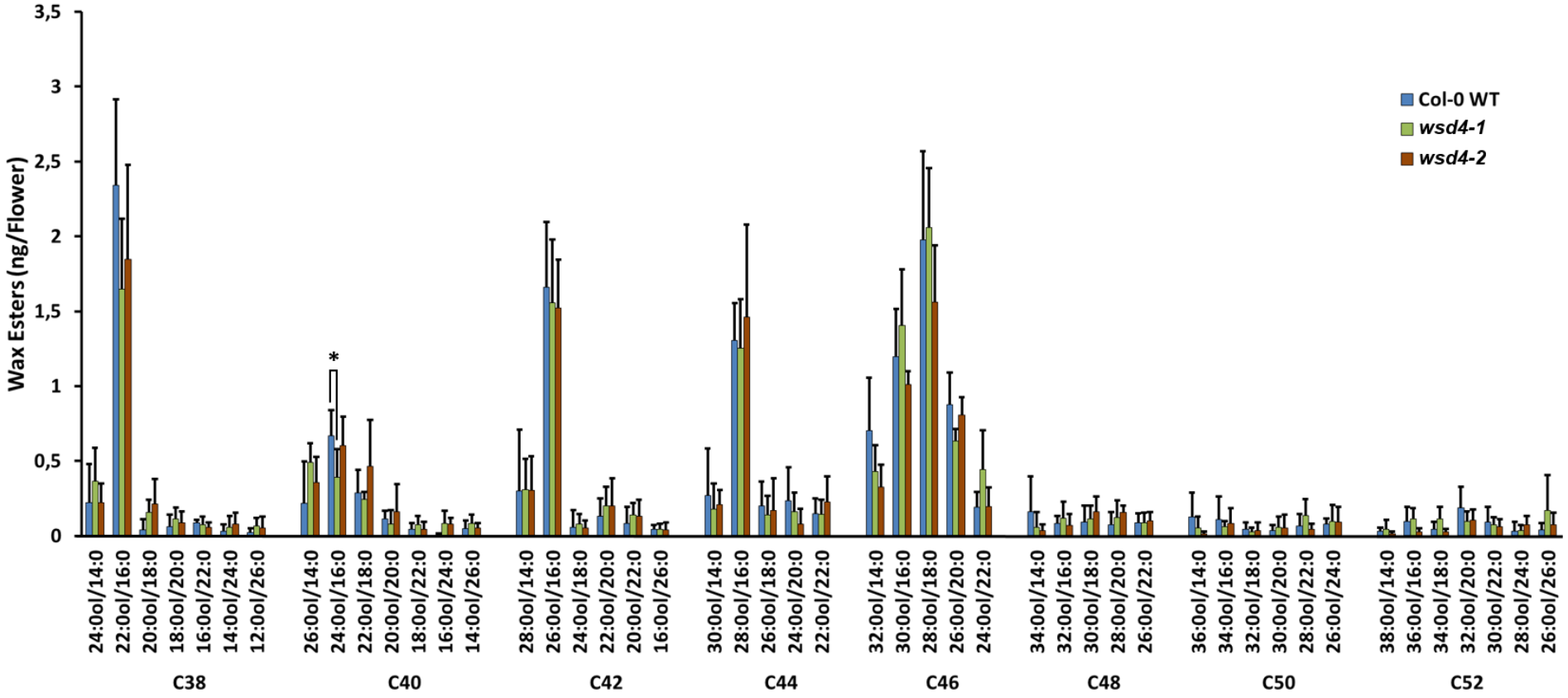

Figure 59: Flower Wax Esters from *A. thaliana* WT and Mutant Lines *wsd4-1* and *wsd4-2*.

Wax from 10 open flowers was extracted by chloroform. The wax extract was fractionated by SPE (hexane/diethyl ether 99/1 (v/v)) and the wax ester fraction analyzed by Q-TOF MS/MS. Data represent mean and standard deviation of 5 measurements. Asterisks indicate values that differ significantly from the wild type control (Student's *t* test, Welch correction, $P<0.05$ (*)).

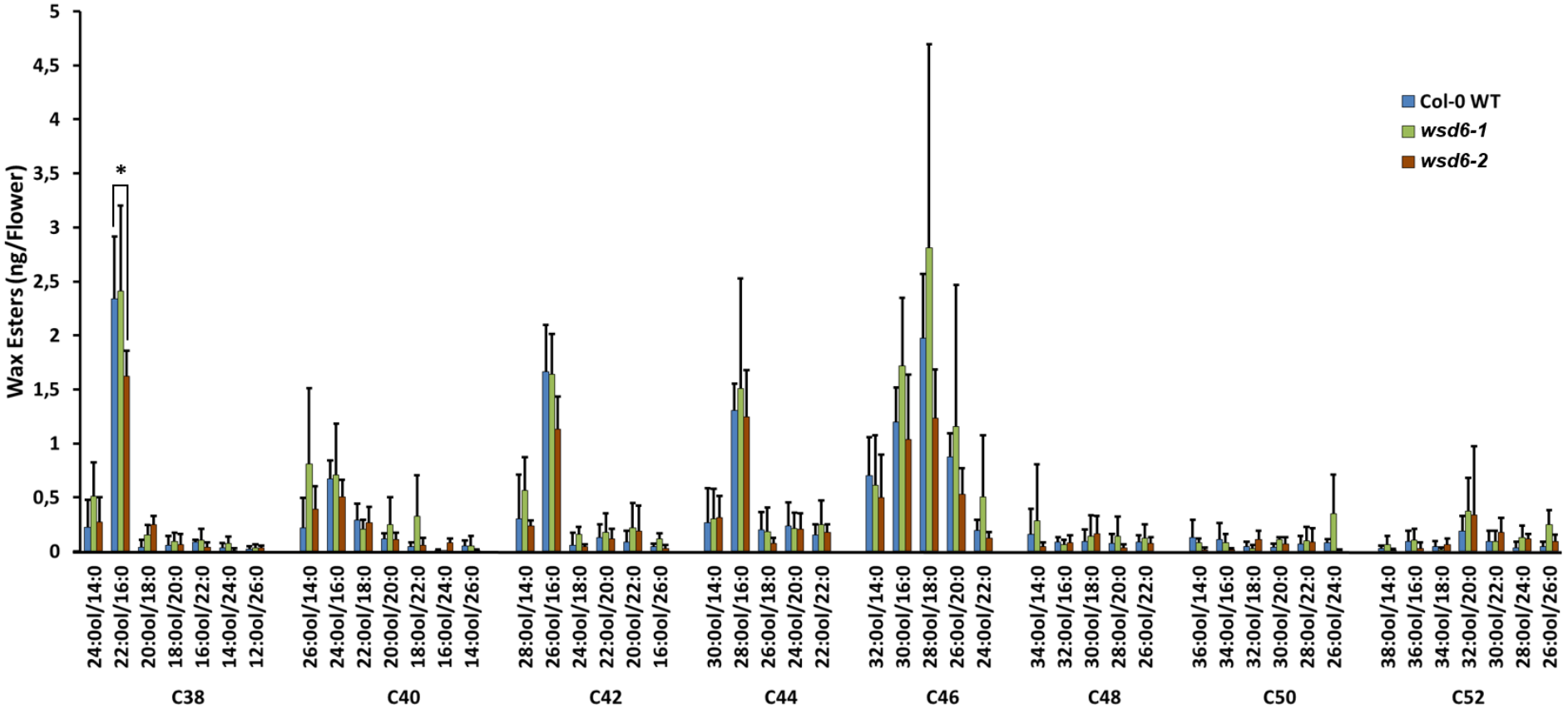

Figure 60: Flower Wax Esters from *A. thaliana* WT and Mutant Lines *wsd6-1* and *wsd6-2*.

Wax from 10 open flowers was extracted by chloroform. The wax extract was fractionated by SPE (hexane/diethyl ether 99/1 (v/v)) and the wax ester fraction analyzed by Q-TOF MS/MS. Data represent mean and standard deviation of 5 measurements for WT and of 4 measurements for *wsd6-1* and *wsd6-2*. Asterisks indicate values that differ significantly from the wild type control (Student's *t* test, Welch correction, $P<0.05$ (*)).

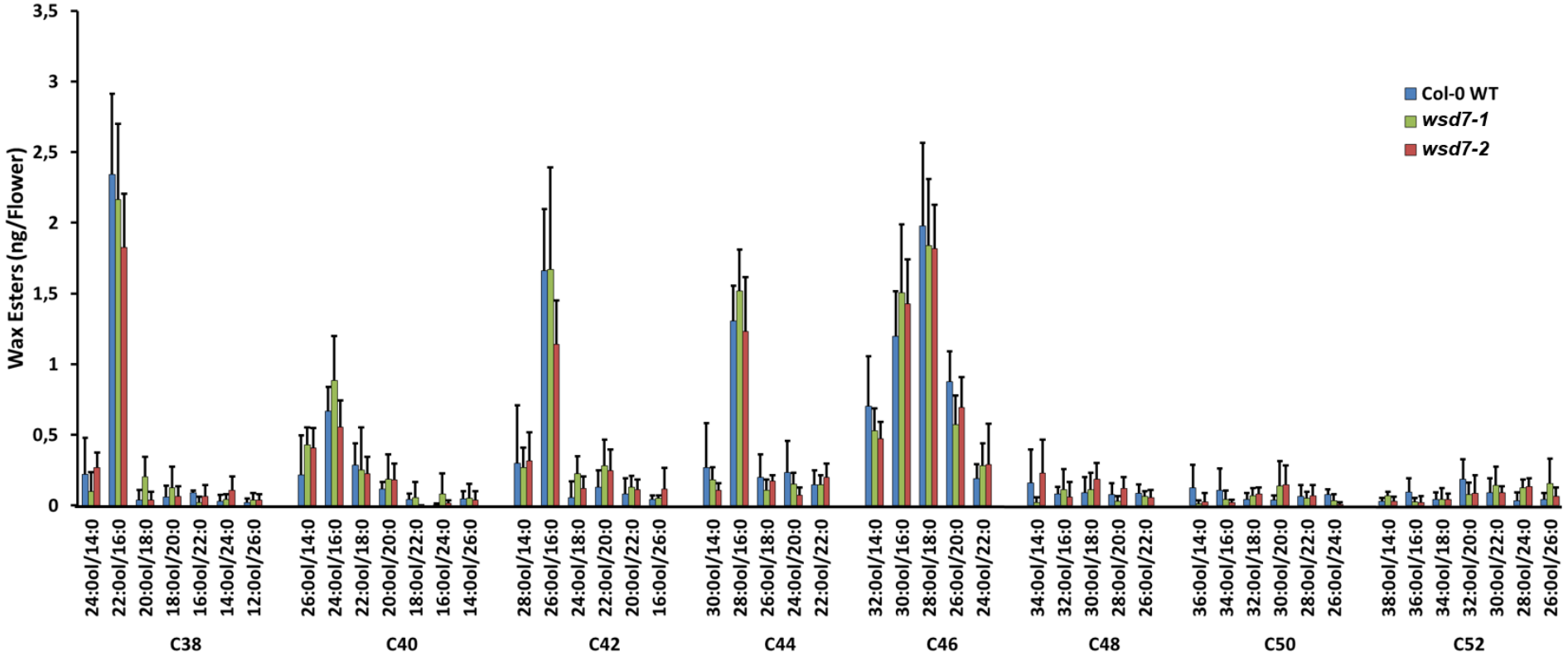

Figure 61: Flower Wax Esters from *A. thaliana* WT and Mutant Lines *wsd7-1* and *wsd7-2*.

Wax from 10 open flowers was extracted by chloroform. The wax extract was fractionated by SPE (hexane/diethyl ether 99/1 (v/v)) and the wax ester fraction analyzed by Q-TOF MS/MS. Data represent mean and standard deviation of 5 measurements.

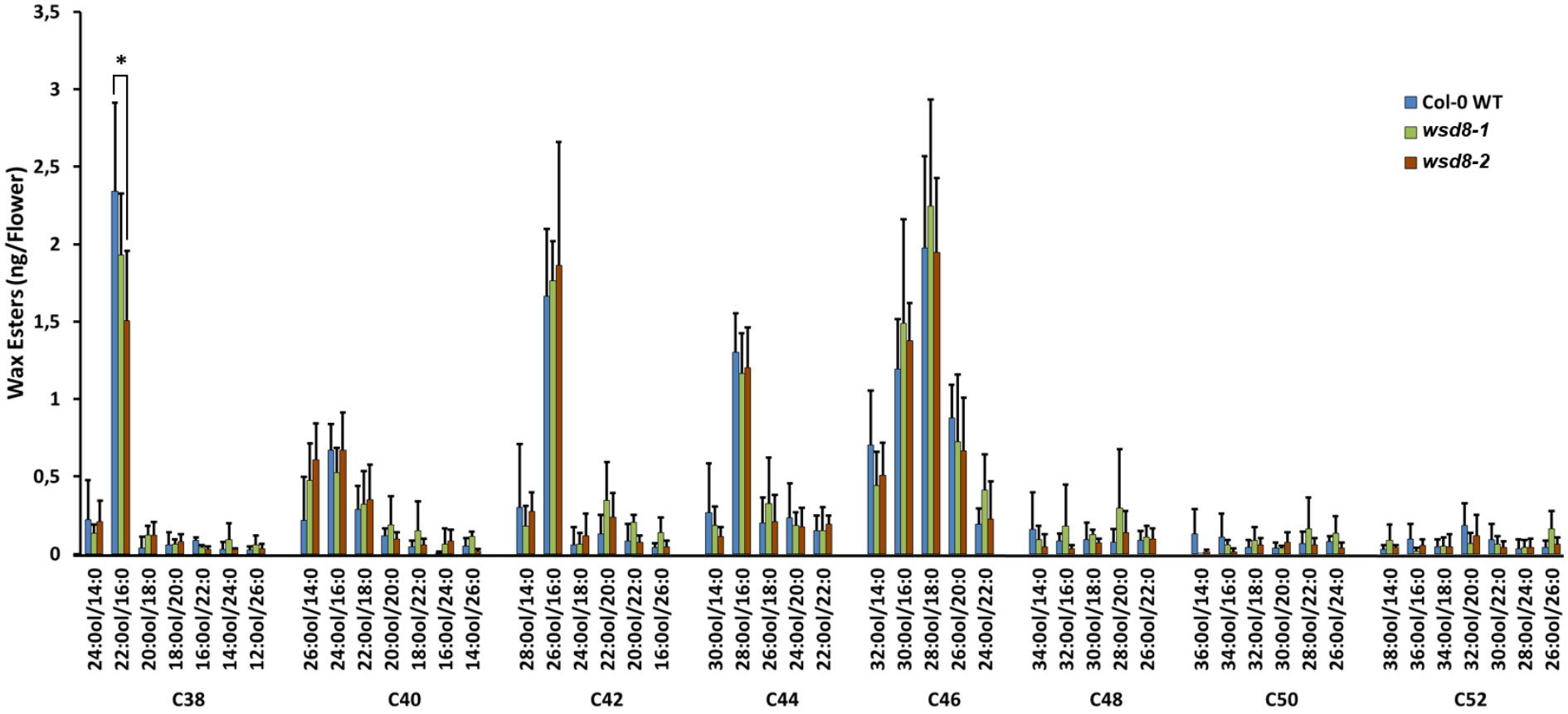

Figure 62: Flower Wax Esters from *A. thaliana* WT and Mutant Lines *wsd8-1* and *wsd8-2*.

Wax from 10 open flowers was extracted by chloroform. The wax extract was fractionated by SPE (hexane/diethyl ether 99/1 (v/v)) and the wax ester fraction analyzed by Q-TOF MS/MS. Data represent mean and standard deviation of 5 measurements for WT and *wsd8-2* and of 4 measurements for *wsd8-1*. Asterisks indicate values that differ significantly from the wild type control (Student's *t* test, Welch correction, $P<0.05$ (*)).

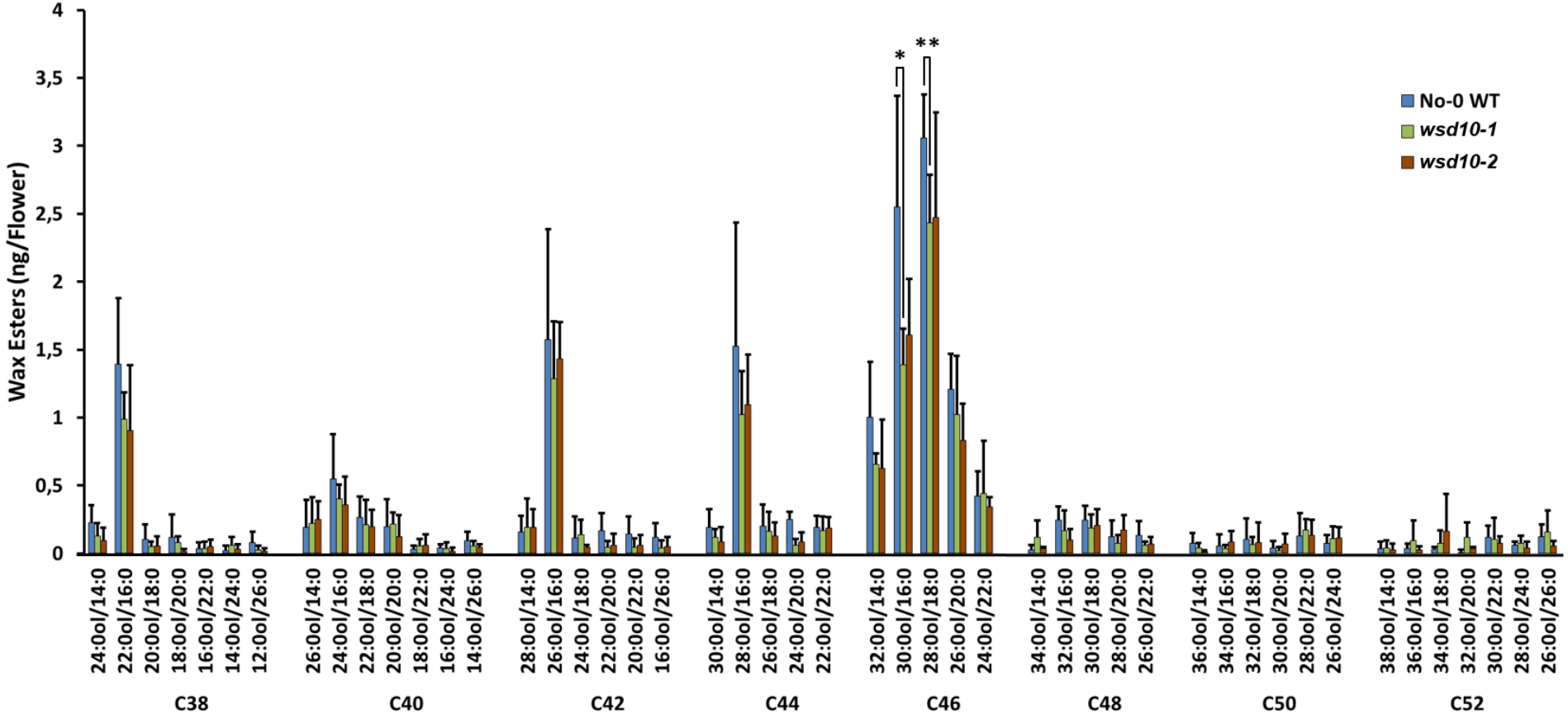

Figure 63: Flower Wax Esters from *A. thaliana* WT and Mutant Lines *wsd10-1* and *wsd10-2*.

Wax from 10 open flowers was extracted by chloroform. The wax extract was fractionated by SPE (hexane/diethyl ether 99/1 (v/v)) and the wax ester fraction analyzed by Q-TOF MS/MS. Data represent mean and standard deviation of 5 measurements. Asterisks indicate values that differ significantly from the wild type control (Student's *t* test, Welch correction, $P<0.05$ (*) and $P<0.02$ (**)).

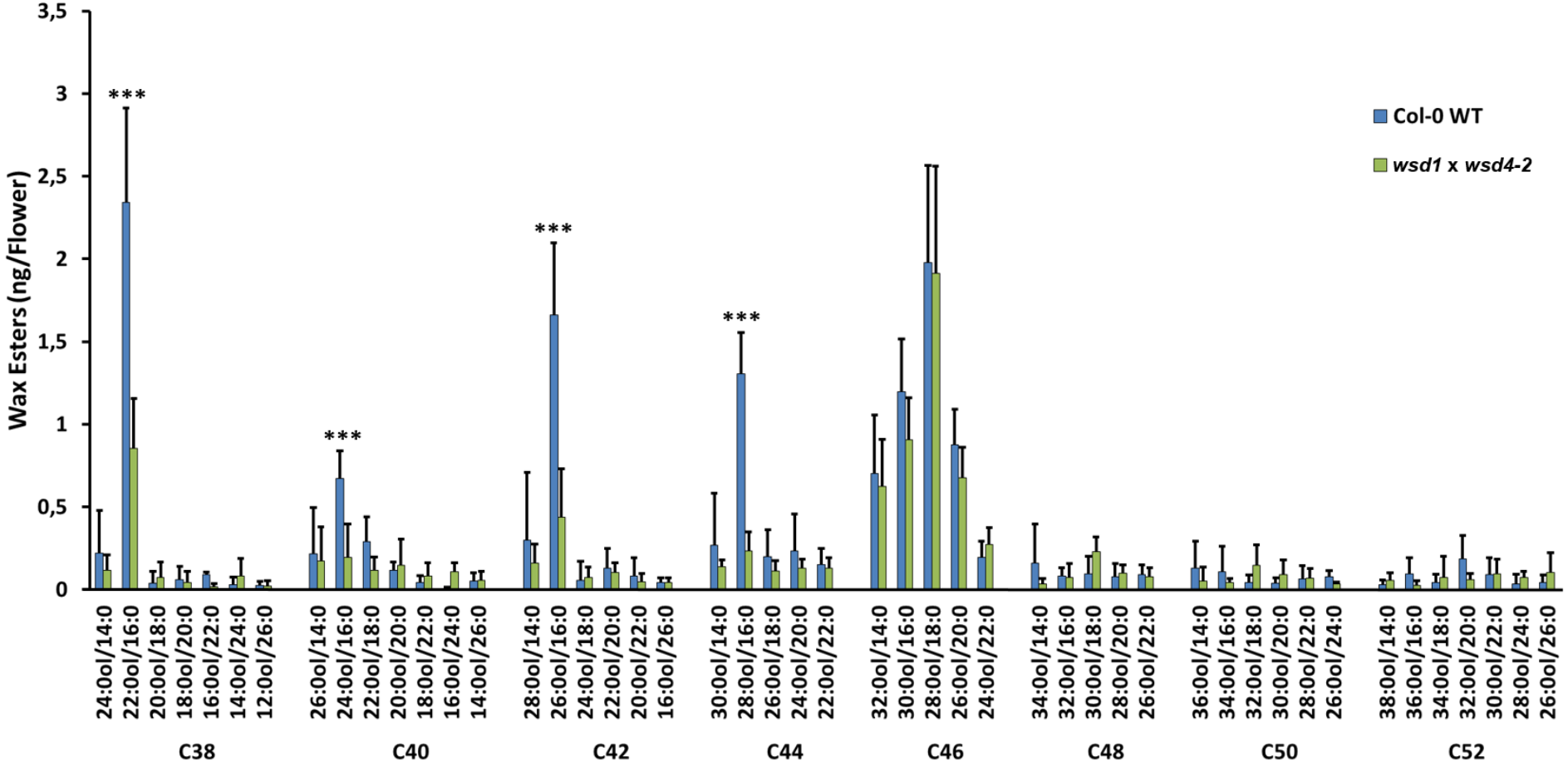

Figure 64: Flower Wax Esters from *A. thaliana* WT and Double Homozygous Mutant Line *wsd1* x *wsd4-2*.

Wax from 10 open flowers was extracted by chloroform. The wax extract was fractionated by SPE (hexane/diethyl ether 99/1 (v/v)) and the wax ester fraction analyzed by Q-TOF MS/MS. Data represent mean and standard deviation of 5 measurements. Asterisks indicate values that differ significantly from the wild type control (Student's *t* test, Welch correction, $P<0.01$ (***)).

7.7 Wax Esters from Silique Surface Wax of *wsd* Mutant Lines

Diagrams are presented on the following pages.

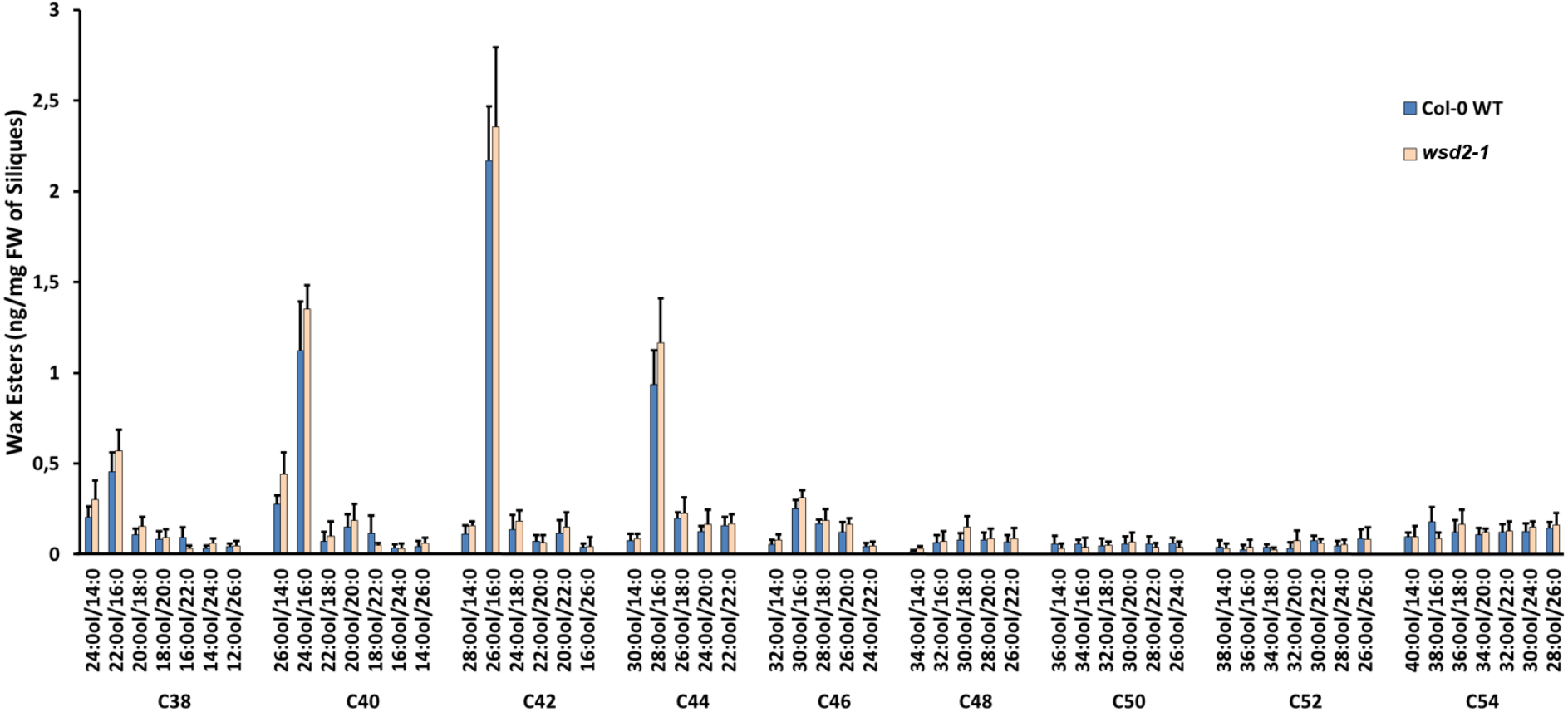

Figure 65: Silique Wax Esters from *A. thaliana* WT and Mutant Line *wsd2-1*.

Wax from 5 siliques, still green but in mature size, was extracted by chloroform. The wax extract was fractionated by SPE (hexane/diethyl ether 99/1 (v/v)) and the wax ester fraction analyzed by Q-TOF MS/MS. Data represent mean and standard deviation of 5 measurements.

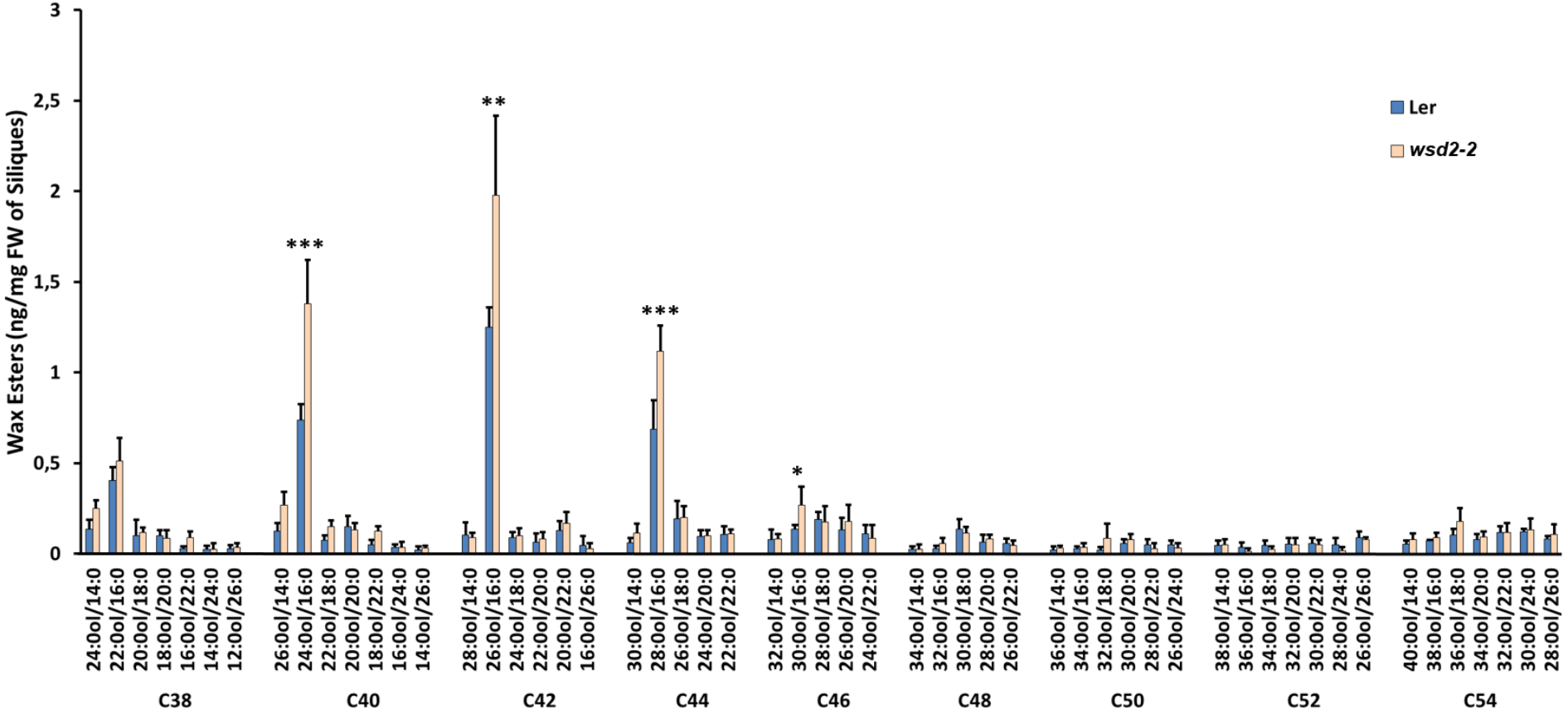

Figure 66: Silique Wax Esters from *A. thaliana* WT and Mutant Line *wsd2-2*.

Wax from 5 siliques, still green but in mature size, was extracted by chloroform. The wax extract was fractionated by SPE (hexane/diethyl ether 99/1 (v/v)) and the wax ester fraction analyzed by Q-TOF MS/MS. Data represent mean and standard deviation of 5 measurements. Asterisks are indicated for the values that are significantly different (Student's *t* test, Welch correction, $P<0.05$ (*), $P<0.02$ (**) and $P<0.01$ (***)).

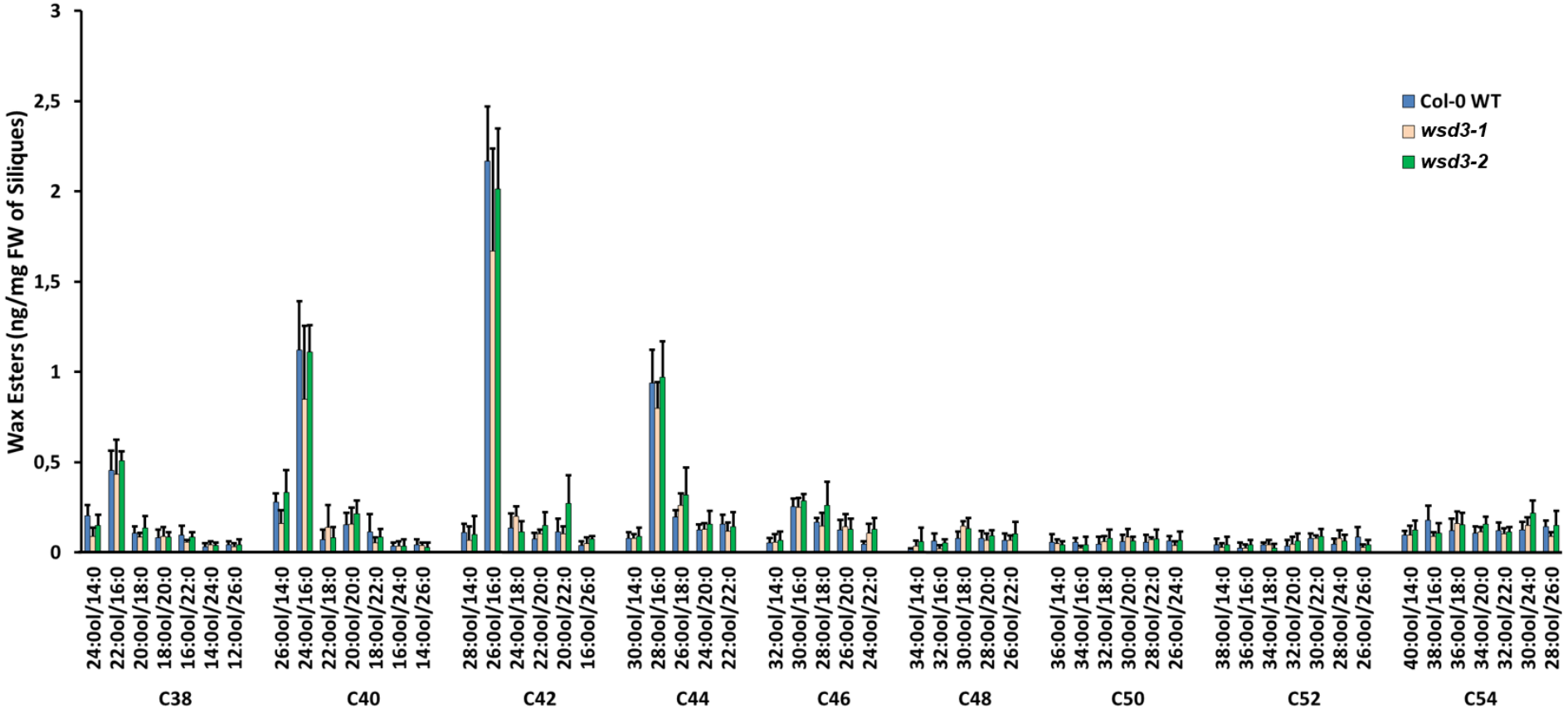

Figure 67: Silique Wax Esters from *A. thaliana* WT and Mutant Lines *wsd3-1* and *wsd3-2*.

Wax from 5 siliques, still green but in mature size, was extracted by chloroform. The wax extract was fractionated by SPE (hexane/diethyl ether 99/1 (v/v)) and the wax ester fraction analyzed by Q-TOF MS/MS. Data represent mean and standard deviation of 5 measurements.

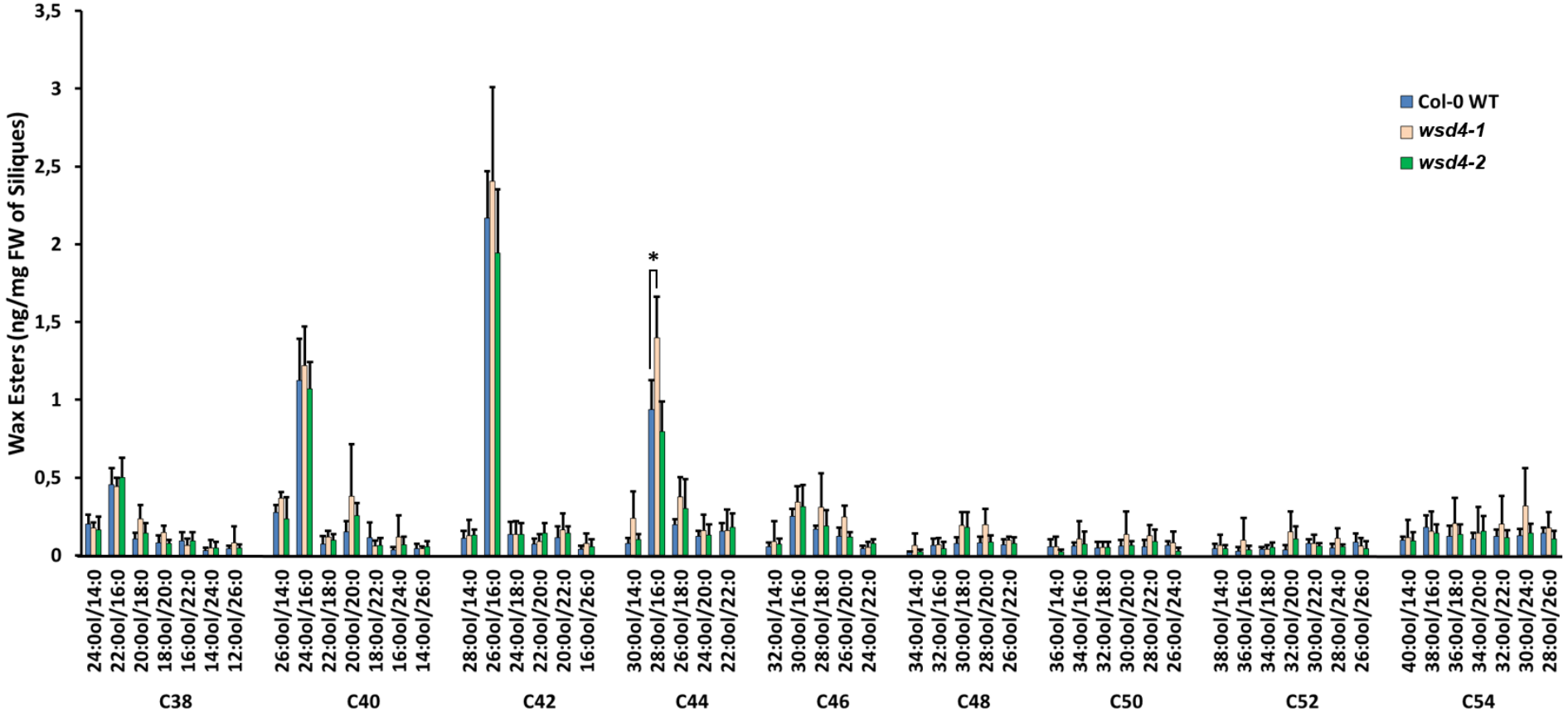

Figure 68: Silique Wax Esters from *A. thaliana* WT and Mutant Lines *wsd4-1* and *wsd4-2*.

Wax from 5 siliques, still green but in mature size, was extracted by chloroform. The wax extract was fractionated by SPE (hexane/diethyl ether 99/1 (v/v)) and the wax ester fraction analyzed by Q-TOF MS/MS. Data represent mean and standard deviation of 5 measurements. Asterisks are indicated for the values that are significantly different (Student's *t* test, Welch correction, $P<0.05$ (*)).

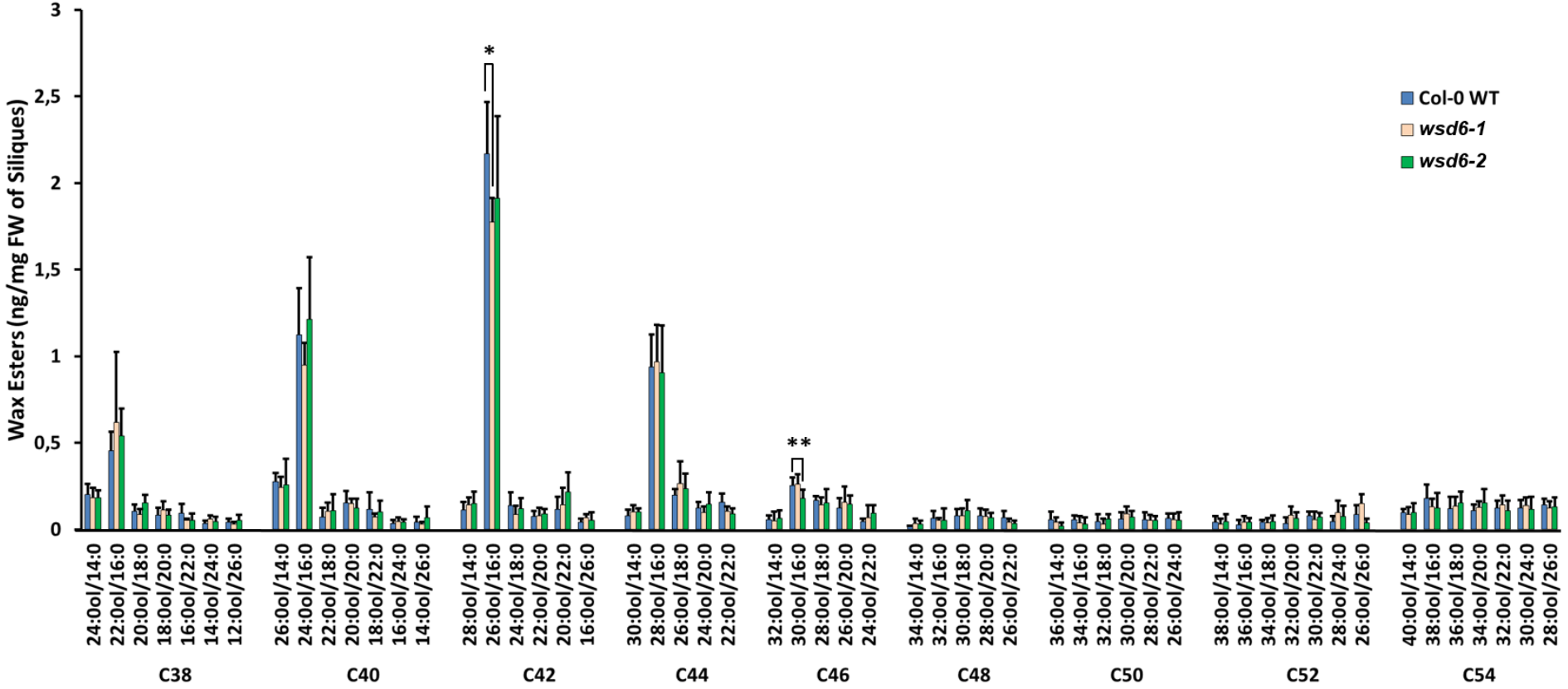

Figure 69: Silique Wax Esters from *A. thaliana* WT and Mutant Lines *wsd6-1* and *wsd6-2*.

Wax from 5 siliques, still green but in mature size, was extracted by chloroform. The wax extract was fractionated by SPE (hexane/diethyl ether 99/1 (v/v)) and the wax ester fraction analyzed by Q-TOF MS/MS. Data represent mean and standard deviation of 5 measurements. Asterisks are indicated for the values that are significantly different (Student's *t* test, Welch correction, $P<0.05$ (*) and $P<0.02$ (**)).

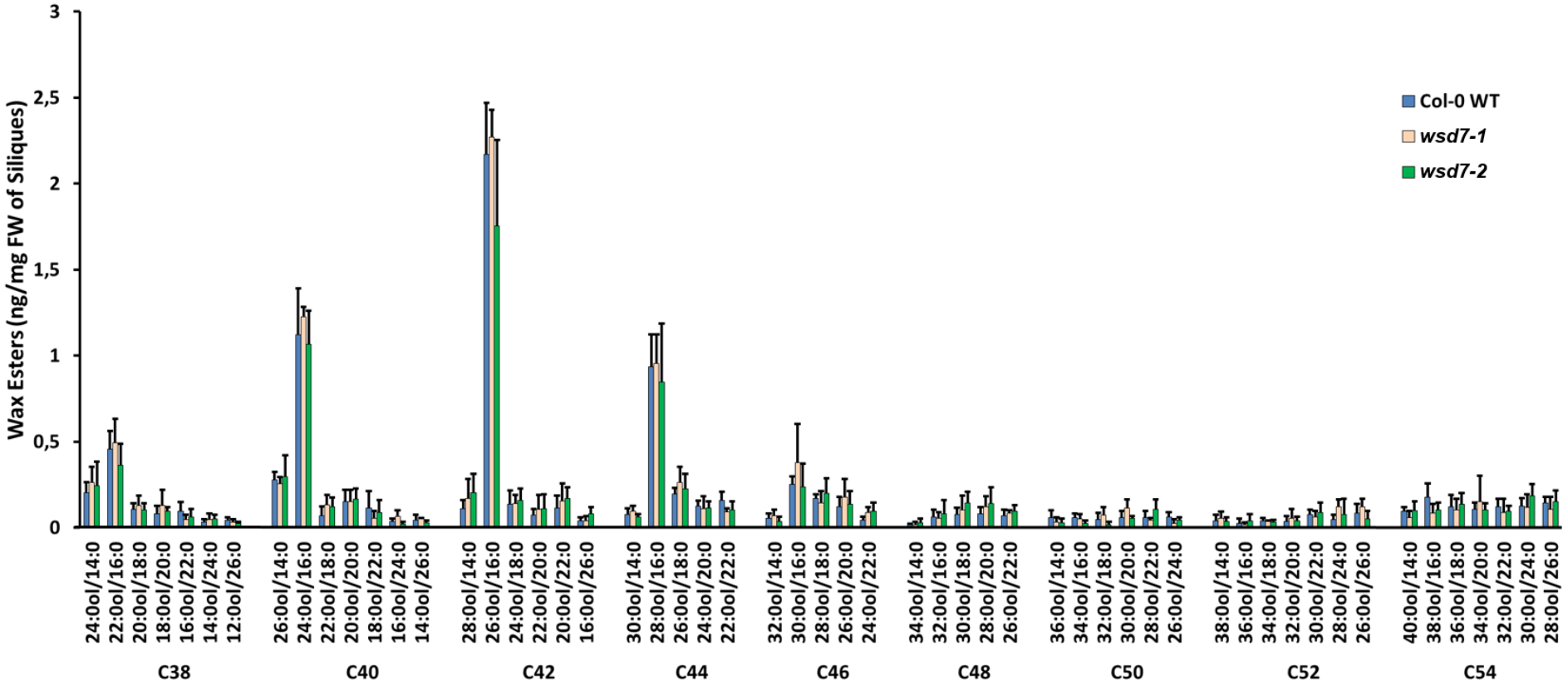

Figure 70: Silique Wax Esters from *A. thaliana* WT and Mutant Lines *wsd7-1* and *wsd7-2*.

Wax from 5 siliques, still green but in mature size, was extracted by chloroform. The wax extract was fractionated by SPE (hexane/diethyl ether 99/1 (v/v)) and the wax ester fraction analyzed by Q-TOF MS/MS. Data represent mean and standard deviation of 5 measurements for WT and *wsd7-1* and of 4 measurements for *wsd7-2*.

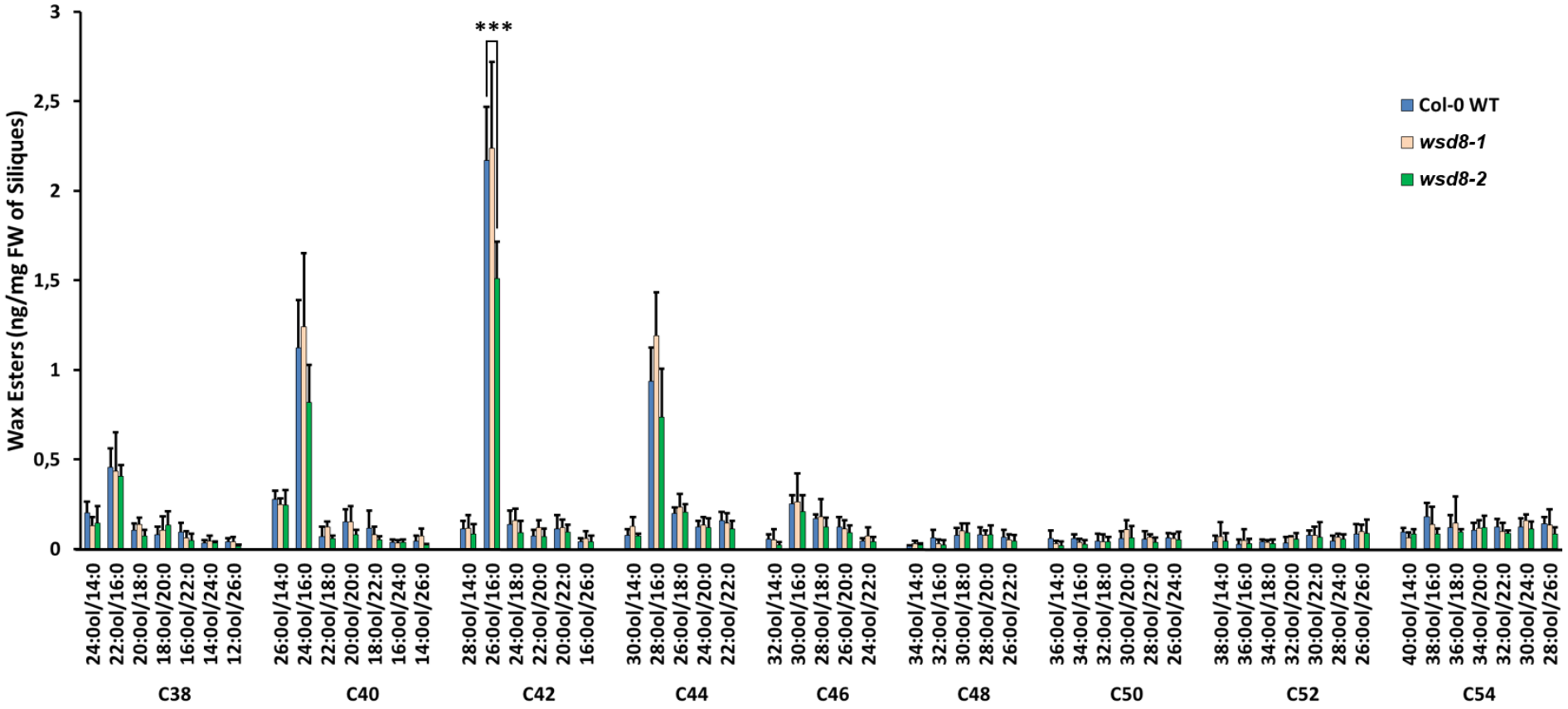

Figure 71: Silique Wax Esters from *A. thaliana* WT and Mutant Lines *wsd8-1* and *wsd8-2*.

Wax from 5 siliques, still green but in mature size, was extracted by chloroform. The wax extract was fractionated by SPE (hexane/diethyl ether 99/1 (v/v)) and the wax ester fraction analyzed by Q-TOF MS/MS. Data represent mean and standard deviation of 5 measurements. Asterisks are indicated for the values that are significantly different (Student's *t* test, Welch correction, $P<0.01$ (***)).

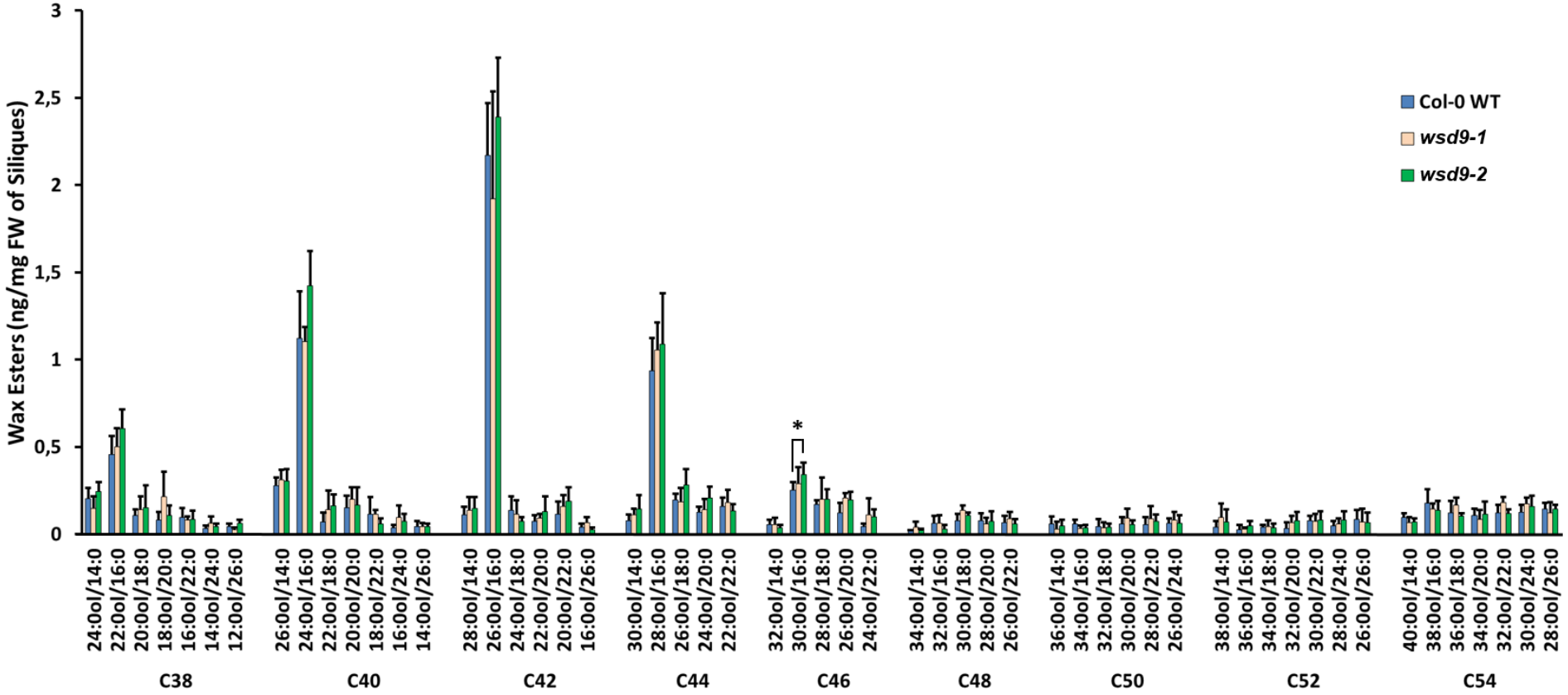

Figure 72: Silique Wax Esters from *A. thaliana* WT and Mutant Lines *wsd9-1* and *wsd9-2*.

Wax from 5 siliques, still green but in mature size, was extracted by chloroform. The wax extract was fractionated by SPE (hexane/diethyl ether 99/1 (v/v)) and the wax ester fraction analyzed by Q-TOF MS/MS. Data represent mean and standard deviation of 5 measurements. Asterisks are indicated for the values that are significantly different (Student's *t* test, Welch correction, $P<0.05$ (*)).

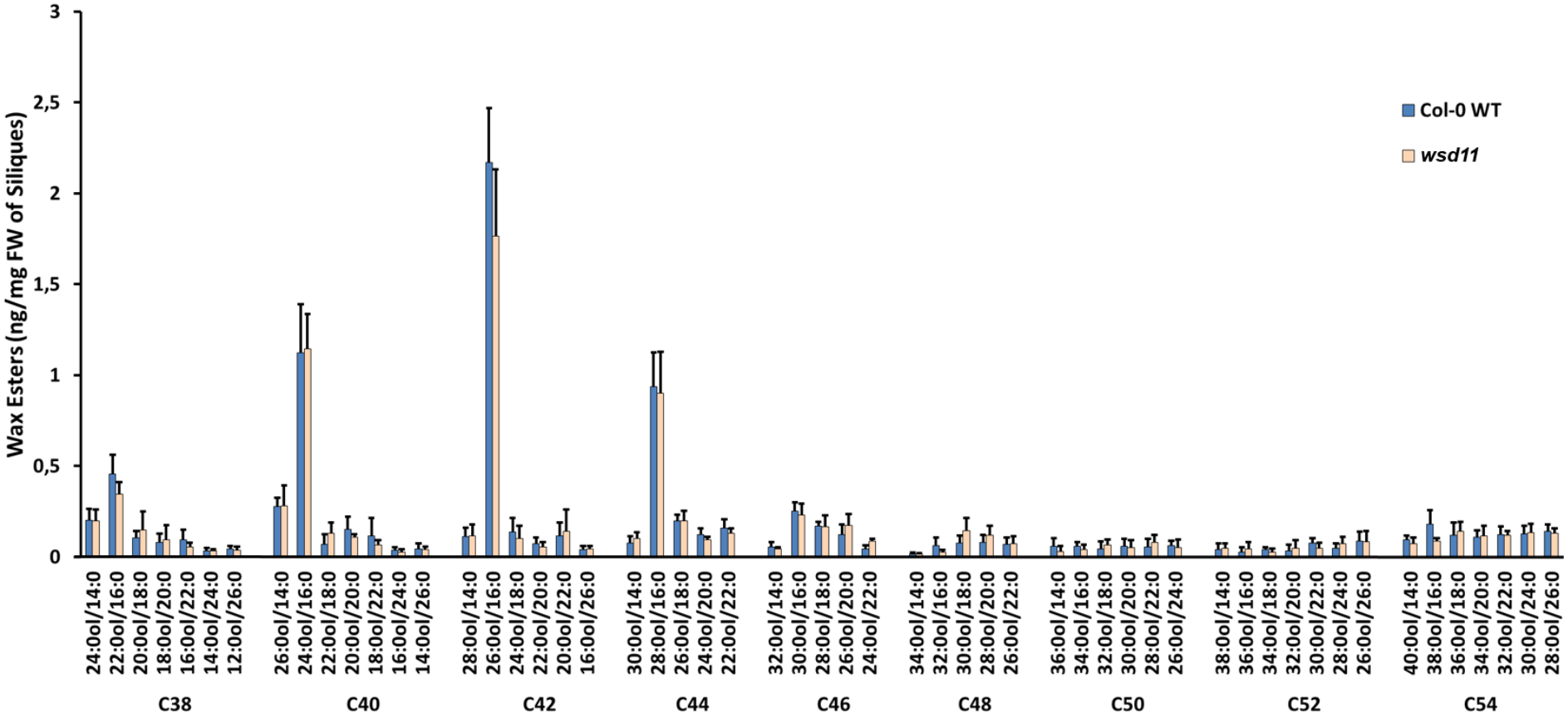

Figure 73: Silique Wax Esters from *A. thaliana* WT and Mutant Line *wsd11*.

Wax from 5 siliques, still green but in mature size, was extracted by chloroform. The wax extract was fractionated by SPE (hexane/diethyl ether 99/1 (v/v)) and the wax ester fraction analyzed by Q-TOF MS/MS. Data represent mean and standard deviation of 5 measurements.

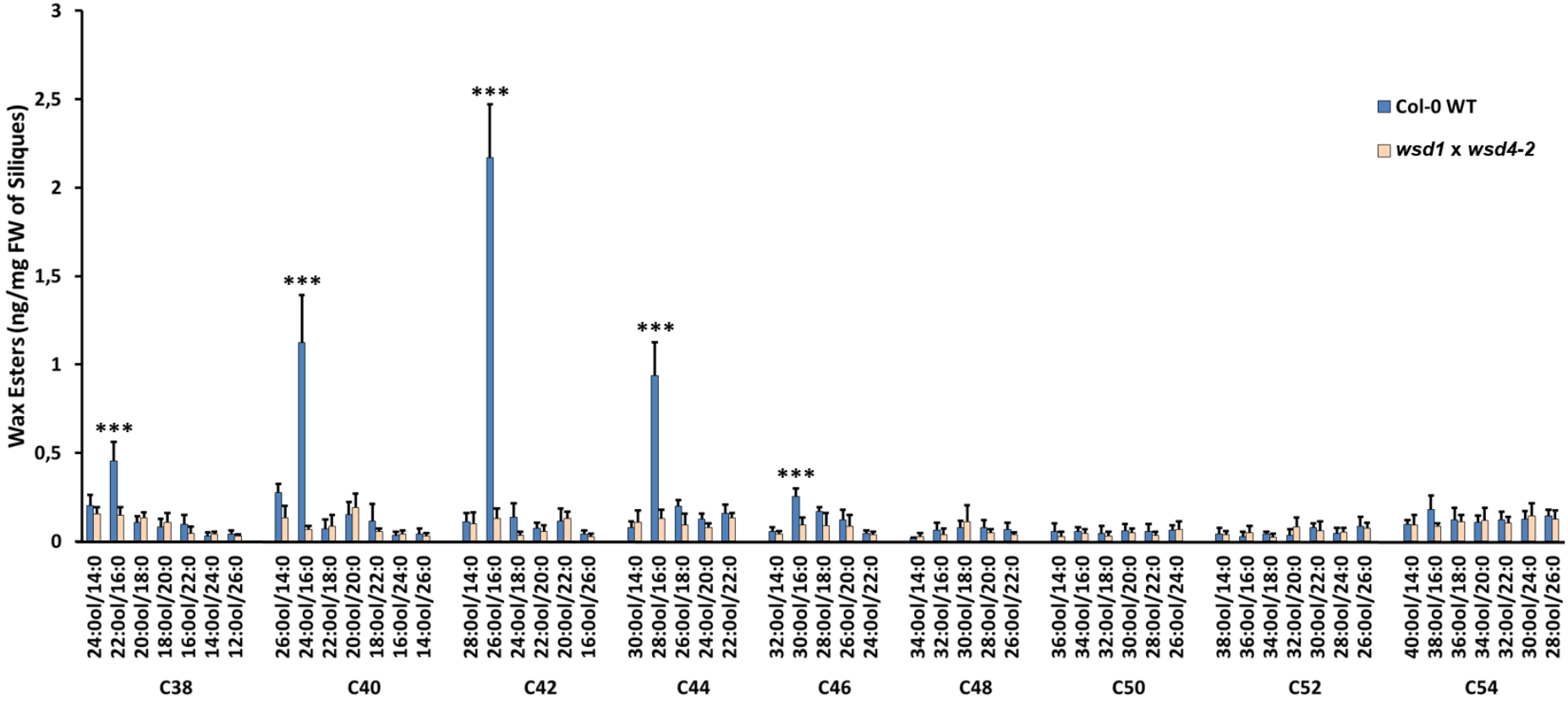

Figure 74: Silique Wax Esters from *A. thaliana* WT and Double Homozygous Mutant Line *wsd1* x *wsd4-2*.

Wax from 5 siliques, still green but in mature size, was extracted by chloroform. The wax extract was fractionated by SPE (hexane/diethyl ether 99/1 (v/v)) and the wax ester fraction analyzed by Q-TOF MS/MS. Data represent mean and standard deviation of 5 measurements. Asterisks are indicated for the values that are significantly different (Student's *t* test, Welch correction, $P<0.01$ (***)).

8 Publication

Patwari P, Salewski V, Gutbrod K, Kreszies T, Dresen-Scholz B, Peisker H, Steiner U, Meyer AJ, Schreiber L, Dörmann P (2019) Surface wax esters contribute to drought tolerance in *Arabidopsis*. The Plant Journal **98** (4): 727-744.